Department of Architecture and
the Built Environment

The University of
Nottingham

UNITED KINGDOM · CHINA · MALAYSIA

ENERGY SAVING POTENTIAL OF GROUND INTEGRATED ARCHITECTURE ON SLOPED TERRAINS

Maria Manuela Marinho de Castro

BA, MSc, MSc

Thesis Submitted to the University of Nottingham for the
degree of Doctor of Philosophy

September 2016

ABSTRACT

Fast urban growth and topographical factors across Europe have contributed to an increase in the total number of hillside residential buildings. In the case of Portugal, a clear need for hillside building design which can fully benefit from the thermal advantage of slope terrains has been identified. Although the energy efficiency of ground-integrated architecture has been the subject of numerous research works, only a small number of those research projects have focused on the thermal potential of ground-integrated buildings constructed on sloped terrains. The research presented in this thesis sheds light on the energy saving potential of ground-integrated buildings on slope terrains and provides design guidelines based on the research findings.

Firstly, through mathematical calculations, this research demonstrates that ground thermal patterns under slope terrains are different from those below flat areas. In Lisbon, terrain inclinations have higher annual ground thermal potential than flat terrains. It is furthermore noted that a transitional zone is formed immediately before and after a slope. As a result of these investigations it is concluded that slopes of 30° to 40° provide the best annual ground thermal potential.

Secondly, through a parametric study using EnergyPlus to simulate ground heat transfer, it is show that ground integration affects buildings thermal performance. It is found that the greater the ground integration the lower the energy demand, but also that total ground integration fails to provide the best solution. Concerning the

levels of slope integration, the steeper the slope, the greater the average annual savings. However the thermal advantage difference between steeper slopes such as those of between 30° to 50° is small. Regarding the impact of building design on annual saving potential, it is found that building design does affect models' thermal performance and that its impact is greatest with shallower slopes.

It is therefore concluded that in temperate climates, new hillside constructions can take advantage of the energy saving potential of ground integration into slope terrain and of slope building designs.

-iii-

PUBLISHED PAPERS RESULTING FROM THIS RESEARCH

De Castro, M. & Gadi, M. B., 2017. Effect of Slope Angle on Energy Performance of Ground-integrated Buildings on Slope Terrain. *International Journal of Sustainable Development and Planning*, 12 (2), 283-293.

De Castro, M. & Gadi, M. B., 2016. Impact of Received Solar Radiation on Energy Potential of Ground-integrated Buildings on Slope Terrain. *In: 15th International Conference on Sustainable Energy Technologies (SET-2016)*, July 19-22, 2016, Singapore.

ACKNOWLEDGEMENTS

TABLE OF CONTENTS

LIST OF FIGURES

LIST OF TABLES

LIST OF EQUATIONS

LIST OF ACRONYMS

ASHRAE: American Society of Heating, Refrigerating and Air-Conditioning Engineers

DOE: Department of Energy (United States)

EAHE: Earth to Air Heat Exchanger

EDSL: Environmental Design Solutions Limited

E+: EnergyPlus

INE: Instituto National de Estatisticas

JRC: Joint Research Centre

kWh/ cons.: Kilowatt hour/ Consumer

kWh/ inhab: Kilowatt hour/ Inhabitant

TAS: Thermal Analysis Simulation

NOMENCLATURE

A_s = annual range of the temperature wave at the ground surface (°C)

b = coefficient of ground surface absorptivity and illumination

f = fraction determined by ground cover and ground moisture content

h_{sur} = soil surface convective heat transfer coefficient (W/m^{2}K)

K = thermal conductivity (W/mK)

r_a = relative humidity of the air (%)

S_a = amplitude of solar radiation wave (W/m^2)

S_m = mean annual solar irradiance (W/m^2)

t = day of year (days)

T_a = air temperature above the ground surface (°C)

T_m = mean annual ground surface temperature (°C)

t_o = phase constant (days) of day with minimum soil surface temperature

T_{sur} = ground surface temperature (°C)

$T_{(x,t)}$ = ground temperature at a depth x (m) and time t (day of the year) (°C)

u = wind velocity (m/s)

x = depth (m)

w = frequency of the temperature range (rad)

α = soil thermal diffusivity (m^2/day)

ε = emittance of the ground surface

φ_a = phase constant (rad)

φ_1 = phase constant (rad)

ΔR = dependent of air humidity values, sky temperature and soil radiative characteristics.

CHAPTER 1. INTRODUCTION

1. INTRODUCTION

"There is much to learn from architecture before it became an expert's art. The untutored builders in space and time (…) demonstrate an admirable talent for fitting their buildings into the natural surroundings. Instead of trying to "conquer" nature, as we do, they welcome the vagaries of climate and the challenge of topography. Whereas we find flat, featureless country most to our liking (any flaws in the terrain are easily erased by the application of a bulldozer), more sophisticated people are attract by rugged country." Rudofsky (1964, p. NA).

Since the early 1960's, two distinct works have set the direction of half a century of design in sustainable architecture. One of these works raised awareness to what today is called vernacular architecture. The other established the basis for sustainable building design by mapping several examples of vernacular architecture. The first, Bernard Rudofsky's *Architecture Without Architects* (1964), opens a window onto numerous examples of world vernacular architecture that it was still possible to see in the early 1960's. The richness and uniqueness of each example of this kind of architecture proves that humans have long been able to design for different climates, generating different construction solutions by taking advantage of local characteristics including topography and available construction materials. The second work, Victor Olgyay's *Design with Climate* (firstly published in 1963) brings to architectural practice the concept of climate design and architectural regionalism based on the legacy of vernacular architecture. Even today, both Rudofsky and Olgyay's concepts form the core principles of sustainable design in architecture.

The reasons why such fundamental aspects as the local climate, topography, and construction traditions have so often been ignored during modern processes of building design and construction is linked to the until-recently ready availability of cheap energy and modern industrial materials (Van der Ryn, 1979, p. NA). However, I believe that this analysis is not complete without taking into consideration economical elements such as prosperity and consumption. For example, the rising access to an increasing number of modern commodities in rapidly developing parts of the world has generated the need for new dwelling layouts, which have become necessary in order to accommodate our increasing consumption, and therefore, perpetuate the escalation between wants and needs.

An illustration of the above problem, which is developed in more detail in Chapter 2, is the effect produced by the Chinese agricultural incentives of the 1980s. In a process that began shortly after the introduction of these economic incentives, the traditional Chinese ground-integrated buildings have been gradually abandoned in favour of newly-constructed above-ground buildings. One of the identified reasons behind this trend is the lack of living space (Golany, 1992, p. 43; Liu et al., 2010, p. 124). Traditional underground buildings present space constraints which mean that they struggle to accommodate new domestic commodities. Consequently, the current cost of constructing buildings ignoring local climate and customs is undermining local construction knowledge (Tong, Chen and Li, 2011, p. 1644) in favour of new construction types. However, these new constructions are less energy efficient (Zhu et al., 2014, p. 159) for the local harsh climate conditions and are less affordable due to the high cost of the new construction materials (Jun and Yan-yung, 2006, p. NA).

The practice of ignoring the land's physical features, by designed buildings without taking site topography into consideration and simply transforming any site in to a flat area is contributing to two distinct losses: land loss and the energy loss. Regarding

the issue of land loss, the relevance of efficient land use is fast increasing due to two well know factors, the global population growth (World Resources Institute, 1994, p. 27) and the much more rapid growth in urban populations (UN-Habitat, 1987, p. 23; World Resources Institute, 1990, p. 66, 1994, p. 31). The rising global population demands larger quantities of food production, but new agricultural land comes at a high cost. New agricultural land is limited by physical constraints such as terrain inclination, and in most cases its expansion inflicts heavy costs on areas that are economically vital and ecologically delicate (World Resources Institute, 1990, p. 88). On the other hand, the existing cropland area is being threatened by the global trend towards urbanization (ibid., p. 88; World Health Organization and UN-Habitat, 2016, p. 102) since *"the expansion of cities often invades rich agricultural lands surrounding them"* (World Resources Institute, 1988, p.42).

We can grasp a way to attenuate the competition for space between construction and agriculture by looking to the particular relation of agriculture and urban land use with topography. This is essentially because flat land and valleys are better for agriculture, while slope terrains can be ideal for human settlements. Flat land and valleys have been identified as more suitable for food production than slope terrains, because the soils are more fertile (Sterling, Carmody and Elnicky, op.cit., p. 29) and there are fewer spatial limitations. From the perspective of construction, which is discussed in more detail in Chapter 4, slope-building constructions are more land efficient. A settlement built on a slope requires less construction area than a flat settlement with the same characteristics (Turan, op.cit., p. 159). Regarding the energy losses, slope areas benefit from a more moderate climate than a flat land or valley. Therefore buildings constructed on hillsides or mountains have lower energy requirements than those built on flat land (Golany, 1996, p. 456) and consequently, produce better thermal performances.

A further thermal advantage of building on slopes is that buildings can take advantage of ground thermal potential through direct contact, which is done by integrating the building into the slope. This was a common practice in ancient slope settlements and it is still used in hillside settlements as the case of Mardin (Turkey), Alicante (Spain), Santorini (Greece) and Matera (Italy).

Although nowadays there is an increasing number of hillside residential areas due to urban development and topographical factors, evidence shows that there is still a lack of relation between recent residential building constructions and the thermal advantage that sloped terrain building designs can provide (Simpson and Purdy, 1984, op.cit, p. 9), in particular in terms of the thermal benefits ground-integration can provide (Benardos, Athanasiadis and Katsoulakos, 2014). Since the global energy crisis of the early 1970's several studies have been conducted, focussing on the energy efficiency of ground-integrated buildings. However, only a few of these studies are focused on the particular case of the thermal performance of ground-integrated buildings on slope terrains. This is particularly true in the case of studies concerning the effect of slope degree or the effect of slope building designs on buildings performance.

In the case of Portugal, Veloso da Veiga's (2009) study identified a clear need for an approach to hillside building design that can take advantage of the hillside thermal comfort potential (ibid., p. 264). According to Veloso da Veiga, the recent increase in hillside building design in the north of Portugal is connected with factors such as local topography, urban development, and lack of available construction land (ibid., p. 264). When studying the '*Encosta do Bom-Jesus*' hillside in Braga, Veloso da Veiga found that most of the houses were constructed recently and their designs commissioned to architects. The study shows that the high-income residents are conscious about solar technologies advantages and aware of energy-saving methods. However, a significant number of households reported little or no

satisfaction with the thermal comfort of the houses, and very few residents use solar technologies (ibid., p. 265).

Newly-built constructions on hillsides miss an opportunity to fully benefit from either ground thermal potential or from building design. Therefore the overall aim of this thesis is to clarify the thermal benefits of ground-integrated buildings on slope terrains. Investigating the thermal patterns produced by different terrain inclinations and verifying how ground thermal affects buildings' annual and seasonal thermal performances, according with levels of ground integration. Considering building design, this research explores the thermal potential of buildings aspect as forms, number of floors, basement, underground courtyard and slope building designs. With the purpose of accomplish the thesis aim the following objectives were determined:

- Identifying gaps on this subject, through the literature review on ground thermal energy, benefits and weaknesses of ground-integrated architecture and advantages of slope-integrated architecture.

- Verifying the ground thermal potential on temperate climates. This is achieved by analysing the ground temperature at six different locations and different depths in Portugal, using a mathematical model to calculate ground temperatures according with depth.

- Investigating the ground thermal potential produced by terrains inclination, by calculating the ground temperatures at different depths using the correspondent solar radiation values.

- Identifying the software and procedure to simulate ground heat transfer by comparing three building simulation packages, Tas, EnergyPlus (E+) and Ecotect.

- Identifying through the available statistic data the average building topology in Portugal to be used to develop the case studies.

- Designing and simulating the parametric case studies based on the findings produced with the above objectives.

- Analysing the parametric case studies that allow identify thermal saving potential produced by ground-integration and building designs.

- Providing energy efficiency design guidelines, based on the findings and conclusions of the parametric case studies.

Methodology

To meet the above aim and objectives, this research deploys the following methodologies. Firstly, this study presents a comprehensive literature review examining ground thermal energy, ground-integrated architecture, slope-integrated architecture and Portuguese building environment and construction context. Secondly, this study deploys quantitative methods and considers particular case studies. Initially, the ground thermal potential and slope thermal potential is investigated using an experimental approach through a mathematical model. Afterwards, the effects of ground-integration and buildings designs are examined, using a parametric study using E+ to simulate ground heat transfer.

Research Structure and Key Outcomes

The structure of this thesis is organised in three parts as illustrated in Figure 1.1. The initial part presents a literature review on subjects such as ground thermal potential, ground-integrated architecture, and slope-integrated architecture. The second part looks into the ground thermal potential of the Portuguese mainland, while also setting the procedure for the computer-based simulations of ground heat transfer. The third part presents the parametric studies of ground-integrated buildings on horizontal and slope terrains. The chapters' contents and outcomes are as follows:
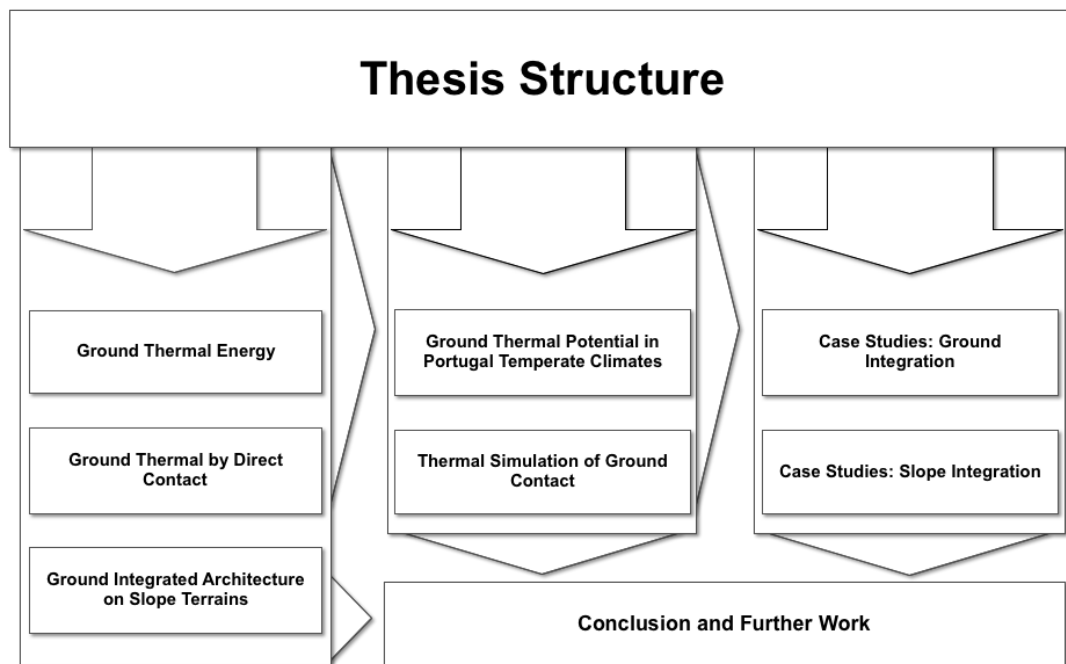
Figure 1.1: Research structure

The structure of this thesis is organised in three parts as illustrated in Figure 1.1. The initial part presents a literature review on subjects such as ground thermal potential, ground-integrated architecture, and slope-integrated architecture. The second part looks into the ground thermal potential of the Portuguese mainland, while also setting the procedure for the computer-based simulations of ground heat transfer. The third part presents the parametric studies of ground-integrated buildings on horizontal and slope terrains. The chapters and correspondent contents are as follows:

Chapter 2. Ground Thermal Energy

This first chapter gives an overview of ground thermal energy sources and its application for the heating and cooling of buildings. It looks into temperature distribution, as well as the factors that affect ground temperature and provides a review of existing literature on ground thermal potential. This chapter also provides a review of ground heating and cooling of buildings through indirect contact by introducing aspects concerning vernacular systems and earth-air heat exchanger

systems (EAHE). Lastly, this initial chapter identify factors that affect EAHE systems performance.

Chapter 3. Ground Thermal by Direct Contact

The second chapter contextualises the study of buildings heating and cooling through direct ground contact. The historical context of ground-integrated architecture is given, as well as terminologies and levels of integration. This second chapter also evaluates relevant advantages and disadvantages of ground-integrated buildings, and gives an overview of the studies on the thermal performance of ground-integrated architecture.

Chapter 4. Ground-integrated Architecture on Slope Terrains

The third chapter focus on the design potential of buildings on slope surfaces. It looks into the issue of lack of suitable land and possible sustainable land use through building on slopes. It provides an overview of slope-integrated settlements and the reasons that lead to this configuration type. Furthermore, this chapter also provides a review of the ground thermal potential of slopes, of the types of slope building designs and of the case studies of slope-integrated buildings.

Chapter 5. Ground Thermal Potential in Temperate Climates

This chapter serves as an introduction to Portuguese mainland temperate climates, and to the Portuguese built environment and energy consumption context regarding residential buildings. It addresses the ground thermal potential in Portugal through mathematical analysis of the ground temperature produced by the Portuguese climate. This chapter also provides a study of the solar radiation received by slopes in Lisbon by looking into how total annual and seasonal solar radiation changes according with slope inclination. Lastly, Chapter 5 presents a study of the slope

thermal potential in Lisbon, which shows how slope surface affects the ground temperature at different depths and therefore its thermal potential.

Chapter 6. Thermal Simulation of Ground Contact

This chapter presents a sequence of studies undertaken in order to determine the most suitable building energy simulation software to conduct research into the benefits of ground-integrated buildings. It analyses the performance of different software packages including Ecotect, Tas and E+ when calculating ground heat transfer, through several comparative and sensibility studies. It also explains the procedure used for the parametric studies of Chapter 7 and Chapter 8.

Chapter 7. Case Studies: Ground Integration

This chapter examines the thermal effects on buildings produced by different levels of ground integration, looking into the annual and seasonal thermal performance and possible energy savings of each level of integration. It also scrutinizes the relevance of design features such as building form, number of floors and the application of basement and courtyards.

Chapter 8. Case Studies: Slope Integration

This chapter presents the slope-integrated building parametric studies. It examines the thermal effect produced by different slope inclinations and by building design, specifically as forms and slope building designs. This is done by analysing the annual and seasonal thermal performance simulation results and the produced energy savings.

Chapter 9. Conclusions and Further Work

This last chapter provides a summary of thesis process and findings. It presents design recommendations based on the main findings of Chapter 7 and Chapter 8 and identifies gaps in the field that can be subject of future research.

Primary Contribution to Knowledge.

This research demonstrates the energy saving potential of ground-integrated buildings on slopes terrains in countries with temperate climates. The primary contributions to this field are the following:

- Demonstrating the high ground thermal potential in different Portuguese temperate climates.

- Proving the superior thermal potential of inclined terrain in a temperate climate as Lisbon.

- Showing why building simulation package need to include terrain inclination and orientation for simulation of ground heat transfer.

- Providing evidence that the use o E+ to compare ground-integrate models on flat and slope terrains needs to be avoided.

- Producing design guidelines for ground-integrated architecture on flat and slope terrains in temperate climates.

The impact of built environment on climate change is too great to be ignored. In the particular case of commercial and residential buildings, the greenhouse gas emissions associated with electricity production are mainly the result of heating and cooling of these buildings. Together, the heating and cooling of homes is responsible for 8% of the total global greenhouse emissions (UN-Habitat, 2011, p. 42). Consequently, controlling and reducing the greenhouse gas emissions in the built environment is our current challenge to mitigate its impact, which can be achieved in part by designing and constructing energy efficient buildings. Newly-built constructions on hillsides can reach this aim through a greater knowledge of the thermal advantages provide by slope terrains and slope building designs.

CHAPTER 2. GROUND THERMAL

2. GROUND THERMAL ENERGY

2.1. INTRODUCTION TO GROUND THERMAL ENERGY

The ground absorbs a large part of the solar radiation received by the earth's surface. To a certain depth, the ground can act as an indirect solar energy source since it is able to collect, store and transmit energy. The other ground' energy sources are atmosphere, geothermal, decomposition of organic matter and radioactivity of rocks (Chang, 1958, p. 43).

The thermal performance of buildings can be improved by using indirect solar energy, as the ground source's heating and cooling can be transferred to a building by direct or indirect contact strategies. In direct contact strategies, a building is totally or partially buried in the ground, so its structure is in direct contact with the soil. In indirect contact strategies, the ground can be used to change the temperature of a fluid, normally air in the case of Earth to Air Heat Exchangers (EAHE), by passing it through pipes placed below ground before being introduced inside a building space.

For an efficient implementation of both earth-coupling strategies it is vital to know the diurnal and annual ground temperature behaviour at different depths. To identify ground thermal patterns it is necessary to determine the ground temperature as well as components that influence ground heat flux.

2.2. GROUND TEMPERATURES

2.2.1. Distribution Zones: Surface, Shallow and Deep
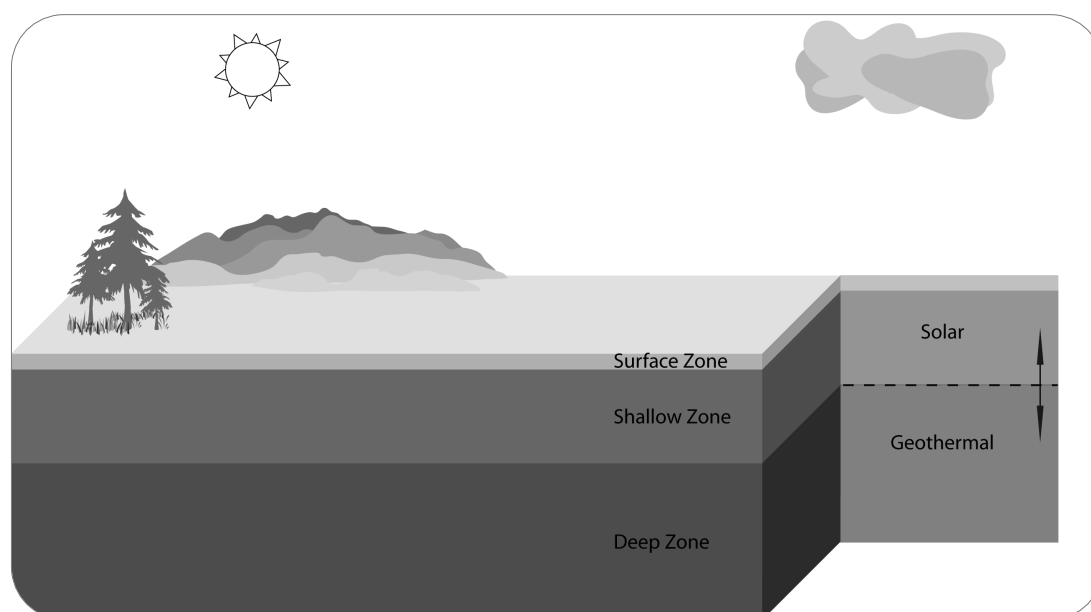
Figure 2.1: Ground energy source and zone temperature distribution

The temperature distribution within the ground varies according to depth, and can be divided into three distinct zones: surface, shallow and deep (Figure 2.1). The surface zone is the soil area immediately below the surface where its temperature is affected by the daily weather conditions, and this immediate influence can be found up to soil depths of 0.5 to 1 m. The shallow zone is the soil area where soil temperatures are more stable and mainly affected by seasonal climate conditions. The extent of this zone depends on the physical properties of the soil, and can be set between 1 to 8 m in most soils, or reach depths of 20 m in some cases.

The deep zone begins immediately below the shallow zone. In this area the soil temperature is almost constant all year round and is no longer affected by diurnal or seasonal climate conditions. Normally the average annual ground temperature is similar to the mean annual ambient air temperature (Chang, op.cit., p. 58; Golany, 1995, p. 193; Popiel, Wojtkowiak and Biernacka, 2001, p. 301; Rantala, 2005, p. 52; Banks, 2008, p. 42). Below the 'permatemp line' (Golany, 1980, p.110) that divides

the shallow zone from the deep zone, the ground temperature is affected by the geothermal heat flux provided by the earth's interior (Popiel, Wojtkowiak and Biernacka, op.cit., p. 301; Banks, op.cit., p. 49), making it a renewable energy source that does not depend on the sun (Brown and Garnish, 2004, p. 342).
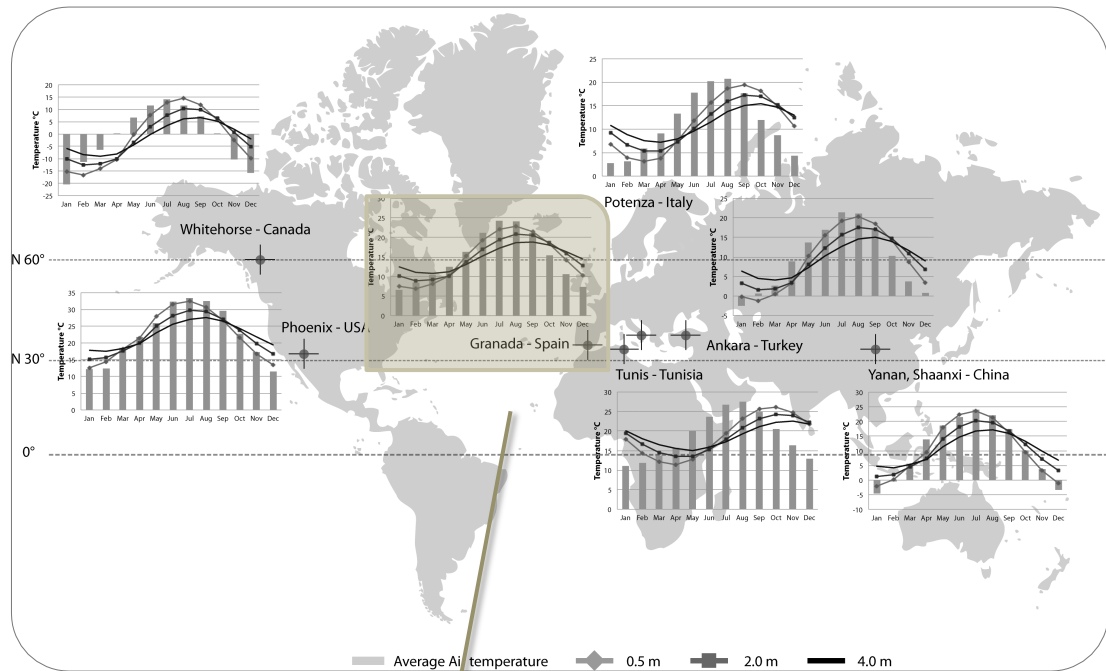
Figure 2.2: Ground temperatures at different depths; by the author, charts based on US Department of Energy weather data
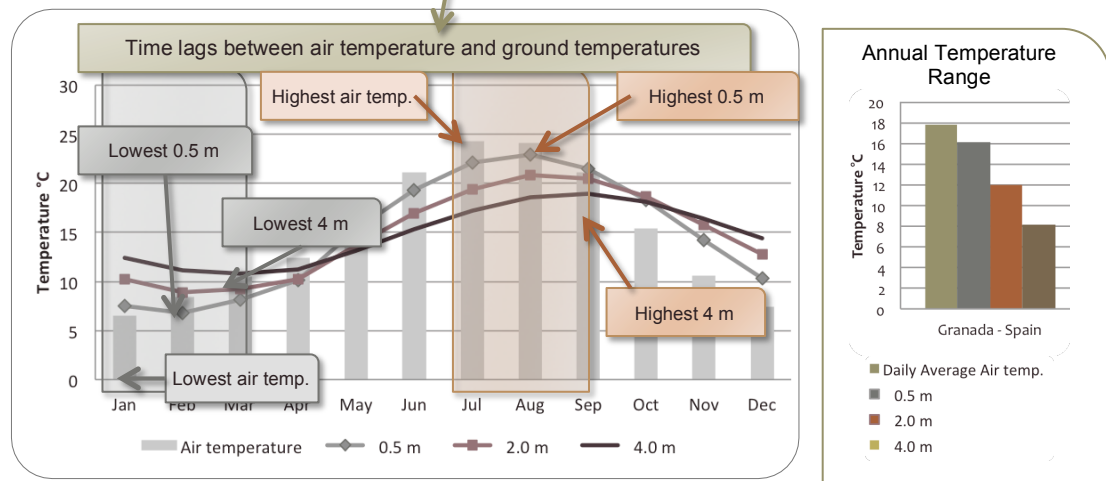
Figure 2.3: Granada, Spain. Air and ground temperatures, time lag and annual temperature range

Figure 2.2 illustrates the air and ground temperature at different locations. At or near these locations, examples of vernacular architecture that apply ground thermal potential can often be found. Similar patterns can be found for time lag and annual temperature range in the graphs above. Looking more closely at a location such as

Granada (Spain), as illustrated in Figure 2.3, we can see that the time lag between the outside air and ground temperature increases according to depth; the greater the depth, the longer the time lag. We can also see that the greater the depth, the smaller the annual temperature range. These undisturbed ground temperatures are defined by fluctuations in the annual pattern of the ground surface temperature and the constant ground temperature at a certain depth (Givoni, 1994, p. 192).

2.2.2. Factors that Affect Ground Temperature

Table 2.1: Factors that affect ground thermal behaviour

Intrinsic factors		External factors
Soil thermal properties	Location characteristic	Climate conditions
• Thermal conductivity • Organic matter • Colour • Moisture content	• Slope orientation • Topography • Nearby elements • Ground coverage	• Solar radiation • Rain • Relative humidity • Air temperature • Wind velocity • Snow

There are several different factors that affect below ground temperature. Table 2.1 presents these factors according to Chang's categories as intrinsic or external (Chang, op.cit., pp. 128-167). The intrinsic factors combine ground thermal properties such as thermal conductivity or density, and location characteristics including topography, cover or slope orientation. The external factors that need to be considered are elements of climate conditions, such as solar radiation, wind velocity, precipitation values, humidity, ambient air temperature and snow coverage.

2.2.2.1. Soil Thermal Properties

The physical characteristics of the soil affects the ground temperatures (Florides et al., 2011, p. 5027). The accurate understanding of soil thermal properties such as soil thermal conductivity is important to earth-contact heat transfer simulations (Rees, Zhou and Thomas, 2007, p. 1485), and these properties depend on factors such as location, depth, density and moisture content (Labs, 1980, p. 127). The impact of the thermal conductivity of the soil is pointed out by Geiger (1950, p. 35)

as the key factor in the ability of the ground to act as reservoir of heat; the higher the thermal conductivity of the soil, the higher the potential of the ground as a heat store. As an example, poorly conductive soil leads to extreme microclimate conditions near the ground with cold nights and hot days, in contrast to soils with high conductivity, which generate more stable microclimates near the ground. However, in defining a design strategy based on time lag or seasonal lag in Australia, Braggs (1982, p. 130) states that soils with low thermal conductivity should be selected to delay the effects of extreme air temperatures on the ground. According to Adjali, Davies and Littler (1998, p. 358) the influence of soil conductivity on ground temperature is greater during the winter.

The organic matter content, colour, and moisture content of the soil affects ground temperature (Chang, op.cit., p. 145). The soil colour affects its absorptivity and therefore influences ground temperature (Chang, ibid., p. 146) since the soil surface temperature is higher when ground absorptivity increases (Mihalakakou et al., 1997, p. 189), and during the summer the influence of soil colour is greatest (Adjali, Davies and Littler, op.cit., p. 358). Regarding the water content of the soil due to changes in weather, variable moister content is, according to Geiger (op.cit., p. 33), the main factor that affects ground temperatures.

2.2.2.2. Location Characteristics

Different characteristics such as latitude, altitude, and slope steepness and orientation are relevant to determine ground temperature values (Chang, op.cit., p. 153). The topographical characteristics (Geiger, op.cit., p. 215; Chang, ibid., pp. 153-167; Labs, op.cit., p. 128; Lewis and Wang, 1992, p. 99; Dimoudi, 1996a, pp. 84-89; Šafanda, 1999, p. 374; Wang, 2009; Ruiz-Arias et al., 2011, p. 1812; Manners, Vosper and Roberts, 2012), ground coverage (Chang, op.cit., p. 166-167; Labs, op.cit., p. 128; Lewis and Wang, op.cit, p. 93; Argiriou, 1996, p. 383; Šafanda,

op.cit., p. 374) or surrounding elements such as, for example, nearby buildings (Kusada and Archenbach, 1965, p. 1), regulate the solar radiation received by the soil (Chang, op.cit., pp. 166-167).

The ground temperature below, or around in the case of ground-integrated structures, a building are affected by the building. Not just because of the area it covers and shadows is produces, but also because of the internal temperatures of the building. Therefore, as Boyer and Grondzir (1987, p. 70) point out, thermal calculations relating to buildings should take in consideration the difference between disturbed and undisturbed ground temperatures. During summer the ground will be *charged* with the building's heat since it flows into the ground, and during the winter the lower temperatures inside the building allow the ground to *discharge* the stored heat (ibid., pp. 80-82).

The ground surface temperature changes according with ground coverage; areas with forest coverage can be 1.7°C to 2.2°C cooler than areas with bare ground (Lewis and Wang, op.cit, p. 93). The ground vegetation cover also affects the precipitation values received by the soil and its moisture content (Geiger, op.cit., 269; Liu et al., 2011, p. 1210). Additionally, ground coverage can change the snow coverage duration, reduce wind velocity, change the air temperature and humidity, and the provision of organic matter (Chang, op.cit., pp. 166-167).

2.2.2.3. Climate Conditions

The weather conditions affect the soil temperature (Figure 2.4). The clearest examples of this relationship are the results of extreme meteorological effects, such as storms and hurricanes, found in deep underground quarries (Perrier, Morat and Le Mouel, 2001). In severe climates, the temperature difference between ground and ambient air becomes larger. This can be observed in cold climate areas or in zones with severe winters and prolonged snow coverage, where the average annual

ground temperature is higher (Fitton and Brooks, 1931, p. 8). Snow, as a ground cover, can affect the ground temperature in two different ways, "first as a cover with its peculiar thermal properties, and second as a source of ground moisture after thawing commences" (Chang, op.cit., p. 137).
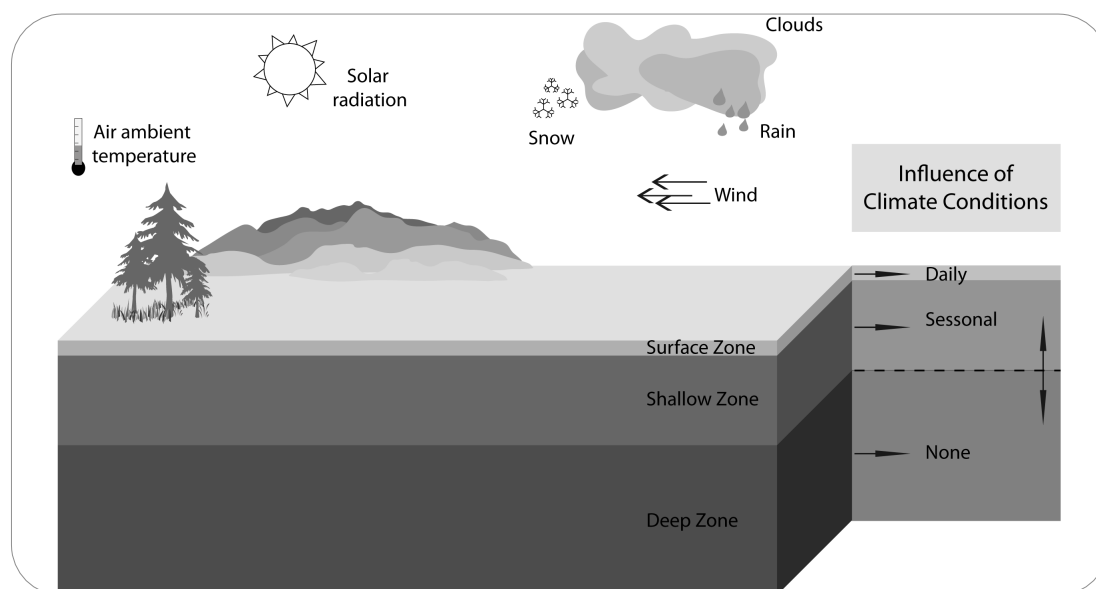
Figure 2.4: Ground temperature distribution - climate influence

Large differences between ground and air temperature can also be found in high altitude areas and in hot dry climates due to higher solar radiation values (Chang, op.cit., p. 59). According to Chang (ibid., p. 129), solar radiation is the principal factor that influences ground temperature. Since solar radiation values can be affected by sky coverage, it should be pointed out that clouds also contribute to ground temperature: during the day by reducing the amount of direct solar radiation received by the ground surface, and during the night by reducing the amount of terrestrial radiation (Chang, ibid., p. 132; Labs, op.cit., p. 128).

One of the most relevant climatic elements, as pointed out by Mihalakakou, Santamouris and Asimakopoulos (1998, p. 19,509), ambient air temperature strongly affects ground surface temperature values (Chang, op.cit., p. 138; Tsilingiridis and Papakostas, 2014, p. 1015) at depths between 0 m to 0.6 m (Liu et al., op.cit., p. 1208). According to Siegenthaler (see Geiger, op.cit., p. 27), the

correlation between air temperature and ground temperature at 10 cm depth is 0.87, which shows how great an impact air temperature has on ground temperature in the area immediately below the surface. As indicated by Rees, Zhou and Thomas (op.cit., p. 1483), near the surface the temperature amplitude is greater because it is more affected by external boundary conditions, while at greater depths the ground is less affected by seasonal temperature amplitude due to being less dramatically influenced by these outside factors.

The amounts of precipitation and irrigation within the soil interfere with ground temperature, since both these factors increase the conductivity and heat capacity of the ground (Givoni and Earth, 1985, pp. 17-18). Soils with higher water content produce lower and more uniform ground temperatures (Fitton and Brooks, op.cit., p. 8). Concerning cooling, rain has the capacity to reduce ground temperature due to evaporative cooling (Labs, ibid, p. 128).

The humidity of the air influences ground temperature due to latent heat; when relative air humidity increases the surface temperature also increases (Mihalakakou et al., op.cit., p. 189). El-Din's (1999) study found that the ground temperature and heat transfer range was affected by relative air humidity, ground absorptivity, evaporation fraction and wind speed. There was an increase in ground temperature and heat transfer range when relative air humidity and ground absorptivity were higher. The ground temperature and heat transfer range decreases as evaporation fraction and wind speed increases (ibid., pp. 487-488).

Lastly, wind is also a climatic parameter to be considered. The wind velocity affects the soil surface temperature: the higher the wind velocity, the lower the surface temperature. This is due to heat transfer by both convection and latent heat transfer through evaporation (Mihalakakou et al., op.cit., p. 189).

2.3. GROUND HEAT TRANSFER AND TEMPERATURE SIMULATION MODELS

Models to calculate ground heat transfer and ground temperatures are crucial to determining the thermal environment of underground constructions and the potential of indirect ground contact systems. During the last four decades several methods or approaches have been used to developed models that simulate ground heat transfer or calculate ground temperatures. The following table provides a list of these models and the approaches upon which they draw.

Table 2.2: Developed models to predict heat transfer and ground temperatures

Modelling approaches:	Based on:

• Analytical model
• Semi-analytical model
• Numerical model
    o One-dimensional model
    o Two-dimensional model
    o Three-dimensional model
    o Response factor elements
• Empirical model (base on experimental data)
• Semi-empirical
• Simplified model
	• Fourier technique
	• Artificial neural network

Kusada and Archenbach (op.cit.) use ground temperature data from 63 stations scattered across the United States to correlate the average monthly temperature values, temperature ranges, phase angles and soil thermal diffusivity. Kusada and Archenbach's study applied a numerical model based on simplified heat conduction theory. Labs and Harrington (1982), on the other hand, use a mathematical model based on the heat conduction and environmental theory developed by Carslaw and Jaeger and by Wijk and Vries to study the ground cooling potential in five regions of the United States. Finally, Braggs (op.cit.) proposes a mathematical model to calculate ground temperatures. Braggs' model is based on Labs' mathematical models but was adapted for the southern hemisphere and uses Kusada's methods of statistical analysis.

Jacovides et al. (1996) demonstrate that the surface and underground temperatures of a specific location could be estimated by using the Fourier technique. El-Din (op.cit.) developed two mathematical models to calculate ground temperature at different depths. The first model presumes that soil surface temperature difference can be described as a sine wave, while the second model develops its analysis through the Fourier series. Wang and Bras (1999) propose a one-dimensional heat transfer method to determine the daily patterns of ground heat flow, based on the relationship between soil surface temperature and ground heat flow. Popeil, Wojtkowiak and Biernacka (op.cit.) propose a semi-empirical model base on Braggs' formula, in order to calculate ground temperature distributions, considering complex soil properties and climate boundaries conditions. Mihalakakou (2002) uses a neural network model to calculate the ground surface temperature by analysing different climate data parameters. Through his research Badescu (2007) developed a numerical model to estimate ground heat exchange that calculates the temperature of the ground surface at different depths. Badescu's model considers the convective energy between air and soil, the solar radiation absorbed by the ground, and the latent heat flow and long-wave radiation. Liu et al. (op.cit.) propose an alternative, simplified, model to estimate underground temperatures during hot weather conditions based on the correlation between air temperature and surface temperature. Recently, Tsilingiridis and Papakostas (op.cit.) developed a set of analytical equations based on the relationship between ground and air temperatures in order to calculate average monthly ground temperatures.

Regarding the difference in the results produced by models approaches, Mihalakakou et al. (op.cit., p. 189) compares a model based on an energy balance equation to a model based on a Fourier analysis of the same data. As a result of this comparison, Mihalakakou found that both models are able to accurately estimate the ground surface temperature as well as the underground temperatures

with a high level of precision. Mihalakakou (op.cit., p. 259) also compares an analytical model and a neural network model that simulate daily and annual patterns of ground surfaces temperatures. In this comparison, Mihalakakou found that, for a warmer period, the predictions of the analytical model are slightly more accurate than those generated by the neural network model. This accuracy gap increases during winter, when the analytical model predictions are significantly more accurate, as it is able to integrate several different weather parameters. Droulia et al. (2009, p. 218) use an analytical and a semi-empirical model to calculate underground temperature patterns. This study found that both approaches' hourly ground temperature results are in accordance with measured data. The study found the same level of agreement for the main annual underground temperature patterns. However, they also found that the semi-empirical model results were more accurate than those of the analytical model.

Several models have been developed to include moister transfer in their prediction of ground temperature. Bharadwaj and Bansal (1981) developed a model to calculate diurnal and annual ground temperature behaviour according to four surface conditions, including dry and wet exposed surfaces and dry and wet shaded surfaces. Thakur (1982) proposes a method that considers soil thermal conductivity as inconstant, since ground water contents change over time. Moukalled and Saleh (2006) propose an unsteady two-dimensional model that applies a finite-volume-based numerical method to simulate heat and moister patterns in soils. This model considers soil physical properties such as moister retention, hydraulic conductivity, thermal conductivity and specific heat. Herb et al. (2008) propose a soil temperature model for dry and wet surfaces. Through the input of climate data this model calculates the heat flux as radiative, convective, conductive and evaporative, taking place on dry or wet surfaces. As a result of this multifaceted analysis the model offered by Herb et al is able to calculate the ground temperatures for rainfall events.

2.4. CASE STUDIES OF GROUND THERMAL POTENTIAL

Fitton and Books (op.cit.) compiled the data of 32 agricultural experimental stations in order to analyse the soil temperature in the United States. As a result, the authors were able to provide a large number of conclusions and verify the results of several previous studies. Some of the reported findings were that air and soil temperature at a shallow depth display a parallel pattern, a daily temperature pattern can be observed up to depths of 0.9 m, and that at depths of 3 m season effects are still visible in ground temperature (ibid., p. 7). However, the time lag between air and ground temperature increases with depth. Regarding soil coverage, it was confirmed that any coverage can reduce the diurnal and annual ground temperature amplitudes (ibid., p. 8).
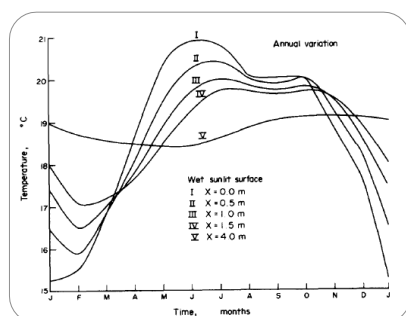
Figure 2.5: Wet sun exposed surface - ground temperature. Bharadwaj and Bansal, 1981
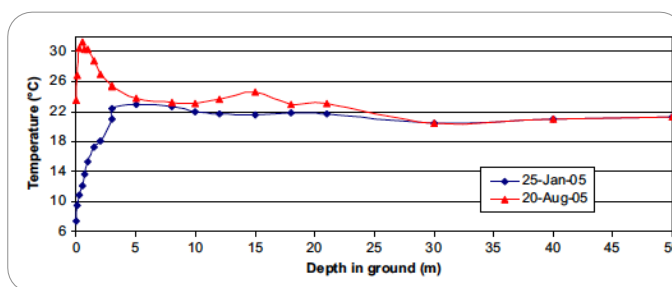
Figure 2.6: Ground winter and summer temperature. Florides and Kalogirou, 2007

Kusada and Archenbach's (op.cit., p. 39) study shows that the average ground temperature is constant according to depth, and that the temperature values are near the same as the annual average air temperature of the location. Labs and Harrington's (op.cit., p.10) report that using the ground as a cooling device produces good results in most areas, except in warm and humid regions. The best cooling results are found in temperate regions with cold winters. Bharadwaj and Bansal's (op.cit., pp. 184-185) study found that diurnal underground temperature in Delhi become stable at a depth of 0.15 m, and that the reported annual variations are constant at a depth of 4 m. The authors conclude that wet shaded or wet solar

exposed surfaces provide the best ground temperatures for heating during winter and for cooling during summer (Figure 2.5). For different locations in India, Ghosal et al.'s study (2004, p. 61) found that the daily amplitude of ground temperatures becomes stable at a depth of 0.3 m and the annual amplitude stabilised at a depth of 4 m.
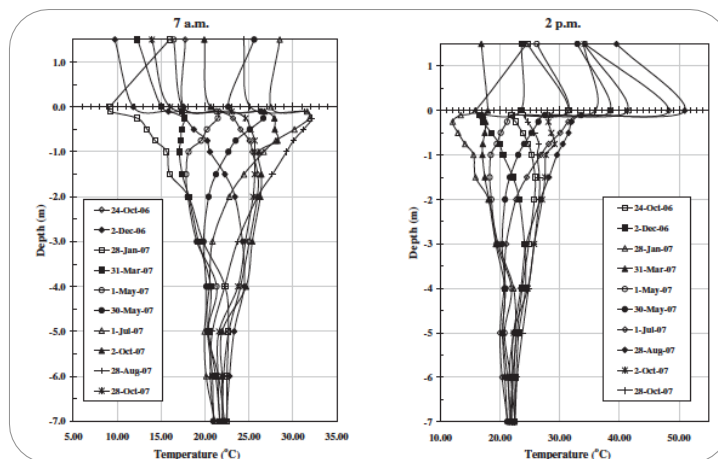
Figure 2.7: Ground temperature at Ariel. Pouloupatis, Florides and Tassou, 2011

In Cyprus, Florides and Kalogirou (2007, p. 2462) observed that the summer and winter ground temperatures in Nicosia were nearly constant for depths below 5 m (Figure 2.6). This proves that the ground could be used for heating and cooling buildings. Pouloupatis, Florides and Tassou (2011, p. 814) measured the ground temperature distribution at three locations in Cyprus. The authors found that the surface zone in these locations can extend to a depth of 0.5 m, and that the shallow zone could extend to a depth of 7 m (Figure 2.7). In a location with a mean annual air temperature of 19.5°C, the almost constant temperature at a depth of 7 m was 22.6°C. The time lag found for soil 1 m below the surface was two weeks, for a depth of 3 m the lag was two and a half months, and for 5 m the lag was three and a half months. Similar results were reported in Florides et al.'s (op.cit., p. 5036) study, which measured the ground temperature of eight locations in Cyprus. In this study Forides et al found that the starting point of the deep zone was at a depth of between 7 and 8 m below the surface, and the constant temperature of this deep zone varied from 18ºC to 23ºC, according to the locations.
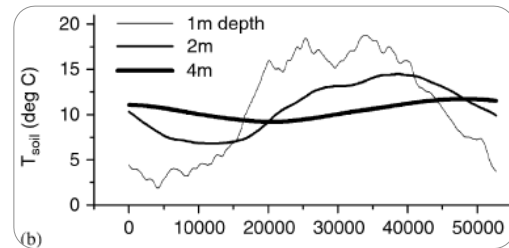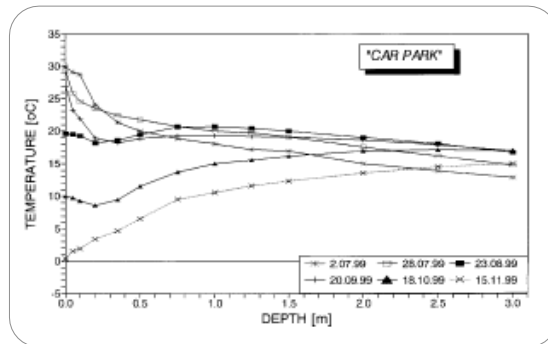
Figure 2.8: (Left) Ground temperature below a car park. Popeil, Wojkowiak and Biernacka, 2001

Figure 2.9: (Above) Ground temperatures. Badescu, 2007

Popeil, Wojtkowiak and Biernacka (op.cit., pp. 306-307) investigated the behaviour of ground temperatures in Poznan (Poland) below a car park surface and below a short-grass covered surface. The surface zone at both locations was extended to a 1 m depth and the boundary between the shallow and deep zone was found at a depth of 10 m. During the summer, and at a depth of 1 m, the ground temperature below the short-grass surface was 4°C lower than below the car park (Figure 2.8). Nassar et al. (2006, pp. 596-597) studied the underground soil temperatures of Tripoli (Libya) by measuring the ground temperatures at a 4 m depth of a dry soil surface and a glass covered soil surface. For both surfaces the temperatures were found to be nearly constant throughout the year.
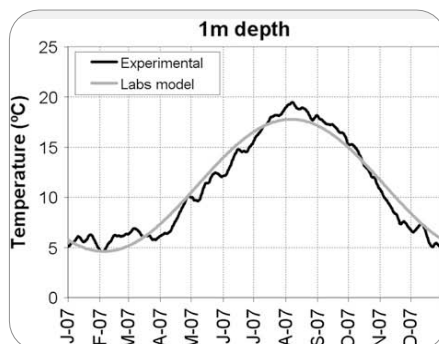
Figure 2.10: Ground temp. at 1m, Mazarron and Cañas, 2009
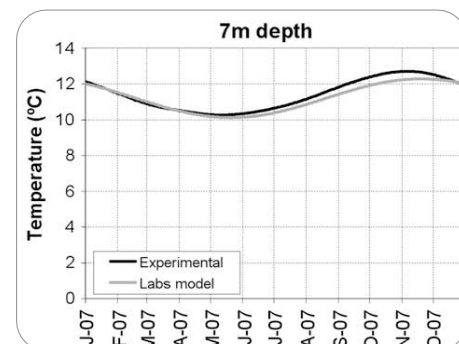
Figure 2.11: Ground temp. at 7m, Mazarron and Cañas, 2009

Badescu (op.cit., p. 851) reports that at Chemnitz in Romania, the ground temperature at a depth of 4 m is almost constant throughout the year with amplitude of only 4°C (Figure 2.9). At a depth of 2 m the ground annual temperature range is 7°C and for 1 m the temperature range increases to around 20°C. Wu, Wang and

Zhu's (2007, p. 1469) study shows that in Guangzhou, Southern China, the average monthly ground temperatures range is lower at greater depths. Mazarron and Cañas' (2009, p. 2489) study demonstrates that at Ribeira del Duero (Spain), the ground temperature at a depth of 7 m is almost constant. From depths of 1 to 3 m, the annual temperature ranges are reduced by nearly one half (Figure 2.10 and 2.11).
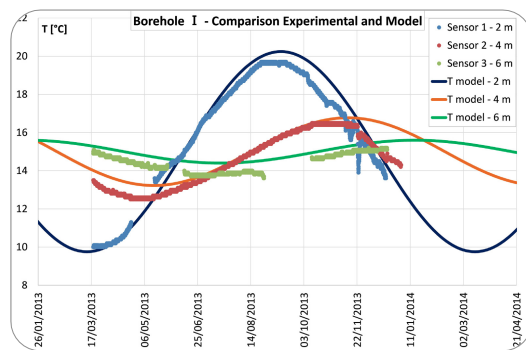
Figure 2.12: Ground temp. borehole I, Tinti et al., 2014
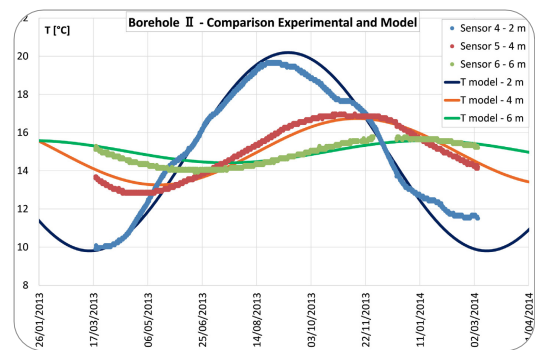
Figure 2.13: Ground temp. borehole II, Tinti et al., 2014

Recently, in Italy, Tinti et al. (2014, pp. 458-459) compared the experimental data retrieved from two boreholes with sensors at depth of 2, 4 and 6 m with the values obtained with a mathematical model (see Equation 5.1). The results proved that at the studied depths, the ground temperatures were not affected by the daily weather conditions. As illustrated in Figure 2.12 and 2.13, the mathematical model produced values similar to those obtained with both sets of boreholes sensors.

2.5. GROUND THERMAL BY INDIRECT CONTACT

A building can benefit from the ground thermal potential through indirect ground contact. As part of a heating and/or cooling strategy, indirect earth contact can be provide with an EAHEs, the air temperature is made temperate by passing through an underground channel, before being introduced into the building. The inlet and outlet air temperature difference changes due to the heat transferred to the soil in the system.

2.5.1. Vernacular Ground Cooling and Heating Systems
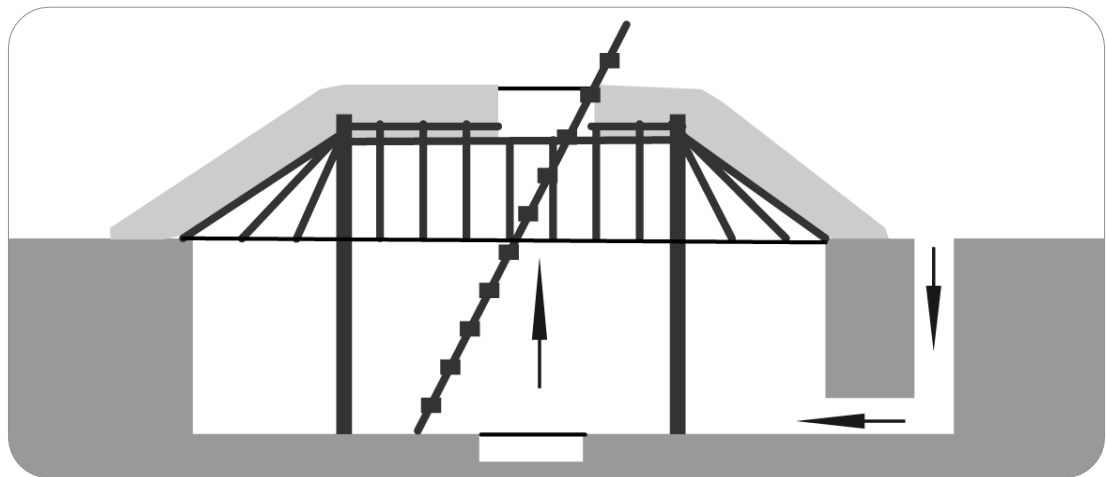
Figure 2.14: *Kiva* - Southwest USA

The use of natural ventilation systems that takes advantage of ground thermal potential can be found in vernacular architecture. These systems are already adapted to be integrated on to below-ground spaces (Labs, op.cit., p. 125) and are more viable for these structures than above-ground ones since their cooling and heating demand is lower (Van Der Meer, 1980, p. 141). Examples of these systems are the *Kiva* from Southwest North American Native architectural traditions, and the *Badgir*, the *Baud-Geers* and Naghb as well as the *Shavadoon* from Persia.

The *Kiva* (Figure 2.14) is an underground dwelling that uses a ventilation system similar to a wind tower system (Labs, op.cit., p. 125) to improve its thermal comfort. The Persian *Badgir* (Figure 2.15) is a wind tower design of an uncertain origin. As

pointed out in Stead (1980, p. 39), one of its possible original uses was to serve as an air duct, a thesis based on archaeological evidence found in Nabupdlassar's summer palace in Babylon.
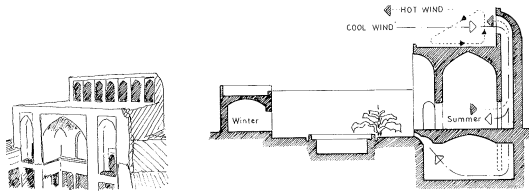
Figure 2.15: Persian house with *Badgir* and basement. Stead, 1980
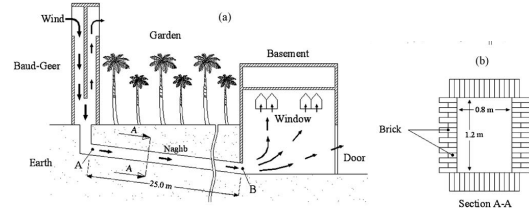
Figure 2.16: *Baud-Geer* and *Naghb*; *Naghb* cross-section. Jafarian et al., 2010
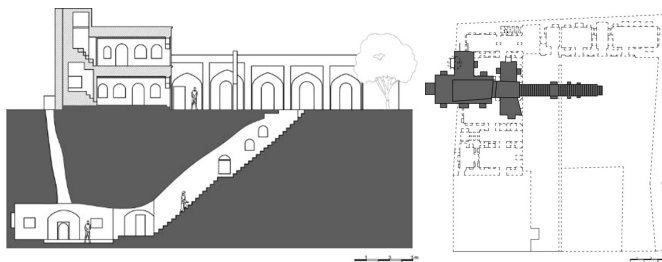
Figure 2.17: Persian house with *Shavadoon* – section and plan. Hazbei et al., 2015
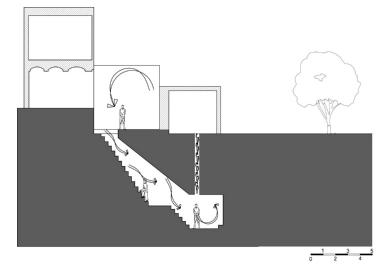
Figure 2.18: *Shavadoon* – Natural ventilation. Hazbei et al., 2015

The *Baud-Geers* and *Naghb* (Figure 2.16) comprise a vernacular cooling system. The first works as a wind-catcher and the second is the underground tunnel that connects the air into a building space (Jafarian et al., 2010, p. 559). A *Shavadoon* (Figure 2.17 and 2.18) is an underground space formed by rooms dug on the ground. These spaces can be found in depths of 5 to 12 m and have a small channel that provides temperate air to the upper building (Hazbei et al., 2015, p. 16).
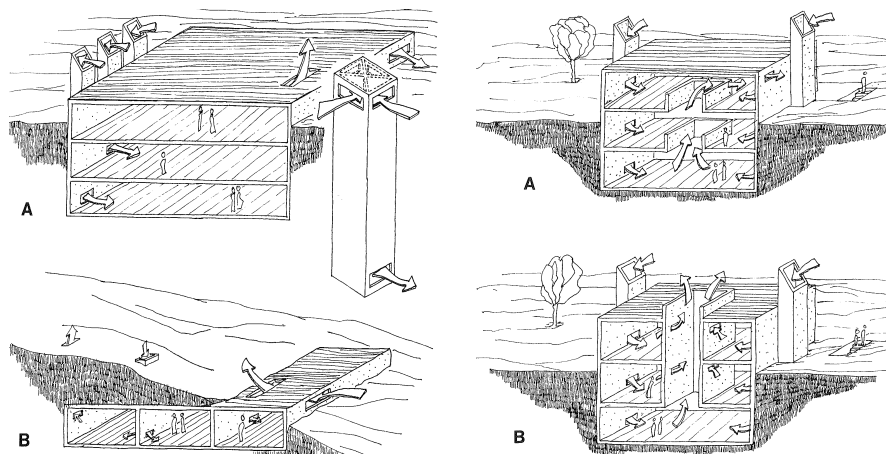
Figure 2.19: Ventilation systems on underground structures. Golany, 1980

Based on these passive ventilation concepts, Golany (1980, p. 112) proposes their application to underground spaces, as illustrated in Figure 2.19. For Golany, the use of passive ventilation systems integrated into subterranean constructions has the economic advantage of providing energy savings. This system can be used to control the temperature of the outside air supply that contributes to better thermal comfort and, therefore, provides additional economic advantages.

2.5.2. Ground Cooling and Heating Through Induce Ventilation: EAHEs
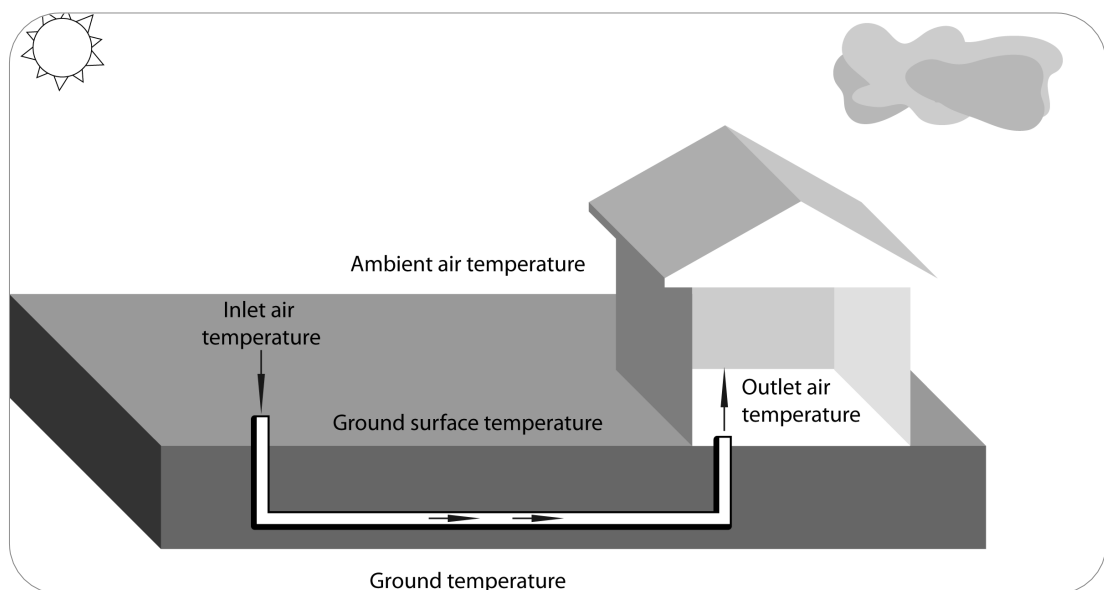
Figure 2.20: EAHE System - indirect ground contact strategy

The EAHE systems take advantage of ground thermal potential to reduce buildings' heating and cooling loads and therefore improve their thermal comfort. Generally, these systems consist of underground channels or pipes, which use air as a carrier fluid for cooling (Banks, op.cit., p. 199). The system illustrated in Figure 2.20 works by conducting outside air into a building space, with the initial air temperature being modified by passing through the buried channels or pipes (Bansal and Sodha, 1986, p. 177; Bansal, Hauser and Minke, 1994, p. 157; Al-Ajmi, Loveday and Hanby, 2006, p. 236; Kwok and Grondzik, 2011, p. 193). The change in air temperature is due to convection transfer between the air and the inner surface of the pipe, and by the conduction between the outer surface of the pipe and heat transfer from the soil

(Al-Ajmi, Loveday and Hanby, op.cit., p. 237). The temperature difference between the outside air and ground temperature where the system is placed determines the cooling and heating potential of the system (Kwok and Grondzik, op.cit., p. 193).

Open loop   Closed-loop
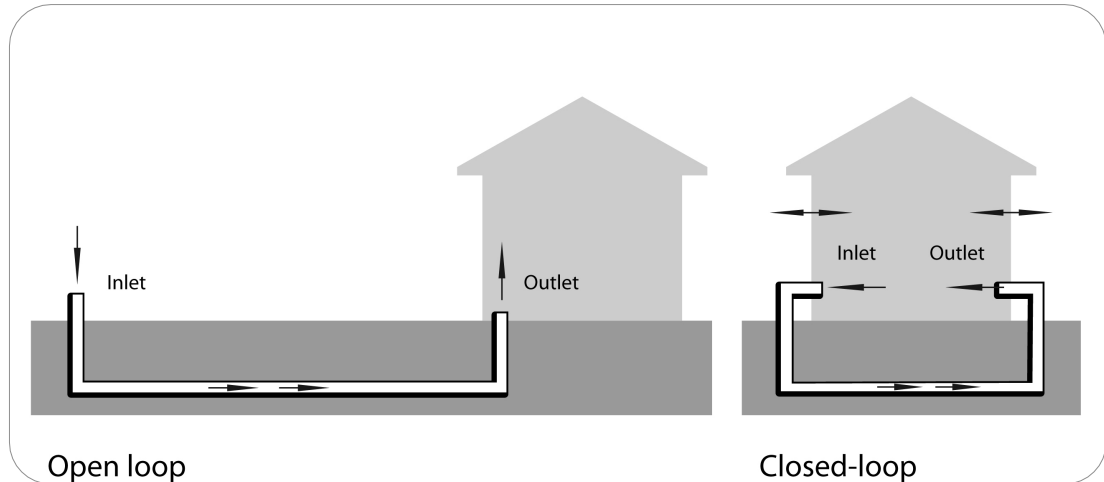
Figure 2.21: EAHE system configuration - open and closed-loop

The EAHE system can be configured as either an open loop or a closed-loop, as shown in Figure 2.21. In an open loop system, the outside air is brought into a building space through an underground pipe (Argiriou, op.cit., p. 367; Kwok and Grondzik, op.cit., p. 193; Ozgener, 2011, pp. 4484-4485). In the closed loop configuration, the inlet and outlet air are both inside the building. Because the cross ventilation in both systems is induced by a fan, EAHE system is a hybrid system since it is not entirely passive.

2.5.3. Advantages and Disadvantage of EAHE Systems

Bansal and Sodha (op.cit., p. 177) make reference to a shift from earth-air tunnel structures to buried tubes. This shift can be linked to the design requirements of these tunnels, as well as their construction and maintenance costs, as well as efficiency problems due to water infiltration, caused by local geological and climate conditions or by negligent maintenance. The EHAE pipe systems are able to minimise some of these problems when compared to tunnels. Its main advantages are lower maintenance (Bansal and Sodha, ibid., p. 182; Shukla, Tiwari and Sodha,

2006, p. 366) and lower energy requirements to operate (Pfafferott, 2003, p. 971; Shukla, Tiwari and Sodha, ibid., p. 365).

Other advantages of the system include its low cost (Argiriou, op.cit., p. 391; Shukla, Tiwari and Sodha, ibid., p. 365), being simple to operate and maintain and not needing skilled labour (Shukla, Tiwari and Sodha, ibid., p. 365), as well as its own simplicity, high thermal performance, and the reduction it causes in the heating and cooling energy demands of a building. These are factors toned to be considered because of the resulting reductions in annual fossil fuel usage (Pfafferott, op.cit., p. 971). Furthermore, the system's equipment is not affected by the severe cold since it is frost-free (Trzaski and Zawada, 2011, p. 1436). However, there are also disadvantages in the use of EAHE Systems, such as water accumulation inside the tubes caused by condensation (Argiriou, op.cit., p. 388), which can cause the growth and development fungi and bacteria within the system (Kwok and Grondzik, op.cit., p. 195) that can produce unpleasant odours (Steemers, 1991, p. 11). Furthermore, during operation, the fan required as part of the system can produce noise (Argiriou, ibid., 389). The performance of an EAHE System can also degrade due to continuous heat transfer from the pipes to the surrounding ground (Kwok and Grondzik, ibid., p. 194).

2.5.4. Factors that Affect EAHE Systems Performance

There are multiple factors that affect EAHE system thermal performance. Table 2.3 summarises the most influential factors reported in different researches. These factors are presented as external climate conditions, geological factors surrounding the system that determine soil thermal characteristics, and factors originating from the system itself including its design and operational. The focus of this section is on case studies examining the external and system-surrounding aspects that determine

performance because both factors also affects the thermal performance of ground-integrated architecture.

Table 2.3: Factors that affect EAHE systems performance reported in different researches

Category	Factor	Sodha et al., 1985	Bansal and Socha, 1986	Trombe, Petit and Bourret, 1991	Krarti and Kreider, 1996	Mihalakakou, Lewis and Santamouris, 1996	Mihalakakou, Lewis and Santamouris, 1996a	Bojic, Papadakis and Kyritsis, 1999	Kumar, Ramesh and Kaushika, 2003	Pfafferott, 2003	Shukla, Tiwari and Socha, 2006	Costa, 2006	Kumar, Kaushik and Garg, 2006	Al-Ajmi, Loveday and Hanby, 2006	Wu, Wang and Zhu, 2007	Badescu, 2007	Lee and Strand, 2008	Bansal et al., 2009	Yoon, Tanaka and Okumiya, 2009	Jafarian et al., 2010	Abbaspour-Fard, Gholami and Khojastehpour, 2011	Ozgener, 2011	Trzaski and Zawada, 2011	Darkwa et al., 2011	Ascione, Bellia and Minichiello, 2011
External fact. — Climate	General					x														x				x	x
	Relative humidity	x	x	x																					
	Air temp.	x		x									x							x	x				
System surrounding factors — Soil thermal properties	General	x															x			x		x	x	x	
	Thermal conduct.					x																x			
	Colour									x															
	Reflectivity												x												
	Moisture content	x	x	x						x			x							x				x	
	Temp.	x	x	x				x					R				x			x		x			
	Nearby elements																					x			
	Ground coverage					x					x											x			
System factors — Design (pipe)	Length	x	x	x		x	x		x	x	x	x		x	x	x	x		x	x		R			x
	Depth	x	x	x		x	x				x			x	x	x			x	x		x			x
	Diameter (surf. area)	x	x	x	x	x	x		x	x		x		x	x	x	x		x	x		x			x
	Material	x	x				x						x		N		N	x	x		N				
	Quantity				x						x					x			x						
	Layout (spacing)				x	x	x									x									
System factors — Operational	Air flow	x	x	R	x	x	x	x	x		x	x		x	x		x	x		x	x		x		x

X - relevant element
R - most relevant element
N - element with no contribution

Trombe, Pettit and Bourret (1991) found that EAHE are affected by external factors such as air temperature and relative humidity, system surrounding factors such as soil temperature and water content, and by system factors. Kumar, Kaushik and Garg (2006, p. 1154) investigate the effect of humidity, ambient temperature, and

-33-

ground temperature both at the surface and at pipes installation depth on an EAHE system's thermal performance. In their study Kumar, Kaushik and Garg found that the supply air temperature is highly dependent upon the ambient temperature and the ground temperature at the installation depth of the system's pipes, which these authors discuss as the most relevant factor.

Mihalakakou, Lewis and Santamouris (1996a, p. 45) analyse the effect of bare soil and short-grass soil coverage on single and multi-pipe EAHE systems performance in Dublin (Ireland). The authors found that during winter bare soil could increase the system's heating performance compared to short-grass covered soil. Regarding the performance of EAHE systems in New Delhi, Shukla, Tiwari and Sodha (op.cit., pp. 374-376) found that is the performance of these systems is affected by the surface conditions as blackened, blackened and glazed, and wetted surfaces produced different performance profiles. During winter, a darker surface can increase the system heating potential, while during the summer, soil with higher moisture content provides the coolest supply air.
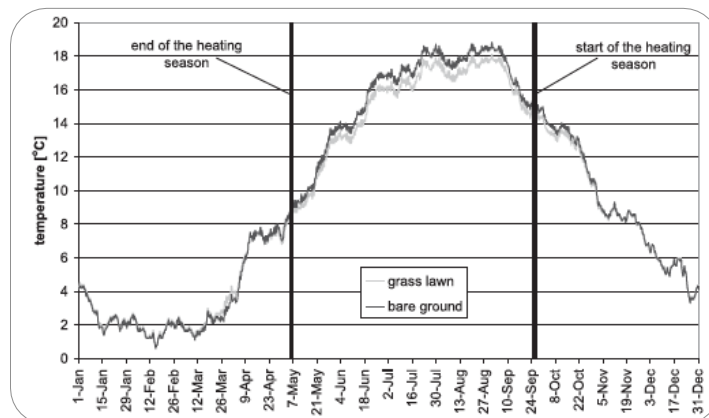
Figure 2.22: Ground temperatures around the end of an EAHE. Trzaski and Zawada, 2011

For climate conditions in Poland, Trzaski and Zawada (op.cit., p. 1442) found that, during summer, the grass-covered soil increased the cooling potential of the system by providing a 1 K lower temperature than the bare soil (Figure 2.22). The winter results from this study show that the temperature difference between the different

kinds of soil coverage is negligible. The authors did, however, state that objects located near an EAHE system could affect its performance.

Concerning ground thermal properties and climate, a study conducted by Ascione, Bellia and Minichiello (2011, p. 2187) shows how an EAHE system performance integrated into an air-conditioned building is affected by the boundary conditions at different climates. The authors found that the system has higher potential with wet and heavy soils and in the colder Italian climate, potentiating thermal energy savings that could go up to 44%. Trzaski and Zawada (op.cit., p. 1442) found that low thermal diffusion coefficient soils had a high cooling performance, but a low heating performance. The authors also found that the opposite was true for soils with a high diffusion coefficient.

2.5.5. EAHE Thermal Performance – Case Studies
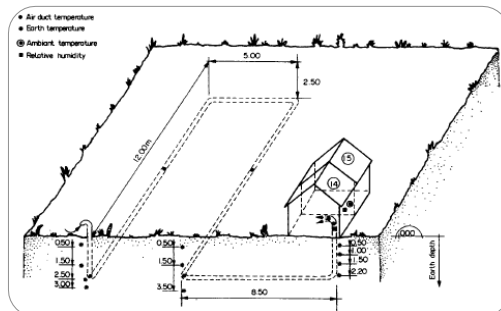
Figure 2.23: EAHE system; experimental set-up. Trombe, Pettit and Bourret, 1991
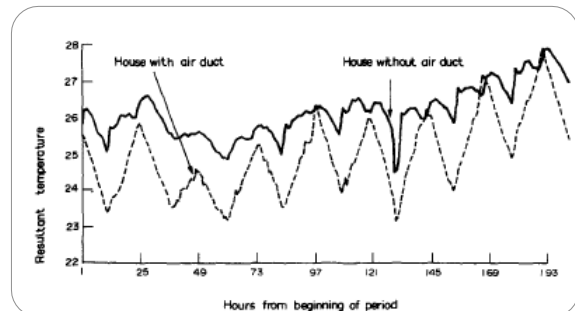
Figure 2.24: Comparison - House with and without EAHE. Trombe, Pettit and Bourret, 1991

Regarding the thermal potential, Trombe, Pettit and Bourret (op.cit.) studied the cooling performance of an EAHE system located in France during the summer (Figure 2.23). The authors assessed the system by measuring temperature data and comparing two similar buildings, one with and another without an EAHE system. The authors found that the air temperature inside the tube decreases in temperature. It had an accentuated decrease in temperature in the initial length of the tube and a more steady decrease in temperature across the rest of the length of the tube. The air relative humidity at the outlet was higher than that at the inlet. The average

difference between the temperatures inside the two buildings was 1.5ºC (Figure 2.24). The authors concluded that the system had a sufficient thermal potential to provide air conditioning for these buildings (ibid., p. 707).

Several studies have reported the cooling and heating potential of EAHE systems. Bojic et al.'s (1997, p. 1151) study establishes that the use of EAHE systems in Greece can reduce the daily heating and cooling energy demands of buildings. The cooling performance of these systems was better than their heating performance, and therefore the energy and cost efficiency saving of these systems was higher during summer than during winter.

Hollmuller and Lachal's (2001, p. 517) investigation states that the use of EAHE systems to preheat the outside cold air during the winter induces energy savings, since it reduces the heating energy demand within the building itself. For the study time set, the use of EAHE systems for air preheating was not sufficient by itself and was more expensive than conventional fuel heating systems. During the summer the cooling provided by these systems could be sufficient by itself when used as a ventilation system. So the systems could substitute for conventional air-conditioner systems, and therefore they were able to reduce energy costs.

Pfafferott's (op.cit., p. 971) study on EAHE systems performance in European office buildings reports that, during winter, these systems can contribute to reducing the heating demands of such buildings by pre-heating the incoming air. During summer, the EAHE systems integrated with building thermal design are sufficient to avoid the use of active air conditioning units. Therefore, Pfafferott considers the system as a passive cooling alternative in moderate climates.

Tittelein, Achard and Wurtz (2009, p. 1691) found that, for the temperate climate in France, the EAHE system could be used as a cooling system for a low-consumption

building during the summer. During winter, however, the system was not recommended as a heating system, since it usage was not justified.
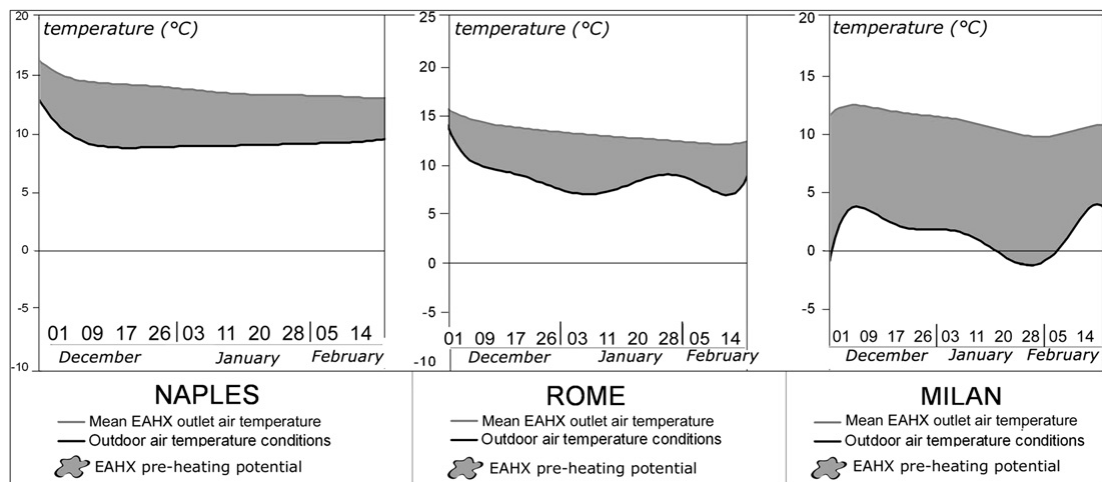
Figure 2.25: EAHE pre-heating potential. Ascione, Bellia and Minichiello, 2011

Ascione, Bellia and Minichiello (op.cit.) evaluated the summer and winter energy performance of EAHE in different Italian climates (Milan, Rome and Naples). During summer, the best energy efficient ratios were registered in Milan (Figure 2.25). Since Milan has the coldest winters of these three Italian climates, during the summer the subsoil temperatures were also lower than the other cities (ibid., p. 2183). For winter conditions, Milan also registered the highest potential, as the air temperature increases are around 10ºC, compared with the temperature increases of around 4ºC obtained in other cities. Thus, the use of EAHE for heating was only convenient for cold Italian climates (ibid., pp. 2183-2184). This study found that thermal comfort is only achieved in Milan, not in the other cities included in the study. For the other climates covered by this study, the use of these passive techniques could improve the thermal comfort, but were only effective with the help of an active cooling system (ibid., p. 2187).

2.6. CONCLUSIONS

As discussed throughout this chapter the temperature of the ground changes according to depth. As also stated, to a certain depth the ground temperature values vary due to the soil's capacity to collect and retain solar energy. This is more clearly the case for the surface and shallow zones, as the ground temperature distribution at both zones closely follows the climate conditions. While the ground temperatures at the surface zone have a diurnal pattern, the shallow zone has a seasonal pattern of temperatures and the time lag can be up to several months. Within the deep zone, the ground temperature is constant all year round and close to the mean annual air temperature of the location, and the ground energy source is geothermal.

The use of ground thermal energy as an energy source to heat and cool buildings can be provided by direct or indirect contact, both of which produce conductive heat gains or losses according with the season. For both strategies, there is a high level of contact with the ground. Most parts of the building structure and most parts of the EAHE pipes are in direct contact with the surrounding soil. For this reason, to determine the ground heating and cooling potential of either strategy it is important to understand the thermal potential of the soil. This is done by determining ground surface temperature and ground temperature at different depths.

For both cases, the main difficulty resides in the multiple factors that contribute to this heat transfer, mutual interference that can disturb ground temperatures, time inconstancies in soil properties or external factors due to various changes. In this chapter it is pointed out that climate conditions such as air temperature and solar radiation are some of the main factors that influence the ground temperature. Furthermore, these external factors depend on location characteristics such as topography, which is described in Chapter 4 and investigated in detail in Chapter 5.

CHAPTER 3. GROUND THERMAL BY DIRECT CONTACT

3. GROUND THERMAL BY DIRECT CONTACT

"We learn that many audacious "primitive" solutions anticipate our cumbersome technology; that many a feature invented in recent years is old hat in vernacular architecture - prefabrication, standardization of building components, flexible and movable structures, and, more specially, floor-heating, air-conditioning, light control, even elevators. (…) we may find that long before modern architects envisioned subterranean towns under the optimistic assumption that they may protect us from the dangers of future warfare, such towns existed, and still exist, on more than one continent." (Rudofsky, 1964, p. NA)

3.1. INTRODUCTION TO GROUND-INTEGRATED ARCHITECTURE

The use of ground thermal potential as applied to the heating and cooling of a building is based on the temperature difference between the ambient air temperature and the ground temperature at a specific depth. Through direct contact with the ground, a large part of the structure of a building is able to take direct advantage of the thermal potential of the ground. To allow for this interaction or coupling between the ground and the structure of the building insulation should be avoided (Givoni, 1994, p. 210). The use of insulation can reduce energy savings because the building structure is decoupled from the surrounding ground (Boyer and Grondzik, 1987, pp. 102-103). However the use of insulation must be considered if thermal resistance is needed in order to minimize heat losses (Givoni, op.cit., p. 210).

Far from being a new way to control building thermal comfort, ground-integrated building concepts can be traced back to ancient times. Subterranean structures such as caves have been used for habitation since the Palaeolithic Era and provided the first shelter for humans. Reasons for using these structures include: protection from severe climate (Golany, 1980, p. 109; Balaras, 1996, p. 2; Jannadi and Ghazi, 1998, p. 102; Al-Mumin, 2001, p. 103; Çorakbas, 2012, p. 1451), preservation of land for agriculture (Golany, op.cit., p. 109), and defensive strategies and ceremonial needs (Golany, ibid., p. 109; Jannadi and Ghazi, op.cit., p. 102). Shelter from local predators, local topographical issues, geological characteristics and lack of construction materials (Erdem, 2008, p. 493; Stasinopoulos, 2014, p. 26) such as timber (Çorakbas, op. cit., p. 1451) also contributed to the use of these structures in ancient times.
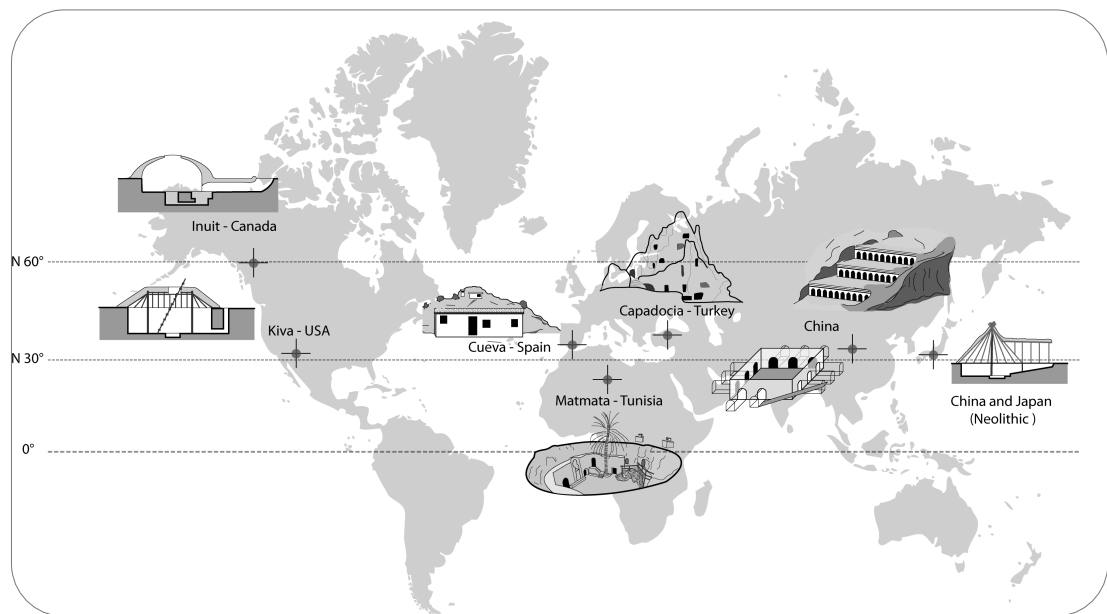
Figure 3.1: World distribution of ground-integrated buildings

The users of these ground-integrated structures noticed that these shelters are able to provide more stable and comfortable conditions when compared to outside ones (Golany, op.cit., p. 109). The use of these habitable spaces provides us with knowledge of the earth's potential as a thermal provider for living and working, and for food storage and security (Golany, 1995, p. 183).

Examples of ground-integrated settlements can be found in many different locations, including the Mediterranean areas of the Göreme Valley of Cappadocia (Turkey), Matmata (Tunisia), Matera and Sicilia (Italy), Santorini (Greece), Andalucia (Spain), Tripolitania (Libya), and in the African area of Seripe (Ghana). Similar ground-integrated settlements can be found in Iran, in the Middle East, in India, in the southwest of the USA, in central and South Australia, and in Asia, particularly in the Chinese Provinces of Henan, Shanxi and Gansu (see Figure 3.1).
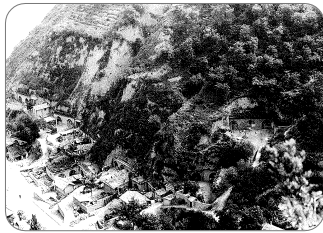
Figure 3.2: Slope-integrated buildings, China. Golany, 1995

Figure 3.3: Ground-integrated buildings, Matmata, Tunisia. Golany, 1995
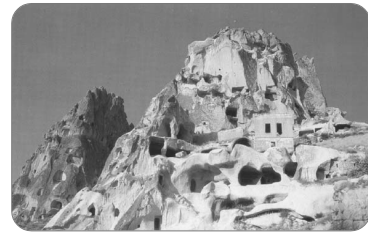
Figure 3.4: Slope-integrated buildings, Cappadocia, Turkey. Aydan and Ulusay, 2003
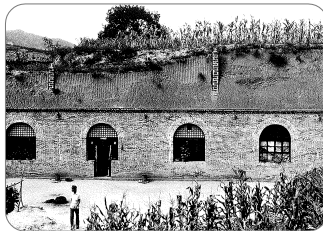
Figure 3.5: Ground-integrated building, Shanxi, China. Golany, 1995
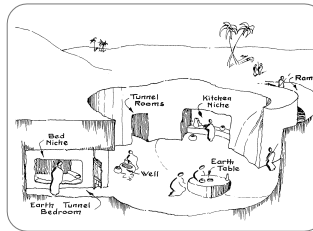
Figure 3.6: Ground-integrated house, Sahara. Callaway, 1980

Figure 3.7: Kaymaklı underground city, Cappadocia, Turkey. Aydan and Ulusay, 2003

The largest below-ground settlements are in China, Tunisia and Turkey. All these areas have in common several factors including severe climate conditions, and the lack of construction resources (Golany, p. 184). China has the world's highest number of below ground residents – approximately ten million people is reported to be currently living underground in China by Tong and Zhang (see Tong and Chen, 2011, p. 5662). Chinese ground-integrated structures (Figure 3.2 and 3.5) have been used for more than four thousand years and can be found in both rural and urban settlements (Stead, 1980, p. 41; Golany, 1995, p. 184). The three main structure types identified in these studies of Chinese underground architecture are

the cliff, pit, and vaulted earth-sheltered dwellings, which are dependent on site selection (Golany, 1992, p. 66).

Matmata (Figure 3.3 and 3.6), in Southern Tunisia, is the second area with the largest amount of belowground settlements. It is composed of approximately twenty settlements (Golany, 1995, p. 184). Its ground-integrated structures are based on a circle generated around a courtyard (Al-Mumin, op.cit., p. 103).

In Cappadocia (Figure 3.4 and 3.7), located in Anatolia (central Turkey), ground-integrated settlements can be traced back to 400 B.C (Erdem, op.cit., p. 493). There are three main settlement types; the cliff or semi-underground, the underground and the modern rock structures, and the locations of these settlements are dependent on the characteristics of the local landscape (Aydan and Ulusay, 2003, pp. 252-253).

3.1.1. Recent Reuse and Abandonment of Underground Structures

The reuse of underground construction was initiated in the USA during the 1960's, as a Cold War military strategy. One decade later, these constructions were studied not as a defence concept but because of their potential energy performance levels, particularly due to the energy crisis of the 1970's which was generated by a sudden increase in fuel prices (Brown and Novitski, 1981, p. 299; Labs, 1982, p. 397; Bartz, 1986, p. 71; Boyer and Grondzik, 1987, p. 1; Jannadi and Ghazi, op.cit., p. 103; Rees et al., 2000, p. 217; Staniec and Nowak, 2011, p. 221). Since then, energy related issues, including thermal comfort, are the main reasons for going underground in contemporary architecture. Another reason for going underground is the provision of additional space, sometimes connected with land preservation, land cost, or land restrictions.

However, whilst there is an increase in attention and some degree of acceptance of ground-integrated structure's thermal potential, the future of these buildings is being

undermined in areas where they were once the dominant architectural form. For example, at the Loess Plateau, one of China's poorest regions, the once predominant ground-integrated buildings are being replaced by conventional constructions, despite the fact that the costs of constructing the latter are higher, due to a lack of conventional construction resources including fired bricks and concrete. In this region, the costs of ground-integrated buildings are 20% lower than conventional constructions, due to the availability of local technology and materials (Jun and Yan-yung, 2006, p. NA). Nevertheless, the popularity of this type of construction is rapidly declining, which could lead to the loss of local knowledge and techniques of vernacular construction (Tong, Chen and Li, 2011, p. 1644). Hayashi (1986, p. 169) reports how the future of earth-sheltered architecture in China has been affected by this change in construction during the 1980's. Hayashi identifies a shift in attitudes towards earth-sheltered houses, as underground construction is no longer an attractive industry. According to Hayashi, the rapid economic growth of Chinese farmers has contributed to a rapid change in housing construction. Earth-sheltered architecture, once the main type of housing construction and the main source of employment for the local workforce and resources, has lost its importance in the face of the rise of modern concrete constructions.

Similarly, Golany (1992, p. 43) identified the same shift in attitudes concerning earth-sheltered architecture during the 1990's. Golany argues that improvements in the economic lot of Chinese farmers have led to the need for larger living spaces, in order to accommodate a larger number of household possessions. Golany also argues that these changes also encouraged the desire to live in above-ground homes, which were seen as more desirable. More recently, Liu et al. (2010, p. 124) reported that the internal space of traditional earth-sheltered houses is no longer appropriate for current living requirements among these farmers, since these constructions are perceived as having low aesthetic value. Consequently, the

increase in the number of brick houses being constructed has increased the energy use of farmers' buildings, as well as claiming good farming land (Zhu et al., 2014, p. 159). The previous estimated global number of 35-40 million below ground residents used by researchers during the last three decades (Stead, op.cit., p. 41; Golany, 1992, p. 42, 1995, p. 183; Wang and Liu, 2002, p. 985; Zeng and Song, 2012, p. 3486), has fallen to 10 million in actual terms since 2007 (see Tong and Chen, 2011, p. 5662), a number revealing a 70-75% reduction in below-ground living. Furthermore, and in the Tunisian case, Golany (1995, p. 208) states that the last underground building in Matmata was constructed in 1975, revealing the discontinuation of these kind of constructions locally.

3.2. CONFIGURATIONS, SITES AND CATEGORIES

3.2.1. Types of Building Configurations

In a building, the source of heat gains can be internal or external. Internal heat gains are mainly produced by the building's users and, therefore, are under human control; these internal gains are caused by factors such as lighting, domestic appliances such as those used for cooking, or by the heat produced by the building's habitants themselves. The external gains are due to the relationship between the local climatic characteristics, such as solar radiation and ambient air temperature, and the design of the building. These external gains can be controlled at the design stage (Dimoudi, 1996b, pp. 35-39).

The shape of a building affects the amount of solar radiation and wind exposure it receives (Balaras, 1996, p. 7), and therefore these factors can be used as a design technique in order to control the amount of heat gains and losses, which are determined by the ratio of exposed surface area to building volume. Another way of controlling heat gains and losses is through increasing the surface area of the building that is in direct contact with the ground, since this will reduce the surface area that is exposed to solar radiation, ambient air temperature and wind. Furthermore, ground-integrated buildings have lower air infiltration due to their airtight structure, and will therefore experience fewer heat gains and losses.
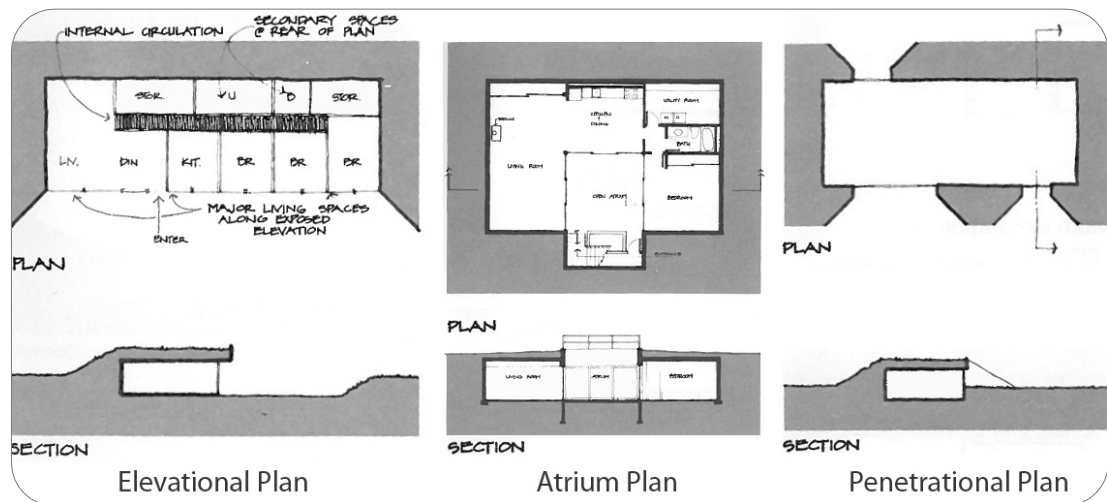
Figure 3.8: Plan concepts – elevational, atrium and penetrational. Underground Space Center, 1979

There is a large range of ground-integrated buildings designs and, usually, their configurations are linked with local climate and site characteristics. Two examples of these configurations are the *elevational* and the *atrium* configurations, as pointed out by Sterling, Carmody and Elnicky (op.cit., p. 104) (Figure 3.8). The elevational house usually has three walls in contact with the ground, leaving the South-facing wall exposed to sun and wind. The roof of elevational houses can either be exposed or covered with soil. The most common shape for this kind of dwelling is a rectangle, with the longest sides facing south and north. This design can be built on a flat site, but sloped sites of to 50% are ideal (ibid., pp. 104-105). Generally, the *atrium* design is a single floor building with a square shape. It can be built on sloped sites of up to 15%, but its construction is easier if erected on a flat site. The main difference between the *elevational* and *atrium* designs is that the atrium design is not dependent on site orientation (ibid., p. 108). The Underground Space Center (1979, p. 42) adds to these two configurations a third, the *penetrational*, a building concept that allows several openings along its perimeter, such as entrance and windows.

3.2.2. Sites and Categories of Ground-integrated Structures

Site	Type			Additional features	
	Total	Semi	Bermed	Courtyard	EAHE systems
Horizontal					
Vertical (Slope)					

Figure 3.9: Ground integration types according with site

Natural, excavated or buried, underground spaces have been used for residential, military, religious, social and educational purposes, as well as for food production or storage, for transportation and for storage of utilities. There are several ways to categorize ground-integrated structures and normally these categories are linked to the type of building site. The site integration is usually divided in horizontal and vertical, the latter referring to slope terrains (Figure 3.9). Stead (op.cit., p. 41), identifies two categories: the ground-integrated structures on flat land, constructed around an underground courtyard, and concerning slope terrains, the slope ground-integrated structures, which are typically composed of several independent rooms carved along a cliff and with a single façade.
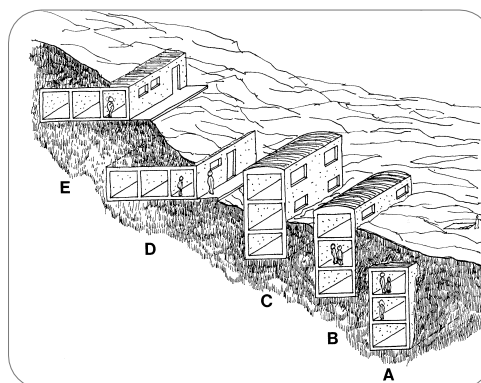
Figure 3.10: Levels of ground-integration. Golany, 1980

Golany (1980, p. 111) defines five levels of ground integration in a model that considers both flat and slope areas. As illustrated in Figure 3.10, there are three

types of ground integrations on flat areas: total subterranean, subterranean and semi-subterranean that is integrated with above ground construction. Regarding the two types of ground integrations on slopes, Golany makes a division between subterranean and semi-subterranean. Contrarily, Van Der Meer (1980, p. 144) considers two main categories of ground integration, based on construction techniques. Van Der Meer refers to these categories as the *'constructed'* and a *'no constructed'* types, with the first requiring all the building elements such as walls, roof, and floor to be constructed, and the second one requiring that the building space be created within the soil. Van Der Meer divides the underground constructed structures into sub-categories, the partially underground, the earth covered, and the totally underground.

Classification	Plan Types		

Figure 3.11: Ground-integrated structures. Boyer, 1980

	Total Underground	Atrium or Courtyard	1 Side Open	2 Side Open	3 Side Open

Figure 3.12: Ground-integrated structures – Building sections, Chamber types. Boyer, 1980

Chamber Types

"True" Underground	Atrium or Courtyard	Hillside Elevational	Side Penetration	"Non-earth" Roof

Figure 3.13: Ground-integrated structures – Building sections, Berm types. Boyer, 1980

Berm Types

"True" Underground	Atrium or Courtyard	Hillside Elevational	Side Penetration	"Non-earth" Roof

Figure 3.14: Ground-integrated structures – Building elevation. Boyer, 1980

Building Elevations

Nonvisible	Roofscape	Mound	Partially Visible	Completely Visible

According to Boyer (1982, p. 202) there are several approaches to applying a ground-integrated structures concept to reality. Boyer's classification of structures is based on the type of building plan, type of cross-section and type of elevation (Figure 3.11 to 3.14). Jannadi and Ghazi (op.cit., p. 103) organise ground-integrated

constructions according to building location and surface. The four structure types they offer are *chamber* (a totally underground building), *atrium* (around a buried courtyard), *elevation* (on a slope) and *bermed* (built above ground and later covered with earth). Anselm (2008, p. 1217) divides ground structures based on two construction concepts: *bermed* spaces and true underground spaces. In Anselm's work *bermed* structure styles are further subdivided into *elevational* or slope design, and *atrium* or courtyard design. As for Kwork and Grondzik (2011, p. 200) their typography of ground-integrated buildings is based on three implementation types: below ground surface on a level site, above or semi- underground surrounded by earth (berm) and integrated into a sloped site.

The types of ground-integrated spaces described by Golany (1995, p. 185) are those determined by the different forms related to the earth and the thermal performance patterns that result, the ways in which they are adapted to the location and climate conditions, and the local construction resources. Golany then divides these sturctures into five main types: earth-sheltered habitat, semi-below-ground habitat, subsurface space, belowground space and *'geospace'* (ibid., pp. 189-190).
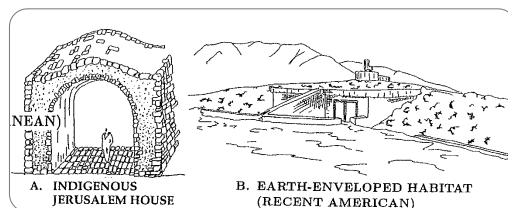
Figure 3.15: Earth-sheltered buildings. Golany, 1995
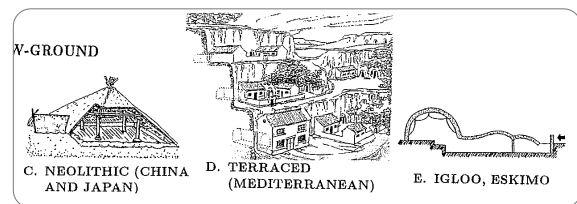
Figure 3.16: Semi-below-ground buildings. Golany, 1995

Earth-sheltered habitats are above-ground constructions where earth is used as thermal insulation. This strategy controls the heat flux, but the storage potential is limited. The use of these constructions can be found in hot-dry regions such as Iran, Turkey and USA and, according to Golany, this style of building was still being used in Jerusalem several decades ago (Figure 3.15). The semi-below-ground habitats, such as basements, are constructions with some elements below and some above

ground. These were considered one of the initial human made constructions and were commonly used in Neolithic settlements in China and Japan, and are still in use in rural settlements in Africa. These can be found in different forms such as the igloo in cold climates, and on slope ground-integrated terrace dwellings in the Mediterranean (Figure 3.16).
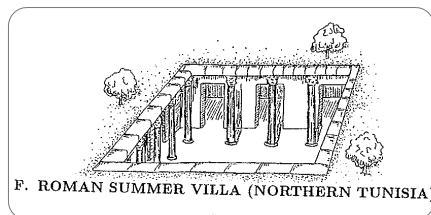
Figure 3.17: Subsurface buildings. Golany, 1995
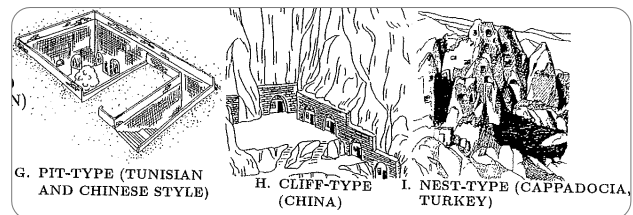
Figure 3.18: Belowground buildings. Golany, 1995

The subsurface building is erected on an underground level but its roof soil coverage is minimal. The distance between the soil surface and the building's ceiling is small, as can be seen at some Roman constructions in north Tunisia (Figure 3.17). The belowground spaces are underground constructions with a soil layer between the ceiling and soil surface of at least 3 m. These constructions depend on the characteristics of the local soil and on topography. These spaces are carved into the soil and are based on three main types; the pit-type, the cliff-type and the nest-type. Pit-type dwellings are used in flat ground areas, such as found in Tunisia and in China. The cliff-type and nest-type constructions are used in areas where the soil is easy to carve and self-sustaining, such as can be found in Turkey and China (Figure 3.18). Finally, the constructions termed by Golany as *'Geospace[s]'*, are all types of below-ground structures.

3.3. ADVANTAGES AND '*DISADVANTAGES*' OF GROUND-INTEGRATED BUILDINGS

The main benefits of constructing buildings at least partially underground are that the structure provides protection against harsh diurnal or seasonal temperatures, as well as providing more stable and moderate thermal values. By controlling the climate conditions the heating and cooling requirements of the building are reduced and, therefore, such buildings provide good energy conservation (Labs, 1980, p. 130; Barker, 1986, p. 59; Carmody and Sterling, 1987, p. 59; Chester and Zimmerman, 1987, p. 414; Golany, 1995, p. 197; Argiriou, 1996, p. 360; Mihalakakou et al., 1997, p. 181; Jannadi and Ghazi, op.cit., p. 108; Al-Mumin, op.cit., p. 105; Liu et al., 2010, p. 124; Li and Wu, 2011, pp. 82-85; Zhang, 2011, p. 6969; Tong and Chen, 2012, p. 4105). Ground-integrated structures are energy-efficient because they require less energy for heating or cooling than above-ground buildings (Brown and Novitski, op.cit., p. 303; Golany, 1992, p. 110; van Dronkelaar et al., 2014, p. 136). These buildings provide a better thermal environment than a standard building (Boyer, op.cit., p. 203), with lower energy costs (Van Der Meer, op.cit., p. 141; Boyer, op.cit., p. 203; Khair-El-Din, 1991, p. 10) which, consequently, leads to the prevention of fuel poverty (Hunt, Jefferson and Rogers, 2011, p. 218). The thermal conditions of ground-integrated structures are good for food preservation (Aydan and Ulusay, op.cit., p. 254; Fuentes Pardo and Canas Guerreiro, 2006, p. 475; Erdem, op.cit., p. 495) and can be used by industries that need stable temperatures such as the film stock preservation (Golany, 1995, p. 199) or wine making industries (Golany, ibid., p. 199; Cañas Guerrero and Ocana, 2005; Ocana and Cañas Guerrero, 2005; Mazarron and Cañas, 2008; Cañas Guerrero and Mazarron, 2009; Mazarron and Cañas, 2009; Mazarron, Cid-Falceto and Cañas, 2012; Tinti et al., 2014).

Furthermore, a good, stable thermal environment has a positive effect on human health (Golany, 1992, p. 125; Tong and Chen, 2012, p. 4106), and its residents live longer (Li and Wu, op.cit., p. 87; Tong and Chen, ibid, p. 4106). Stable temperatures decrease the time needed to heal external injuries by up to 20% (Golany, 1995, p. 199). Yan (1986, p. 173) reported that living in an earth shelter dwelling environment could contribute to a reduction in upper respiratory infections, and a similar reduction in the incidence of rheumatism, nasal bleeding and infection, and skin conditions. Furthermore, a stable thermal environment has the potential to reduce infections, and to protect against health-related problems caused by noise due to the ability of the ground to act as sound barrier.

Regarding heritage and urban planning, underground constructions are identified as good ways to generate open space without additional land costs, and can be used as no-visual barriers (Aughenbaugh, 1980, p. 151; Van Der Meer, op.cit., p. 141; Givoni, 1994, p. 219; Al-Mumin, op.cit., p. 105; Erdem, op.cit., p. 492; Hunt, Jefferson and Rogers, op.cit., p. 218). These constructions contribute to preserving the landscape by maximizing the land use potential of an area (Aughenbaugh, op.cit., p. 151; Labs, 1980, p. 130, 1982, p. 410; Barker, op.cit., p. 59; Golany, 1995, p. 199; Jannadi and Ghazi, op.cit., p. 101; Kumar, Sachdeva and Kaushik, 2007, p. 2450), and reducing the visual impact of buildings (Van Der Meer, op.cit., p. 141; Barker, op.cit., p. 59; Khair-El-Din, op.cit., p. 10; Argiriou, op.cit., pp. 363-364; Jannadi and Ghazi, op.cit., p. 101; Al-Temeemi and Harris, 2004, p. 253). Another advantage of ground-integrated urban planning is that such buildings have a lower impact on the local ecology and microclimates (Van Der Meer, op.cit., p. 141).

Considering security and safety issues, underground shelters provide privacy thanks to their safe and secure environment (Golany, pp. 197-198; Argiriou, op.cit., p. 365; Mihalakakou et al., op.cit., p. 181; Jannadi and Ghazi, op.cit., p. 109; Al-Mumin, op.cit., p. 105). These buildings also protect their occupants from exterior generated

noise (Aughenbaugh, op.cit., p. 105; Van Der Meer, op.cit., p. 151; Labs, 1982, p. 410; Barker, op.cit., p. 59; Boyer and Grondzik, op.cit., p. 36; Carmody and Sterling, op.cit., p. 59; Golany, 1995, pp. 197-198; Argiriou, op.cit., p. 364; Mihalakakou et al., op.cit., p. 181; Jannadi and Ghazi, op.cit., p. 109; Tong and Chen, 2012, p. 4106), and provide protection against high winds and tornados (Labs, 1980, p. 130; Van Der Meer, op.cit., p. 141; Labs, 1982, p. 410; Barker, op.cit., p. 59; Boyer and Grondzik, op.cit., pp. 187-188; Chester and Zimmerman, op.cit., p. 414; Argiriou, op.cit., p. 365; Mihalakakou et al., op.cit., p. 181; Jannadi and Ghazi, op.cit., p. 109), sand storms (Labs, 1980, p. 130) and fire propagation (Aughenbaugh, op.cit., p. 151; Labs, ibid., p. 130; Boyer and Grondzik, op.cit., p. 193; Chester and Zimmerman, op.cit., p. 414; Golany, 1995, pp. 197-198; Argiriou, op.cit., p. 365; Mihalakakou et al., op.cit., p. 181; Tong and Chen, 2012, p. 4107). When efficiently designed, underground constructions also withstand earthquakes better than above-ground structures (Luo, 1987, p. 205; Yucheng and Liu, 1987, p. 216; Golany, 1992, p. 126, 1995, p. 199; Argiriou, op.cit., p. 365; Al-Mumin, op.cit., p. 105; Erdem, op.cit., p. 495; Tong and Chen, ibid., p. 4107), since their structural elements move with the ground as a unit and not *"as an unrelated assemblage of parts"* (Boyer and Grondzik, op.cit., p. 192).

There is no consensus regarding the comparative construction costs of underground compared to above-ground constructions. The divergence in different cost analyses of ground-integrated buildings is caused by the construction context as well as soil characteristics, excavation problems due to hard rock, water table locations or the need for special drainage design. Wendt (1982, p. v) reports that, on average, an underground house could cost 10% to 35% more than a above-ground house. It should be added that for the market conditions of 1981, and taking in account a life cycle cost of a building, this extra amount might not add any benefits. According to Egg and Howard (2011, p. 9), prohibitive construction cost is one of the reasons why

people do not build entire dwellings underground. For Labs (1980, p. 137), however, the construction costs and technologies required for underground buildings are not obstacles to building underground constructions. Other researchers have perceived low construction costs as an incentive for ground-integrated structures (Aughenbaugh, op.cit., p. 157; Golany, 1992, p. 78, 1995, p. 197; Al-Mumin, op.cit., p. 107; Liu et al., op.cit., p. 124; Tong, Chen and Li, op.cit., p. 1645). For Golany (1995, p. 197), ground-integrated building construction costs proved to be up to 50% lower than above buildings constructions with similar dimensions, as the land price for sites suitable for ground-integrated dwellings is normally low because they often feature slope terrain, and the soil itself can be used as the construction material. Aughenbaugh (op.cit., p. 157) states that underground construction costs are economically viable, since they are able to compete against above ground buildings, with his research showing a 10-20% reduction in construction costs for underground compared to above-ground dwellings. Studies by Al-Mumin (op.cit., p. 107) proved that, in Kuwait at least, an underground courtyard building with one floor is less expensive than a similar above-ground building. And as for underground courtyard buildings with two floors, the final costs for these buildings are, according to Al-Mumin, similar to above-ground construction of similar buildings. However, if the running costs were added to the equation, the sunken courtyard design would improve its total costs when compared to above-ground constructions of the same type.

When considering maintenance, the building envelope of a sheltered house has fewer surfaces affected by climate conditions and therefore the maintenance needs of underground buildings are lower and less demanding than those of an above-ground building. This includes a reduction in exterior maintenance costs (Aughenbaugh, op.cit., p. 151; Van Der Meer, op.cit., p. 141; Barker, op.cit., p. 59; Argiriou, op.cit., p. 365; Mihalakakou et al., op.cit., p. 181; Jannadi and Ghazi,

op.cit., p. 109; Al-Mumin, op.cit., p. 105) and lower water systems maintenance due to pipes' lower exposure to freezing temperatures (Golany, 1995, pp. 197-198). However, Wendt (op.cit., p. 38) pointed out that this analysis depends upon the objects compared. If we compare an underground house with a well-built above-ground house the maintenance cost difference would not be so pronounced.

The most commonly accepted issue concerning below-ground buildings is the general perception or conceptualization of such buildings (Labs, 1980, p. 137), making social and psychological problems the greatest obstacle to the spread of these constructions (Golany, 1980, p. 120; Jannadi and Ghazi, op.cit., p. 105). Van Der Meer points out that underground housing construction acceptance is low in the USA due to a negative perception of such buildings in the country's collective memory. In the US, underground dwellings are associated with a primitive culture and with poverty due to the use of basement accommodations during the Great Depression of the 1930s (Van Der Meer, op.cit., p. 141), as well as with the post-World War II basements accommodations of unfinished houses (Jannadi and Ghazi, op.cit., pp. 106-107). In China, religious buildings were always built above ground to be *'pure'* (Golany, 1992, p. 7). It was also common in these areas for buildings with a higher monetary value to be built above ground, which makes living in ground-integrated buildings not a choice, but rather a result of economic restriction (Golany, 1995, p. 200). This history has contributed to the perception of ground-integrated spaces as dark places, humid and with poor ventilation, which provide a poor health environment and a sense of claustrophobia. In the case of the Cappadocia constructions, Çorakbas (op. cit., p. 1451) argues that carving underground spaces was more economical and took less time than constructing the same area above ground. Furthermore, the underground spaces at this location could be adapted or reused. For Çorakbas, this fact leads to the argument that underground structures were not a preference but probably a necessity.

Aughenbaugh (op.cit., p. 157) provides a new perspective to this problem. For Augenbaugh the main obstacle to the construction of underground buildings is not the negative public perception of such buildings, but rather the planner's assumptions. On the few occasions where the public was informed of the living conditions in underground dwellings and was able to see different house plans and studies, it became clear that all objections to these buildings ceased. In a similar manner, Boyer (op.cit., p. 209) argues that the psychological problems associated with living underground fail to be borne out when confronted with the reality of underground living. With regard to schools, Boyer reported that sheltered buildings provided a good learning environment. As for workspaces, Boyer stated that the experience was similar to working in large above ground workplaces. Bartz (1986, p. 80) found that the residents of earth-shelter houses developed a more positive opinion of such dwellings after living in earth-shelter homes. Before moving, residents reported some concerns and divided negative, positive and neutral attitudes. After the experience, the residents' attitude changed, becoming universally extremely positive. Al-Mumin (op.cit., p. 111) also states that occupant of below ground dwellings in Kuwait expressed high satisfaction and positive reactions to the conditions provided by the design.

Other reported disadvantages of these constructions are the high relative humidity and insufficient air quality (Khair-El-Din, op.cit., p. 6; Argiriou, op.cit., p. 366; Jacovides et al., 1996, p. 167; Liu et al., op.cit., p. 124; Zhang, op.cit., p. 6969), excessive weight of roofs due to a large amount of soil waterproofing (Khair-El-Din, op.cit., p. 6), size requirements or restrictions (Van Der Meer, op.cit., p. 142; Liu et al., op.cit., p. 124; Tong and Chen, 2012, p. 4107), lack of appropriate sites (Jannadi and Ghazi, op.cit., p. 109), slow reaction to new conditions (Steemers, 1991, p. 11) and finally, construction codes, regulations and financial impediments due to lending restrictions (Van Der Meer, op.cit., p. 142).

3.4. CASE STUDIES

3.4.1. Initial Studies

In order to assess the potential of underground construction, Golany (1995) studies the thermal comfort of a below-ground residential building in the Ya'nan City area in Shaanxi Province (China), of a hotel in Matmata (Tunisia) and of the Hunt House, an uninhabited Roman subsurface house structure in Bulla Regia (Tunisia).
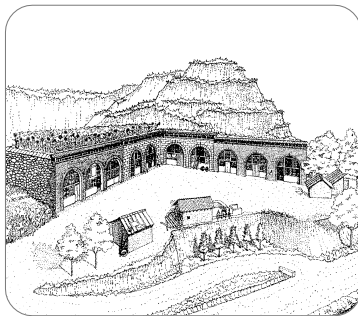
Figure 3.19: Studied building, Ya'nan City, China. Golany, 1995
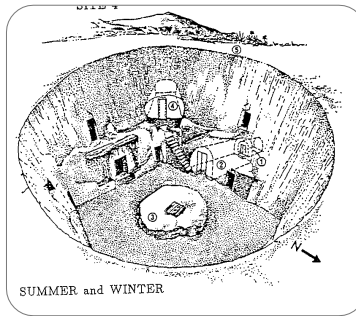
Figure 3.20: Marhala Hotel, Tunisia. Golany, 1995
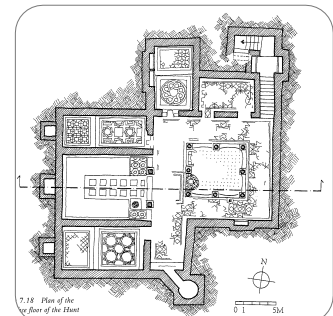
Figure 3.21: Hunt House, Bulla Regia, Tunisia. Golany, 1995

The family building in China shown in Figure 3.19 consisted of a south facing L-shape, with five rooms on both sides. The right wing of the building was carved into a cliff so that its structure has soil coverage 15 m deep, and the left wing is an earth-sheltered structure with 2 m roof soil coverage. During the summer, which featured an outside maximum temperature of 28ºC and diurnal amplitude of 14ºC, the cliff-type wing provided good thermal comfort with a low temperature oscillation of 3ºC and a maximum temperature of 21ºC. The earth-sheltered wing had the highest temperature and thermal oscillation. Through the winter it was found that both wings required some sort of heating. The cliff-type wing had more stable temperatures than the earth-sheltered wing, but it also registered the lowest ones. However, in summer and winter the humidity level was lowest and almost constant in the earth-sheltered wing (ibid., pp. 202-204).

The below-ground Marlhala Hotel in Tunisia consisted of a pit-type construction (Figures 3.20). During the summer all the rooms' temperatures were stable. In the

intermediate room, with 4 m soil coverage, the temperature was highest and registered the biggest thermal oscillations. A smaller room with a soil coverage of 10 m registered temperatures 17ºC lower than the outside temperatures. In winter Golany found that all rooms registered higher temperatures than those found in the outside areas. The lower rooms had the most stable thermal conditions throughout the year. Golany concluded that the soil structure influences the below ground spaces, and this provided both a more stable temperature and better thermal comfort than those found in above ground buildings. At depths of up to 10 m, Golany observed that the deeper the space is buried, the better its thermal performance. The humidity values are also lower and the diurnal and seasonal humidity and temperature oscillations are reduced the deeper a room is buried (ibid., pp. 204-210).

The Hunt House, illustrated in Figure 3.21, is formed of five rooms that are connected via an open patio. Its structure was built 5 m below the surface and the soil roof coverage is less than 1 m. The house's structure works as a thermal insulator and does not provide thermal storage. All rooms have an internal duct for light and ventilation. By analysing the site temperature measurements once in the winter and once in the summer, Golany found that the temperatures found in the structure were lower than the outside temperatures on both occasions (ibid., pp. 210-214).

3.4.2. Location and Climate

Protected by UNESCO since 1993, the *"Sassi"* district of Matera, Italy, is formed by a number of semi-underground excavated constructions. These buildings' main problem is the high humidity. In the case of Santa Maria of the Paloma Sanctuary, this high humidity caused the degradation of the mural frescos, a degradation which could have been prevented by improving the natural ventilation of the space

(Cardinale and Ruggiero, 2002, p. 412). Cardinale, Guida and Ruggiero (2001, p. 302) argue that the semi-cave settlement of *"Sassi of Matera"* was a bio-climatic architecture able to use soil, location and climate to provide a good thermal environment.
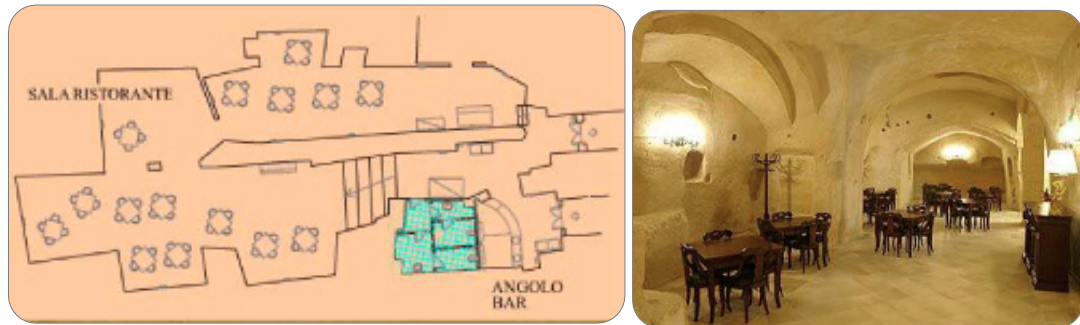
Figure 3.22: Restored underground space. Guida, Pagliuca and Rospi, 2008

Guida, Pagliuca and Rospi (2008, p. 149) studied the thermal performance of two reconverted underground buildings adapted into hotels, shown in Figure 3.22. They concluded that these underground constructions provided passive cooling and heating and delivered a thermal environment in accordance with recent European directives. Later, Cardinale, Rospi and Stazi (2010, p. 94) confirmed that the walls' thermal mass was sufficient to control the daily and annual internal thermal environment by avoiding large thermal amplitudes. After restoration, the spaces provided good thermal comfort and could be used with a reduced technology system. Recently, Cardinale, Rospi and Stefanizzi (2013, p. 598) analysed two examples of vernacular buildings in southern Italy. The experimental research proved that both the *"Sassi of Matera"* and *"Trulli of Alberobello"* structures produce outstanding energy performances.

Khair-El-Din (op.cit., pp. 15-16) analysed earth sheltered constructions through their design characteristics based on location, climate and environmental impact. Khair-El-Din's study concludes that these types of structures should be part of future housing construction in hot and dry climate locations. Al-Temeemi and Harris (op.cit., p. 404) studied the effect of earth-contact buildings in Kuwait by measuring

the energy efficiency of a wall with ground contact at different depths. The study confirms that by increasing the ground contact of a subterranean wall at up to 2 m depth, the heat flux decreases (Figure 3.23). By comparing earth-contact walls with above ground walls Al-Temeemi and Harris found that the heat flux could be reduced by up to 51.6%.
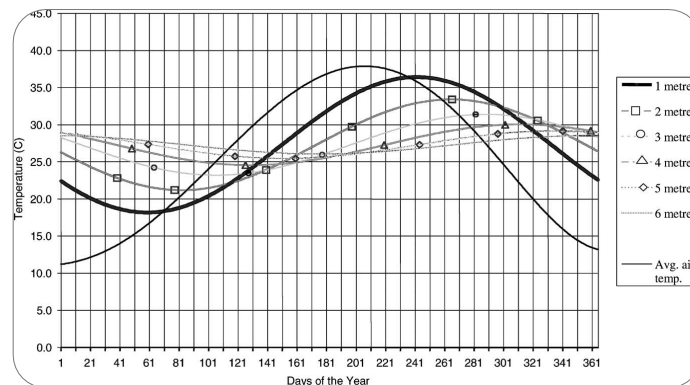
Figure 3.23: Ambient air and underground wall surface temperatures. Al-Temeemi and Harris, 2003

In Japan, Yoshino et al. (1992) conducted a study that collected the thermal performance data of the semi-underground dwelling in Sendai. This study was carried through five years, measuring internal temperatures, soil temperatures, and an analysis of the heating energy demands of the building in four different scenarios. Hasegawa, Yoshino and Matsumoto (1997, p. 435) analysed the annual temperatures measurements inside the Sendai dwelling. They confirmed that the temperature amplitude inside the house was far smaller than the outside temperature swing.

The Sendai data was used also by Sobotka, Yoshino and Matsumoto (1996, p. 165) to study and compare the thermal performance of semi-underground rooms (Sendai) and totally earth integrated rooms (Brhlovce, Slovakia). In temperate climates, totally integrated constructions without insulation and with good solar gains designed through fenestration were found to be too cold, with poor thermal comfort during spring and a part of the summer. Therefore, the use of insulation was recommended. In hot climates, where the cooling needs are more accentuated, this

insulation can be omitted. The key design parameters for the passive, solar-earth sheltered building are, according to these authors, the level of ground integration, the structure insulation levels and the percentage of south-facing walls that are glazed.

Rantala (2005, p. 52) studies the thermal behaviour of slab-on-ground structures. According to Rantala, a heated building changes the ground thermal behaviour by providing a more constant heat flux, creating a *'warm cushion'* below the building. However, the surrounding ground without coverage limits the extent of the depth of the *'warm cushion'* effect. Below this limit, the ground temperature registers similar values to the average annual subsurface.
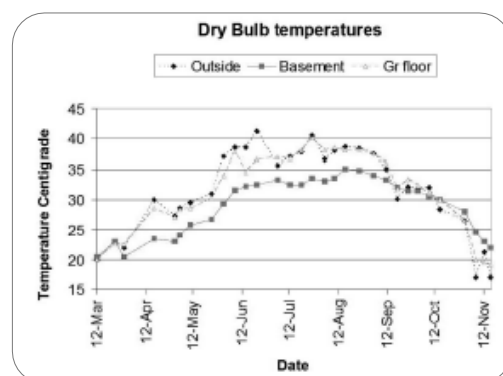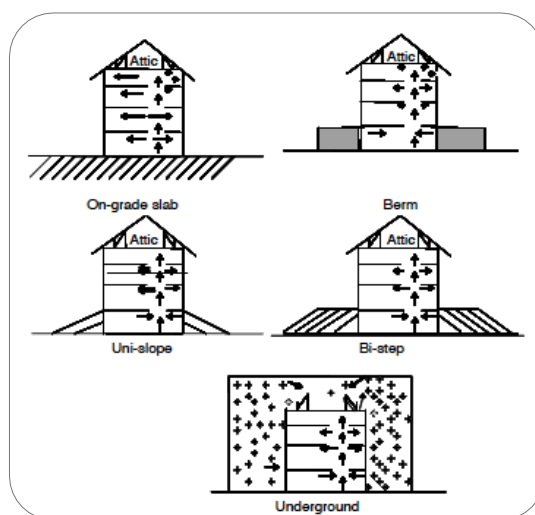
Figure 3.24: (Left) Ground contact structures. Kumar, Sachdeva and Kaushik, 2007
Figure 3.25: (Above) Air temperatures. Kharrufa, 2008

Kumar, Sachdeva and Kaushik's (op.cit) study focuses on five different ground contact structures configurations, as illustrated in Figure 3.24. These five configurations are a slab with ground contact, a raised bank, a single-slope, a double-set slope configuration and an underground structure. The results of this comparison show that the configuration which had the highest energy conservation value, and therefore the best comfort zone, was the underground structure. The underground structure was followed by the double-set slope, single-slope and raised bank configurations (ibid., p. 2458). It is therefore possible to confirm that the heat flux through the structures' envelope is affected by the amount of ground contact.

The higher the amount of soil contact the lower the heat transfer value. Kumar, Sachdeva and Kaushik's results prove that ground contact structures are highly valuable as passive technology, and that underground walls at different depths have a direct effect on the total energy demand of a building (ibid., p. 2460).

In Iraq, according to Kharrufa (op.cit., p. 411), traditional building space was used based on a cyclic rotation between the living areas of the basement, the courtyard and the roof, which depended on daily activities and external and internal air temperatures. More recently, this space-use pattern was abandoned in favour of air conditioning systems. This shift was caused by the low cost of energy and the rise of underground water levels, which increased the costs and risks of underground construction. Recently, this scenario is changing due to general land cost increases, the unreliable electricity supply in Iraq throughout the last decade, and the impression of safety against stray bullets and shrapnel (ibid., p. 412). Kharrufa's (ibid., p. 416) study of cooling thermal performance in underground spaces in Iraq proves that, during the summer, basements provided better thermal comfort than above ground areas, with the air temperature measuring 4.5ºC lower than above ground areas (Figure 3.25). Therefore, basement spaces require less energy to improve their thermal environment.

3.4.3. Soil Characteristics Influence

Ocana and Cañas Guerrero (op.cit., p. 708) demonstrate that soil thermal characteristics and construction depth set the air temperature range inside the underground space. Staniec and Nowak (op.cit., pp. 233-234) consider the influence of soil characteristics on the heating and cooling demands of an earth sheltered building. According to Staniec and Nowak, for underground buildings the type of soil affects the building's thermal behaviour, as 80-90% of the building envelope is in direct contact with the ground, while an above ground building has, in general, only

30% of its envelope in contact with the ground. The type of soil affects an the energy demand of an above ground building by only 3-11%, and affects an earth-sheltered building's energy demand by 11-80%. Soil with a low thermal conductivity coefficient leads to a building with low heating and cooling energy demands.

3.4.4. Patios and Courtyards Impact

Regarding the influence of the patio and courtyard on a ground-integrated building's thermal comfort, Brown and Novitski (op.cit.) consider two underground building designs in different climates of North America: one with an atrium and the other with a courtyard facing south. The authors found that earth sheltered buildings have the potential to respond to the climate patterns (ibid., p. 299). Brown and Novitski's study argues that the immediate outside spaces around the earth-sheltered building could contribute to, as well as benefit from, better thermal comfort (ibid., p. 304).
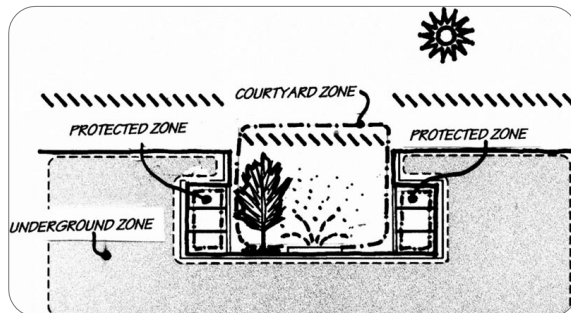
Figure 3.26: Ground-integrated building with courtyard. Al-Mumin, 2001

Figure 3.27: Ground-integrated house with courtyard. Al-Mumin, 2001

Al-Mumin (op.cit., p. 111) investigates the cooling performance of a ground-integrated building with a case study of a courtyard situated in Kuwait. This structure, according to Al-Mumin, has three major advantages for a hot, dry climate. Firstly, it avoids the direct and indirect solar radiation heat gains through the roof and walls; secondly, it reduces the heat gains through infiltration and, thirdly, it reduces the heat gains that could be transferred to the roof and wall through the outside air temperature in the summer (Figure 3.26 and 3.27). Al-Mumin's study demonstrates that the sunken courtyards have a 23-35% reduction in annual energy demand.
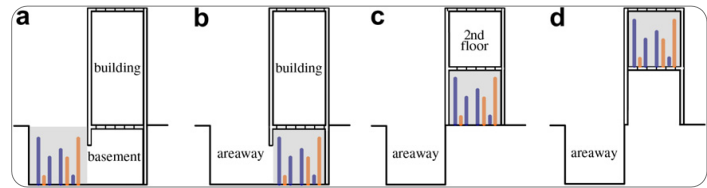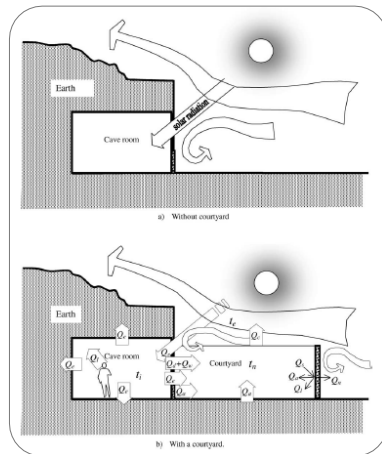
Figure 3.28: (Left) Heat flux- with and without a courtyard. Wang and Liu, 2002

Figure 3.29: (Above) Case study *"a) Areaway space; (b) basement; (c) 1st floor; (d) 2nd floor."* Bu, Kato and Takahashi, 2010

Concerning the heating potential of a courtyard, Wang and Liu (op.cit., p. 1000) examine its effects on earth-sheltered constructions in Northern China through the interaction between the rooms, the courtyard area and the outside ambient temperature. Wang and Liu establish that the courtyard functioned as a buffer zone (Figure 3.28), which reduced the heat losses from the rooms, controlled the winds effect on the building's facade and collected solar radiation throughout the day. The data collected for Wang and Liu's study show that the temperature inside the courtyard is constantly 2ºC higher than the outside ambient temperature and its amplitude is 3ºC lower than the outside temperature. The three main reasons for this result, as argued by the study's authors are, firstly, the increase in received solar radiation and, secondly, the shelter effect provided by the room's and courtyard's walls and, lastly, the courtyard's ability to collect heat lost from the adjacent rooms.

Bu, Kato and Takahashi (2010) studied the benefits of areaways (open sunken courtyards) in urban residential areas (Figure 3.29). The areaway spaces these authors studied are identified as buffer zones and can control the inside thermal conditions of building areas such as basements, improving their natural ventilation and light conditions (ibid., p. 2263). Compared to the pit cave dwelling courtyards found in China, the areaways in Japan are smaller spaces. The authors conclude

that in an urban setting, areaway spaces are sustainable elements able to provide ventilation to below ground spaces and, therefore, improve the underground environment (ibid., p. 2271).

3.4.5. Earthships Constructions Performance
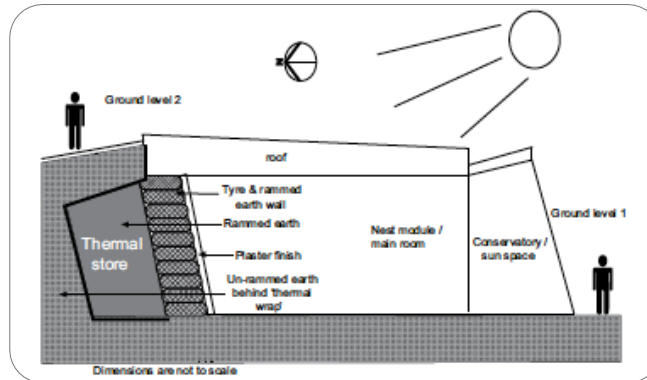
Figure 3.30: Earthship section, Brighton, UK. Ip and Miller, 2009

Michael Reynolds developed the *Earthship* construction, which is a ground-integrated structure characterised by operating in self-sufficient mode and which utilizes recycled and local construction materials (Figure 3.30). Grindley and Hutchinson (1996, p. 154) investigated the thermal behaviour of an *Earthship* building in New Mexico (USA), simulating its behaviour in a southeast location in the UK. Grindley and Hutchinson found that the building suffered from overheating during the summer months in both New Mexico and in the UK. The building in New Mexico provided good thermal conditions during the day for the rest of the year, with some heating needs during the night and during winter. The same building in the UK only required a small amount of heating during winter. Similarly, Ip and Miller (2009, p. 2043) analysed the performance of an *Earthship* building's seasonal thermal storage system in Brighton, UK. The initial measurement shows that the unoccupied building is able to minimise the outside extreme temperatures. The thermal store, as described by the authors, was working as an initial *'charging'* cycle. This cycle was expected to continue throughout the first years, with an annual increase in thermal comfort during winter.

3.4.6. Wine Cellars

Ocañas and Cañas Guerreno (op.cit., p. 1393) investigate the summer and winter thermal behaviour of four underground wine cellars in the Ribera del Duero region, Spain. Their study found that the internal temperature of the cellars were stable compared to the outside air temperature. However, the internal temperature and humidity level varied between the cellars. The mean temperature difference between all cellars was smaller during the summer than during the winter. The authors concluded that the outdoor temperature did not affect the cellars internal temperature.

Figure 3.31: Slope-integrated wine cellars. Ocañas and Cañas Guerreno, 2005
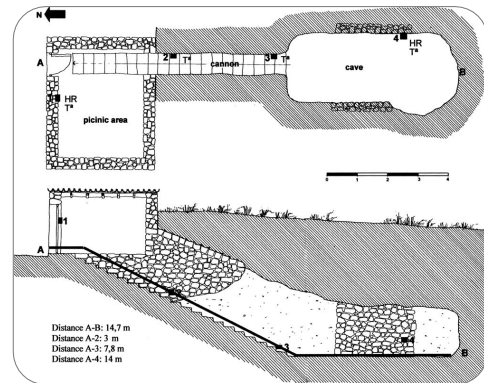
Figure 3.32: Studied wine cellars, plans and section. Cañas Guerreno and Ocañas, 2005

Cañas Guerrero and Ocañas (op.cit.) studied the hygro-thermal cooling patterns of two traditional wine cellars (Figure 3.31 and 3.32). To understand the best thermal conditions for a wine cellar, the authors based their study on knowledge of the local wine producers of Morcuera (Soria, Spain) (ibid., pp. 46-48). The study proves that these cellars have high passive cooling potential by providing stable temperatures much lower than 18ºC during the summer (ibid., pp. 53-54). The cellars carved on hillside sites registered air temperature variations of 0.8ºC with a minimum value of 11.4ºC. The cellar carved at a lower depth registered a stable temperature of around 9ºC, 2.4ºC lower than the hillside cellar minimum.

Cañas Guerrero and Mazarron (op.cit., p. 1825) investigated the effects of natural ventilation on the hygrothermal patterns of underground wine cellars in Ribeira del Duero. This study proves that underground wine cellars with and without wind vents (zarceras) provide good temperature and relative humidity conditions for wine maturing, by controlling the large annual temperature variations. Therefore, the benefits of these traditional cellars also include no energy costs compared to above ground cellars that need air conditioning systems. The wine cellar without vents had lowest temperature oscillations. Both cellars registered constant relative humidity values; however the cellar without vents registered high values during the summer. Cañas Guerrero and Mazarron also found that wind vents improved the underground cellar's hygrothermal patterns. The natural ventilation provided by this feature only worked from September to April, which contributes to the removal of the CO_2 generated by wine fermentation during this period without compromising the internal air temperature.

On further investigation, Mazarron and Cañas (op.cit., p. 2484) found that wine cellars' internal air temperature is determined by the ground temperature at the average depth of the construction space, and by the outside air temperature through ventilation. The stability of the thermal environment changes according to the seasons. Mazarron and Cañas found that the cooling thermal performance of the underground cellars was better than their heating performance (ibid., pp. 2491-2492). During the warmer period of spring and summer, the influence of ground temperatures dominated the inside air temperatures. During the autumn and winter, the air temperature of the cellars temperature is more highly influenced by the outside air temperatures due to an increase in ventilation.

Mazarron, Cid-Falceto and Cañas (op.cit.) developed a modelling procedure to simulate the annual air temperature pattern of underground cellars in different locations. Their study used the climate data of twenty wine producing regions; it

considered future global warming and its effects on the underground wine cellars'
thermal environment, on locations with a mean annual air temperature higher than
15ºC (ibid., p. 57). Mazarron, Cid-Falceto and Cañas found that for all the wine-
producing locations the ideal thermal environment could be secured by constructing
the cellar at the right depth, a depth that was determined by the thermal properties
of the soil and external climate conditions (ibid., p. 61).

3.5. CONCLUSIONS

Natural, excavated, or buried, ground-integrated spaces have been used for residential, military, religious, social and educational purposes, or for food production or storage, transportation and utilities. The categories of ground integration can be based on site integration for both slope and flat land, and by ground integration as total, semi and *bermed*.

The ground integration of a building's envelope is a ground thermal strategy that enables the building to take advantage of the ground thermal potential through direct heat transfer. These buildings are able to control and decrease heat loss during the cold seasons and to avoid heat gains during the warmer seasons. The increase in surface area with direct ground contact reduces the effect of external parameters such as solar radiation, ambient air temperature and wind, as well as reducing air infiltration. The use of insulation produces lower or total decoupling between ground and building structure and, therefore, its use should only be considered when there is high ground heat loss.

The thermal environment of below ground spaces is influenced by multiple factors such as local climate, site topography and orientation, soil characteristics, the level of ground integration, depth and nearby elements.

Other than energy conservation, thermal comfort and land preservation are the main advantages of ground-integrated buildings, followed by security and safety, maintenance and health benefits. Most of the disadvantages, such as high humidity, poor air quality, reduced lighting and size restrictions, can be prevented through careful design. Other disadvantages to consider are the lack of suitable sites and increased construction costs in areas where these types of constructions are uncommon.

CHAPTER 4. GROUND-INTEGRATED ARCHITECTURE ON SLOPE TERRAINS

4. GROUND-INTEGRATED ARCHITECTURE ON SLOPE TERRAINS

4.1. POTENTIAL APPROCHES FOR A SUSTAINABLE LAND USE

A large part of the world's population lives in areas with severe climate conditions such as hot dry, hot humid, and cold dry climates. The increasing urban population of these areas could lead to the use *"of new natural resources. In this situation, intense development of the mountain slopes (…) will become inevitable, creating a new urban frontier and new challenges for urban designers and climate specialists."* (Golany, 1996, p. 464).

Three decades have passed since Simpson and Purdy (1984, p. 1) pointed to an increasing tendency toward building on slope terrains in the UK, a trend which was linked to the scarcity of flat land and to a rising appreciation of the need to preserve agricultural land (ibid., p. 248). Both these issues are global, as the shortage of flat construction land is an on going problem, and the rapid urban development of the past three decades had led to steep increases in land prices and to the claiming of farming land for building purposes (Hayashi, 1986, pp. 167-168; Burger, 1987, p. 288; Golany, 1992, p. 115, 1998, p. xi; Liu et al., 2010, p. 125). To continue the practice of building on flat land could lead, in the near future, to food shortages due to the waste of good agriculture land.

For sustainable land use, the three main ground integration strategies currently used are the use of underground space, the reuse of existing underground spaces and the exploration of slope ground-integrated spaces.

Firstly, going underground permits a dual use of land, below and above ground, thereby taking advantage of space. Reclaiming urban underground levels is not a new solution. Below ground spaces have long been used for infrastructural projects such as sewers, utilities and transportation (Hunt, Jefferson and Rogers, 2011, p. 215). Although understood as a legacy of the Cold War defence strategy of the 1950s and of the 1970s energy crisis, land preservation or urban land limitations are currently the main incentive for the increasing interest in below ground dwelling spaces. Lack of available land is normally linked with a land cost increase, which has been a reason for recent interest in and studies on underground spaces (Golany, 1995, p. 186) such as the reclamation of land in Japan through the use of underground rooms (Yoshino et al., 1992, p. 339; Sobotka, Yoshino and Matsumoto, 1996; Hasegawa, Yoshino and Matsumoto, 1997) and areaways (Bu, Kato and Takahashi, 2010), or the reintroduction of basement spaces in Iraqi constructions (Kharrufa, 2008, pp. 411-412).

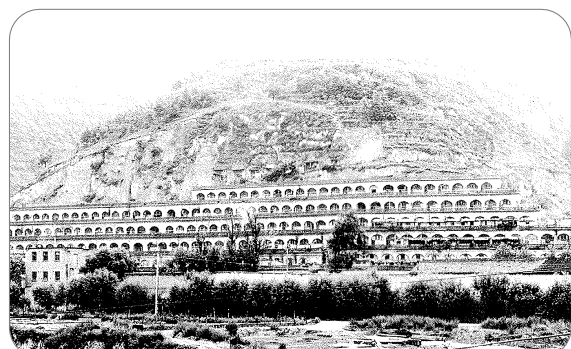Figure 4.1: Weels of the Fouggara. Amara, Nordell and Benyoucef, 2011

Figure 4.2: Slope students' dorm -Yan University, Shaanxi. Golany, 1995

Secondly, already-available unused underground spaces can be adapted to different functions. This could be the case with inactive mines, which could be converted into housing and commercial spaces (Aughenbaugh, 1980, p. 156; Golany, 1980, p.

120), and underground wine cellars (particularly in Spain), which could be converted into social and cultural spaces (Fuentes Pardo and Canas Guerreiro, 2006; Fuentes Pardo et al., 2010). Other examples are the *Fouggara* (Figure 4.1), formerly underground channel systems in Sahara, Algeria used for water transport, these tunnels have the potential to be re-used for building ventilation, heating and cooling systems (Amara, Nordell and Benyoucef, 2011).

A third potential strategy for reclaiming underground levels for construction is the maximization of slope land. Ground-integrated buildings are considered ideal for sharply inclined sites (Aughenbaugh, op.cit., p. 154; Sterling, Carmody and Elnicky, 1981, p. 26; Lee and Shon, 1988, p. 409; Kwok and Grondzik, 2011, p. 199). Since flat land tends to have the richest soils, ideal for agriculture (Sterling, Carmody and Elnicky, op.cit., p. 29), slope-integrated buildings are able to maximize the use of land generally not suitable for agriculture proposes (Golany, 1992, p. 84). This is the case of the main student dorm at Yan University, shown in Figure 4.2, an example of a slope-integrated structure design with the main purpose of saving local agricultural land (Golany, 1995, p. 229).

This last approach, which is the focus of this research, is far from being a new concept. Old hill towns are proof that vernacular architects understood and knew how to take advantage of ground thermal potential and slope microclimate, such as moderate ambient air temperatures and slope airflow. However, this clever and sustainable use of land, a common building practice for millennia in several parts of the world, has become an unfamiliar and almost unusual concept, particularly during the last century.

4.2. SLOPE EFFECT ON CLIMATE

4.2.1. Topography Effects on Air Temperature and Solar Radiation

As previously discussed in Chapter 2, different location characteristics, such as latitude, altitude, slope steepness and orientation affect ground temperature. The characteristics of topography regulate the solar radiation received by the soil (Šafanda, 1999, p. 374; Bennie et al., 2008, p. 47), and therefore have great influence on ground temperatures (Šafanda, ibid., p. 374). Thus it can be safely assumed that topography also affects the thermal performances of slope-integrated buildings.

Latitude effects the amount of solar radiation received by a location, and the higher the latitude, the lower are the insolation values (Chang, 1958, p. 153). Fitton and Brooks (1931, p. 9) noted that the amount of solar radiation received by the ground increased with altitude, which affects the ground temperatures and annual temperature amplitude, since both values decrease with altitude. For each 300 m altitude increase, there is an air temperature decrease of approximately 1.9 °C (Sterling, Carmody and Elnicky, op.cit., p. 50).
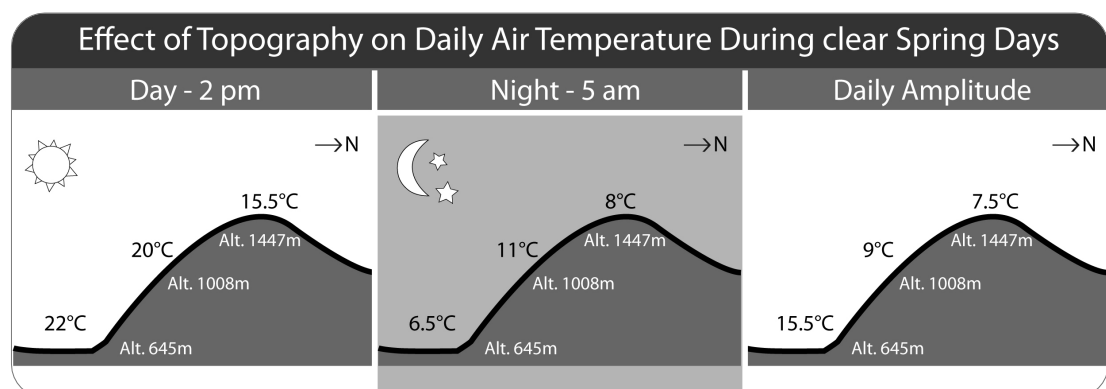

Figure 4.3: Air ambient temperatures at different heights at Arber; illustration based on Geiger (1950)

The ambient air temperatures on slopes are more temperate and their range smaller than those found in the lower and upper areas of a mountain (Dimoudi, 1996a, p. 85). The above illustration (Figure 4:3), based on Geiger (1950, pp. 249-250), shows

how topography affects daily air temperatures during the spring. Although during the day the hill base has the best temperature values, during the night the temperature is the lowest, providing the highest daily air temperature amplitude. As shown in Figure 4.4, the best building site is located in the middle zone of a slope because, both during winter and summer, this zone benefits from less extreme conditions (Sterling, Carmody and Elnicky, op.cit., p. 50). However, slope orientation produces different patterns. As altitude increases, the annual average air temperature decrease is higher on a north-facing slope than on a southern slope. The annual average diurnal temperature amplitude is higher on the southern slope but the annual average temperature amplitude is higher on the north-facing slope (Tang and Fang, 2006, p. 200).
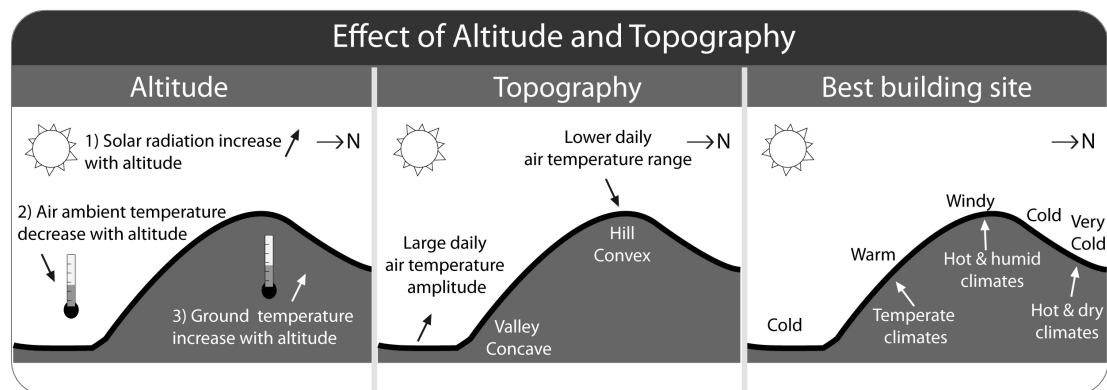

Figure 4.4: Effects of altitude and topography on ground and air ambient temperature based on Geiger (op.cit., pp .219-249); slope best building site for different climates, based on Dimoudi (1996a, p. 98) and Sterling, Carmody and Elnicky (op.cit., p. 156)

Slope orientation contributes greatly toward building heat gains and loss, as well as light access (Golany, 1983, p. 11). South oriented slopes in the Northern hemisphere receive the highest amount of solar radiation and hours of sunshine. In contrast, north-facing slopes receives the lowest (Fitton and Brooks, op.cit., p. 9; Chang, ibid., p. 156; Dimoudi, 1996a, p. 86; Šafanda, op.cit., p. 367; Littlefair, Santamouris and Alvarez, 2011, p. 29) and, therefore, south facing slopes have higher ground temperatures (Sterling, Carmody and Elnicky, op.cit., p. 155).

South facing slopes have the best light access, and buildings produce a lower solar obstruction (Littlefair, Santamouris and Alvarez, ibid., p. 29). Through semi or total slope-integration, it is possible to reduce a building's mutual obstruction to null values, which means good day light access in a compact land area. Geiger (op.cit., p. 219) links the relevance of slope orientation with latitude, and slope orientation has a greater influence on total solar radiation values at middle latitudes and low impact at either low or high latitudes.
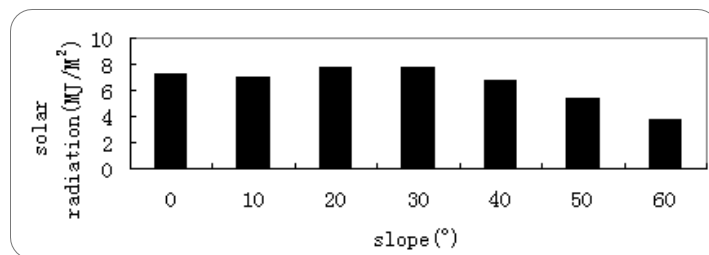

Figure 4.5: Solar radiation variation of the slope. Wang, 2009

The angle of a slope also affects the solar radiation received by the ground (Chang, op.cit., p. 159; Wang, 2009, p. 2184). According to Chang, *"by changing the degree of slope, the effect of latitude is simulated on a small scale. The temperature differences between exposures are usually accentuated by the slope."* (Chang, ibid., p. 159). Wang's (op.cit., p. 2187) study found that for slopes between 10° to 20° there is a gradual increase in solar radiation values received by the slope surface, from 20° to 30° a small decrease, and between 30° to 60° there is a clear decrease in solar radiation values. With the exception of 20° and 30° slope surfaces, all studied slopes, of whatever steepness received lower solar radiation than a flat surface (Figure 4.5).

According to Tian et al. (2001, pp. 69-70), the effect of slope angle is higher during winter and summer than during spring and autumn. The effect of slope orientation is considerable during winter in the northern hemisphere, due to shadows produced by the lower position of the sun. On complex terrain the effect of orientation is just as

evident, as solar radiation received by the soil is affected by terrain shading (Ruiz-Arias et al., 2011, p. 1812; Manners, Vosper and Roberts, 2012, p. 721).

4.2.2. Slope Flow - Katabatic and Anabatic Winds

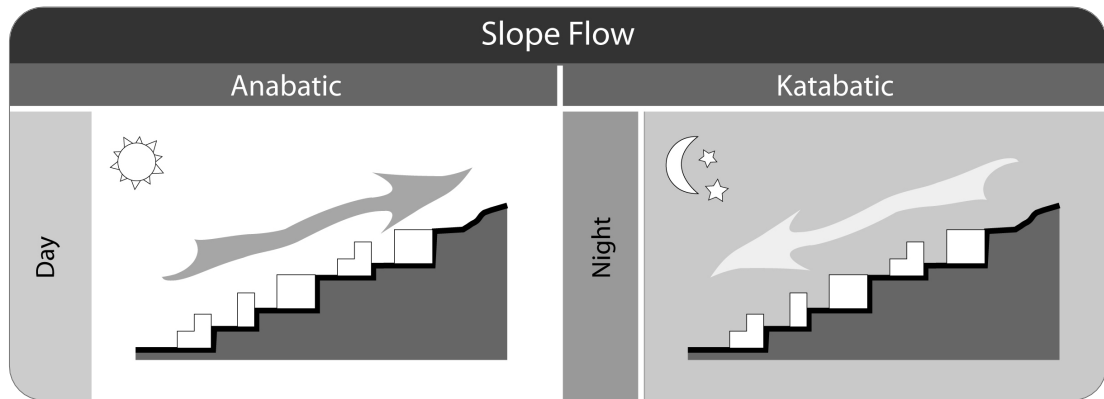Figure 4.6: Slope flow occurancy

Slope flow is a thermally-induced airflow produced in mountainous areas where there is a large temperature difference between the ground surface and the ambient air (Luo and Li, 2001, p. 5946). There are two types of slope flow, the anabatic and the katabatic winds. Both winds have high relevance for the air quality of a slope settlement (Catalano and Cenedese, 2010, p. 1859).

As illustrated in Figure 4.6, the first slope flow occurs during the diurnal period, and the second during the night period (Simpson and Purdy, op.cit., p. 21; Dimoudi, op.cit., p. 86; Luo and Li, op.cit., p. 5947). An anabatic wind develops when the ground temperature of a slope is greater than the ambient air temperature, causing an up flow of air movement ascending the slope. The katabatic wind is formed during the night by a rapid ground heat loss under clear skies, when cold air descends along the slope, cooling the ambient air temperatures. This effects the ground surface temperature (Chang, op.cit., p. 166; Luo and Li, ibid., p. 5947).

Highly populated, compact cities have higher potential to generate urban heat island environments, which are normally linked with urban pollution islands. To mitigate urban heat island environments, Luo and Li (ibid.) have studied the potential of

slope flow for urban ventilation in cities located in a mountainous area. This research found that slope flow was relevant to urban ventilation and its importance increased when there was a lack of wind. Luo and Li concluded that *katabatic* winds are a favourable way of avoiding the urban heat island effect throughout the night period.

4.3. SLOPE-INTEGRATED SETTLEMENTS

4.3.1. Landscape Integration

Slope settlements are one of the earliest settlement configurations, and they have been used since the Neolithic period (McHenry, 1980, p. 97; Turan, op.cit., p. 159). Generally these settlements provided natural advantages due to their south face oriented terrains that attenuate local climate conditions (McHenry, ibid., p. 97). An example of southern oriented sloped settlement is Akkoy, in Cappadocia where buildings are terraces, arranged in different platforms following the land topography. This organization contributes to good natural light access due to the advantageous solar exposure of southern slope settlements (Turan, ibid., pp. 148-151).
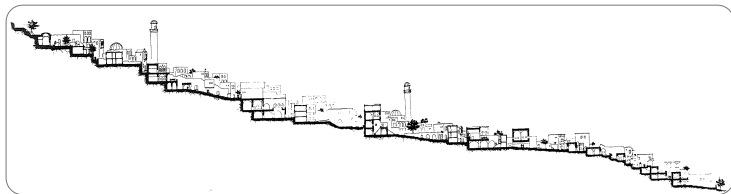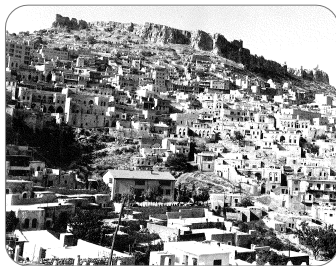
Figure 4.7: (Left) Mardin, slope-integrated buildings, Imamoglu, 1980
Figure 4.8: (Above) Mardin, cross section. Turan, 1983, p. 158

Figure 4.9: Macchu Picchu, Andes, Peru. Burger, 1987

Figure 4.10: Matera, Basilicata. Lembo, Marino and Calcagnoa, 2011

Figure 4.11: Pietrapertosa, Basilicata. Lembo, Marino and Calcagnoa, 2011

Similarly, the ancient city of Mardin, in southeast Turkey (shown in Figure 4.7) was developed over a south-sloping hillside with a 30 to 40° gradient (Imamoglu, 1980, p. 53). Rebuilt by the Romans during the 6th century (BC) the origins of Mardin can be traced back to approximately 1230 BC. This slope settlement takes advantage of prevailing wind directions and *katabatic* winds to provide thermal comfort throughout the year (Turan, op.cit., p. 155). These terraced houses are semi-integrated along

the slope, as shown in Figure 4.8. Its underground spaces are reported to provide good thermal comfort throughout the year (Imamoglu, ibid., p. 62). Other examples of ancient slope ground-integrated settlements are the Mesa Verde settlement in Colorado (USA), the city of Machu Picchu (Figure 4.9) in Peru (Burger, op.cit., p. 289), and the Matera (Figure 4.10) and Pietrapertosa cities (Figure 4.11), both in Basilicata, Italy (Lembo, Marino and Calcagnoa, 2011).

4.3.2. Contemporary Landscape Integration

Burger (op.cit. pp. 288-289) provides more recent examples of slope settlements, which are classified by the author as *Geomorphic Architecture*. This is a building design concept able to solve issues around land constraints by exploring the physical features of sloped terrains and hillsides. According to Burger this slope-integrated design appeared in western European countries where available land was limited and mostly reserved for farming. In general, the design of *geomorphic* constructions is based on nature or develops from a natural process. This design fits within the natural contour of the place, and becomes part of the landscape and is semi- or total ground-integrated. These geomorphic constructions have proven to be land efficient, to provide high physical and physiological benefits and privacy, as well as to be highly energy efficient.

4.3.3. Advantages of Sloped Settlements

Table 4.1: Comparison between ground-integrated buildings on flat and slope land

Flat land constructions		Slope land constructions	
Disadvantages	• Floods • Deposit of dust (sand storm) • Limited light • Claustrophobia • Reduce perception of surrounding elements or landscape • Limited ventilation	Advantages	• Good drainage, so avoids floods • Lower impact to dust storms • Can provide good light since it does not limit light through obstruction • Reduce claustrophobic feelings • Can provide good views also with lower levels of obstruction • Good ventilation • Underground and semi-underground slope integration
		Disadvantages	• Construction costs due to soil characteristics (rock) and land accessibility it might be need additional road construction

Housing on slopes can enjoy a large number of benefits compared to a flat site. The above table provides a comparison summary based on Golany (1980, pp. 110-111). Examining the advantages and disadvantages of flat and slope land constructions, Golany (ibid., p. 110, 1995, p. 229) concludes that ground-integrated constructions in slope hills are better than those on flat land, and achieve the best thermal performance in a moderate climate. Other benefits of sloped urban sites, as opposed to low-flat sites, are the better views and the reduction of health risks, due to better air ventilation a reduction in air pollution (Golany, 1992, p. 121, 1996, p. 456). The energy consumption of sloped land settlements is lower than flat land settlements. Sites on flat land or valleys are subject to higher air temperature amplitudes and, therefore, their heating and cooling demands are higher (Golany, 1996, p. 456). A flat land settlement in a hot dry climate consumes 50% more energy than an equivalent south-sloped settlement (Turan, op.cit., p. 159).

Slope-integrated construction contributes to efficient land use (Liu et al., op.cit., p. 124; Zhang, 2011, pp. 6968-6969). Underground buildings integrated on flat land require higher percentages of land than slope-integrated buildings (Golany, 1992, p. 115). Flat land settlements occupy double the area of slope settlements with the same characteristics (Turan, op.cit., p. 159). In addition, due to safety concerns, the area above ground-integrated building on flat land cannot be used for agriculture, resulting in a waste of land. For this reason, in the Chinese province of eastern Gansu, the construction of underground-integrated buildings on flat land was prohibited (Golany, ibid., pp. 116-118).

However, the benefits of building housing on slopes are not always considered and normally ignored. As Simpson and Purdy (op.cit, p. 9) point out, a sloped site most often *"appears to be regarded as a nuisance to be overcome rather than as an opportunity to be exploited"*.

4.4. SLOPE BUILDING DESIGN
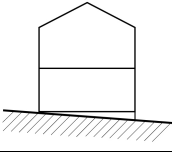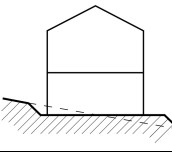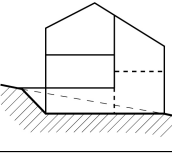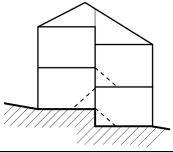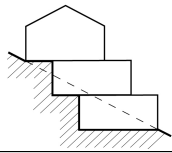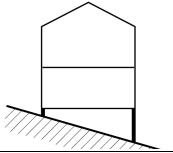
4.4.1. Slope Site Approach

Figure 4.12: (Left) Site inspired design. View and section, NP House by NO Arquitectos, Lda., Famalicão, Portugal. http://architizer.com
Figure 4.13: (Above) Special design. View and section, Mediterrani 32 by Daniel Isern Associates, Sant Pol de Mar, Spain. http://architizer.com

According to Simpson and Purdy (op.cit, pp. 34-35) there are three ways to approach a slope site, as a *site inspired*, *land-form adapted* and *special designs*. Examples of *site inspired* designs are hill towns, where buildings and access to them have been developed around the topography in an organic way. Figure 4.12 shows an example of a pre-existing building that was extended by adapting to the surrounding landscape. A *land-form adapted* approach is normally used in site adaptations for slopes lower than 7°. With this approach any slopes on the site are levelled into flat areas, creating terraced sites, in order to implement flat site constructions. Finally, the *special design* approach is used when slopes are higher than 8° and, therefore, too high to be flattened (Figure 4.13).

4.4.2. Building Design

Slope site design adaptation can be tackled in three ways, as illustrated in Table 4.2. One way is by adapting (in either a simple or complex way) a building planned for a flat site, a process that normally occurs in sites with small slopes. Simple adaptations consists of adding *extra masonry* for small adjustments of building walls on the lowest side of the site, and *cut-and-fill* operations that level the site into a flat area.

Table 4.2: Slope site design adaptation for houses; by the author based on Simpson and Purdy (op.cit, pp. 87-89)

Adaptation of the site		Slope building design			Site detached
Extra masonry	Cut-and-fill	Amended section	Split level	Cascade	Building on posts
Lower slopes		Median slopes		Median to high slopes	Median to high slopes
0° to 4°	1° to 6°	6° to 13°	4° to 8°	11° to 26° or +	8° to 26° or +

The second way is to design a building by taking site slope in consideration. This is the case in the *amended section*, *split level* and *cascade* or *step-hill* designs that are normally found on average to high slopes and are the designs studied in Chapter 8. The *amended section* uses several floor levels that normally have different access depending on the terrain configuration. With the *split level* design the building floors are organised in several levels, which can be based on half storey variation of levels. The *cascade* or *step-hill* designs generate an off-set that is linked with slope degree (Figure 4.14). With the latter design it is possible to create horizontal and or vertical subdivisions, forming several individual units (Figure 4.15). The last way is by erecting *houses on posts*. As illustrated in Figure 4.16, the building is suspended and, therefore, detached from the ground (Simpson and Purdy, op.cit, pp. 85-86).

Figure 4.14: Cascade house. Casa Tóló by Álvaro Leite Siza Vieira, Vila Real, Portugal. http://ultimasreportagens.com

Figure 4.15: Cascade multi unit housing by Ken Architekten BSA AG, Brugg, Switzerland. http://architizer.com

Figure 4.16: House on posts. by Hiroyuki Arima, Fukuoka, Japan. http://architizer.com

Slope building design, as *cascade* is commonly understood to be the best solution for steep slopes, as the "*profile keeps close to the natural slope and so helps the building to integrate with its immediate landscape. The stepped profile can provide*

clear, unobstructed views without loss of privacy. It is hardly surprising that it is a favoured form with those seeking to exploit the full potential of sloping sites where the land is to be use intensively" (Simpson and Purdy, op.cit, p. 129).

4.4.3. Structure Integration and Roof Coverage

The elevational design described in Chapter 3 is generally pointed out as the ideal design for slope-integration. Although the long shape of an elevational design requires larger sites than a (more compact) conventional building, the design can be adapted to be integrated into slope sites, and building density can increase according with the slope. In steeper slopes there is the advantage of increasing the building density, but also the disadvantage of limited site selection. Considering passive solar gains, only south, south-east and south-west slopes are suitable for buildings with an elevational design (Sterling, Carmody and Elnicky, op.cit., p. 105).

As explained above, elevational design can be used to create multiple attached configurations, forming single or multiple units with several floors or side by side. By combining units the construction costs of each unit can be reduced, as can land use, and the units become increasingly energy efficient (Sterling, Carmody and Elnicky, op.cit., p. 105). It should be noted that the building shape affects its thermal performance, and this is due to surface area. Comparing a square shaped building with a rectangular building with equal floor area it is evident that the surface area changes. A compact form such as a square has a lower surface area than the longer form of a rectangle and the higher the surface area the higher the building's heat losses will be (Underground Space Center, 1979, p. 35). Therefore, instead of constructing just one floor, if the total area is distributed between two or more floors the building shape is more compact, and consequently the total surface area and resultant heat losses decrease. This design can also reduce the circulation problems that one floor plan units often experience (ibid., p. 40).
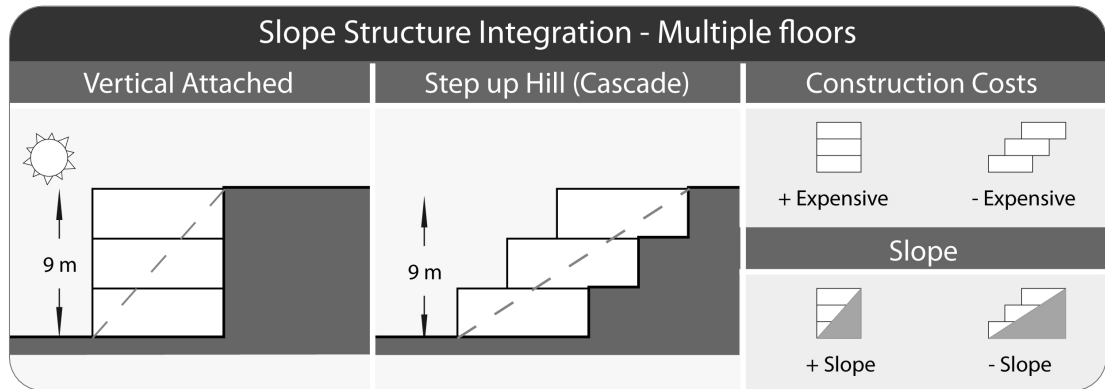
Figure 4.17: Slope structure integration of multiple floor building; based on Sterling, Carmody and Elnicky (1981)

Although several units can be vertically attached, the costs of retaining an earth berm of 9 m or higher are large (Figure 4.17). A *cascade* or *step-hill* approach is a better solution since it is easier to construct and has lower construction costs (Sterling, Carmody and Elnicky, op.cit., p. 105). This last approach also does not require steeper slopes, as it facilitates the provision of individual access to each unit and it benefits from separate external areas if the front façade follows the slope.

Figure 4.18: Grass roof coverage, Edgeland House by Bercy Chen Studio, USA. http://www.bcarc.com

Figure 4.19: Bare soil coverage, Sustainable House in Douro Valley by Utopia - Arquitectura e Engenharia Lda. Vila Real, Portugal http://architizer.com

Regarding roof coverage, and as previously discussed in Chapter 2, generally the daily weather conditions cease to affect the ground temperatures from 30 cm depth, and consequently this would be the minimum roof soil coverage value necessary to produce some energy savings. Roof soil coverage, however, needs to also consider ground surface type, because bare soil surface or a grass surface will require lower depths than a soil covered roof with shrubs or trees (Figure 4.18 and 4.19).

Therefore, it needs to be pointed out that the structural costs could increase with the amount of roof coverage. Soil depths of 30 to 46 cm are advisable for grass covered roofs, small shrubs require 61 to 76 cm of soil, and large shrubs and trees should need soils depths of around 152 cm (Underground Space Center, op.cit., p. 46).

4.4.4. Topography Influence on Building' Solar Access and Density
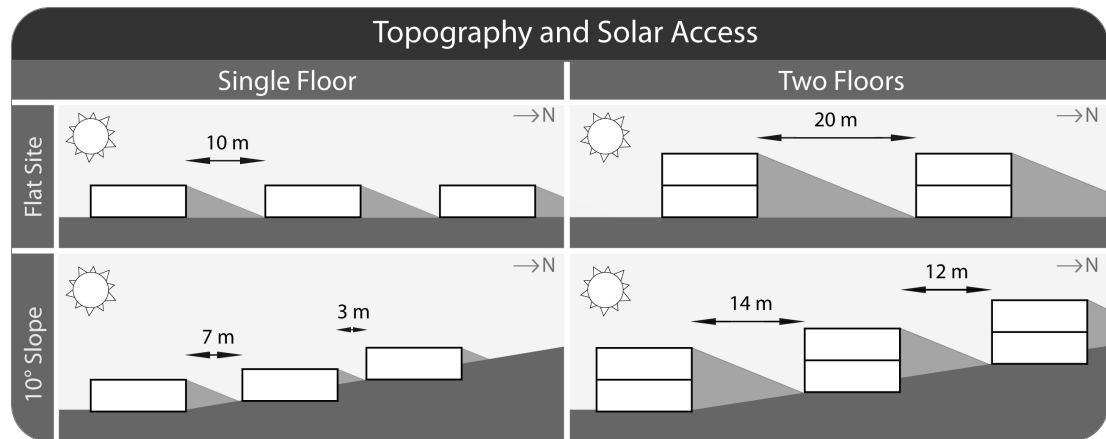
Figure 4.20: Density based on floor number and topography

Building design should take in consideration local topographical aspects such as slope degree and orientation from the earliest design stages. The number of buildings that can be constructed on a site is closely affected by the topography of the site because it will influence buildings' solar access, as shown with Figure 4.20. Designing for a flat site, a south-facing slope site or a north-facing slope site will require different spacing between buildings. The site density on a south-facing slope is higher than a flat location, and a north facing slope requires a larger area to achieve similar building numbers (Sterling, Carmody and Elnicky, op.cit., p. 123). Another factor that interferes with site density is the number of floors planned for each unit. A single floor building is more appropriate for a flat site and a two-storey building is more appropriate for terrains with a 20% inclination (Sterling, Carmody and Elnicky, op.cit., p. 137).

Table 4.3: Topography effect on buding density

Topography*		Lot size (4 units)*	Building density (units/hectare)*	Percentage of building density (%)	
Flat		36 m x 118 m	9.4	100**	-
Slope	10%, south-facing	27 m x 112 m	13.2	140.4	+ 40.4
	10%, north-facing	48 m x 127 m	6.56	69.8	- 30.2
	20%, south-facing (two floor units)	24 m x 70 m	23.8	253.2	+ 153.2

*Values retrieved from Sterling, Carmody and Elnicky (1981); data converted to units per hectare;
**Value set as 100% for comparison with different slopes.

The topography, lot size and building density values presented in Table 4.3 are based on Sterling, Carmody and Elnicky study (op.cit., p. 137). These values allow us to compare the relationships between topography, floor numbers and site density. The author used those values to add to the table the percentage difference of building density according to the site inclination and orientation. The values of this new column assume that the flat terrain is 100%. From this assumption, all remain values were calculated based on the following relation: if a density of 9.4 is equal to 100, then a density of 13.2 will be equal to x. Therefore x will be obtain by multiplying 13.2 with 100, which will be divided by 9.4. This operation was repeated for all the table rows. The following step, the density percentage of the flat area was assumed as the pivot value: above this values the percentage difference is positive and below this values the percentage difference is negative.

With the values resulting from this procedure it was possible to verify that the lot size required for a 10% south-facing slope is lower than for a flat site and, without compromising solar access, the site density can be expanded to 40.4%. However a north-facing slope requires 30.2% more land than a flat site because the density of unit per hectare is lower. When the living area of the units on a site is spread between two floors the individual lot size is reduced. If this configuration is set on a 20% south-facing slope the overall density increases by 153.2%, when compared with the single floor units on a flat site. This shows that site density is dependent on topographical aspects such as slope orientation and degree, as well as a lot size resulting from single or multi floor unit designs.

4.5. CASE STUDIES

4.5.1. Slope Ground Integration – New Concepts and Proposals
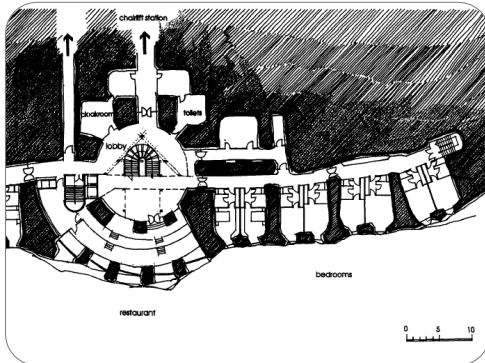
Figure 4.21: Hotel plan. Labbe and Duffaut, 1995
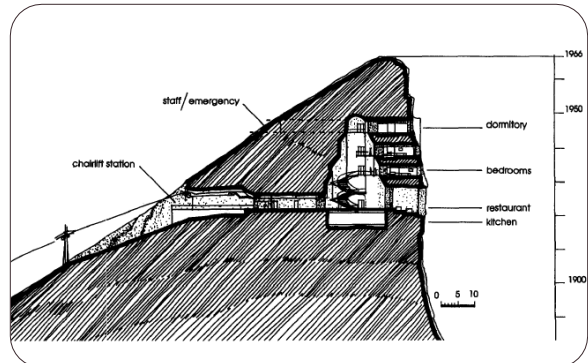
Figure 4.22: Hotel section. Labbe and Duffaut, 1995

Labbe and Duffaut (1995) propose the design of an underground hotel inside a hilltop in Grenoble, France. Labbe and Duffant's design (illustrated through Figure 4.21 and 4.22) explores the advantages of underground constructions on slope sites by using the hill's internal space. The design solution took into account the preservation of the landscape, which provided both technical and psychological benefits. The listed technical advantages are thermal and sound insulation provided by the ground, good ventilation, use of solar and wind energy sources, and manageable access routes (ibid., p. 158). As for the psychological benefits, elevated underground constructions can offer good views. Also, the access is ascendant, which could remove issues surrounding claustrophobia or disorientation as the greater the slope gradient, the shorter the building access (ibid., p. 159).
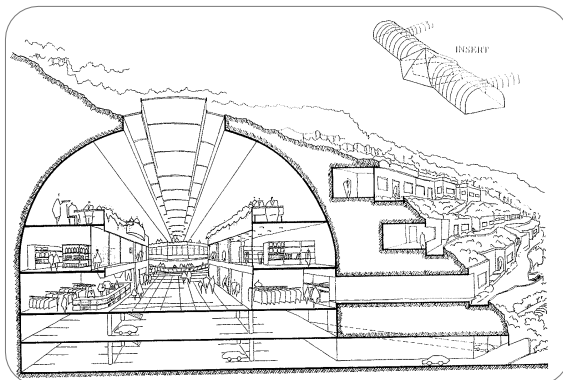
Figure 4.23:Slope-integrated houses and shopping area. Golany, 1995
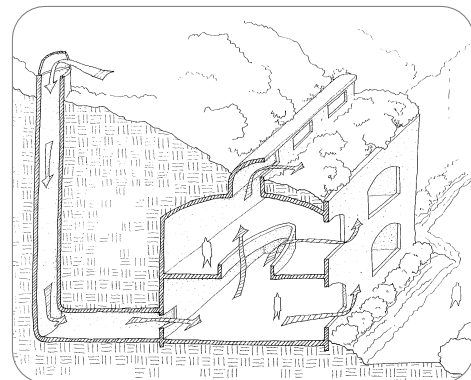
Figure 4.24: Passive ventilation system for slope buildings. Golany, 1995
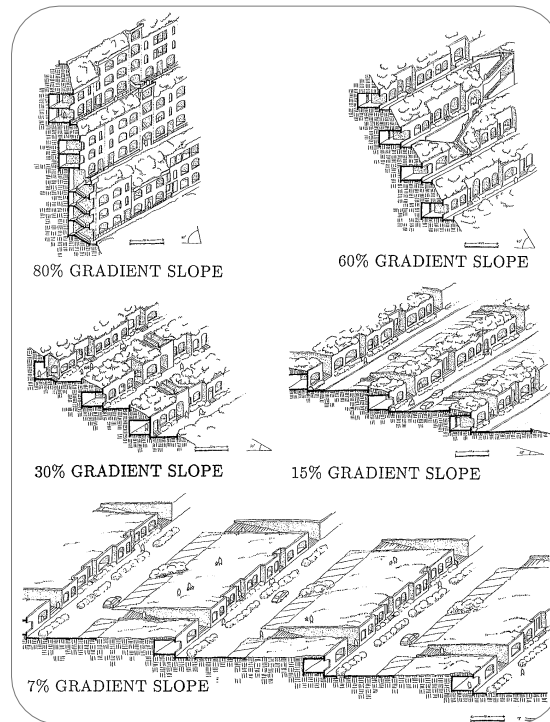
Figure 4.25: Slope-integration for different gradients. Golany, 1995

Golany's (1995, p. 220-231) *geospace* city concept seeks to maximise the land topology and the levels of integration through different ground depths. Sloped terrains are the core element for these spaces, and are considered the ideal site topology. In this concept, the slope works as a pivotal point for the city structure and as a gateway between internal and external areas, as illustrated in Figure 4.23 and 4.24. This deployment of the slope maximises light, land, solar exposure and natural ventilation potential. The slope's habitat design could use to its advantage gradients from 7% to 80%, and the ground integration can vary between total and semi-integration, or can be combined with above ground zones (Figure 4.25).
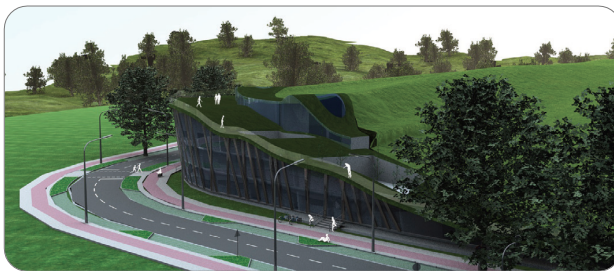
Figure 4.26: View - projected building. Lembo, Marino and Calcagnoa, 2011
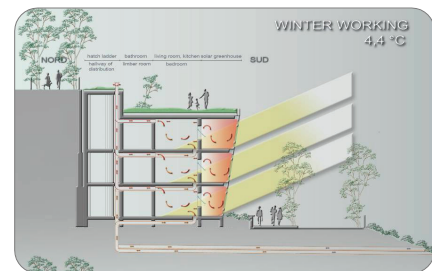
Figure 4.27: Cross-sections; winter. Lembo, Marino and Calcagnoa, 2011

Lembo, Marino and Calcagnoa (op.cit., p. 570) propose a semi-underground building for the rehabilitation of urban mountainous areas in Basilicata, where these semi-underground constructions are part of local building traditions. Their proposal takes advantage of the site's climatic and morphological characteristics. The semi-underground building is integrated into the environment by being placed on a south-facing hill, allowing the roof to be used as a garden and for walking paths, as shown in Figure 4.26 and 4.27 (ibid., pp. 573-577). It benefits from daily and seasonal thermal control and avoids overheating through reduced surface solar exposure and avoids cold winter winds. The project considers the use of earth to air pipes (indirect contact) and ventilation chimneys (stack ventilation) to provide better ventilation and thermal environment.

4.5.2. Reuse of Old Concepts - New Cave Dwelling Design
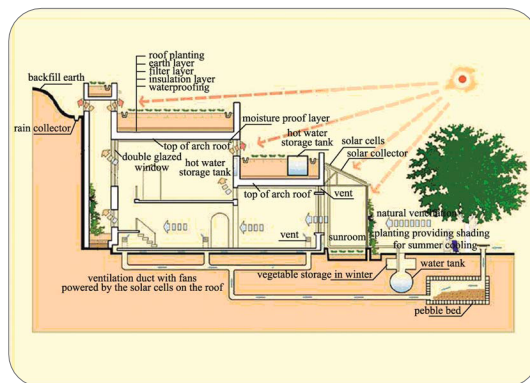
Figure 4.28: Cross-section. Liu et al., 2010

Figure 4.29: Cave dwelling. Liu et al., 2010

Liu et al. (op.cit., pp. 122-123) proposes a new cave dwelling model for slope terrains, as illustrated in Figure 4.28 and 4.29. Based on Chinese traditional ground-integrated houses, the prototype tackles main problems of these traditional constructions such as reduced internal space, irregular temperature distribution, poor indoor air quality and poor natural light. The traditional one-floor house is adapted into a two-floor space, with a sunspace integrated on the front façade. This design also incorporates an EAHE system and takes advantage of green roofs (ibid., 125). The constructed buildings proved to be energy efficient. The comfort

conditions were reported to be satisfactory for 70% of the inhabitants during the winter, and by 85% of those during the summer. With regard to its natural light and ventilation, the satisfaction values were nearly 100% (ibid., 129).

4.5.3. Thermal Performance and Construction Cost

Lee and Shon (op.cit., p. 409) studied the thermal performance of a sloped ground-integrated house, comparing its efficiency to an above ground house. Since hill terrains form 80% of South Korea's land and 70% of this area is forested, most of the population is concentrated on a limited percentage of land. According to the authors, ground-integrated buildings are able to preserve energy and land area, and can be better adapted on the available slope land. This type of construction achieves the best thermal behaviour and provides better thermal comfort throughout the year (ibid., p. 416). The ground-integrated house has lower diurnal temperature range, which provide a more stable inside air temperature. The outdoor air temperatures had a lower effect on the internal temperatures compared to similar above-ground dwellings.
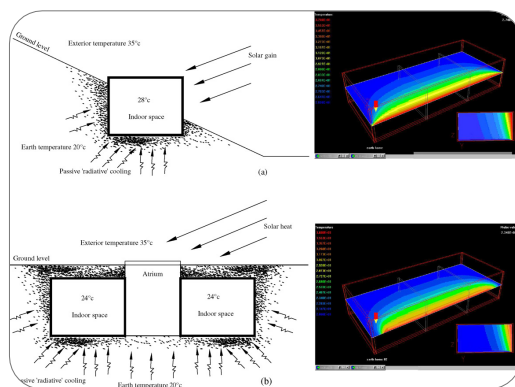
Figure 4.30: Summer performance of a slope design and a courtyard design structure. Anselm, 2008
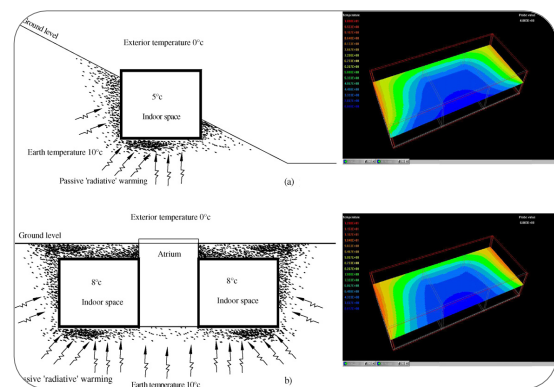
Figure 4.31: Winter performance of a slope design and a courtyard design structure. Anselm, 2008

Anselm (2008) studies the potential of ground-integrated buildings as an energy conservation system. The study analyses the heat flux patterns to identify the potential of ground-integrated buildings as an energy conservation system through computer simulation (Figure 4.30 and 4.31). Two ground-integrated structures are

compared in Anselm's study: a slope design model with 50% ground direct contact, and a courtyard design structure with 80% direct earth contact. The study concludes that the higher the level of ground integration, the better the building's thermal performance.
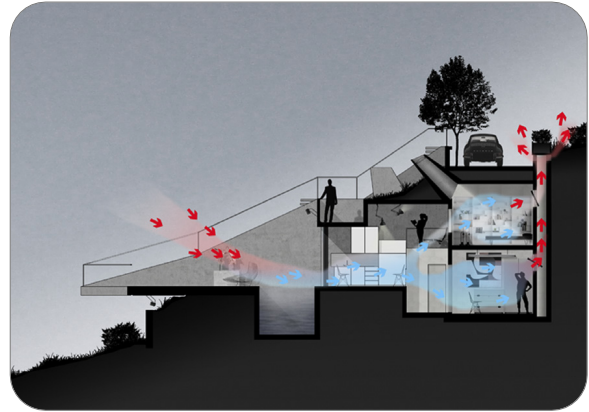
Figure 4.32: Left up: Front view of slope-integated residence. Benardos, Athanasiadis and Katsoulakos, 2014
Figure 4.33: Left down: Front view of above ground residence. Benardos, Athanasiadis and Katsoulakos, 2014
Figure 4.34: Up: Buiding section with air flow - Slope-integated residence. Benardos, Athanasiadis and Katsoulakos, 2014

Benardos, Athanasiadis and Katsoulakos (2014) use one slope-integrated design and one above ground residence design of similar characteristics to compare the thermal performance and building costs of the two buildings (Figure 4.32 to 4.34). The location of the study is the Kea Island in Greece, which according to the authors, is suitable for slope-integrated buildings due to its topography and warm climate. The calculation of energy needs and energy consumption is made with the EN 13790 standards. The results of the study showed that the thermal performance of the slope-integrated design is better than the above ground design, as it provide cooling savings of 25% and total energy demand savings of 42% (ibid., p.50). The authors believe that with a dynamic energy analysis method the difference in results between the designs would be greater. The construction cost analysis indicates that above ground design is 8% lower than the slope-integrated design. This small cost difference reveals that a slope design was affordable, and its reduce maintenance as well as operational cost could bring this gap even closer (ibid., p.52).

4.6. CONCLUSIONS

The world's rapid urban growth demands more construction land. This demand is contributing to the reclamation of agriculture land for construction. The rising global population and the expected food shortage intensifies these problems. Current construction practices not only consume large amounts of arable land also waste considerable energy resources. The use of hillside sites for construction has the benefit of using land that is considerably less suitable for farming.

Topographical aspects such as altitude, slope orientation and degree have a great effect on air temperature, total solar radiation and wind. These factors can affect daily and seasonal air temperature values and patterns, and determine the solar radiation values received by a surface, as well as produce katabatic and anabatic winds.

Slope-integrated settlements are an old construction configuration that has proved to be land and energy efficient. By maximizing the spatial potential of slopes through building ground-integration there is an increase in thermal advantages. These settlements provide better thermal comfort and ventilation than flat land settlements and benefit from slope flow.

Slope-integrated buildings reflect a *site inspired* or a *special design* approach to architecture, since site form and restrains are embraced during the design process. These approaches are in opposition to a *land-form* adapted approach, where a slope site is flattened. The site slope angle can be the base for the slope building design, which can be an *amended section*, *split level* and *cascade* or *step-hill*. The building structure integration needs to take into consideration building floor levels and slope degree. These issues can be addressed through *vertical attached* and by *cascade* or *step-hill*, which for multiple levels can be less expensive. Covering the roof with large amounts of soil can also be expensive; therefore, if there are no thermal benefits this solution should be avoided. Southern slopes are ideal for slope-integrated buildings, as it provides good solar access with higher site density.

CHAPTER 5. GROUND THERMAL POTENTIAL IN TEMPERATE CLIMATE

5. GROUND THERMAL POTENTIAL IN TEMPERATE CLIMATE

As discussed in Chapter 2, climate conditions have a great impact on ground thermal potential. Ground temperatures are largely dependent on air temperature, on solar radiation values that are in turn affected by latitude and, as discussed in Chapter 4, by topographical characteristics such as altitude, slope degree and orientation. Considering these characteristics, this chapter analyses the potential of the use of ground thermal in a temperate climate, by looking into its application in Portugal's mainland. Since Portugal's temperate climate features a diverse range of conditions, it makes for a good base of study, as conclusions drawn from its range of conditions offers a broad range of potential applications to a larger number of countries with a particular type of temperate climate.

5.1. THE STUDY AREA

5.1.1. Climate Zones

Mainland Portugal is located on the western side of the Iberian Peninsula, between latitudes of 37° to 40°N. The country's northern and eastern areas are bordered by Spain and its western and southern areas are limited by the Atlantic Ocean. The average altitude differs between northern and southern areas. While the north landscape is formed of mountainous terrain, with 90% of the land above 400 m, the southern areas are flatter, with around 60% of the land below 400 m above sea level (Inácio, Pereira and Pinto, 2008, p. 22).

Portugal's temperate climate is modulated by factors including latitude, altitude, and proximity to the Atlantic Ocean. The average maximum temperatures during the summer are between 30ºC to 40ºC, and the average minimum temperatures range between 10ºC and 15ºC. During the winter, the average maximum temperatures are between 10ºC to 25ºC and the minimum average temperatures are typically between -7ºC and 3ºC.
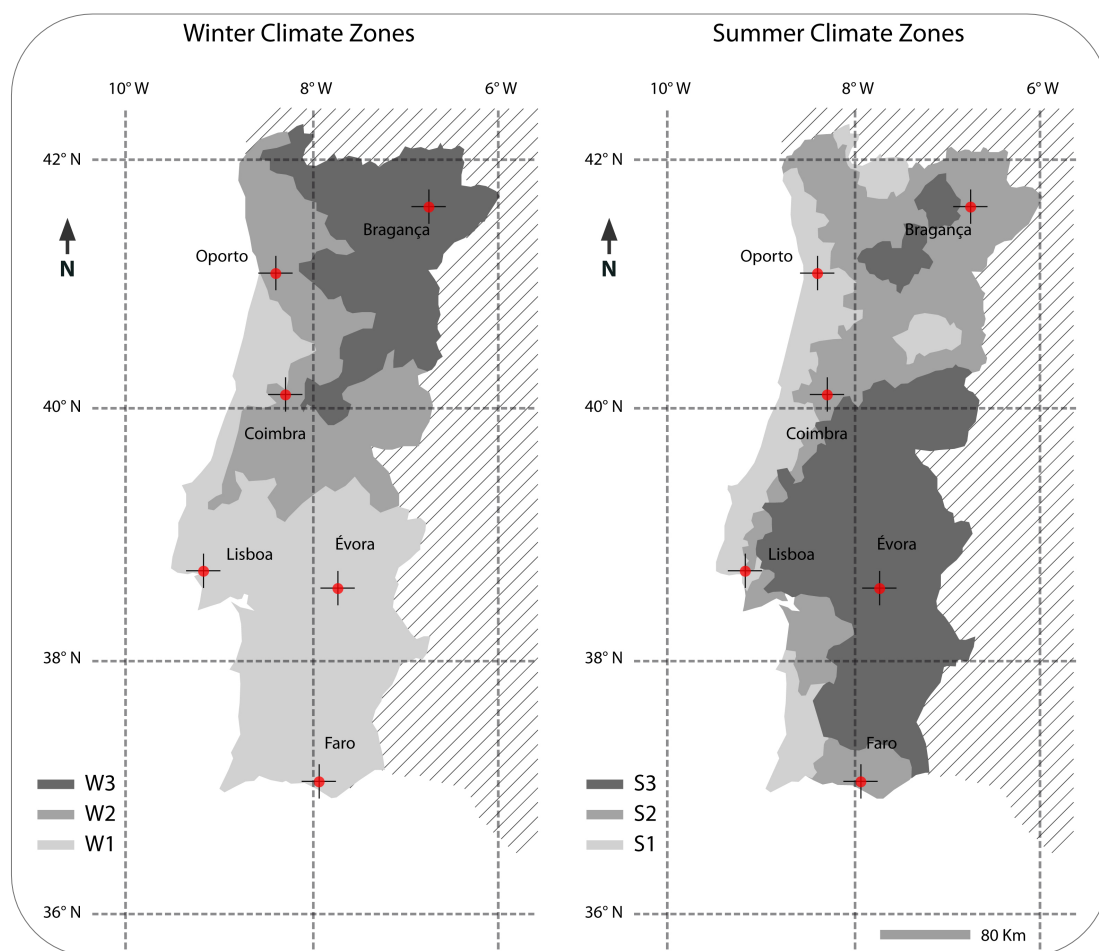
Figure 5.1: Portugal, Main land – Winter and summer climatic zones. Illustration based on Ministério Das Obras Públicas & Comunicações, 2006

Table 5.1: Portugal's winter and summer climate zones - average temperature limits values based on Ferreira and Pinheiro (2011, pp. 7667-7668).

Winter Climate Zones		W1	W2	W3
Ave. Temp. (°C)	November	> 12	10.5 – 13.5	0 – 9
	December	> 10	8 – 12	0 – 6
	January	> 9	7 – 11	0 – 7
	February	> 9	7 – 9	0 – 7
	March	> 11	9.5 – 12.5	0 – 8
Summer Climate Zones		S1	S2	S3
Ave. Temp. (°C)	June	23 – 29	25 – 29	> 29
	July	23 – 31	31 – 35	> 35
	August	> 23 – 30	30 – 34	> 34
	September	25 – 28	25 – 28	> 28

The Portuguese climate is divided into several different winter and summer climatic zones. As illustrated in Figure 5.1 and shown in detail in Table 5.1, there are three winter climatic zones (W1, W2 and W3) and three summer climatic zones (S1, S2 and S3) (Ministério das Obras Públicas and Comunicações, 2006, p. 2477), the order of these zones is defined as mild (1), moderate (2) and severe (3).
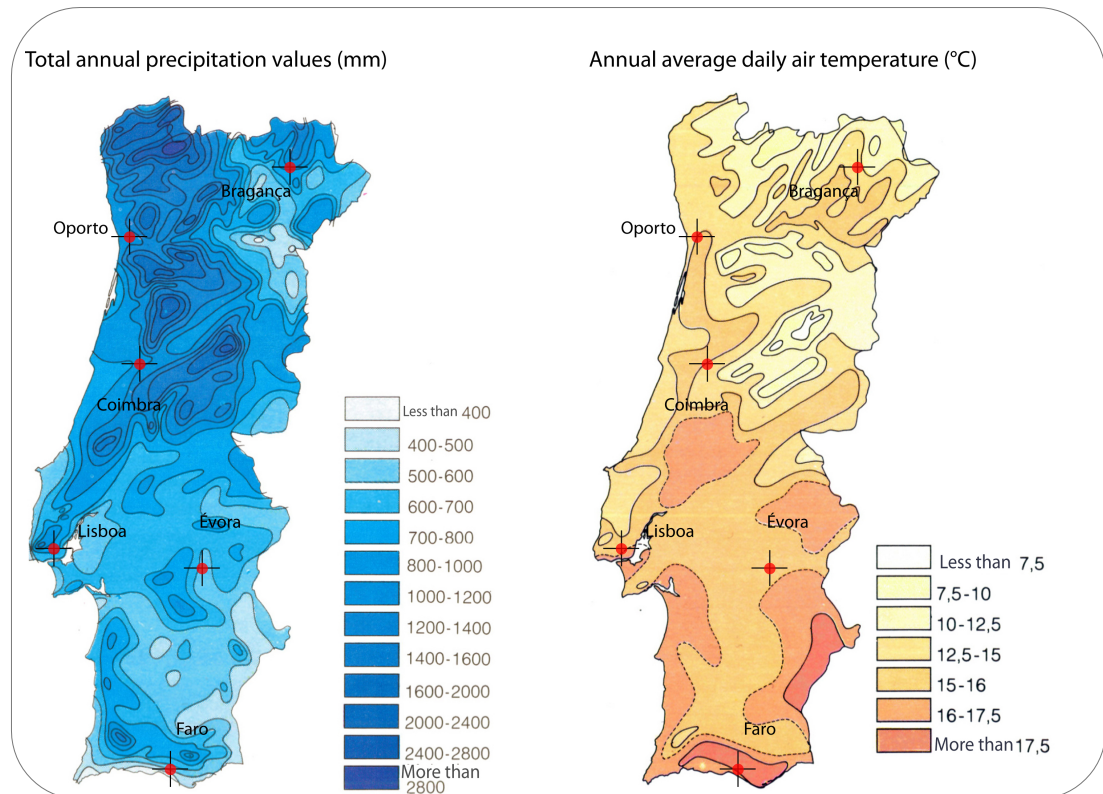
Figure 5.2: Annual precipitation and average daily temperature, portugal. Illustration adapted from Selecções do Reader's and Instituto Geográfico (1988, p. 59).

Areas near the Atlantic coast, such as Oporto, Lisbon or Faro, benefit from less extreme temperatures during the year. On a North-South axis, northern areas of Portugal are subject to higher heating demands. During the winter, low temperatures and occasional snowfall are registered at northern high-altitude areas such as Bragança, Vila Real and Guarda. As can be seen in Figure 5.2, areas including the north (Oporto) and north-central littoral (Coimbra) zones have higher annual precipitation values and consequently lower annual solar radiation values than south-centre inland and southern coastal areas (Lisbon and Faro).

5.1.2. Energy Production and Consumption in Portugal

According to data from Eurostat (2015), which is shown in Figure 5.3, during 2013 the percentage of Portuguese gross final energy consumption that originated from renewable sources was 25.7%, which is above the average values for the rest of the European Union. The Portuguese targets for 2020 show that there is a clear interest in increasing the use of renewable sources by 5.3%.
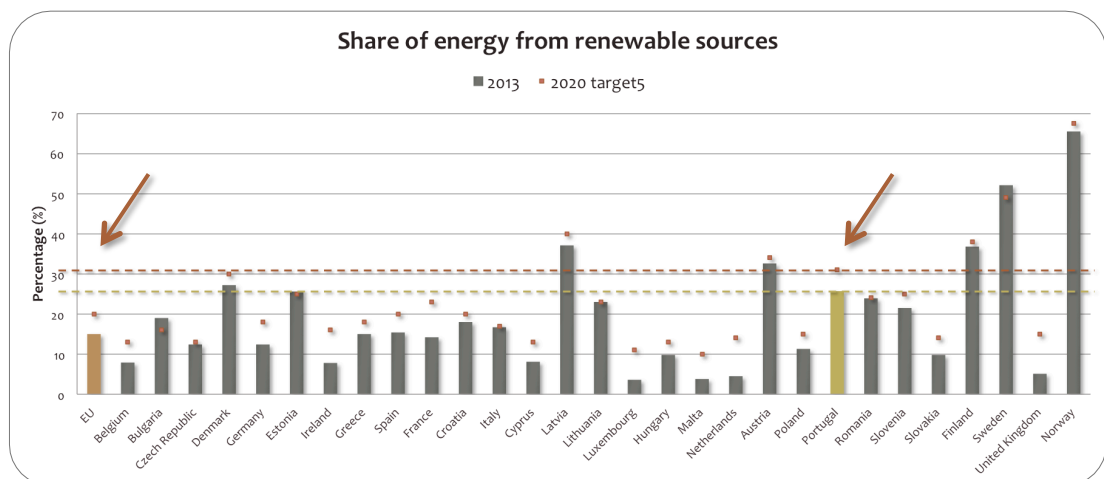
Figure 5.3: European share of energy from renewable sources, 2009 and 2013. Eurostat, 2015

During the same period, the annual consumption of electric energy by inhabitants of Portugal was 4425 kWh/inhab. Of this consumption, 1177.2 kWh/inhab was household consumption (INE, 2015), a number that corresponds to a quarter of the total electric energy consumption. The relevance of these values comes from the fact that renewable sources were able to produce almost half (49.2%) of the total electricity generated in Portugal (Eurostat, 2015), with wind and hydro energy as the main sources, followed by thermal, photovoltaic and geothermal (INE, 2015).

Looking further into the energy consumption of Portugal, and especially the annual quota of final energy consumption per sector in Figure 5.4, it is visible that during 2013 more than one third (36%) of this energy quota was used by the transport sector, almost one third (30%) was used by industries, and the domestic sector was the third main consumer, using 17%.
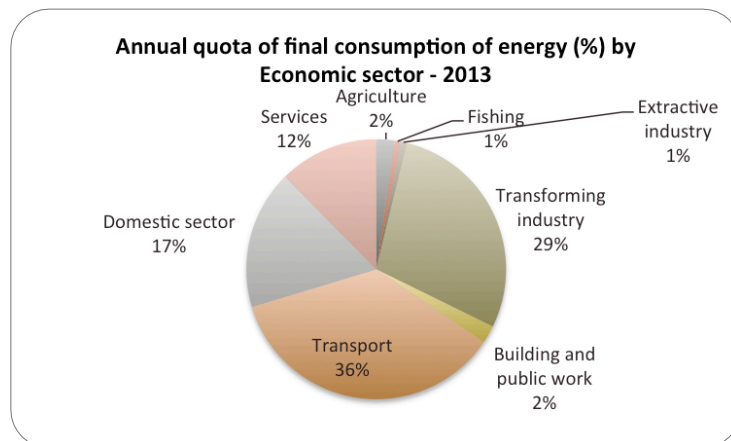
Figure 5.4: Portugal's quota of final energy consumption, 2013. INE, 2015

Table 5.2: Average of energy consumption by dwelling and Consumption of electricity by type of utilization, 2010. INE, 2015

Average energy consumption (%) by dwelling				
Heating	Cooling	Water heating	Kitchen	Lighting, appliance etc.
17.5%	-	20%	33.3%	29.2%
Consumption of electricity (%) in conventional dwellings by type of utilization				
Heating	Cooling	Water heating	Kitchen	Lighting	Small appliances, entertainment and computer related equipment)
9.06%	1.60%	2.39%	40.52%	13.56%	32.86%

Based on the 2010 statistics, heating energy needs correspond to 17.5% of the average energy consumption per dwelling (Table 5.2), which includes several types of energy sources as heating oil, firewood, solar thermal, natural gas, electricity and others. Regarding only the electricity consumption per type of utilization, 9.06% of total electricity production is used for heating, while only 1.60% is for cooling, which shows that heating has a much higher impact on building energy consumption.

5.1.3. Residential Building Statistics

Table 5.3: Building density, 2001. INE, 2015

Buildings density 2001 No./ km²	Mainland	North	Centre	Lisbon	Alentejo	Algarve
	33.6	51.6	35.1	133.1	11	32.1

The dwelling density of Portugal's mainland in 2001 (Table 5.3) shows a large concentration of dwellings in the northern areas of the country and a very high concentration around Lisbon. The lowest building density is in the upper south areas including Alentejo, which registered a density value well below the mainland values.
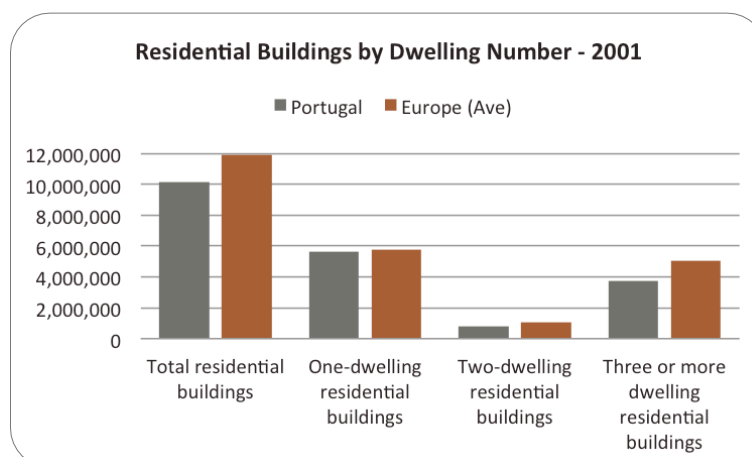
Figure 5.5: Residential buildings by dwelling number, 2001. Eurostat, 2015

The total number of residential buildings in Portugal closely follows the European average (Figure 5.5), with the single-family house being the main type of dwelling. According to the data from Eurostat (2015), in 2001 Portugal's one-dwelling residential buildings corresponded to 55% of the total number of residential buildings, a value which is 7% higher than the European average of 48%. Residential buildings with two dwellings corresponded to 8% and buildings containing three or more dwellings accounted for 37% of total domestic buildings.

Table 5.4: Conventional dwellings by Building in Portugal's mainland 2001. INE, 2015

Conventional dwelling by building, 2001	Mainland	North	Centre	Lisbon	Alentejo	Algarve
	1.6	1.4	1.2	3.2	1.2	1.7
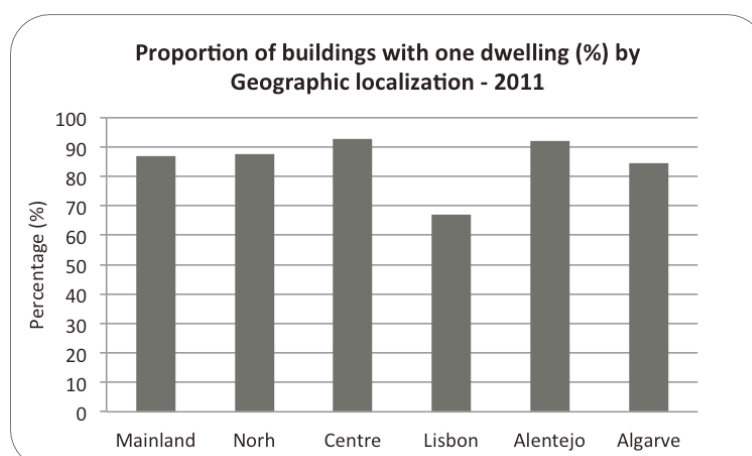
Figure 5.6: Proportion of buildings with one dwellings in Portugal, 2011. INE, 2015

Looking at the proportion of conventional dwellings by building (Table 5.4) in 2001, and based on the percentage of buildings with one dwelling and their distribution across the Portuguese mainland in 2011 (Figure 5.6), it can be argued that the

single-family house is the main type of dwelling in non-urban areas. In contrast to this, in urban areas such as Lisbon multiple occupancy buildings are the most commonly found type of building, particularly apartment buildings.

Table 5.5: Number of floors and rooms, and average room utility area per complete residential building. INE, 2015

	Mainland	North	Centre	Lisbon	Alentejo	Algarve
Number of floors, 2014	2.1	2.2	2.1	2.6	1.6	2.6
Number of rooms, 2014	5	5.3	5	5	5.1	4.2

Recent INE statistics from 2014 (Table 5.5) show that the average number of floors per completed building in new family housing constructions are 2.1. At Alentejo the traditional one floor dwelling is still the norm among newly constructed buildings, while the buildings in the Algarve and Lisbon have equally the highest number of floors with an average 2.6. The average number of rooms in newly constructed family housing in 2014 is five.

5.2. GROUND THERMAL POTENTIAL IN PORTUGAL

To identify the ground thermal potential in Mainland Portugal it is necessary to know the ground temperature at different depths. This section examines the ground thermal potential of six different locations in Portugal by using mathematical formulae to calculate the corresponding ground temperatures at different depths during the year.

5.2.1. Formulas to Calculate Ground Temperature

The annual ground temperature at different depths can be calculated through Labs' (1979) one-dimensional sinusoidal equation that is expressed below in Equation 5.1 and using values from Mihalakakou et al.'s (1997) Equations 5.2 and Equation 5.7, and also using Szokolay's (2014, p. 10) soil surface convective heat transfer Equation 5.6.

$$T_{(x,t)} = T_m - A_s e^{-x\sqrt{\frac{\pi}{365\alpha}}} \cos\left\{\frac{2\pi}{365}\left[t - t_o - \left(\frac{x}{2}\right)\left(\sqrt{\frac{365}{\pi\alpha}}\right)\right]\right\}$$

Equation 5.1

Where:

- $T_{(x,t)}$ = ground temperature (ºC) at a depth x (m) and time t is the day of the year, the reference day is January 1st;

- Tm = mean annual temperature of the ground (ºC);

- As = annual amplitude of the temperature wave at the soil surface (°C);

- x = depth (m);

- t = day of year (days);

- to = phase constant of day with minimum soil surface temperature (days);

- α = soil thermal diffusivity (m2/day).

$$T_m = \frac{1}{h_e}\left[h_r T_{ma} - \varepsilon\Delta R + bS_m - 0.0168 h_{sur} fb(1-r_a)\right]$$

Equation 5.2

Where:

- T_{ma} = mean air temperature at time $2\pi/\omega$ (°C);

- ω = frequency of the temperature wave, as $2\pi/365$ (rad/day);

- ε = emittance of the ground surface;

- ΔR = value dependent on humidity values of air over ground surface, sky temperature and soil radiative characteristics;

- b = coefficient of ground surface absorptivity and illumination;

- S_m = mean annual solar irradiance at the ground surface (W/m2);

- h_{sur} = soil surface convective heat transfer coefficient (W/m2K);

- f = fraction determined by ground cover and ground moisture content;

- r_a = relative humidity of the air above the ground surface.

The coefficient of ground surface absorptivity and illumination can be calculated by using the following equation.

$$b = 1 - albedo$$

Equation 5.3

Fraction f can be calculated for bare or grass covered soils. The fraction for bare soils increases with the soil moisture content (wet soil f = 1; humid soil f = 0.6-0.8; dry soil f = 0.4-0.5; arid soil f = 0.l-0.2). The fraction for grass covered soil is estimated by multiplying the above bare soil fraction values by a coefficient of 0.70 (Mihalakakou et al.'s, op. cit., p. 185; Mihalakakou, 2002, p. 253).

The h_e and h_r values can be calculated using Mihalakakou et al.'s (op.cit.) Equation 5.4 and Equation 5.5.

$$h_e = h_{sur}(1+0.0168af)$$

Equation 5.4

$$h_r = h_{sur}(1+0.0168ar_a f)$$

Equation 5.5

Where a is equal to 103.00 (Pa/K).

The soil surface convective heat is calculated with the following equation (Szokolay, op.cit.).

$$h_{sur} = 5.8 + 4.1 \times u$$

Equation 5.6

Where u is the wind speed.

The annual amplitude of the temperature wave at the soil surface is calculated with the following equation (Mihalakakou, et al.,op.cit.).

$$A_s = [h_r A_{sa} - b S_a \exp(i\varphi_1 - \varphi_a)] / (h_e + K_s)$$

Equation 5.7

Where:

- A_{sa} = amplitude of air temperature wave at 2π/ω (°C);

- Sa = amplitude of solar irradiation wave (W/m2);

- φ1 = phase constant (rad);

- φa = phase constant (rad);

- Ks = ground thermal conductivity (W/mK).

5.2.2. Locations and Ground Temperature Calculations Inputs

Table 5.6: Locations and correspondent climate zones

Location	Winter climate zone	Summer climate zone	Zone	
Oporto	W2	S1	North	Littoral
Bragança	W3	S2	North	Inland
Coimbra	W1	S2	Center	North littoral
Évora	W1	S3	Center	South inland
Lisboa	W1	S2	Center	South littoral
Faro	W1	S2	South	Littoral

The selected locations are Oporto, Bragança, Coimbra, Évora, Lisbon and Faro. The winter and summer climate zones are displayed in Table 5.6, in accordance with official project data from Ministério das Obras Públicas e Comunicações (2006, pp. 2477-2478).

Table 5.7: Nomenclature and values used on the ground temperature calculations at different locations

Location		Oporto	Braganca	Coimbra	Evora	Lisbon	Faro
Mean air temp, °C	T_{ma}	17.73	12.36	15.32	15.77	16.29	17.73
Amplitude of air temp wave, °C	A_{sa}	12.10	17.40	11.50	14.20	12.00	12.10
Phase constant	φ_a	0.10	0.10	0.10	0.10	0.10	0.10
Phase constant	φ_1	0.28	0.28	0.28	0.28	0.28	0.28
Mean annual solar radiation - ground surf, W/m^2	S_m	426.57	369.23	365.40	406.34	388.14	426.57
Amplitude of the solar radiation wave, W/m^2	S_a	342.29	397.00	342.00	370.71	349.29	342.29
Phase constant soil surf - Day with min. soil temp, Day	t_0	40	35	35	40	40	40
Value dependent of humidity and air, W/m^2	Δr	63.00	63.00	63.00	63.00	63.00	63.00
Pa/K	a	103.00	103.00	103.00	103.00	103.00	103.00
Emittance, 0 to 1	ε	0.93	0.93	0.93	0.93	0.93	0.93
Wind, m/s	u	3.61	2.61	2.31	4.40	4.99	3.61
Relative humidity, %	r_a	0.67	0.70	0.77	0.68	0.68	0.67
Soil absorptivity and illuminance = 1 - Albedo	b	0.70	0.80	0.80	0.70	0.75	0.70
Fraction of the soil, 0 to 1	f	0.50	0.50	0.50	0.40	0.50	0.50

The ground temperature calculations at different depths for the six locations were produced using Equation 5.1. The mean annual temperatures of the ground (T_m) are calculated with Equation 5.2; the annual amplitude of the temperature wave at the soil surface (A_s) is calculated with Equation 5.7. The inputs used for each location are displayed in Table 5.7, with their values based on monthly weather data, which are displayed in Appendix 1. This data is retrieved from the weather files distributed by E+ and are produced with public data published by the Instituto de Meteorologia, which are combined by Instituto Nacional de Engenharia, Tecnologia e Inovação data and made available to the DOE.

Table 5.8: Main types of rocks/soils

Location	Rocks/soils					
	Granite	Limestone	Sandstone	Shale (schist)	Clay	Sand
Oporto	X	-	-	X (wet)	X (wet)	X (wet)
Bragança	X	-	-	X	X	X
Coimbra	-	X	X	X	X	-
Évora	X	-	X	X	X	-
Lisboa	-	X	X	-	X	X
Faro	-	X	X	-	X	X

X	Materials used for the initial comparisons
X	Additional materials used for the amplitude damping comparison

Based on the geological characteristics (Selecções do Reader's and Instituto Geográfico, op.cit, pp. 42-45) of each location, four predominate type of soils have been selected. As displayed in Table 5.8, the highlighted rock or soil values are used for the ground temperature comparisons between these locations. To analyse the amplitude damping at each location the four correspondent soils are used in the calculations.

Table 5.9: Thermal properties values of selected rocks and soils – medium values

Class	Material	Dry Density (kg/m^3)	Conductivity (W/(m K))	Diffusivity (m^2/day)
Rocks	Granite	2650	3	0.107
	Limestone	2600	3.1	0.107
	Sandstone	-	2.8	0.38
	Shale, wet	2650	1.9	0.0745
	Shale, dry	2650	1.55	0.0645
Soils	Heavy clay, wet 15% water	1925	1.65	0.0515
	5% water	1925	1.2	0.054
	Heavy sand, wet 15% water	1925	3.3	0.097
	5% water	1925	2.2	0.1165
	Light sand, 5% water	1285	0.9	0.0875

The thermal properties of the rock and soil, such as conductivity (K_s) and thermal diffusivity (α), are based on the thermal properties values of selected rocks and soils, as presented in Table 5.9. These values correspond to the normal range of median values provided by ASHRAE (2011, p. 34.15), and its full range is display in Appendix 1.

5.2.3. Results and Discussion

Observing the ground temperature results at the different locations, which are presented in Figure 5.7, we can see that the values vary according with location. The results show a clear division between three main areas, divided into northern and centre-north littoral, northern and centre interior and centre-south and southern littoral.
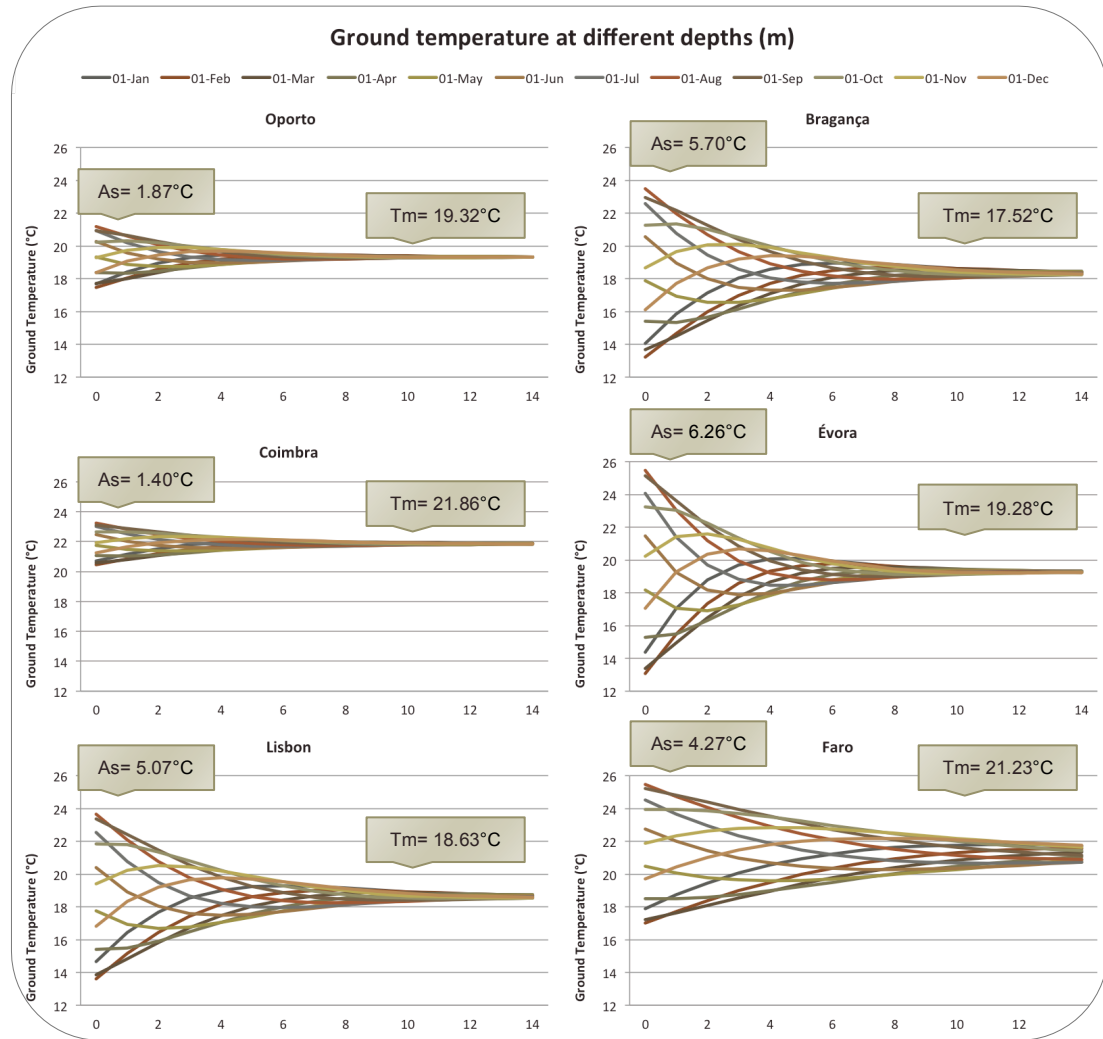
Figure 5.7: Ground temperature at different depths according with location

The northern and centre-north littoral area, which includes Oporto and Coimbra, has high mean ground temperature (T_m) values and low annual temperature amplitudes (A_s). This is due to the high precipitation values in the region and, the high ground moisture content that results from this precipitation. The northern and central interior areas, which include Bragança and Évora, provide the greatest annual temperature amplitudes (A_s) of all areas, because of the contrast between winter and summer climate conditions in these areas. The mean ground temperature (T_m) values are 17.52ºC at Bragança and 19.28ºC at Évora. The centre-south and southern littoral area, which comprises Lisbon and Faro, presents larger annual temperature amplitudes (A_s), and the average ground temperature (T_m) values are 18.63ºC in Lisbon and 21.23ºC in Faro.
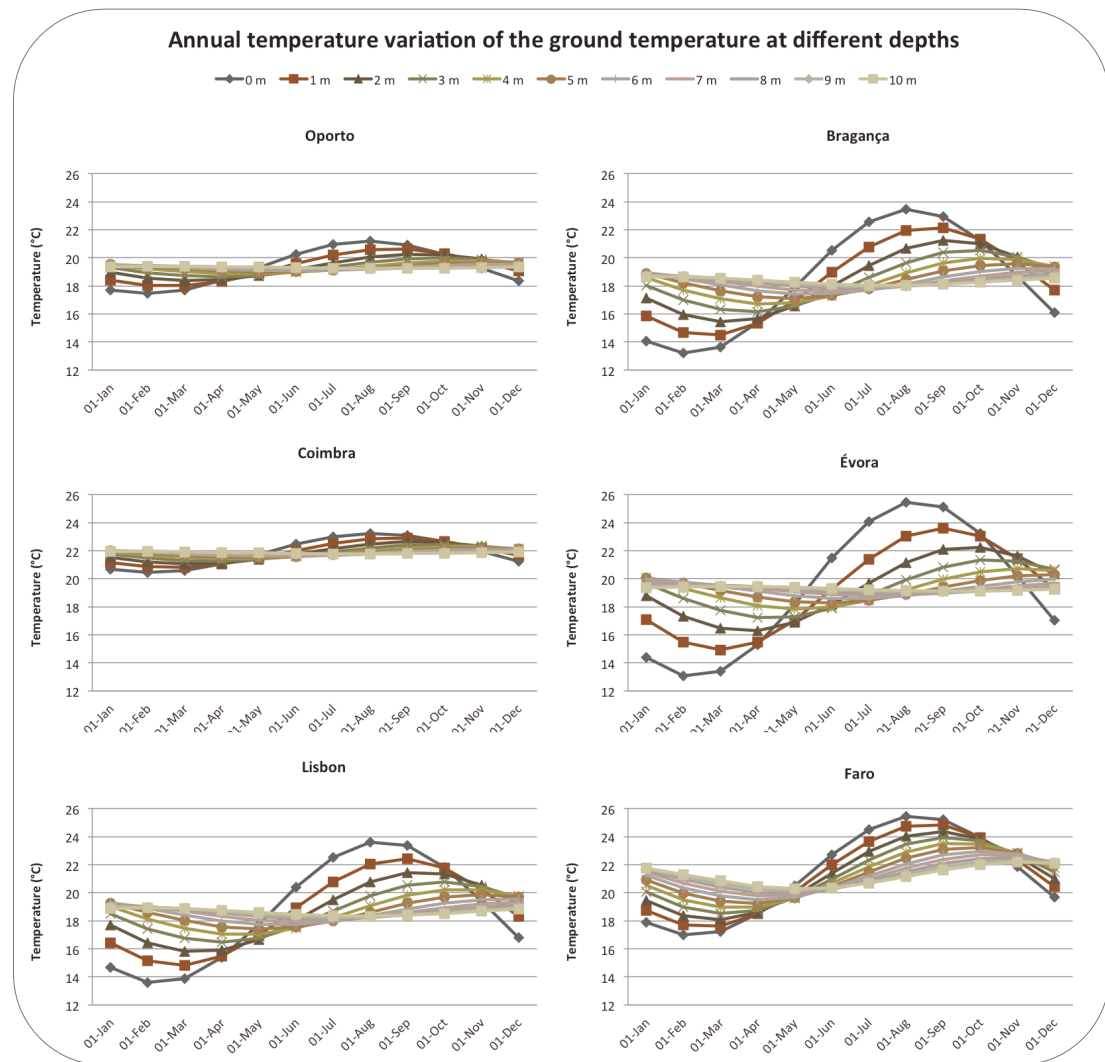
Figure 5.8: Annual amplitude of the ground temperatures at different depths and locations

Figure 5.8 shows the decrease in annual ground temperature variation and the time lag with depth. For all locations, while at the ground surface the coldest temperatures are found in February and the warmest in August, at 4 m the temperature lag is extend up to four months. The coldest temperatures at this depth are registered in May and the warmest temperatures are registered during November.

Figure 5.9 shows the ground heating and cooling potential at 3 m depth in the six studied locations. These figures establish that all locations can benefit from ground thermal potential. At this depth, the ground cooling and heating potential at Bragança and Évora are the highest, as these northern and central interior locations

provide the greatest ground thermal potential of all areas. The great ground thermal potential of these areas results from a combination of factors including high daily and annual air temperatures, moderate to high annual solar radiation values and low to moderate annual precipitation values.
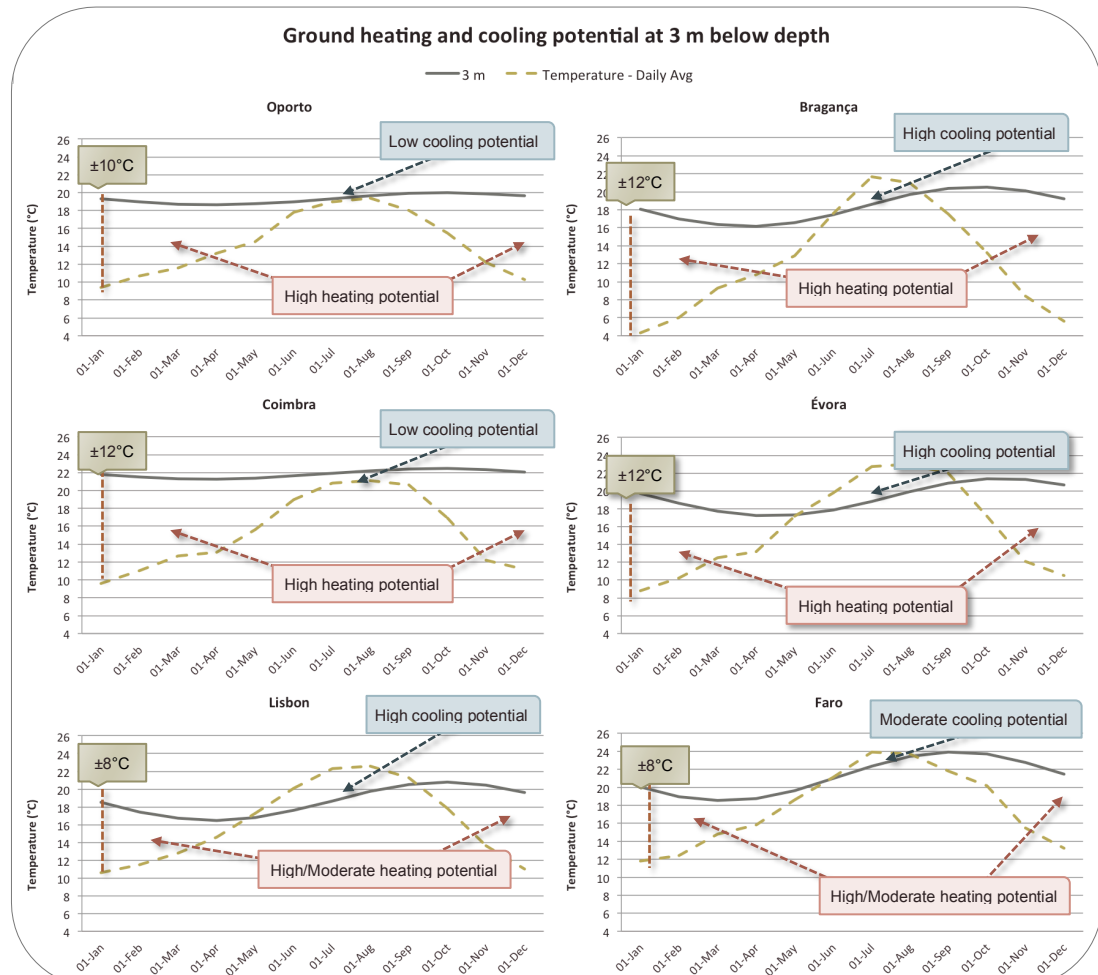
Figure 5.9: Ground heating and cooling potential at 3 m depth and at different locations

At Oporto and Coimbra, in the northern and centre-north littoral area, the heating potential is higher but the cooling potential is limited. Regarding Lisbon and Faro in the centre-south and southern littoral areas, the ground heating potential is considerable, in view of the mild winters, as well as the ground cooling potential, which is high at Lisbon. As for Faro, the ground cooling potential is moderate due to the high mean ground temperature.

Another factor to consider is the amplitude damping. The amplitude damping is the relation between the ground annual temperature amplitude and the depth where the mean ground temperature value is constant. This relation depends on soil characteristics such as soil thermal diffusivity. A fast temperature damping means that the mean ground temperature is reached at a depth closer to the ground surface. This is a relevant indicator in defining ground thermal potential because although the mean ground temperature is equal at all depths for a specific location, the depth that this value becomes constant through all year changes according with type of soil present in a location. Using the values from Table 5.7 and 5.9 the amplitude damping of the main soil type at the six locations (Table 5.8) was calculated using Labs' (1979, p. 48) Equation 5.8 and the results are illustrated in Figure 5.10:

$$A_x = A_s e^{-x\left(\frac{\pi}{365\alpha}\right)^{\frac{1}{2}}}$$

Equation 5.8

Where:

- A_s the annual amplitude of the temperature wave at the soil surface (°C);

- x the depth (m);

- α is the soil thermal diffusivity (m^2/day).

The results shown in Figure 5.10 demonstrate that soil characteristics such as thermal diffusivity, which varies with moisture content, produces different amplitude damping. It is observable that light and dry soils have faster damping than heavy soils. The soil thermal diffusivity is far more relevant in Lisbon, Évora and Faro than at locations such as Oporto and Coimbra. This is because of the moisture content of the ground, as greater moisture values have a higher impact on thermal diffusivity than soil types. Therefore, at locations with high annual precipitation values, such as Oporto and Coimbra, the type of soil produces a low effect on ground temperatures.
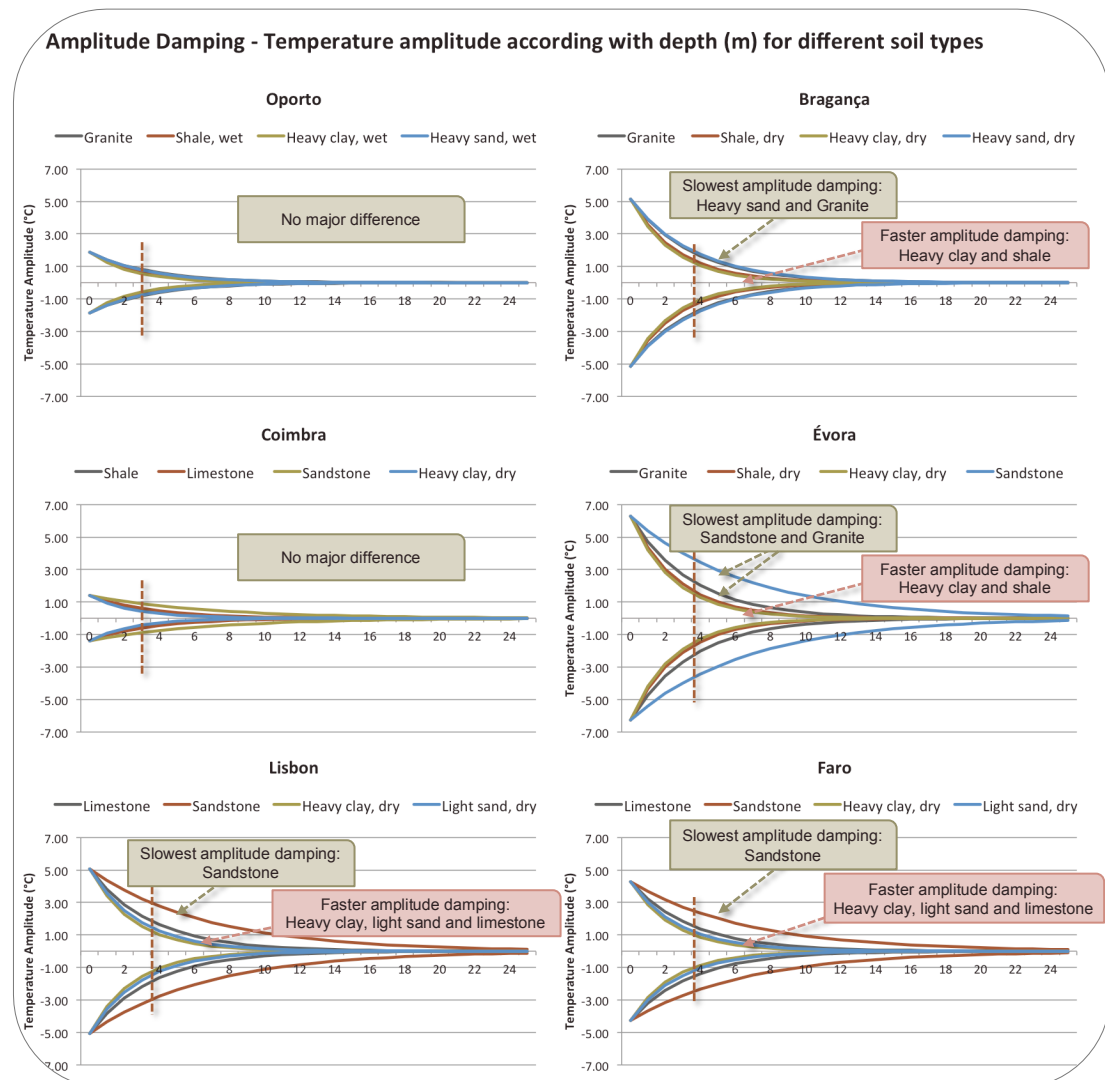
Figure 5.10: Amplitude damping – according with depth, soil types and locations

By comparing the different values of soil amplitude damping at Lisbon it is observable that a ground-integrated building at this location can benefit from greater thermal potential when constructed in soils such as heavy clay, light sand or limestone due to the fast amplitude damping. While a sandstone soil has slow amplitude damping, meaning that it has the lowest thermal potential. At Évora the best soils for ground-integration are heavy clay and shale soils, followed by granite soils. For the compared soils at this location, sandstone produces the slowest amplitude damping and, therefore, it has the worst performance. Regarding Faro, it is found that the best soils are heavy clay, followed by light sand and limestone. Sandstone is, once again, the soil type with the lowest ground thermal potential.

5.3. SOLAR RADIATION ON SLOPES

5.3.1. Location
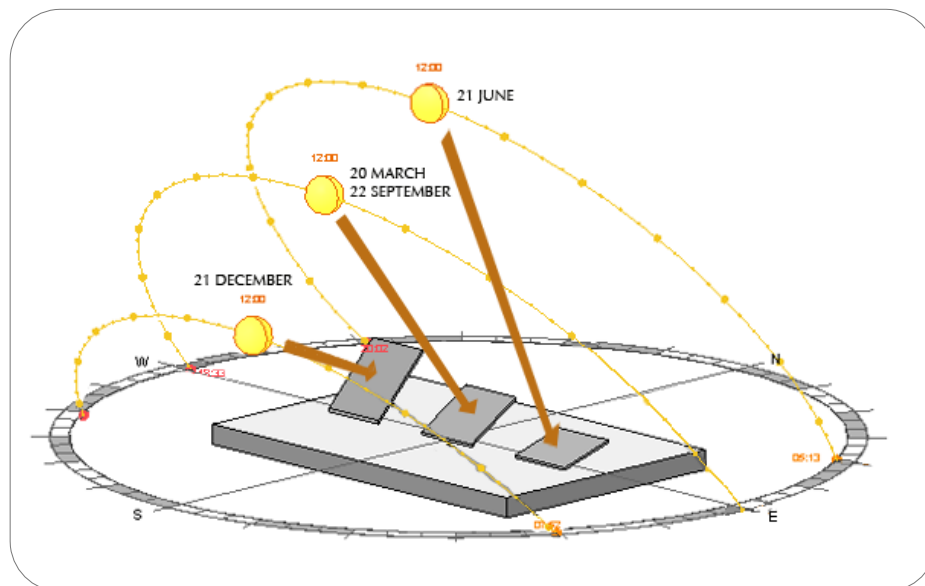
Figure 5.11: Sun's rays angle at winter and summer sostice, and spring and autumn equinox - Lisbon 12pm; sun path study using Revit

The solar radiation values received by slopes and flat surfaces are different, and this difference depends on latitude, slope gradient, orientation, as well as day of the year and hour of the day. As illustrated in Figure 5.11, in the Northern hemisphere during spring and autumn equinox at midday, a terrain surface with the same angle as the latitude is perpendicular to the sun's rays. Therefore, during these periods a south oriented surface with the same inclination as the latitude receives the greater amount of solar radiation.

To confirm the main solar radiation patterns that can be observed in Portugal throughout the year, a brief study was conducted according with terrain surface tilt. The Portuguese mainland territory ranges across latitudes 37°N to 42°N. Since the total range of these latitudes is only 5°, it is relevant to select Lisbon as the central location for this study.

5.3.2. Interactive Application and Used Inputs

Table 5.10: Input parameters

Constant Parameters		Changed Parameters	
Latitude	38.74	Month No.	1 (Jan) to 12 (Dec)
Surface Azimuth (-180;180):	0	Surface Tilt (90 = vert.)	0, 5, 10, 15, 20, 25, 30, 35, 40, 45, 50, 55 & 60

The monthly average solar radiation values for this study were obtained from the online Photovoltaic Geographical information system - interactive maps made available by the Joint Research Centre (JRC) from the European Commission. The surface tilts compared ranged from 0° to 60° with 5° degrees intervals. The parameters used to retrieve the monthly data are displayed in Table 5.10.

5.3.3. Results and Discussion

The annual average results showed in Figure 5.12, demonstrated that the total solar radiation values in this location change according with surface angle. From a horizontal surface to a 35° slope there is a substantial increase of the solar radiation received in proportion with the increasing steepness of the slope studied. From 35° to 60° slopes, the steeper the slope the lower the solar radiation received by its surface, meaning that the total annual solar radiation values decrease.
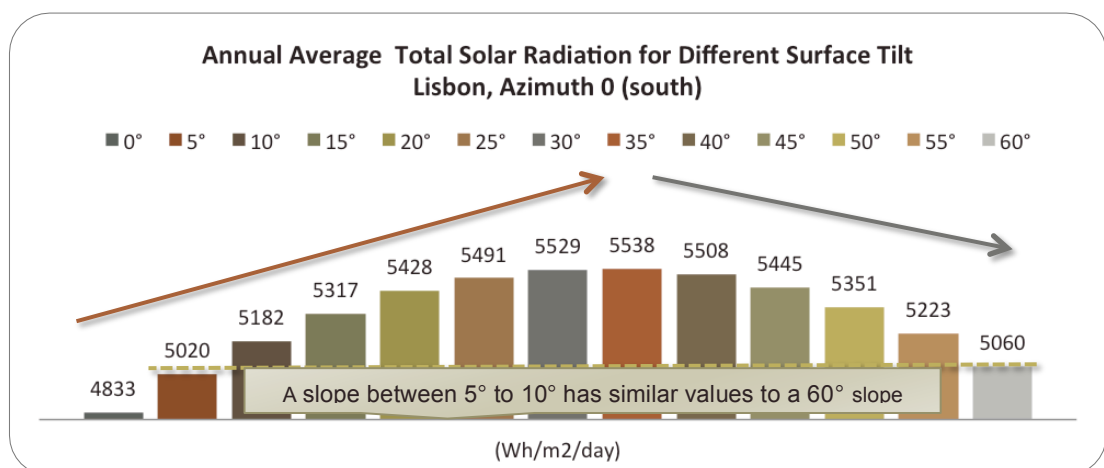
Figure 5.12: Lisbon - Annual average total solar radiation for different surface tilt

To maximize the annual solar radiation at this location the most effective slopes are those closer to the latitude, which in this case are slopes with angles of 30° to 40°,

which are further perpendicular to the sun's rays during autumn and spring. It is also evident that small slopes can improve the solar radiation values received by a surface. A small slope of 10° received more solar radiation than a slope of 60°, and a 25° slope is better than 55° and 60° slopes.
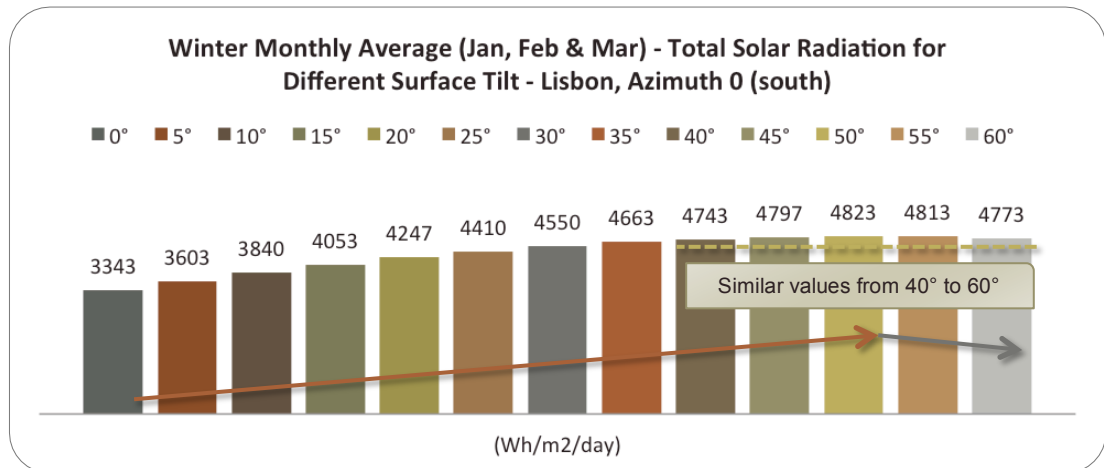
Figure 5.13: Winter monthly average of total solar radiation according with surface tilt

Regarding the seasonal monthly solar radiation patterns for different tilts, shown in Figure 5.13, analysis shows that during wintertime the amount of solar radiation rises from the horizontal surface to a gradient of 50°. From 0° to 40° the increase is substantial, and from 40° to 50° the increase is minimal. The solar radiation values decrease in slopes of 50° to 60°. At this period the best slopes are from 45° to 55° and the optimum gradient is of 50°.
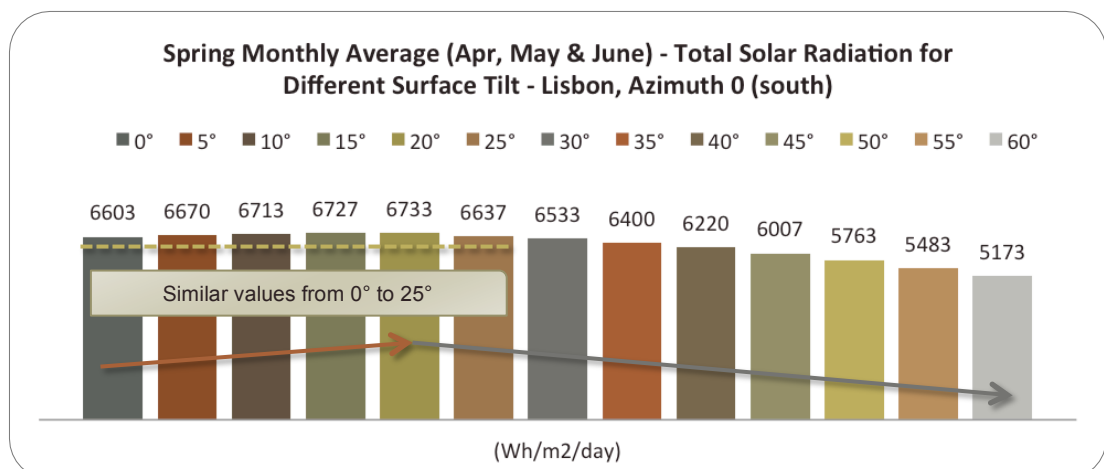
Figure 5.14: Spring monthly average of total solar radiation according with surface tilt

As shown in Figure 5.14, during spring the solar radiation pattern changes. The smaller slopes receive the highest amounts of solar radiation. The greatest value was received by a 20° slope, and from 20° to 60° the values of solar radiation decrease. It should also be noted that the values received by 0° to 25° slopes are very similar. This is because at early spring the sun's rays are perpendicular to angles closer to the latitude but at later spring the shallowest terrain inclinations receive higher amounts of solar radiation. For this period, and especially in the early months of the year when the ground heating potential is reduced, the steeper slopes are not recommended. However, if the objective is to produce lower ground temperatures for cooling in the summer, then steeper slopes are ideal.
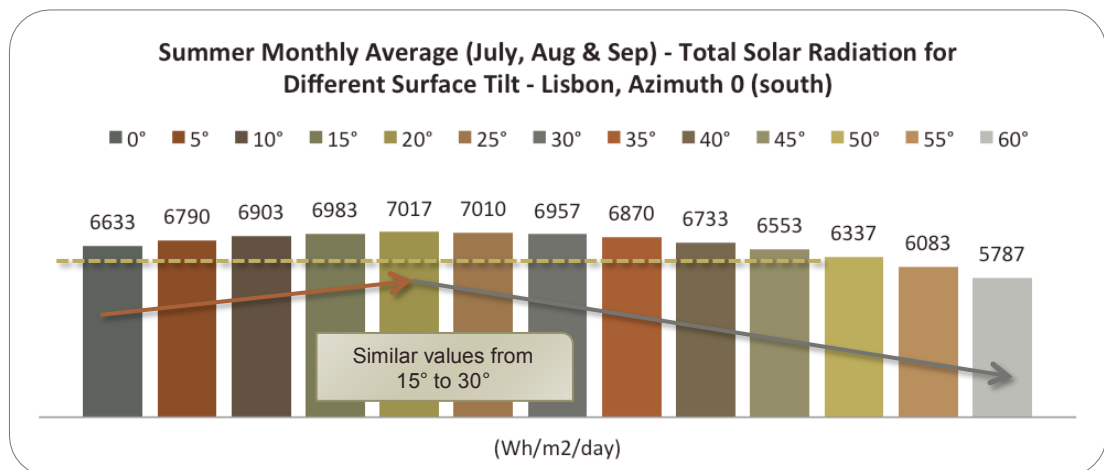
Figure 5.15: Summer monthly average of total solar radiation according with surface tilt

As shown in Figure 5.15, during summertime the solar radiation values rise in slopes of 0° to 20° and fall in those from 20° to 60°. During this period a horizontal surface receives more solar radiation than 45° to 60° slopes. The highest values are received by slopes of 10° to 35°, and the optimum slope is of 20°. As illustrated with Figure 5.11, at early summer the sun's rays are perpendicular with the lowest terrain inclinations, and this gradually change until late summer, when the sun's rays are perpendicular with the latitude. If the intention is to harvest the maximum solar radiation for a greater ground heating potential at autumn, then the best surface

inclinations should be lower than the latitude, in this case the best inclinations are slopes of 10° to 35°.

During autumn the total solar radiation improved with gradient, since the steeper the slopes greater are the values (Figure 5.16). This is because at early autumn the sun's rays are perpendicular to terrain surfaces with inclinations similar to the latitude, and by late autumn, when the sun path is lower, terrain surfaces with greater angle are more perpendicular to the sun's rays. Therefore, the 55° slope receives the maximum value, and 50° to 60° slopes have similar results.
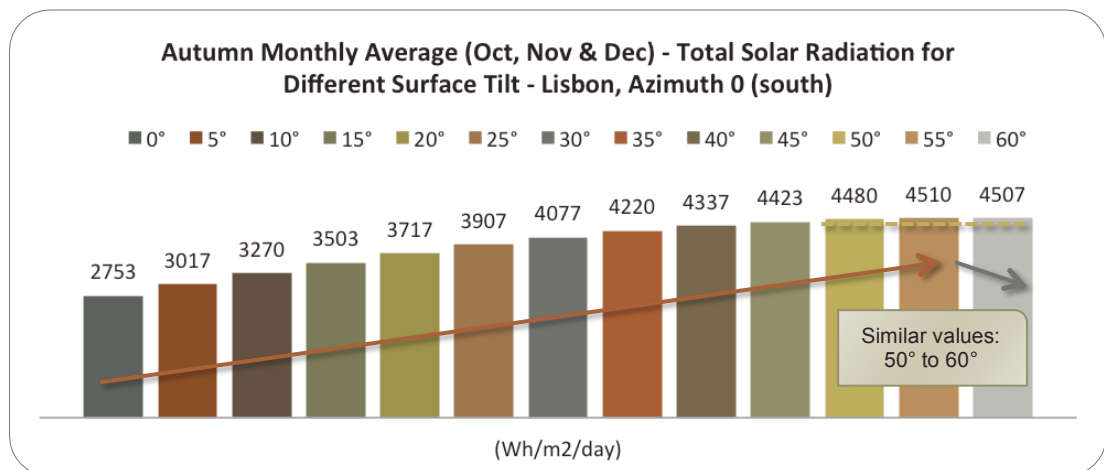
Figure 5.16: Autumn monthly average of total solar radiation according with surface tilt

To conclude, the seasonal monthly average total solar radiation received at different surface tilts reveals how these values change throughout the year. The steeper slopes receive the greater solar radiation values during autumn and winter, and the shallower slopes during summer.

5.4. SLOPE GROUND THERMAL POTENTIAL

5.4.1. Slope Ground Temperature and Zone of Influence

As discussed in Chapter 4, topography can affect the climate near the ground. It is already known that tilt, orientation and altitude determines the direct solar radiation received by a surface, and at higher latitudes the solar radiation received by a sloped surface is higher than for a flat one. This implies that flat and slope terrains' underground temperatures are different, which leads to the question of how different the produced temperature values and patterns might be.
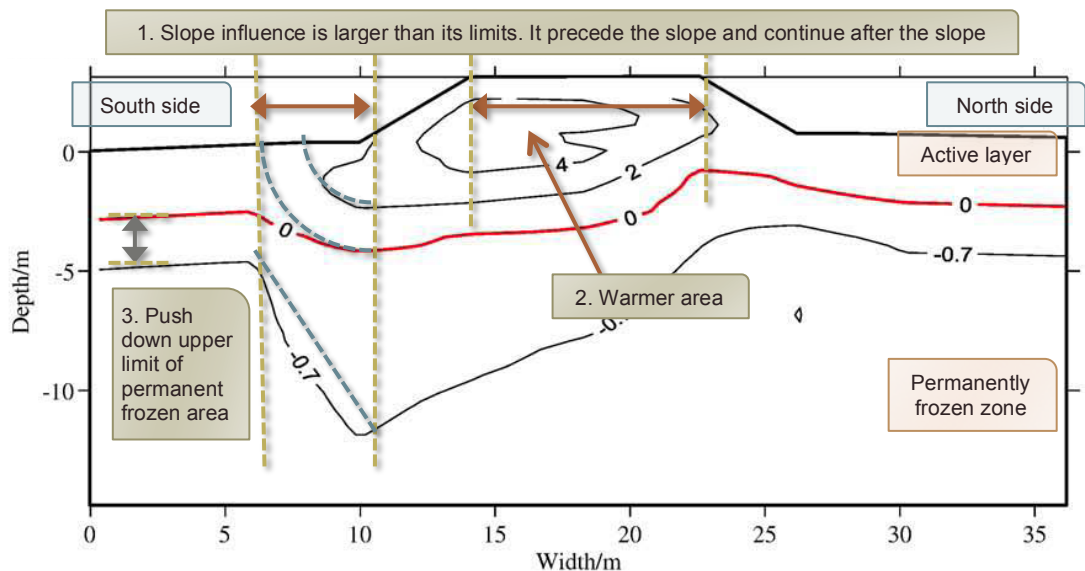
Figure 5.17: Ground section temperatures; Slope influence on ground temperatures at a permafrost region. Chou et al., 2010

A further point to be considered is the slope influence zone. The impact of a slope is not limited to its starting and finishing points. Underground areas that precede or are positioned after a slope terrain are still affected by the slope. Considering this issue, Chou et al. (2010) studied the impact of sunny-shady slopes on the thermal performance and deformation stability of the highway embankment on the Qinghai-Tibet Plateau. This study can be used as an example to illustrate the extent of slope influence zones. Looking at the ground temperature section of Chou's research (Figure 5.17) it can be noted that the effects of a slope are not limited to the slope area. In the case of this warm permafrost region it can be seen that the slope effect

precedes and continues after the tilted area, producing a warm temperature area below the slope and pushing down the upper temperature limit of the permanently frozen area. The beginning of the slope is working as a pivot point between the ground temperatures below a slope and flat terrain.
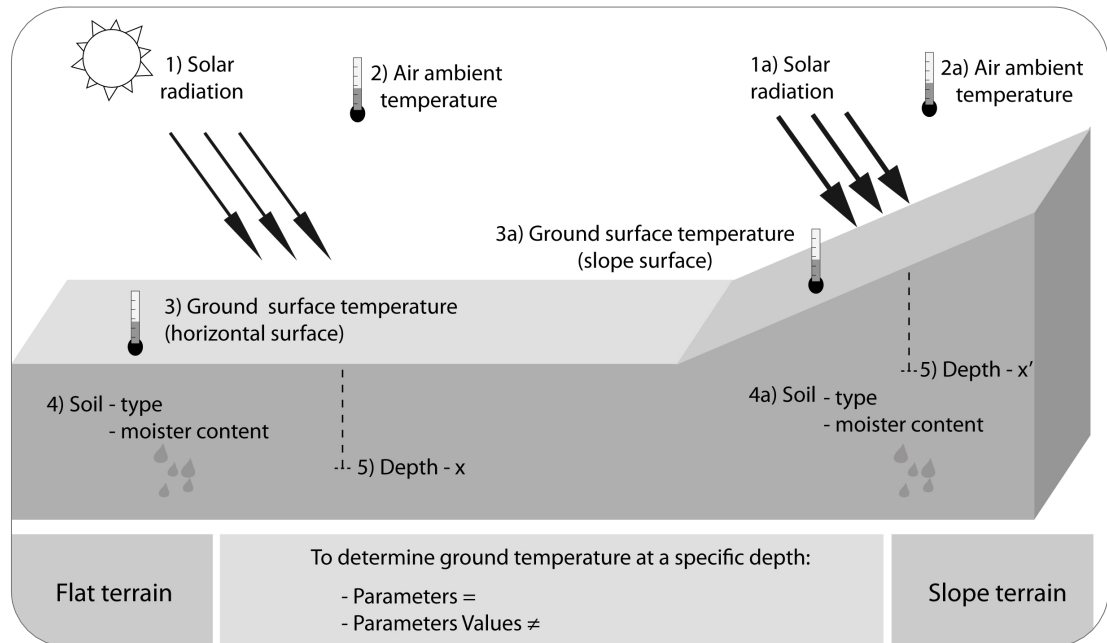
Figure 5.18: Topography effect on ground temperature

As summarised in Figure 5.18, flat and sloped terrains share the same parameters to calculate ground temperature at a specific depth. These parameters are solar radiation, air temperature, ground surface temperature, soil type, soil moisture content and depth. This section of the chapter is focused on the solar radiation parameter. It does so by using the values received by a surface according with its inclination, with all the other parameters remaining unchanged.

The two elements that form Equation 5.1 ($T_{(x,t)}$), require solar radiation values (see Table 5.11). These values are the mean annual temperature of the soil surface (T_m) and the annual range of the temperature wave at the soil surface (A_s). The correspondent equation for T_m is Equation 5.2 and for A_s the corresponding equation is Equation 5.7. In this study, the values for the mean annual solar energy at the

ground surface (S_m), used to calculate T_m, as well as the values for the amplitude of solar radiation wave (S_a) for calculating A_s, are changed in accordance with the tilt.

Table 5.11: Solar radiation aspects from Equation 5.1, 5.2 and 5.7

$$T_{(x,t)} = T_m - A_s e^{-x\sqrt{\frac{\pi}{365\alpha}}} \cos\left\{\frac{2\pi}{365}\left[t - t_o - \left(\frac{x}{2}\right)\left(\sqrt{\frac{365}{\pi\alpha}}\right)\right]\right\} \quad \text{Equation 4.1}$$

$$T_m = \frac{1}{h_e}[h_r T_{ma} - \varepsilon\Delta R + bS_m - 0.0168 h_s fb(1-r_a)] \qquad A_s = [h_r A_{sa} - bS_a \exp(i\varphi_1 - \varphi_a)]/(h_e + K_s)$$

Equation 4.2   Equation 4.7

T_m = mean annual temperature of the soil surface
S_m = mean annual solar energy at the ground surface

A_s = annual range of the temperature wave at the soil surface
S_a = amplitude of solar radiation wave

The T_m equation allows us to track the changing mean annual solar radiation on the ground surface (S_m) value according with its slope, while with the A_s equation the annual amplitude of the solar radiation wave (S_a) value can be changed also according with the study slope. Based on this, the ground temperatures in Lisbon can be calculated using the correspondent T_m and A_s equations for tilt surfaces from 0° to 60° with 5° intervals. The T_m and A_s values are found using the correspondent S_m and S_a values for each slope.

5.4.2. Ground Temperature Calculations Inputs

Table 5.12: Nomenclature and values uses on the ground temperature calculations at Lisbon for different slope terrains

Slope Terrain		00°	10°	20°	30°	40°	50°	60°
Mean annual solar radiation - ground surf, W/m²	S_m	388.14	419.46	441.88	453.75	454.91	444.72	423.36
Amplitude of the solar radiation wave, W/m²	S_a	349.29	307.77	272.46	231.08	187.33	156.67	136.67

Using this method, the ground temperatures for different tilt terrains in Lisbon were calculated using the corresponding solar radiating values, as displayed in Table 4.12. These values are based on the monthly data retrieved from the online Photovoltaic Geographical information system - interactive maps (JRC), and that are available in Appendix 1. All other parameters used in this section correspond to the Lisbon values, which are displayed in Table 5.7 in Section 5.2.

5.4.3. Results and Discussion
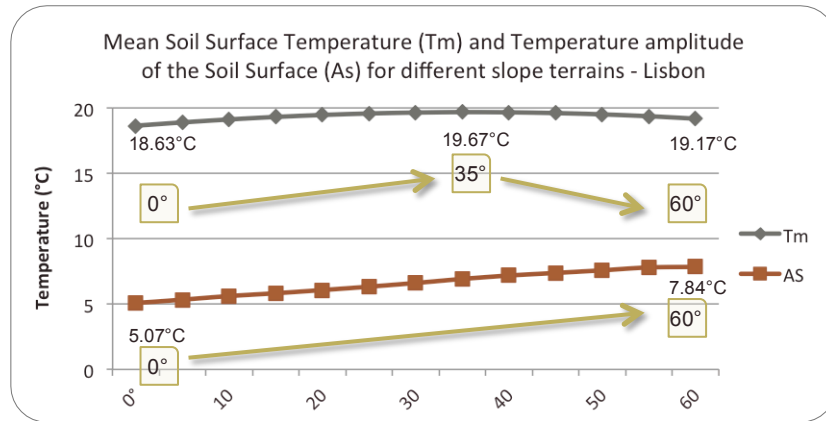
Figure 5.19: T_m and A_s according with slopes - Lisbon

Using these data the author found that by changing the received mean annual solar radiation values (S_m) according with the slope, different mean soil surface temperatures (T_m) can be produced. As illustrated in the above figure, the T_m value increases in slopes from 0° to a 35°, with a total range of 1.04°C, and it decreases in slopes from 35° to a 60°. It can also be seen that the T_m value for a 15° slope is higher than for a 60° slope.

Regarding the temperature amplitude of the soil surface (A_s), it is observed that these values are also affected by the inclination of the terrain. As can be seen in Figure 5.19, that by using the correspondent annual amplitude of the solar radiation wave (S_a) the solar radiation values increase with the steepness of the slope. The total A_s value range produced ranges of 2.77°C, from 5.07°C for a 0° slope to 7.85°C for a slope of 60° slope. It should be pointed out that the steeper slopes, such as 55° and 60°, have a small amplitude difference between them.

Therefore it is proved that by using the correspondent mean annual solar radiation (S_m) and temperature amplitude of the soil surface (A_s), the values of the terrain inclination affects both T_m and A_s values and, consequently affecting the ground temperature calculations.
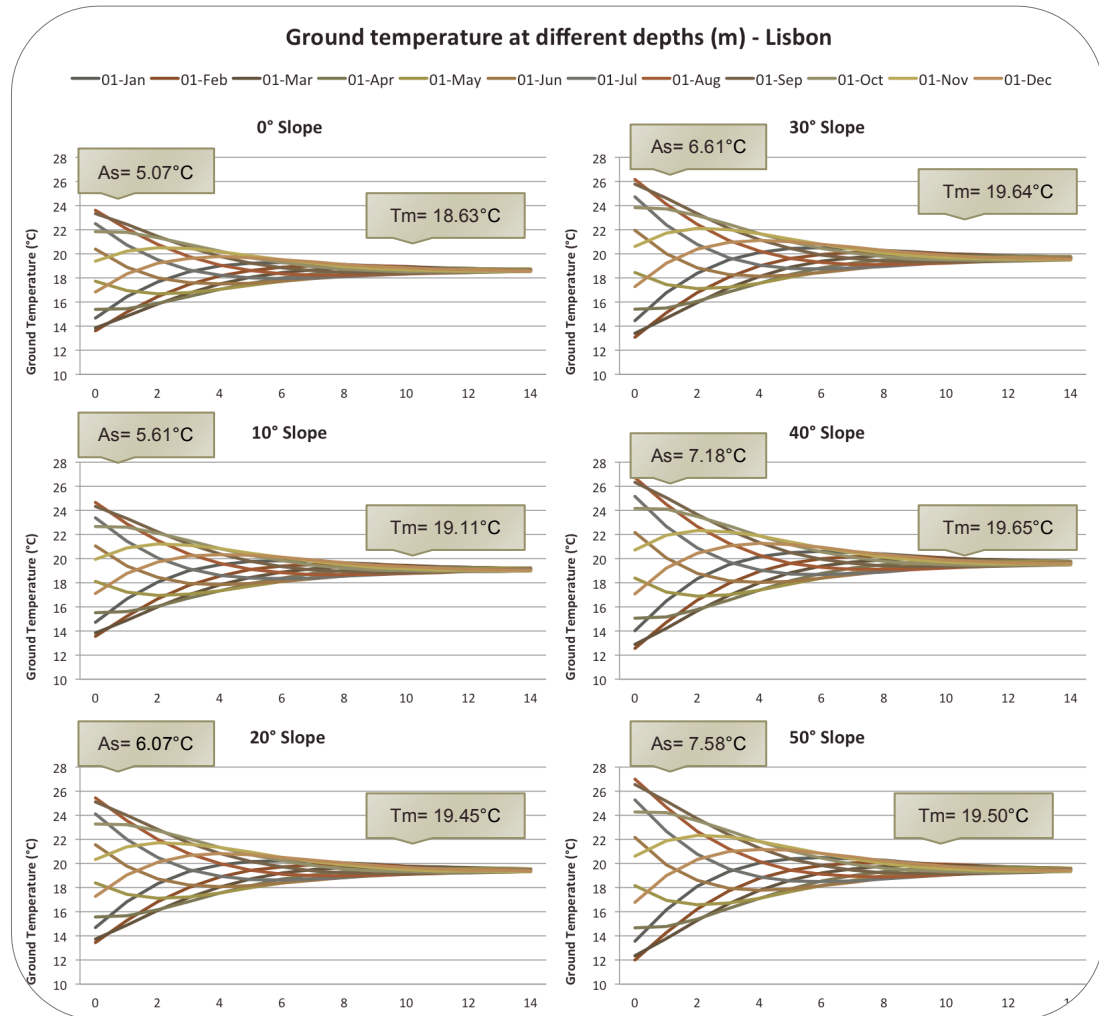
Figure 5.20: Ground temperature at different depths according with slope - Lisbon

The impact of T_m and A_s values on ground temperatures according with slope inclination are visible in Figure 5.20. It can be observed that for the same location both values change due to tilt, leading to different ground temperatures values. This shows that ground temperature calculations need to use the appropriate solar values according with terrain inclination.
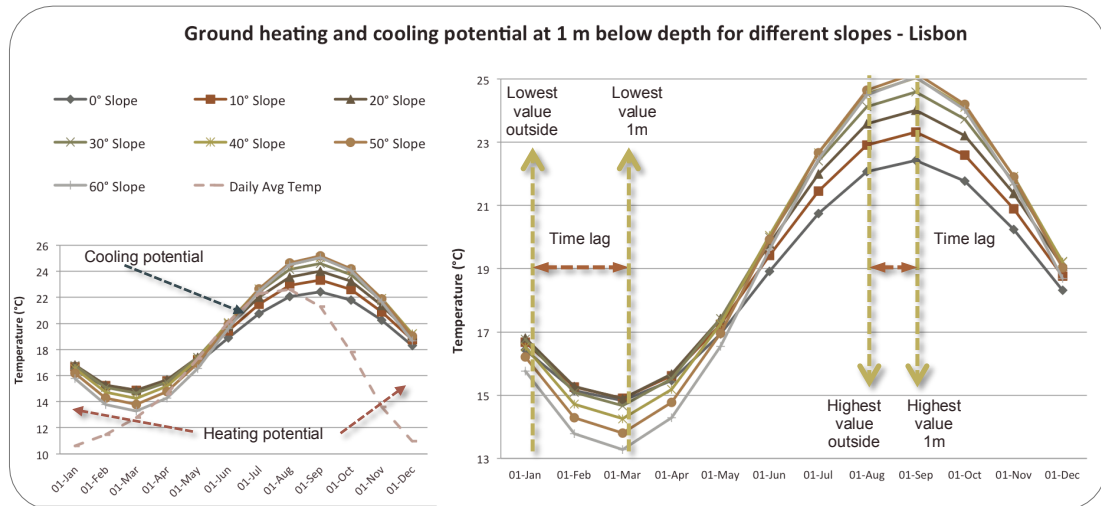
Figure 5.21: Ground heating and cooling potential for different depths, Lisbon – 1 m depth

The annual ground temperature values for a 1 m depth can be seen in Figure 5.21, show that they are affected by terrain incline degree and the pattern of temperature change during the year. These figures reveal a considerable heating potential from October until March but the cooling potential is limited. This limitation exists because most slopes produce higher values than the daily average temperature. During January, slopes of 20° and 30° produce the best results, in April a 20° slope is the best inclination, in July a 0° slope produce the best values and in October a 50° slope has the best temperatures, the latter closely followed by a 40° slope. Overall, at this depth, the best annual temperatures are provided by slopes of between 20° to 40°. Regarding the time lag, the author found that in winter it is of around two months and in summer of one month.
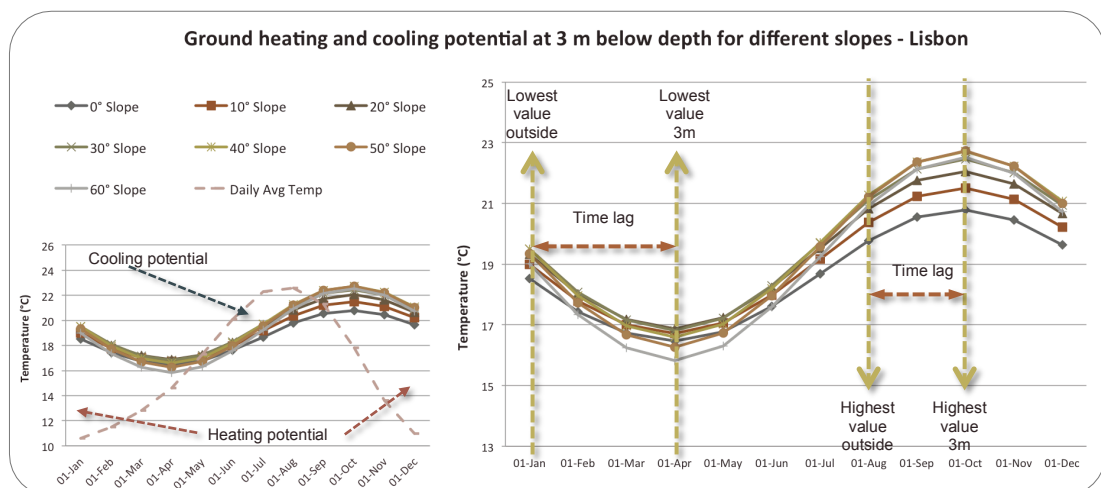
Figure 5.22: Ground heating and cooling potential for different depths, Lisbon – 3 m depth

Examining the values presented in Figure 5.22 it is clear that at 3 m depth all terrain inclinations have a good ground thermal potential. The temperature gap between the inclinations is reduced. During January the best slopes are of 30° and 40°, in April of 20°, in July 0° and in October the best slope is of 50°. The best annual temperatures are provided between 30° to 40° slopes. The time lag at the coldest period is around three months, while the warm ground temperatures are felt during October, that is, two months after the outside air temperature heat peak.
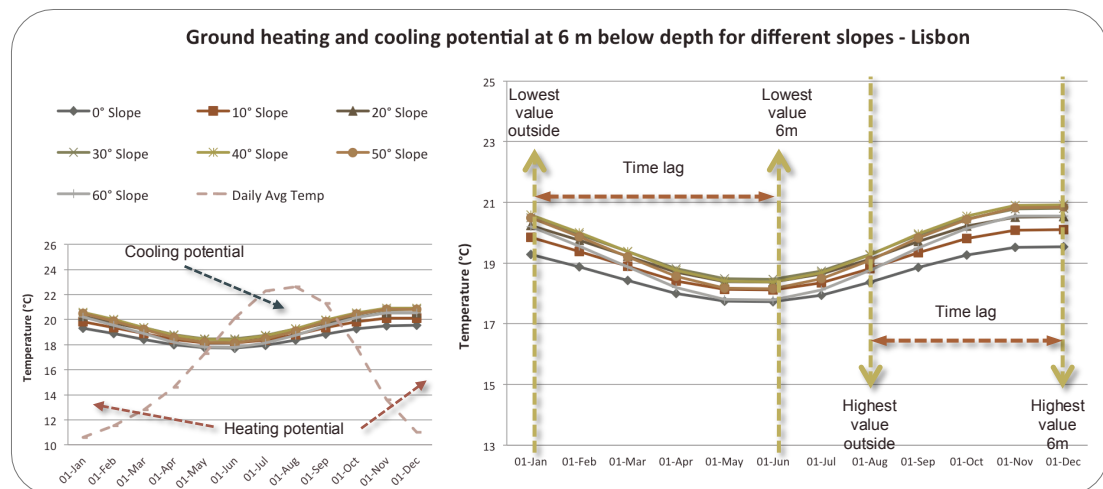
Figure 5.23: Ground heating and cooling potential for different depths, Lisbon – 6 m depth

As illustrated in Figure 5.23, in the case of 6 m below ground the ground thermal potential is improved with higher heating and cooling potential than in the lower studied depths. Due to more constant values throughout the year, the temperature amplitude value between the slopes and the annual temperature range for each inclination is narrow. During January and October the best values are registered by a 40° slope, followed by a 30° slope. In April this is reversed, with a 30° slope providing the best values, and closely follow by a 40° slope. In July the best value is for 0° and 60° slopes. At this depth, overall, the best slope is 40°, closely followed by a 30° slope. The time lag is increased to up to five months for the coldest temperature values, coinciding with the beginning of the summer, and the warmest ground temperatures are registered in December, four months after the hottest period of the year.

As previously explained, the ground is able to collect and store solar energy, and this energy can be transmitted to a building by direct and indirect contact. Slope terrains receive a higher amount of solar radiation than flat terrains. The higher amount of collected and stored energy is verified by comparing the ground temperature at 3 m depth below a flat terrain, against the location at which the same temperature is found under different slope terrains. This verification was done for single days at the beginning of January, April, July and October.
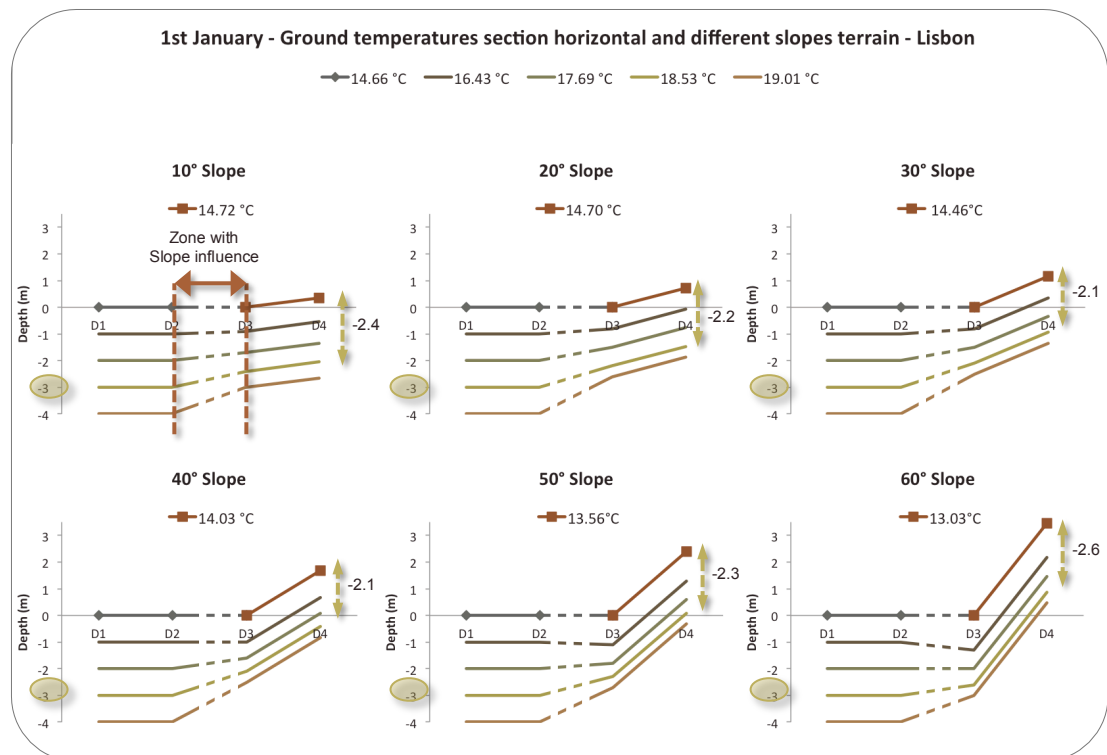
Figure 5.24: Ground temperature comparison between flat and slope terrains, Lisbon – 1st January

Sloped terrains produce different ground temperature patterns than flat terrains. An intermediate zone is produced between a flat and a sloped area. The slope affects the ground temperatures in this intermediate zone.

At the beginning of January a warm ground temperature of 18.53°C can be found below a flat surface at 3 m depth. Following the same temperature value, Figure 5.24 shows that its distance from the surface changes with the steepness of the slope. At this winter day the warmer values are closer to the ground surface below

all slopes. With a 10° slope the 18.53°C is found at 2.4 m depth and it reaches the lowest depth of 2.1 m with a 30° and 40° slope. This shows that ground-integrated buildings in, as well as near, slope terrains can benefit from higher ground thermal potential during winter.
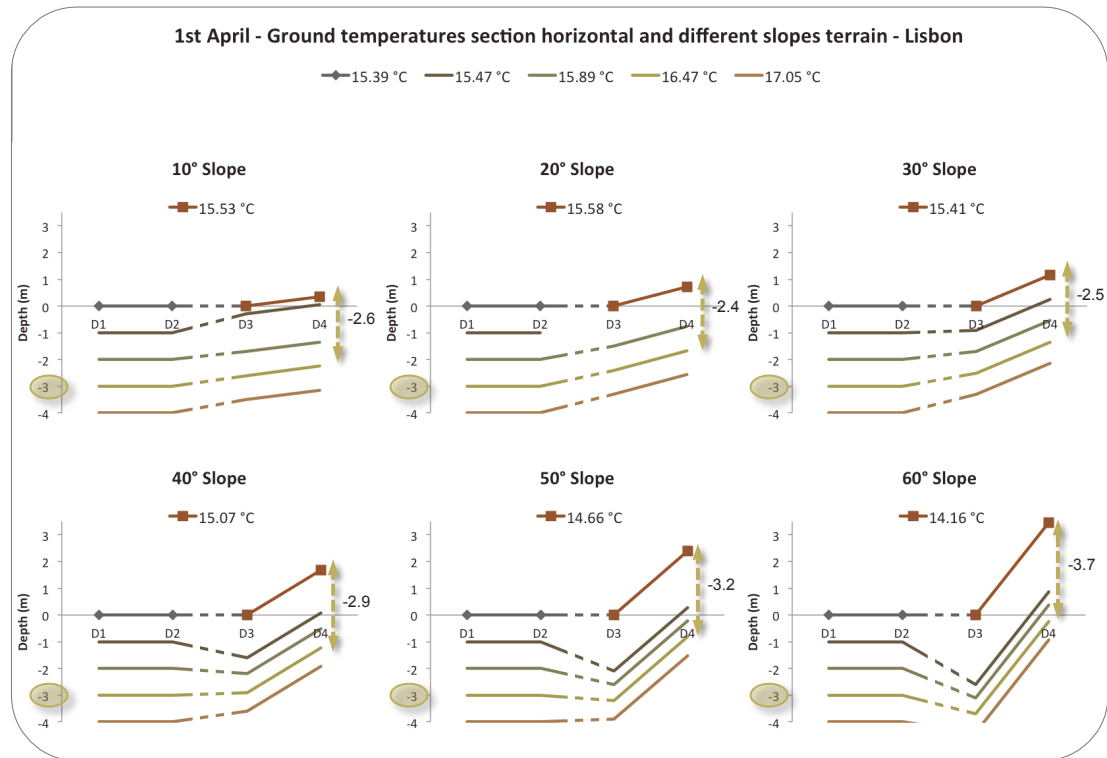
Figure 5.25: Ground temperature comparison between flat and slope terrains, Lisbon – 1st April

In Figure 5.25 it is can be seen that by early spring the ground has released a great part of its energy. At this period, although the surface temperatures are warmer comparing with winter values, all other ground temperatures up to 4 m depth have reached their annual lowest.

The author found that slopes from 10° to 40° are able to provide better ground temperature values than flat terrain. The 16.47°C value registered at 3 m depth below the flat surface moves closer to the surface below a 10° to 40° slope. Its proximity to the surface is greatest under a 20° slope located at a 2.4 m depth. It is also confirmed that slopes higher than 50° produce the worst ground temperatures, since the 16.47°C temperature is only found at depths below 3 m.

It can therefore be concluded that at this period slopes between 10° to 40° can increase ground heating potential. However, slopes greater than 50° have less ground heating potential than a flat terrain.
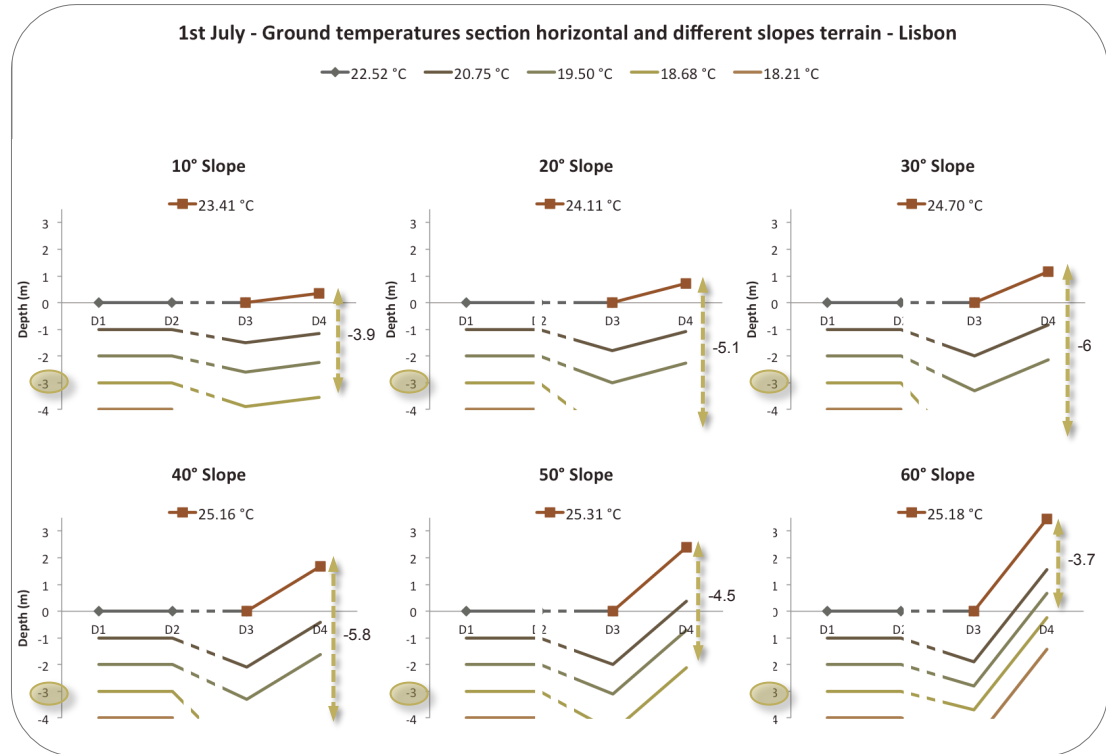
Figure 5.26: Ground temperature comparison between flat and slope terrains, Lisbon – 1st July

Observing the ground temperature positions below flat and inclined areas in the beginning of July (see Figure 5.26) it is clear that all slopes produce higher ground temperature values than flat terrain. The temperature value of 18.68°C registered at a 3 m depth below a flat terrain is pushed down to 3.9 m below a 10° slope, and the maximum depth of 6 m for this temperature value was found under a 30° slope. Although this shows that the ground cooling potential at a slope area is reduced when compared with a flat terrain, it indicates that the annual heating potential at any slope will be greater, since during this period the ground it is at a charging mode.
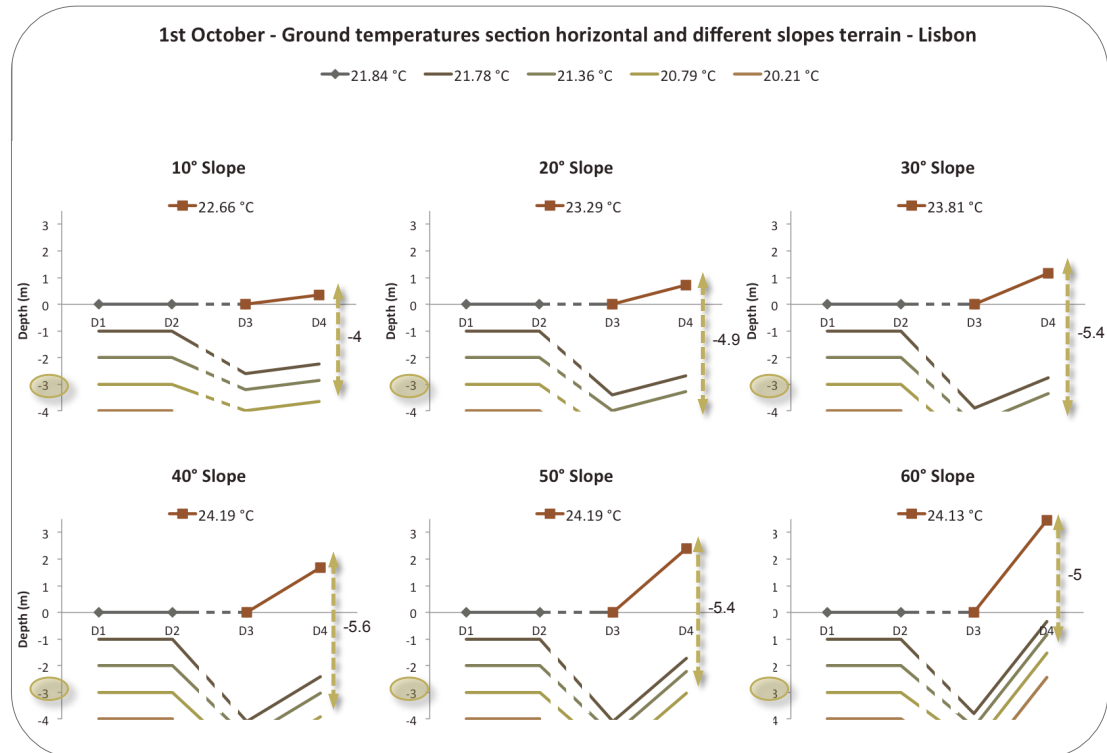
Figure 5.27: Ground temperature comparison between flat and slope terrains, Lisbon – 1st October

As a consequence of this charging mode observed during the summer, it is evident in Figure 5.27 how the ground has stored the received solar energy by the 1st of October and is now totally charged. At the beginning of the autumn, all slope terrains have higher heating potential than flat terrain. The 20.79°C ground temperature value found at 3 m below a flat area appears further down below all slopes. Inclinations between 30° to 50° have good thermal potential, and 40° is the optimum slope during this period.

5.5. CONCLUSIONS

Portugal's temperate climate is divided into three winter climatic zones and three summer climatic zones, split between mild, moderate and severe. In 2013, the Portuguese annual quota of final consumption of energy per sector shows that the domestic sector was the third main consumer, accounting for 17% of all energy consumption. For this sector, in 2010, 17.5% of the average energy consumption per dwelling was used for heating. The electricity consumption values per type of utilization indicate that heating contributes to a larger energy usage than cooling, since 9.06% of the total electricity is used for heating and only 1.60% is for cooling.

The dwelling density of Portugal's mainland in 2001 indicates a higher concentration of dwellings in the north, rather than in the south, and with a very high concentration around Lisbon. A single-family dwelling is the main type of residence in Portugal, corresponding to 55% of total residential buildings, 7% higher than the European average. A two-dwelling building corresponded to 8% and buildings containing three or more dwellings are 37% of total domestic buildings. Data from 2001 and 2011 makes reference to the amount of conventional dwellings by building and the percentage and distribution of buildings with one dwelling. This data shows that the single-family house is more predominant at non-urban areas, while in urban areas (such as Lisbon) there is a prevalence of multiple occupancy buildings, mostly apartment buildings. In 2014 the average number of floors per completed buildings in new families housing constructions was 2.1. The lowest number of average floors is found in the single floor dwellings of Alentejo, and the highest is an average of 2.6 at the Algarve and Lisbon. The national average number of rooms per dwelling is five.

The author conducted a study in order to identify Portugal's ground thermal potential. This was done by analysing six locations at which the ground temperature

at different depths was calculated. The result of this analysis shows that all locations can benefit from ground thermal potential. The length of the potential is dependent on the mean ground temperatures (T_m) and annual temperature amplitudes (A_s).

Three main ground thermal areas were identified by the conducted study analysis: Firstly, the north and centre-north littoral zone, which includes Oporto and Coimbra, and that has high heating potential but limited cooling potential due to higher precipitation values; secondly, a north and centre interior zone in which Bragança and Évora are included, which has the greatest thermal potential across the whole year due to the contrast between summer and winter weather; lastly, a centre-south and south littoral area, which includes Lisbon and Faro, with good ground heating potential, and with good cooling potential in Lisbon and moderate potential in Faro, the latter due to the mild winters and moderate summers.

Regarding the relevance of soil types on ground thermal potential, this effect was found to be lower in zones with high annual precipitation, as it is the case of north and centre-north littoral, compared with zones with lower annual precipitation such as Lisbon, Évora and Faro. At these three locations, sandstone produces the worst ground thermal potential due to its slow amplitude damping. The result order for best to worst soil types in Lisbon is heavy clay, followed by light sand and limestone; in Évora it is heavy clay, shale and granite, while in Faro it is heavy clay, light sand and limestone.

The author studied the solar radiation on slopes in Lisbon in order to understand annual and seasonal variations. The author found that at this location all slope terrains have higher annual solar radiation exposure than flat terrain. Between low to medium slopes the impact on annual solar radiation values is greater than between medium-steep slopes, as 5° slope receive 26.5% more solar radiation when comparing it with a flat terrain. As for slopes between 30° to 35°, the increase

difference is only 1.3%. The author also found that a 10° slope terrain have higher solar exposure than a 60° slope, while a 25° slope produces higher annual values than slopes between 55° and 60°. Gradients between 25° to 45° provided the greatest annual values, and the optimum slope is of 35°. Regarding the seasonal patterns, the author found that the highest slopes receive the greatest solar radiation values during winter and autumn, while the medium low and low slopes have the highest values during spring and summer.

The slope ground thermal potential for Lisbon was studied by calculating the ground temperatures using the correspondent solar radiation data. For each tilt surfaces the appropriate S_m and S_a values were used. The analysis shows that, as consequence, T_m and A_s values are affected. This proves that ground temperature below slopes is different from that registered under a flat terrain. Between all studied slopes, changing the S_m generate a T_m results range of 1.04°C increases from 0° to 35° slope and decreases for 35° to 60° slopes. Whereas by altering the S_s values the A_s value range increased by up to 2.77°C, with 5.07°C for a 0° slope and 7.85°C for a 60° slope.

The author therefore concludes that in Lisbon, all terrain inclinations produce higher annual ground thermal potential than flat terrains. The author found that, for depths greater than 3 m, a 30° to 40° slope provides better temperatures in winter, spring and autumn than the other slopes studied. These are the seasonal periods when most energy is required. For summer, both slopes provide greater temperatures than shallower slopes as 0°, 10° and 20°. However this season corresponds to the annual period with lower energy needs and, therefore any form of ground integration is an advantage. This makes 30° to 40° slopes the best angles to maximise the annual ground thermal potential. The author observed that time lag increased with depth, as at 3 m the coldest ground temperature values are register three months after the outside cooling peak, while at 6 m the difference is increase to five months.

The author has demonstrated that slopes terrains produce different ground temperature patterns than flat terrains. Also, that between a flat and a slope area, an intermediate zone is produced since the slope affects is not limited to its own area. At the beginning of January, the author found that the ground temperature value at 3 m below a flat terrain appears closer to the surface under all slopes. This proves that all slopes have higher ground heating potential than flat terrain. It is below 30° and 40° slopes that the temperature value reaches its lowest depth at 2.1 m. In early spring, the ground temperature value at 3 m under a flat terrain is visible closer to the surface beneath a 10° to 40° slope. This shows that these slopes produce the best ground thermal potential. During July, all slopes produce greater ground temperature when compared with a flat terrain. This indicates that the flat terrain has higher ground cooling capacity but also shows that the slope terrains are in charging mode, which means that their heating potential during autumn and winter is greater. During early October the optimum slope is found to be 40°.

The next chapter looks into how ground heat transfer is simulated by different building simulation software. This is done to identify the software and methodology to be used in Chapter 7 and Chapter 8.

CHAPTER 6. THERMAL SIMULATION OF GROUND CONTACT

6. THERMAL SIMULATION OF GROUND CONTACT

Over the past two Decades several building energy simulation programs have been developed by private companies, universities and government bodies made available as both commercial and as free software. At the initial stage of this research, the author had access to three software packages that were identified as possible tools for studying ground integration effect on buildings thermal performance. The university provided two of those packages, Ecotec and Tas, while a third one, E+, was freely available. The author was only familiar with Ecotec. During the process of self-learning Tas and E+, it became evident to the author that each program has different strengths as well as limitations. As consequence of these different strengths and weaknesses, the ground thermal outputs can vary depending on the software used to calculate them. Therefore, the author placed a considerable emphasis on identifying a suitable software tool to conduct this research into ground thermal potential. This chapter analyses how different packages including Ecotect, Tas and E+ perform when simulating ground heat transfer.

The selection process for this comparison was performed in four stages: an initial case, a second case, a sensibility case, and lastly a slope simulation case. The initial case study compares the three software packages made available to the author, Ecotect, Tas and E+. The results of this initial comparative study led to the second case study, where further comparisons between two of the software packages were conducted. This second case study focuses on defining the

simulation procedures for E+ simulations and looks specifically at ground contact effects through comparative tests. The third case studies tests additional results patterns and discrepancies between the different software packages, and determines which building energy simulation package the author will use across the rest of the thesis. The last case study looks into the limitations of each software package and outlines procedures for ground heat transfer simulations, in particular when simulating ground integrations on slope terrains.

6.1. INITIAL CASE MODEL - ECOTECT, TAS AND E+
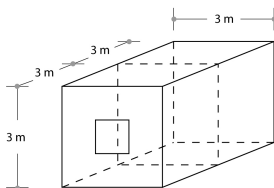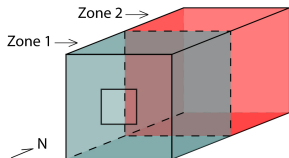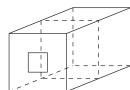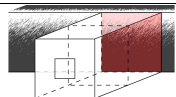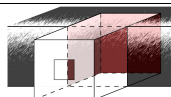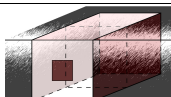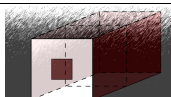
6.1.1. The Computer Simulation Packages

The software packages for building thermal simulation available to the author were Ecotect, Tas, and E+. Intending to identify the most suitable tool for this research, the author modelled an initial comparative case study test and simulated its ground thermal outputs using the three software packages.

At the time of this comparative study, Ecotect was an Autodesk analysis software which was being marketed by the company as a sustainable building design software. Since 2015 the functionality of this software has been integrated into the Revit package. Regarding Tas, this package was a Bentley building energy simulation product and it is currently commercialised and distributed by EDSL. Finally, E+ is an energy simulation software developed by the United States Department of Energy, it is free, open-source, and cross-platform. The software versions used in this chapter were Ecotect Analysis 2010, Tas 9.2 and E+ 7.2.

6.1.2. Model Dimension and Simulation Input Data

Table 6.1: Model Dimension, Zones and Level of Ground Integration

Dimensions	Zones

Surface with Ground Contact

	Case 00	Case 01	Case 02	Case 03	Case 04
Zone 1	Floor	Floor	Floor	Floor East wall West wall	Floor Roof All walls except South wall (Zone 1)
Zone 2	Floor	Floor North wall	Floor North wall East wall West wall	Floor North wall East wall West wall	

The model building used for the case study consists of a two zone building structure with an interior partition and a 1.2 m^2 south-facing window. Each zone has a total area of 9 m^2 and a volume of 27 m^3. The case model variations are based on five different levels of ground integration. For each level the surface elements with direct ground contact vary, as illustrated in Table 6.1.

The location used in this study is Bragança, Portugal. The reasons for this choice of location are the cold winters and hot summers found at this location, as these characteristics can produce greater contrasts in the simulation results, and therefore making the result patterns clearer. Details about the weather file are explained in Chapter 5 Section 5.2.2. The models assume that there are no internal gains and that no heating and cooling systems are used. The building materials are listed in Appendix 2. The winter day and summer day results used in this study correspond to the 1st January and 1st August.

6.1.3. Simulation Results and Discussion

The a priori hypothesis expected to be verified with this case study was that during winter the inside air temperature would increase as the ground-integration level of the model was increased. While with the summer results the opposite was expected, the inside air temperature should decrease as the ground integration was increased.
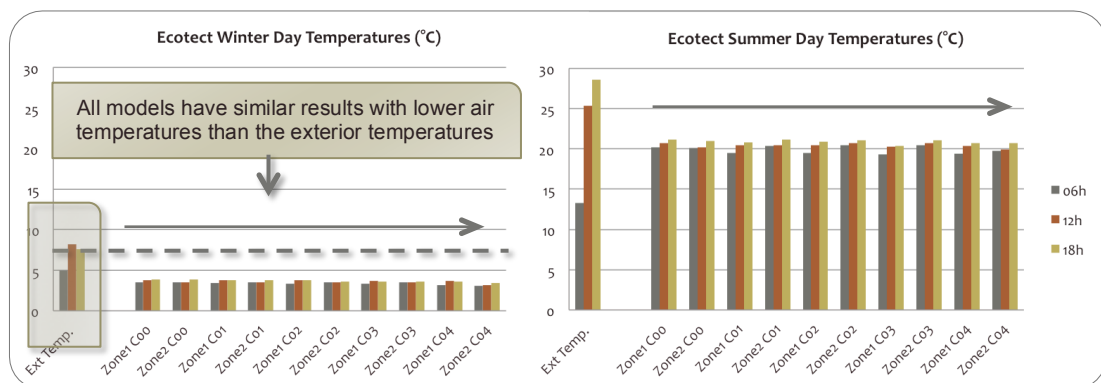
Figure 6.1: Ecotect - Models winter and summer day air temperature
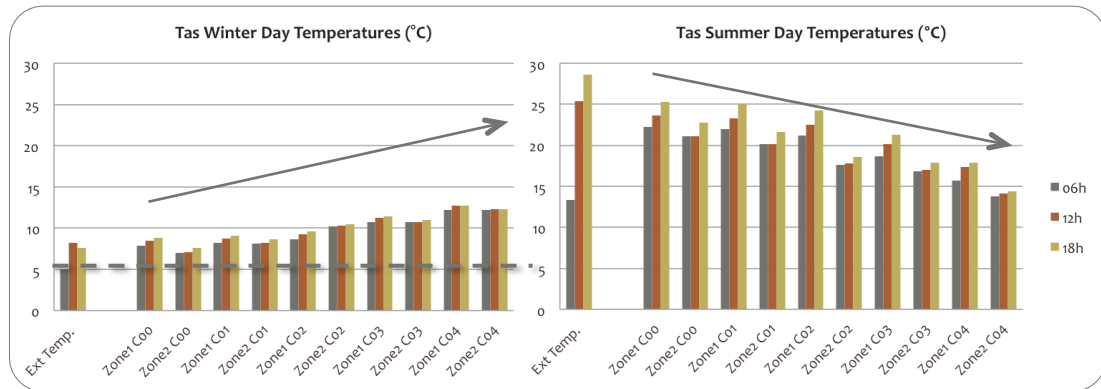
Figure 6.2: Tas - Models winter and summer day air temperature
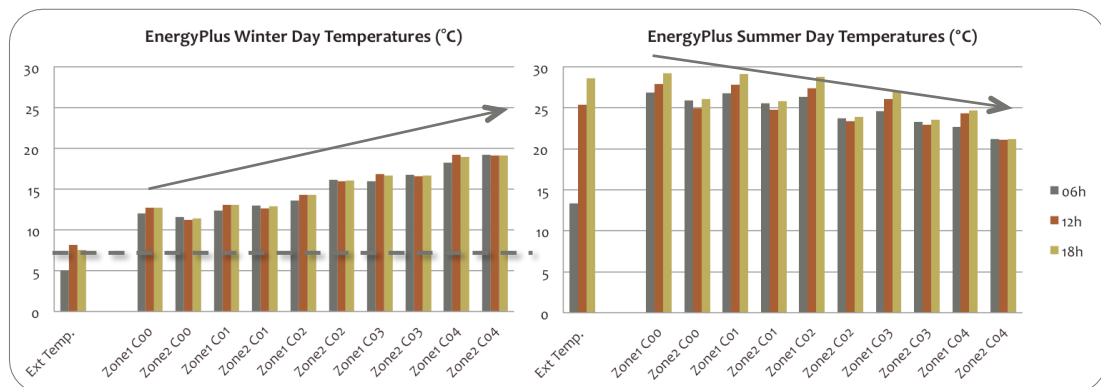
Figure 6.3: E+ - Models winter and summer day air temperature

The a priori hypothesis was confirmed by Tas and E+ simulation results. However, this was not the case with Ecotect generated results. As can be seen in Figure 6.1, for both the winter and summer days, the Ecotect results registered an almost constant inside air temperatures which consistently presented lower values than the exterior temperature. This clearly shows that Ecotect's thermal simulations are not taking ground contact into consideration. In contrast, the results that Tas and E+ generated indicate that these models are able to benefit from ground integration during winter and summer. These models found that the higher the ground integration the better the temperature values in both zones (Figure 6.2 and 6.3).
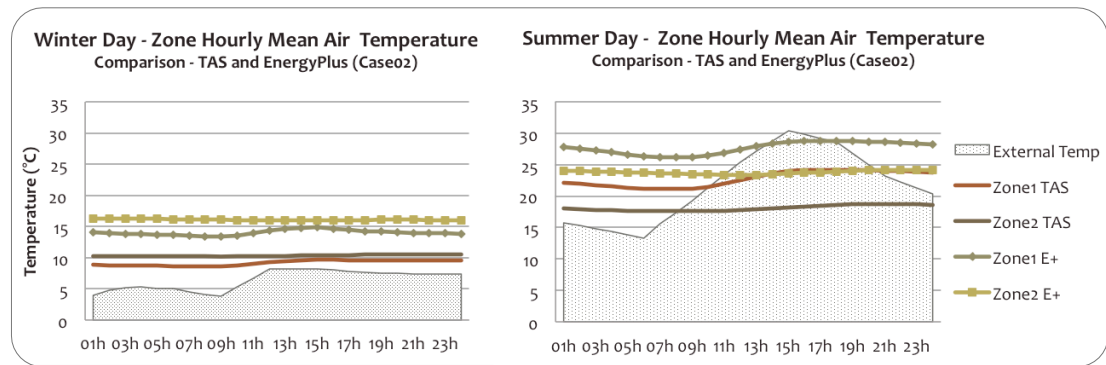
Figure 6.4: Model Case 02 Tas and E[+] winter and summer comparison

When using Case 02 (see Table 6.1) to compare Tas and E+ results the author observed that Tas registers lower temperature results than E+, on the winter and the summer day. The lower amplitude difference between the programs is found at the winter results, as illustrated in Figure 6.4, which show a mean disparity of 5°C at Zone 1 and of 5.4°C at Zone 2. During the summer the gap increases to a mean difference of 5.3°C at Zone 1 and 5.5°C at Zone 2.

6.1.4. Findings and Conclusions

As a result of this initial case study Ecotect was found to be unsuitable as a tool option for this research. It is found that the results produced by Ecotect did not follow the basic a priori hypothesis. This lead to the conclusion that ground contact, as an input parameter, is not been simulated by Ecotect. However, it is evident that Tas and E+ results show that the level of ground contact does affect the models performance, as initially expected. However the result values differ between these two software packages. For this reason, further tests are needed to clarify the difference and identify the most appropriate research tool for this project.

6.2. SECOND CASE MODEL – TAS AND E+

Table 6.2: Stages and analysed parameters
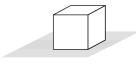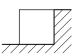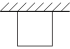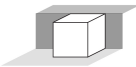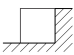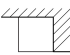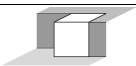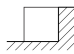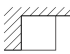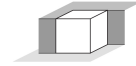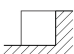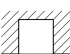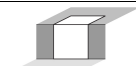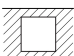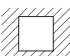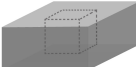
Software	Stage	Analysed parameters
E+	Defining procedure	• Results produce by different *'First run'* methods • Results patterns and discrepancies between E+ methods • Effects of simulation period: 1 Day versus 1 Month
	Comparative test	• Effects of ground contact on ground-integrated buildings
Tas	Comparative test	• Effects of ground contact on ground-integrated buildings
E+ & Tas	Comparative test	• Effects of ground contact on ground-integrated buildings

The second case study is divided in two stages. Firstly, it defines the procedures for E+ simulations and comparative tests (Table 6.2). Since E+ provides multiple ways to simulate ground heat transfer, defining a procedure is an essential step. For this reason the initial part of this case study is focused on testing different methods and settings. The second stage is focused on the analysis of the effect produced by ground contact on ground-integrated buildings. This is achieved through a comparative test between Tas and E+ results.

6.2.1. Model Dimension and Simulation Inputs

Table 6.3: Second Case models detail

Second Case Models

Name	Configuration and Level of Ground Integration			Floor	North Wall	East Wall	West Wall	South Wall	Roof
	Sections	Plans	Perspectives						
Model 00	No ground integration			X S					
Model 01	1 Side (N wall)			X S	X B				
Model 02	2 Sides (N + E walls)			X B	X B	X B			
Model 03	2 Sides (N + W walls)			X B	X B		X B		
Model 04	3 Sides (N + E + W walls)			X B	X B	X B	X B		
Model 05	4 Sides (N + E + W walls + Roof)			X B	X B	X B	X B		X B

X – surface with ground contact
S – E+ Models - outside surface temperature from the Slab auxiliary program
B – E+ Models - outside surface temperature from the Basement auxiliary program

The second case study model consists of a single zone block with no windows. The 3 m by 3 m model has a total area of 9 m^2 and a total volume of 27 m^3. The model's levels of ground integration are summarised in the Table 6.3.

As in the previous section, this study' simulations use the weather file of Bragança, Portugal. For higher contrast, the winter and summer days analysed correspond to the coldest and hottest days of the year - 19st January and 19st August. To prevent result differences due to complex material inputs and to amplify the impact of ground contact, all models use a single construction material of 20 cm thick concrete (Table 6.4).

Table 6.4: Models materials

Material	Width (cm)	Conductiv. (W/m.°C)	Convec. Coeff. (W/m^2.°C)	Density (kg/m^3)	Specific Heat (J/kg.°C)	Thermal Resist. (m^2.°C/W)
Concrete	20	0.51	-	1400	1000	R=0.2/0.51=0.392
	Thermal Absorpt.	Solar Absorpt.	Visible Absorpt.			U value (W/m^2.°C)
Concrete	0.9	0.65	0.65			1.772

6.2.2. E+ – Ground Heat Transfer Simulation Methods Using Slab and Basement Auxiliary Programs

With more or less complexity, E+ allows for the simulation of ground heat transfer in multiple ways. The main difference between processes is how the building surface temperatures in contact with the ground are obtained. The most complete and also most complex way to find surface temperatures is by using the Slab and Basement auxiliary programs. Slab and Basement auxiliary programs are part of the E+ package. These extra programs can be used to simulate ground heat transfer, and can be accessed through the EP-Launch window under the utilities tab (Department of Energy, 2012b). These pre-process programs generate monthly average zone air temperatures that can be later used. However, there are three different methods that can be used to generate these temperature values (Department of Energy, 2003; Andolsun et al., 2011, pp. 1664-1668, 2012, pp. 190-194; Department of Energy,

2012, pp. 81-116). Therefore these methods are compared in order to determine the simulation procedure.

Table 6.5: Different methods to apply when using Slab and Basement programs

	'First Run' Methods
Method 1 Building surface temperature as 18 °C	Site: Ground Temperature: Building surface = 18 °C (all year) Building Surface Detailed: ○ Outside Boundary Condition: Ground ○ Construction: Concrete floor
Method 2 Floor with external insulation	Building Surface Detailed: ○ Outside Boundary Condition: Ground ○ Construction: Concrete floor with Insulation
Method 3 Floor as an internal surface	Building Surface Detailed: ○ Outside Boundary Condition: Surface ○ Construction: Concrete floor

Buildings affect ground temperatures and for this reason undisturbed ground temperatures cannot be used as a final ground temperature input. In an initial stage, a model is simulated to calculate the initial building monthly average indoor temperature value. This first stage can be set in three ways, as described in Table 6.5. In a second stage, the 'first run' monthly average air zone temperature results for the model are run through the Slab and Basement pre-process programs. Both Slab and Basement auxiliary programs produce customised monthly average surface temperatures by generating output files that contain a Schedule: Compact list and a SurfaceProperty:OtherSideCoefficients list.

In a third stage, these results lists are inserted into the .idf files. While the Slab results have to be inserted manually, the Basement data can be inserted by copying and pasting the objects generated by the out_bsmt.idf file. Finally, this data can be accessed as an Outside Boundary Condition Object that can be selected for each structure element listed at BuildingSurface:Detailed, with the Outside Boundary Condition set to OtherSideCoefficients.

6.2.3. E+ - Results Produce by Different *'First Run'* Methods
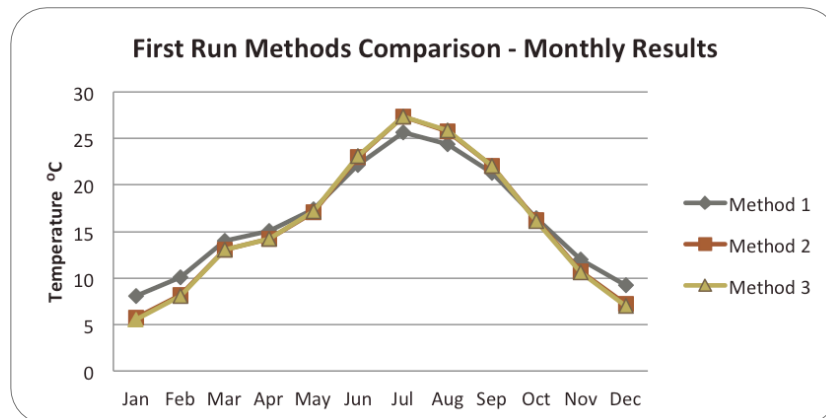
Figure 6.5: Monthly ground temperature results using different methods

As previously described, E+ allows to determine ground-surface temperature using three different methods. To identify the method used in this research a comparison between the values produce using those methods was made. With the comparison it was verified that the methods generate different monthly average zone air temperature results. The author found that Method 2 and Method 3 results are similar, but Method 1 generates different results. The result disparity is more visible during the coldest months of December and January and during the hottest months of July and August. As can be seen in Figure 6.5, for the coldest period Method 1 provides the warmest temperature as for the hottest period it generates the coldest ground temperature; therefore, Method 1 produces the results most inline with the a priori hypothesis.

6.2.4. E+ - Results Patterns and Discrepancies Between Different Methods

To identify the appropriate '*first run'* method, the corresponding monthly air temperature values of each method are used with the Slab and Basement auxiliary program simulations. Later, Models M00 to M05 are simulated for each of the three methods, using the corresponding building surface temperatures. To conduct this research, the winter and summer day data is retrieved from the model simulation results and compared.

Table 6.6: Models's winter and summer internal temperatures - different methods results

		Winter day (ºC)			Summer day (ºC)		
		M00	M05	Range	M00	M05	Range
Method 1	Min.	-0.87	7.76	8.62	27.44	24.23	3.21
	Max.	1.14	8.46	7.32	32.3	25.59	6.7
Method 2	Min.	-1.23	6.22	7.76	27.63	25.14	2.48
	Max.	0.8	6.93	6.13	32.48	26.51	5.97
Method 3	Min.	-1.26	6.09	7.35	27.64	25.19	2.44
	Max.	0.77	6.81	6.03	32.49	26.56	5.93

As shown in Table 6.6, temperature ranges are largest during the winter day than during the summer day. However, this temperature range increases or decreases depending on which method's results are used. The models that use the data obtained from Method 1 have the highest temperature values in winter, followed by results from Method 2 and Method 3. The temperature difference between the models (M00 to M05) is also larger when using data from Method 1. Concerning the summer results, the results are reversed: Method 1 registers the lowest temperature values and the range difference between models M00 and M05 is, again, the largest. The results produced by models that use Method 1 output values are closest to the anticipated ones.

Table 6.7: Methods temperature ranges and average temperature difference

		Methods Temperature Range (ºC)		Ave. Temp. Diff. Between Methods (ºC)	
		19th Jan.	19th Aug.	19th Jan.	19th Aug.
Model 00		2.02	4.85	0.37	0.19
Model 05		0.71	1.36	1.65	0.97

Regarding the effect of ground contact, the results amplitude differs according with level of ground integration, meaning that the higher the ground contact better the results. For all methods and both studied days, the author found that the temperature range decreases as ground contact increase (Table 6.7).

During winter, the average internal temperature differences between methods increases as the ground contact increases. For all methods, during the summer day the average internal temperatures decreases as ground contact increases.

For both days, the results generated by Methods 2 and 3 are almost identical, as shown in Table 6.6. The temperature difference between these two methods and Method 1 increases with ground contact, so the higher the ground integration the larger the difference in temperature. This relationship is more evident during the winter day, with a 1.65ºC average temperature difference between methods for Model 05 (see Table 6.7).

By comparing the *'first run'* procedures the author found that although all the result patterns for all methods are similar, the use of different methods can affect the simulation values. Methods 2 and 3 present closer temperature values and Method 1 results are most inline with the a priori hypothesis than Method 2 and 3 in the summer and winter days. Since the results generated by Method 1 are closer to the expected results, this method was chosen as the approach for the following E+ simulations.

6.2.5. E+ - Effects of Simulation Period: 1 Day versus 1 Month

During this study the author observed that the results are affected by the input simulation period. To identify how this input affect the results and what simulation period should be used, a brief comparison is made between results retrieved from one single day period input (19 Jan and 19 Aug), with a day result retrieved from a monthly period input (21 Dec to 21 Jan; 21 Jul to 21 Aug).
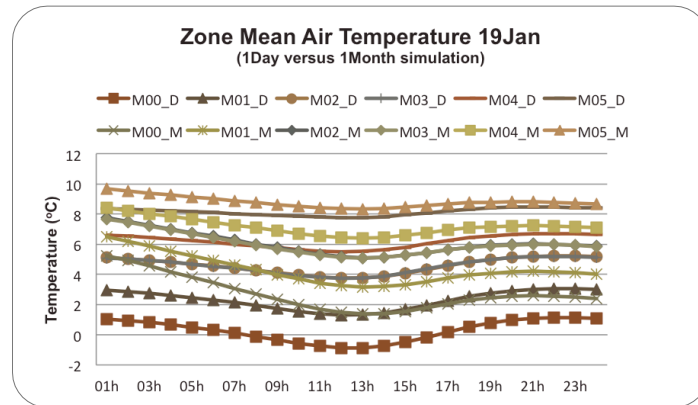
Figure 6.6: Model 00 to 05 – Winter day results from different simulation periods (1 day /1 month)
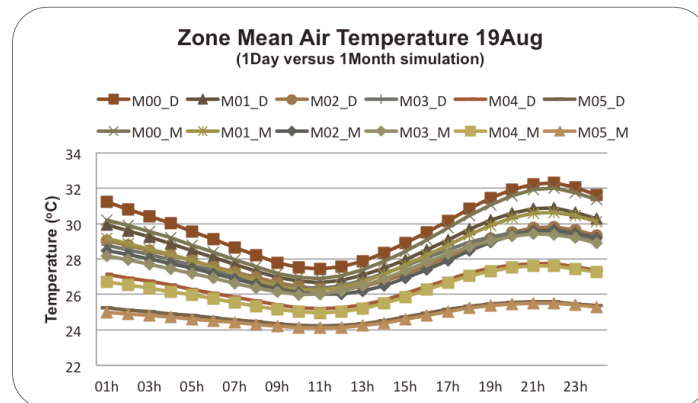
Figure 6.7: Model 00 to 05 – Summer day results from different simulation periods (1 day /1 month)

For all models, it is found that the internal temperature results for the studied winter and summer days are affect by simulation period. As can be seen in Figure 6.6 and 6.7, the monthly simulation produces higher temperature results in winter and lower temperature results in summer than a single day period simulation.

Table 6.8: Period comparison - single day versus month simulation results
Results difference between single day and monthly simulation period (ºC)

	Day time	M00	M01	M02	M03	M04	M05
19th Jan	00 am - 01 am	4.21	3	2.64	2.58	1.82	1.3
	23 pm - 00 am	1.28	1	0.7	0.68	0.44	0.27
19th Aug	00 am - 01 am	1	0.78	0.55	0.62	0.43	0.25
	23 pm - 00 am	0.26	0.19	0.14	0.15	0.1	0.07

The largest differences between results are found during the initial hours, and the gap gradually narrowed during the day, as shown in Table 6.8. This indicates that the single day period simulation results are not taking the weather conditions of previous months or even days into consideration. Because ground thermal potential

follows the weather conditions with a specific time lag, the ground temperatures at a particular depth can be affected by the weather conditions of previous weeks or even seasons. The use of larger simulation input periods ensures that E+ is considering a larger weather sample and therefore the results should be more consistent.

The author studied the effect of the simulation period as an input by comparing the results between a single day and one month simulation period. The results demonstrated that temperature outputs are affected by the simulation period. The monthly period simulation produced better results: during winter the monthly period results are higher, and during summer the monthly period results are lower. Therefore it is concluded that larger simulation input periods such as monthly or yearly data are preferable to single day inputs.

6.2.6. E+ - Effect of Ground Contact on Ground-integrated Buildings
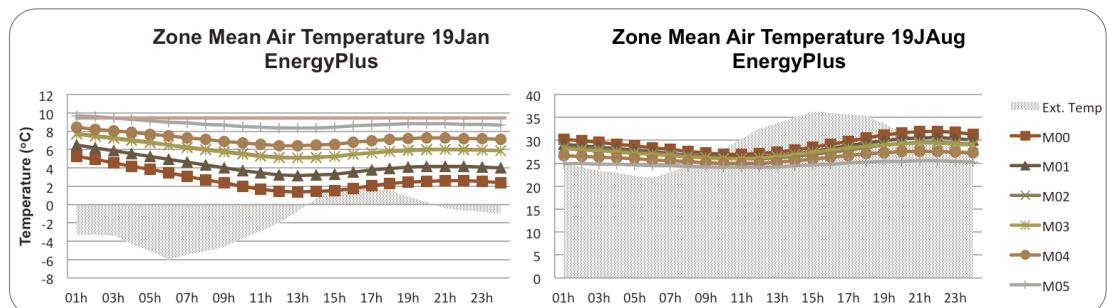
Figure 6.8: Winter and summer day internal air temperature according with models ground contact – E+ Model 00 to 05

This section examines in more detail the effect of ground contact on the E+ model results. It is found that for summer and winter, the larger the model's ground contact the greater the difference between the outside ambient air temperature and models air temperature, therefore greater is the thermal comfort. As visible in Figure 6.8, during winter the internal temperatures are higher when ground contact increases, and in summer the temperature decreases when ground contact decreases.

It is also observed that the higher the ground integration, the lower the internal air temperature amplitude range, generating more constant internal temperatures. It is therefore concluded that the level of ground contact affects the models' results. The increase in ground contact generates a better annual thermal performance, since the internal temperatures are more stable and less affected by outside climate conditions.

6.2.7. TAS – Effects of Ground Contact on Ground-integrated Buildings
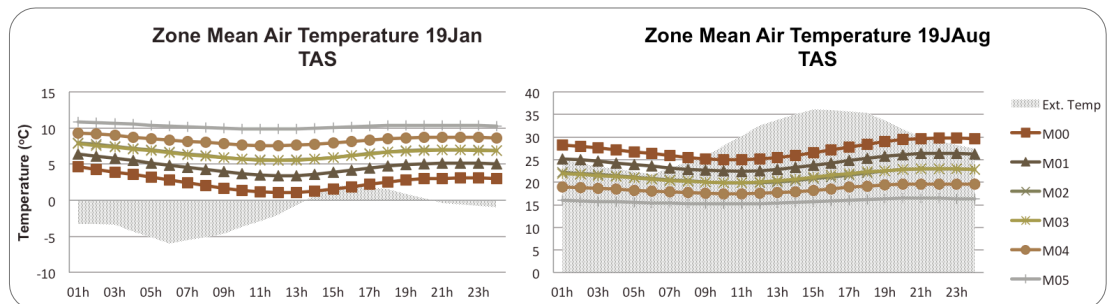
Figure 6.9: Winter and summer day internal air temperature according with models ground contact – Tas Model 00 to 05

Regarding the results produced by Tas, it is found that across the whole year, the amount of ground integration affects the thermal performance of the model. In winter, the higher the ground contact the higher the internal average air temperature. During summer the opposite is found, so the higher the ground contact the lower the internal average air temperature (Figure 6.9).
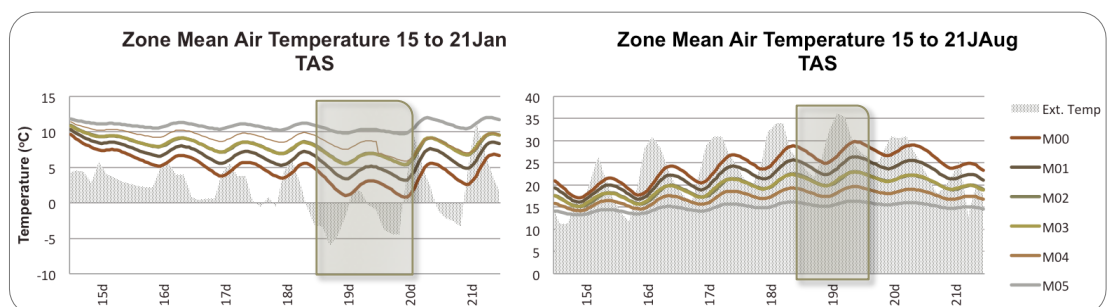
Figure 6.10: Winter and summer week: Internal air temperature according with models ground contact – Tas Model 00 to 05

The largest temperature difference between the study models was found in the summer and occurs when the maximum outside ambient temperature is registered. The models' temperature ranges are smaller in winter and the largest temperature

difference is found when the minimum internal temperatures are registered. With the weekly results, displayed in Figure 6.10, it is observed that the temperature difference between models increases in winter when outside minimum and maximum temperature decrease, and during summer, when external temperatures increase. This shows a greater influence of daily weather conditions on models with lower levels of ground contact.

Through this comparative test between models with different levels of ground integration the author concluded that level of ground contact influences the Tas models' internal air temperature. The higher the ground integration better the annual thermal performance. Also, the internal air temperatures are more constant and less dependent on outside climate conditions.

6.2.8. Comparison Between E+ and TAS Results

Table 6.9: Tas and E+ results comparison

Temperature difference between Tas and E+ simulation (ºC)

Models		M00	M01	M02	M03	M04	M05
19th Jan	Min.	0.33	0.23	0.44	0.41	1.14	1.49
	Max.	0.65	0.10	0.18	0.15	0.91	1.19
	Ave.	0.19	0.35	0.52	0.50	1.18	1.44
19th Aug	Min.	1.91	3.82	6.14	6.12	7.52	8.95
	Max.	2.21	4.23	6.60	6.46	7.98	9.08
	Ave.	2.00	3.98	6.32	6.26	7.73	9.01

Through the comparison between Tas and E+ results, it is found that the internal temperature difference is smaller in winter with average values between 0.19ºC to 1.44ºC, than in summer when average values ranged from 2ºC up to 9.01ºC (Table 6.9). This difference increases with ground contact since the higher the ground contact value, the larger the range between the results generated by different software packages.
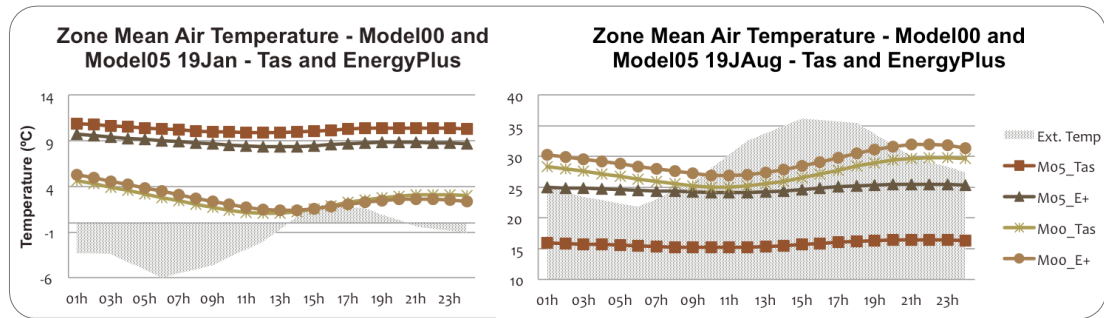
Figure 6.11: Winter and summer day: Internal ait temperature – Model M00 and M05 – Tas and E+ comparison

The level of ground contact affects both software results. Tas registers better thermal performance on both the summer and winter days, with the largest difference between programs results found on the summer day. The higher the ground contact the larger the gap between the different results generated by each software package. As can be seen in Figure 6.11, during the summer day Tas temperature results for model M05 are below the maximum and minimum daily outside temperatures. While the E+ model M05 results are above the minimum outside temperature. To identify what causes the discrepancy of results between Tas and E+, an additional case study based on a sensible test was made.

6.2.9. Findings and Conclusions

This study establishes the methodology used by E+ to calculate ground heat transfer. E+ provides multiple processes to take ground contact effect into consideration during building energy simulations. One of the processes used by E+ are the Slab and Basement auxiliary programs, which produce pre-process data to be later inserted into the E+ .idf files. This process allows E+ simulations to use the disturbed ground temperature produced by the building itself. To perform this process there are three methods to determine the initial internal temperatures for the auxiliary programs simulations. Overall, the author found that although all methods produce similar patterns, the values can differ. Therefore, the method selected was Method 1, which sets the initial building monthly surface temperature at 18°C.

Additionally, the author found that E+ results are affected by the simulation period, since the longer the simulation period the better the results. This study shows that E+ 'builds up' the results as a continuous simulation process over the course of the simulation period. For this reason larger simulation periods such as one-year are recommended.

Regarding the ground integration effects, both software results show that the higher the ground integration, the better the internal air temperatures. The author found that the temperatures found inside ground-integrated buildings are more constant and less dependent on outside climate conditions since the internal temperature ranges decrease as ground integration increases. When comparing both programs, it is found a result discrepancy between Tas and E+, which increases when simulating models with greater levels of ground contact. Regarding the model with the highest ground integration, during the winter day, the average result difference between the two software packages is 1.44ºC and during the summer day, when the difference was greatest, it is 9.01ºC. To identify the cause for this results discrepancy and sensible case study was made.

6.3. THIRD CASE STUDY – TAS AND E+

Table 6.10: Stages and analysed parameters
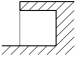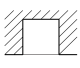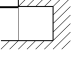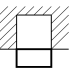
Software	Stage	Analysed parameters
E+	Sensible test	• Effects of ground contact, insulation and shadow device
Tas	Sensible test	• Effects of ground contact, insulation and shadow device
E+ & Tas	Results Comparison	• Effects of ground contact, insulation and shadow device

This third case study analyses how each program simulates ground integration effects through a sensible test. The study is based on testing the impact of parameters such as ground contact, insulation, and shadow device (Table 6.10). The simulation package used in this thesis is determined with the comparison between E+ and Tas results.

6.3.1. Model Dimension and Simulation Inputs

Table 6.11: Third Case models detail

Third Case Models (Sensible test)

Name	Configuration and Level of Ground Integration	Floor	North Wall	East Wall	West Wall	South Wall	Roof
	Sections Plans Perspectives						
Model C01	4 Sides (N + E + W walls + Roof)	X B	X B	X B	X B	Insulated	X B
Model C02	4 Sides (N+E+W walls + Roof+shadow device)	X B	X B	X B	X B	Insulated; shadow device	X B
Model C03	5 Total ground integration - Underground	X B	X B	X B	X B	X B	X B

X – surface with ground contact
S – E+ Models - outside surface temperature from the Slab auxiliary program
B – E+ Models - outside surface temperature from the Basement auxiliary program

This case study uses the same model as Section 6.2. and it focus on two levels of ground integration, a four sides and a total ground integration, as shown in Table 6.11. It uses the same weather file and winter and summer days described in Section 6.2. All surfaces are made of a single construction material of 20 cm concrete. Damp proof and insulation is not used with any models surface apart of the south wall of Model C01 and C02, which has an extra layer of insulation (Table

6.12). A shadow device is introduced in Model C02. Its size is designed to minimize the direct solar radiation received by the insulated south wall.

Table 6.12: Models materials

Material	Width (cm)	Conductiv. (W/m.°C)	Convec. Coeff. (W/m^2.°C)	Density (Kg/m^3)	Specific Heat (J/Kg.°C)	Thermal Resist. (m^2.°C/W)
Concrete	20	0.51	-	1400	1000	R=0.2/0.51=0.392
Insulation	30	0.03	-	140	1380	R=0.3/0.03=10
	Thermal Absorpt.	Solar Absorpt.	Visible Absorpt.			U value (W/m^2.°C)
Concrete	0.9	0.65	0.65			1.772
Insulation	0.9	0.6	0.7			0.098

6.3.2. E+ - Effects of Ground Contact, Insulation and Shadow Device
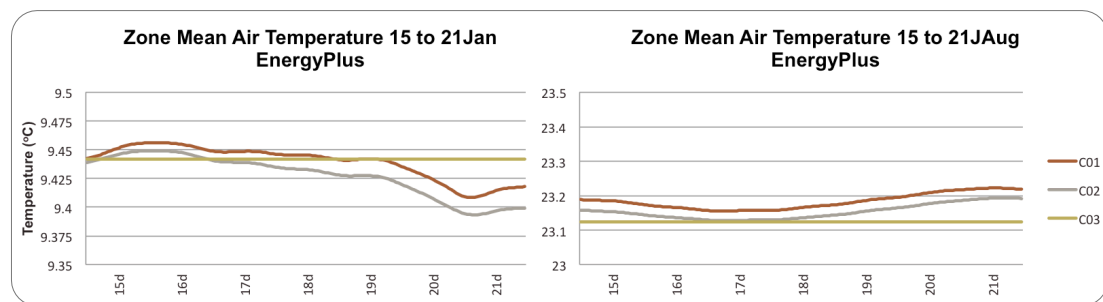
Figure 6.12: Winter and summer week: Daily internal air temperature – E+ Model C01 to C03

This section investigates the effects of ground contact, insulation, and shadow device. It is observed that during winter and summer the results for the totally underground model (C03) are constant and not influenced by the weather conditions of the studied period (Figure 6.12). The temperatures of Model C01 (with insulation) and C02 (with insulation and shadow device) are almost constant. Moreover, by crossing information displayed in Figure 6.12, Figure 6.14 and Figure 6.15 it is found that this small weather influence has a time lag of one day. This demonstrates that, although by a small degree, Model C01 and C02 are affected by the outside weather conditions, while Model C03 is only affected by the ground thermal conditions. Regarding the shadow device on Model C02, it is found that this feature is able to reduce the gap between Model C01 and C03.

The author therefore concluded that all elements are able to affect buildings' thermal performance. However, ground contact has a higher impact on heat gains and losses shown by these models than the insulation and shadow device.

6.3.3. TAS - Effects of Ground Contact, Insulation and Shadow Device
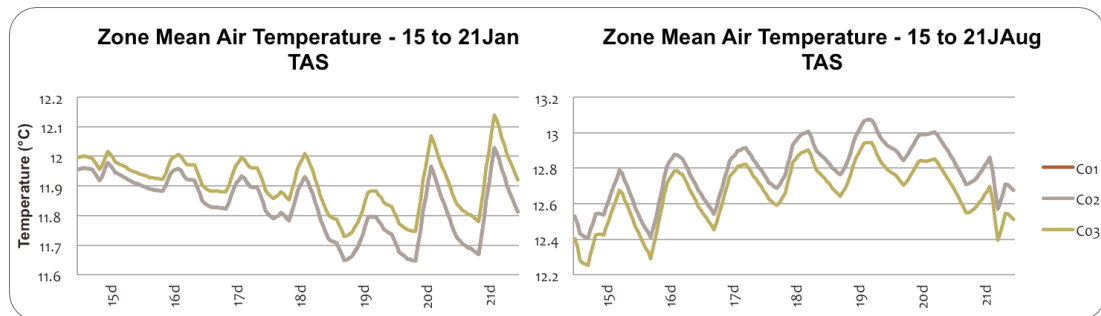
Figure 6.13: Winter week: Internal air temperature – Tas Model C01 to C03

By comparing the results from the Tas models it is found that Model C01 and C02 values are identical (Figure 6.13). Both models register an average 0.05°C lower temperature during winter, when compared with Model C03, and an average 0.1°C higher temperature in summer. These results show that the shadow device effect on Model C02 is not being taken in account by the Tas simulations.

Overall, the results indicate that ground contact is able to reduce heat gains and losses, and the use of insulation generates a reduction of heat gains and losses. It is found that insulation has a greater effect on the exposed south façade wall since the shadow device contribution on Model C02 results is not being considered. However the most surprising finding is that the daily weather conditions continue to affect all models results, even when Model C03 is underground. As an underground structure, the model's internal air temperature for the sample periods should be constant.

6.3.4. E+ and TAS - Effects of Ground Contact, Insulation and Shadow Device
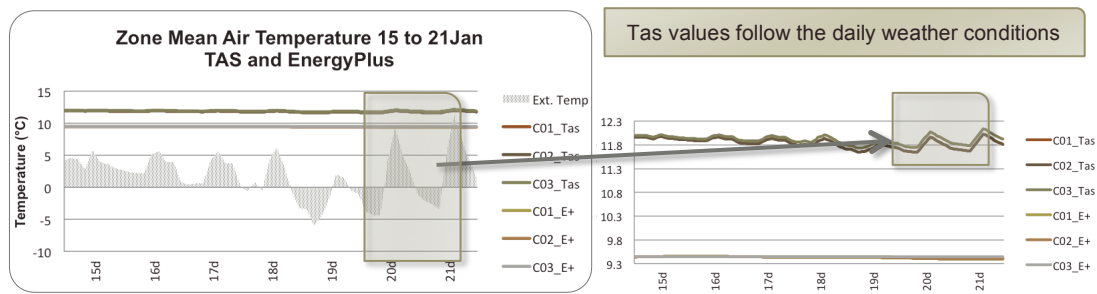
Figure 6.14: Winter week: Internal air temperature - Model C01 to C03 - Tas and E+ comparison
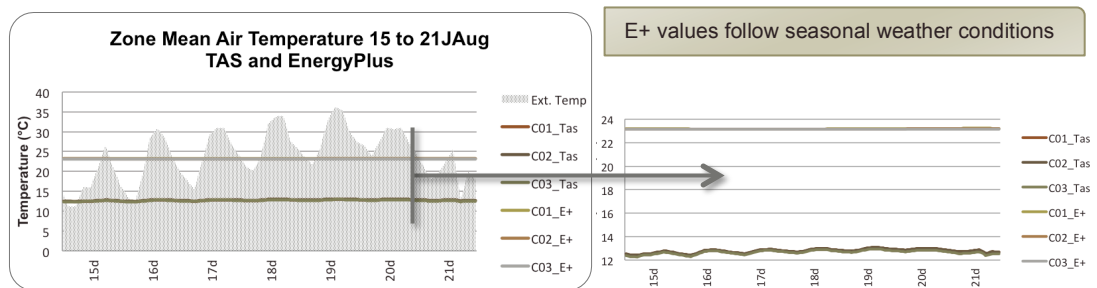
Figure 6.15: Summer week: Internal air temperature - Model C01 to C03 - Tas and E+ comparison

Table 6.13: Tas and E+ average temperature difference according with Model C01 to C03 averages results

Ave. temp. diff. between Tas and E+ (ºC)	19th Jan.	19th Aug.
	2.42	10.41

The comparison of the results from Tas and E+ indicates that one of the main differences between the two software packages is found in the average air internal temperature values. Tas temperatures are 2.42°C higher in the winter and 10.41°C lower in the summer than E+ (Figure 6.14, 6.15 and Table 6.13). The second difference is that the temperature patterns are different. All Tas models' results follow the daily outside temperature changes, whereas in the results obtained from E+, only Model C01 and C02 follow the average daily outside temperatures, instead of the daily ones. As for Model C03, this underground model produces consistent winter and summer results with E+.

During the winter and summer days, the Tas simulation results for Model C01 and C02 are identical (Figure 6.16 and 6.17). The south façade insulation blocks heat gains or loss, which explains why Model C02' shadow device has no effect on the

results. Concerning Model C03, totally underground, it registers the warmest temperature in winter and the coldest in summer, which indicates that the increased level of ground contact produces the best results. However, for all Tas models it is visible that, during both winter and summer, the internal average air temperatures follow the daily ones without any time lag. This goes against the fact that the daily weather conditions should stop affecting ground temperatures below depths of around 20 to 30 cm (Krarti and Kreider, 1996, p. 1564).
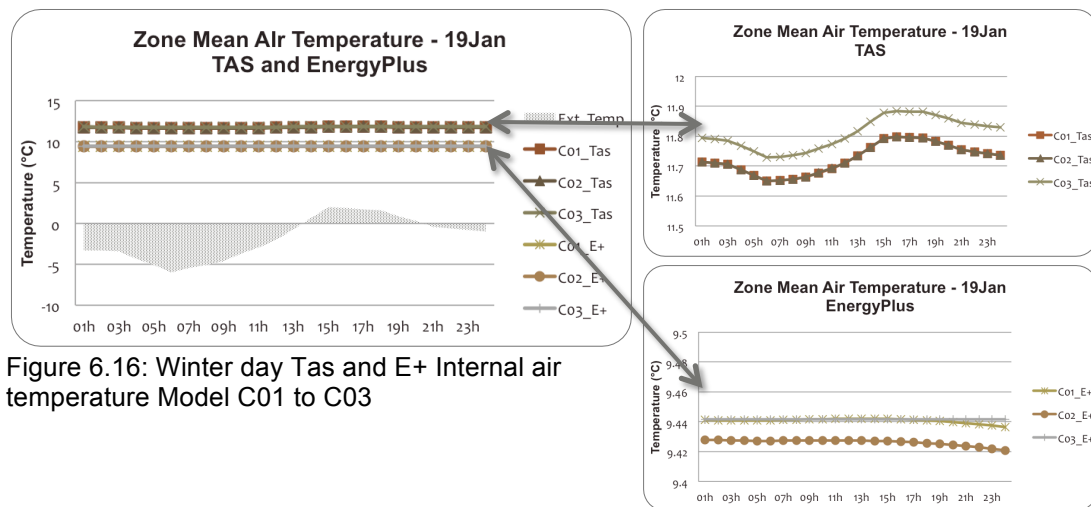
Figure 6.16: Winter day Tas and E+ Internal air temperature Model C01 to C03

Contrasting with this result, E+ temperature results pattern for Model C01 and C02 do not follow the daily temperatures. Instead, the results follow the average daily temperature with a time lag of one day, so their changes are more gradual as if following a 'seasonal' pattern. In the case of Model C03, the temperature results are constant for the sample periods, as expected for an underground model.

In winter, the difference of results registered by E+ temperature in all models is reduced (Figure 6.16). However, the temperature values for Models 01 and 03 are almost identical, and Model 02 has the lowest temperatures. This shows that the solar gains received by the insulated South façade allows Model 01 to have similar results as Model 03. Therefore, the lack of solar gains experienced by Model 02 produces the lowest internal temperature. Although the input insulation is equal for both software packages, the result outcome is different.

During summer, the E+ temperature results difference between all models is once again small and increases throughout the day (Figure 6.17). Model C03 has the lowest temperature values, while Model C01 has the highest ones. Temperature results for Model C02 are lower than Model C01 because the shadow device is reducing the solar gains.
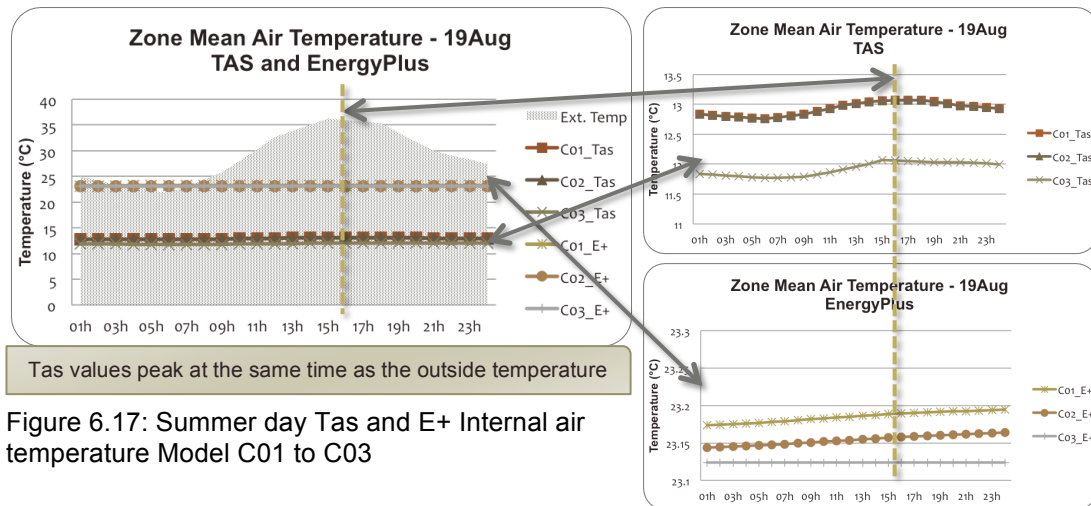
Figure 6.17: Summer day Tas and E+ Internal air temperature Model C01 to C03

In this comparison, it is clear that Tas and E+ present different behaviours. Tas results have a daily pattern that follows the outside temperature, as expected from a steady-state calculation. Results from E+ have a seasonal pattern, which shows that E+ simulations take weather data into consideration in a cumulative way.

Regarding the temperature difference, in summer the results show a large gap between the two software packages. During this period Tas' internal temperatures are approximately 10°C lower than E+. Concerning the insulation, the author found that it has a greater effect on Tas results than on E+ results. For this reason the shadow device effect on Model C02 is not been considered on Tas results, but is visible on E+ results.

6.3.5. Findings and Conclusions

This study shows that although Tas results are better than E+, the results are proved to be misleading, as they just follow the weather conditions as a steady-state

calculation. Regarding ground contact effect, the results for the underground model put through Tas are not able to produce a constant temperature. This proves that its ground heat transfer calculations have limitations. Furthermore, the ground temperatures found around a ground-integrated structure are affected by the same structure. Tas simulation results appear to not take this into account, and therefore its good results might be caused by the use of undisturbed ground temperature.

Taking the results presented above into consideration, the author decided that E+ was the most reliable software to use on the research. Although more complex and time consuming to use, its simulation results have proved to be more consistent, particularly when compared with the results obtained by Tas.

6.4. SLOPE SIMULATION WITH ENERGYPLUS

The last part of this chapter presents a study which has two purposes. Firstly, to verify what difference, if any, would be found by comparing flat and slope ground integration models with equal ground contact and the same outside surface temperatures. The assumption is that, in these circumstances, the final results should be identical. Secondly, this study aims to define the procedure which should be adopted when simulating slope ground integrations, by identifying what outside surface temperature should be used on walls with slope integration.
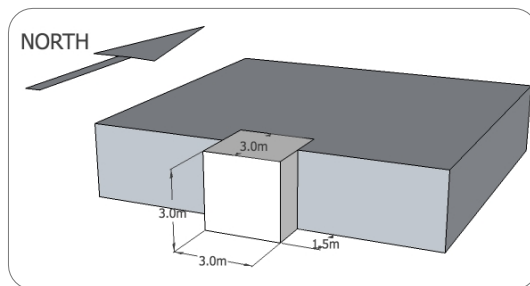
Figure 6.18: Flat ground integration model
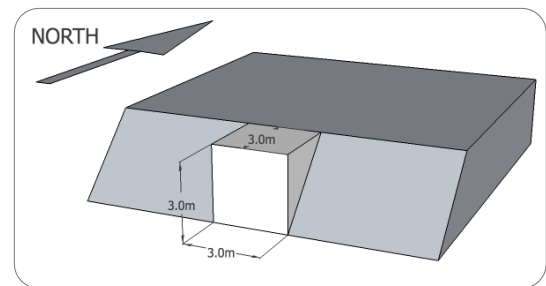
Figure 6.19: Slope ground integration model
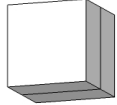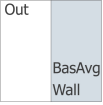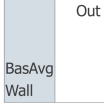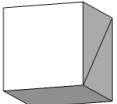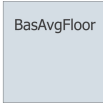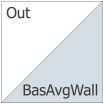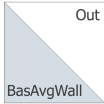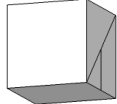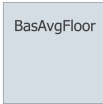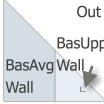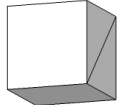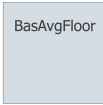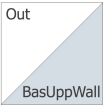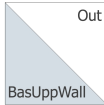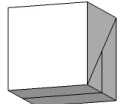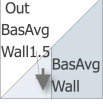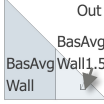
As previously discussed in Chapter 5 (Section 5.3), slopes affect the solar radiation values received by a surface, and as a consequence the ground surface temperature differs according with the ground surface gradient as verified in Section 5.4. This means that the ground temperatures at a specific depth are different for flat and sloped surface areas. However, when basement outside surface temperatures are simulated, the depth of the wall bellow the ground is considered, but it is assumed that these values are constant. This means that these simulations assume that the ground integration of their models occurs on a flat surface. Consequently, the ground temperatures are calculated by applying the solar radiation amounts received by a flat surface.

6.4.1. Model Dimension and Simulation Inputs

All models have the same dimensions and use the same construction material. As shown in Figure 6.18 and 6.19, the models share the same amount of direct ground

contact. Both models' north walls have full ground integration, while half of the east and west walls are in direct contact with the ground.

Table 6.14: Models inputs – surfaces with ground contact

Name	Surface with Ground Contact				
		Floor N	North Wall	East Wall N	West Wall N
01_Flat		BasAvgFloor / SlabAvgFloor	BasAvgWall	Out / BasAvgWall	Out / BasAvgWall
02_Slope		BasAvgFloor	BasAvgWall	Out / BasAvgWall	Out / BasAvgWall
03_Slope1		BasAvgFloor	BasAvgWall	Out / BasUppWall / BasAvgWall	Out / BasUppWall / BasAvgWall
04_Slope2		BasAvgFloor	BasAvgWall	Out / BasUppWall	Out / BasUppWall
05_Slope3		BasAvgFloor / BasAvgFloor 1.5m	BasAvgWall	Out / BasAvgWall1.5 / BasAvgWall	Out / BasAvgWall1.5 / BasAvgWall
Floor	SlabAvgFloor - Outside surface temperature: SlabAverage BasAvgFloor - Outside surface temperature: BasementAvgFloor; Depth=3m BasAvgFloor1.5 - Outside surface temperature: BasementAvgFloor; Depth=1.5m				
Wall	BasAvgWall - Outside surface temperature: BasementAvgWall; Depth=3m BasUppWall - Outside surface temperature: BasementUpperWall; Depth=3m BasAvgWall1.5 - Outside surface temperature: BasementAvgWall; Depth=1.5m				

The outside surface temperatures generated by the Basement auxiliary program provides three different wall surface values named as BasementAverageWall, BasementUpperWall and a BasementLowerWall. The BasementAverageWall gives the mean outside surface temperature of the wall, the BasementUpperWall provides the values for depths closer to the ground surface and the BasementLowerWall gives the surface outside temperatures on the deepest area of the wall. The ground integration of 01_Flat's east and west walls are delimited by a vertical axis at the walls centre. As for the slope models, the ground integration is limited by a diagonal axis. This raises the question of what outside surface temperatures should be used. Consequently Models 02_Slope to 05_Slope in Table 6.14 explore a mix of different approaches to identify the most appropriate one to be used across this thesis.

6.4.2. Results and Discusssion

The initial assumption that the final results would be identical is not confirmed by analysis of the results of this test. The 01_Flat and 02_Slope models with equal amount of ground-integrated area and outside surface temperature fail to produce identical results. In fact, the models' total annual loads results, presented in Figure 6.20, show that all slope models produce better outcomes than the flat model.
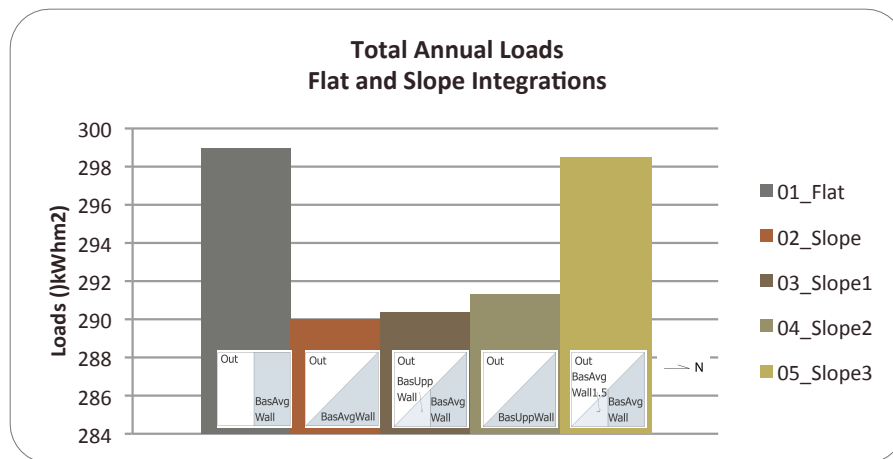
Figure 6.20: Total annua loads values for flat and slope ground integrations models

Floor inputs affect the results' gap between 01_Flat and 02_Slope models. The slope model floor has the advantage of having a large area with the basement average floor temperatures. In the case of the flat model, the floor is divided in two areas, a north side floor area that uses the basement outside surface temperatures, and a south floor area that uses the slab outside surface temperatures. The flat and slope results only come close in 05_Slope when the floor, east and west walls use a mix input of basement average temperatures for 3 and 1.5 m depth.

Through this study the author argue that a comparison between models with flat and slope integration using the same outside surface temperatures is not an accurate procedure. Therefore the author established that for future ground integration studies, flat and slope integrations should not coexist. For slope models it is adopted the outside temperatures input scheme presented in 04_Slope, as it presents a balance between all slope input configurations.

6.5. CONCLUSIONS

As a result of the comparative tests explained above, the author concluded that E+ presents the most adequate performance to be used on this research. The simulation outcomes of this program proved to be more consistent than results obtained when using Tas. The reason why Tas internal temperatures are so different from E+ can be explained by the calculations presented by Tas, which use undisturbed ground temperatures. On the other hand, E+ uses disturbed ground temperature, through the use of the outside surface temperatures generated during the simulation process.

Regarding the simulation methodology, the ground heat transfer method to be used with E+ is identified and the running period is defined. The author determined the use of Slab and Basement auxiliary programs, in order to find the outside temperature of surfaces with directed ground contact. It was also established that the *'first run'* simulation is made by setting the initial building monthly surface temperature as 18°C. For the final simulations, it is recommend the use of larger simulation periods such as one full year.
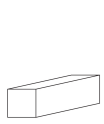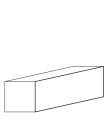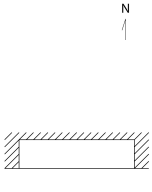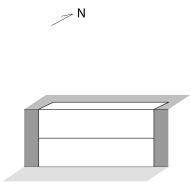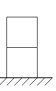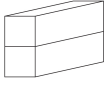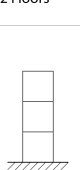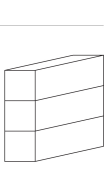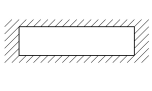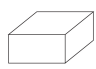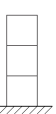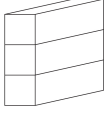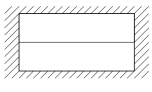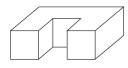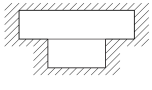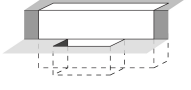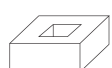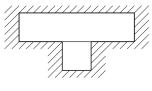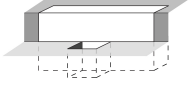
The objective of the slope simulation study is to identify the simulation procedures that should be used in applying outside surface temperatures to structures with slope-integration. Although E+ is not able to use ground inclination as a ground temperature parameter, this does not detract from its greater potential for modelling the thermal performance of buildings with direct ground contact. The results involving slope integration can be used to identify thermal patterns. However, the thermal performance comparisons between flat and slope integrations are not recommended, since the Basement auxiliary program does not have inputs for slope terrains. Therefore the process to calculate the exterior temperature of the structure elements with direct ground contact is limited to horizontal surfaces. Consequently,

the following chapters present cases studies divided in ground and slope integration. In Chapter 7 the author analyse the effect of direct ground contact is by assuming that the terrain is horizontal and Chapter 8 examines ground effect generated with slope gradients.

CHAPTER 7. CASE STUDIES: GROUND INTEGRATION

7. CASE STUDIES: GROUND INTEGRATION

Table 7.1: Chapter studies - Forms, Floors and Basement and Courtyard

Forms		Floors		Basement and Courtyards	
Plan	Perspective	Section	Perspective	Plan	Perspective
Long - long depth		1 Floor		Above Ground	
Long - Short depth		2 Floors		Basement	
Compact		3 Floors		Basement with Courtyard 1/1	
Semi-courtyard				1/2	
Courtyard				1/3	

In this chapter the author discuss the effect of direct ground contact on the thermal performance of buildings by analysing the annual and seasonal thermal patterns provided by changing levels of ground integration. This study is divided into three sections, based on three design features: building form, number of floors, and the use of basement and courtyards. As illustrated in Table 7.1, the Forms section looks into the thermal performance of five models based on four shapes as long, compact, semi-courtyard and courtyard. The results of this initial section are used to develop

the models and ground integrations which are applied in subsequent sections. The Floors section compares how the number of floors can affect buildings thermal performance. The last section looks at how the thermal performance of buildings can benefit from elements such as basements and courtyards.

Simulation settings and inputs data:

1. Software Version: EnergyPlus 8.1.
2. Simulation Method: follows the proposed EnergyPlus simulation method for ground-integrated buildings described in Chapter 6.2.
3. Location: Lisbon.
4. Weather File: the weather data described in Chapter 5 Section 5.2.2. uses the Climate Design Data 2009 ASHRAE Handbook design conditions.
5. Internal Gains: no internal gains were used.
6. Ventilation: no ventilation was used.
7. Infiltration: no infiltration was used.
8. Comfort Zone: the annual comfort range at this location it is assumed to be between 20°C to 26°C.
9. HVAC: the heating SetPoint is 20°C and cooling SetPoint is 26°C.
10. Openings: no openings were used.
11. Materials: all surfaces are assumed to be 20 cm concrete, see Table 6.4 in Chapter 6.
12. Seasonal data: it is assumed that winter period correspond to January, February and March; the spring period combines April, May and June; the summer season is formed by July, August and September; the autumn period is formed by October, November and December.

7.1. FORMS STUDY

From early sketch conceptualisation to construction, a buildings' design develops around a form. For different locations and climates, building shape and volume are elements that can affect building's thermal performance in different ways. This case study aims to identify the most appropriate building form for the 38-degree-latitude location of Lisbon. It also aims to understand how the thermal performance of buildings is affected by direct ground contact. The five main models used in this study are a long form with an East-West axis, a long form with North-South axis, a compact form, a U shaped model with a south facing open atrium or semi-courtyard, and an square shape model with a central courtyard. This section's results identify the base models for the following simulation studies by identifying the best model and the most relevant levels of ground integration.

7.1.1. Models Description and Levels of Ground Integration

Table 7.2: Models characteristics - Forms study with ground integration

Model Name	Model F01	Model F02	Model F03	Model F04	Model F05
Models					
Area (m^2)	168	168	168	168	168
Perimeter (m)	62	62	52	70.8	73.6
Ratio A/P	2.7	2.7	3.23	2.41	2.28

The five models illustrated in Table 7.2, share the same height, floor area and volume, and are based on a single floor unit. Model F01 and F02 differ on their orientation, while F01 is oriented around an East-West axis, so the walls with larger surface areas are facing north and south. F02, meanwhile, has a North-South axis so the walls with the smaller surface area are facing north and south. The most compact shape is F03, has the smallest perimeter. The models F04 and F05 have a larger number of walls and, therefore, the largest perimeter and lowest ratio of area to perimeter.

The following table provides further details of these five modules, identifying the models' names, dimensions, type of ground integration and the reference name used to refer to each model during the simulations.

Table 7.3: Models details - Forms study with ground integration
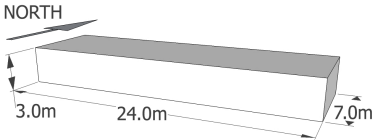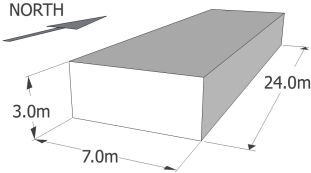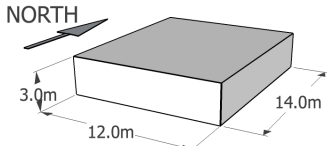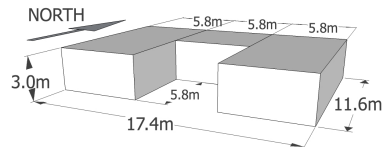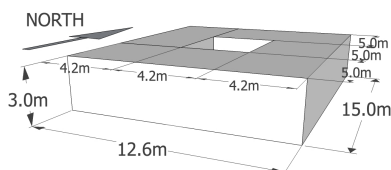
Models Dimensions	Ground Integration	Ref. Name
	01 – No Ground Integration	F01_01
	02 - North Wall	F01_02
	03 - North & West Wall	F01_03
Model F01	04 - North & East Wall	F01_04
	05 - North, West & East Wall	F01_05
	06 - Roof, North, West & East Wall	F01_06
	07 - Total Underground	F01_07
	01 – No Ground Integration	F02_01
	02 - North Wall	F02_02
	03 - North & West Wall	F02_03
Model F02	04 - North & East Wall	F02_04
	05 - North, West & East Wall	F02_05
	06 - Roof, North, West & East Wall	F02_06
	07 - Total Underground	F02_07
	01 – No Ground Integration	F03_01
	02 - North Wall	F03_02
	03 - North & West Wall	F03_03
Model F03	04 - North & East Wall	F03_04
	05 - North, West & East Wall	F03_05
	06 - Roof, North, West & East Wall	F03_06
	07 - Total Underground	F03_07
	01 – No Ground Integration	F04_01
	02 - North Wall	F04_02
	03 - North & West Wall	F04_03
Model F04	04 - North & East Wall	F04_04
	05 - North, West & East Wall	F04_05
	06 - Roof, North, West & East Wall	F04_06
	07 - Total Underground	F04_07
	01 – No Ground Integration	F05_01
	02 - North Wall	F05_02
	03 - North & West Wall	F05_03
Model F05	04 - North & East Wall	F05_04
	05 - North, West & East Wall	F05_05
	06 - Roof, North, West & East Wall	F05_06
	07 - Total Underground	F05_07

Table 7.4: Level of ground integration - Forms study with ground integration

Levels of Ground Integration	Sections ⟶N	Plans N	Perspectives ⟶N	Walls Depth
01 – No Ground Integration				0 m
02 – North Wall (1 Side)				
03 – North & West Walls (2 Sides)				
04 – North & East Walls (2 Sides)				3 m
05 – North, West & East Walls (3 Sides)				
06 – Roof, North, West & East Walls (4 Sides)				
07 - Total Underground				3.5 m

This case study uses seven levels of ground integration, as illustrated in Table 7.4. It starts from null ground integration, when the building is above ground (01) and only the floor is with direct contact with the ground, to total ground integration (07), when the whole exterior is in direct contact with the ground. For integration 02, 03, 04 and 05 the walls in contact with the ground assumes a wall height of 3 m. For integration 06 and 07 the walls with ground contact are 3.5 m below ground and there is a roof ground coverage of 0.5 m (see Chapter 3 Section 3.4.3).

7.1.2. Results Analysis

7.1.2.1. Annual Results
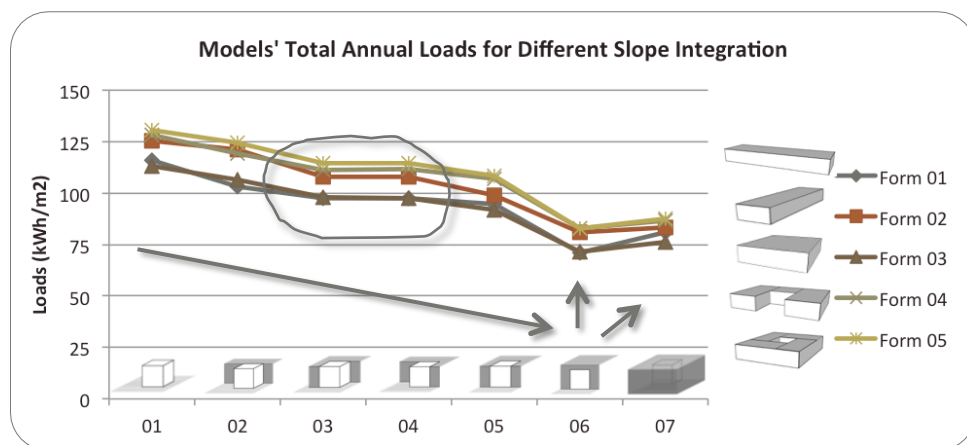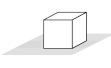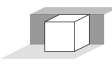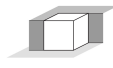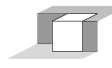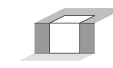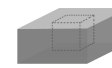
Figure 7.1: Ground contact effect on Form models' total annual load

The annual results for all models show a similar pattern, as shown in Figure 7.1. The total annual energy demand for each building can be reduced through ground-integration. By increasing the level of ground contact the energy needs of each building decrease. The exception in all models is the total underground integration, which achieved only the second best results. These results show that total underground integration is not the best approach for this climate.

Table 7.5: Form models' annual thermal performance according with ground integration
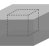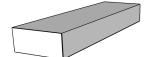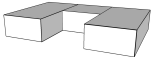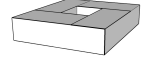
Effect of Ground Integration on Models Annual Thermal Performance

01	02	03	04	05	06	07
Above Ground	1 Wall (3m)	2 Walls N&W (3m)	2 Walls N&E (3m)	3 Walls (3m)	Roof & 3 Walls (3.5m)	Total Und. (3.5m)
7	6	5**	4**	3	1	2

← Scale 1 to 7 →

* Performance Scale 1 to 7 (1= Best performance & 7= Worst performance); ** For Form 01 and 04 the order is reverse, and for all forms: Ground Integration 03 and 04 have similar results.

The results for each model are summarised in Table 7.5 according with their thermal performance, ordered from best (1) to worst (7). The best annual results are found in ground integration 06, in which only the south facing wall is not in contact with the ground. The second best result was achieved by the total underground integration (07). The use of ground integration 05 produces the third best solution, demonstrating that this integration is a good compromise if there is no desire to cover the roof of the building, due to design restrictions or construction costs. Ground integrations 03 and 04 share similar annual results. Looking at the annual savings produced by the ground coupling displayed in Table 7.6, it is clear that these values of ground integration 03 and 04 are almost identical in all the models.
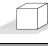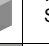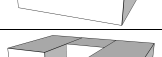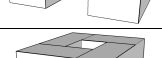
As displayed in Table 7.6, it is also clear that the average annual energy savings difference between two walls (03 and 04) and three walls (05) ground integrations is 4%, which is a small performance gap. Greater savings of 37.87% can be achieved with ground integration 06, an almost 20% average annual savings, which are much higher than ground integration 05.

Table 7.6: Form models' annual savings percentage according with ground integration

Ground Effect - Annual Savings (%) per Model

Models		Levels of Ground Integration						
		01	02	03	04	05	06	07
F01		0.00	12.38	18.33	18.31	21.26	44.89	34.86
F02		0.00	3.28	13.74	13.88	21.03	35.48	33.56
F03		0.00	5.56	13.42	13.51	18.58	36.83	32.39
F04		0.00	6.85	13.02	13.01	16.52	35.40	32.36
F05		0.00	4.91	12.33	12.43	16.98	36.73	33.13
Average Savings % per Ground Integration		0.00	6.59	14.17	14.23	18.87	**37.87**	33.26

In order to identify how the thermal performance of each model is affected by its design, the annual savings per ground integration for each model are compiled in Table 7.7. Also, each models' overall results are based on average energy saving and thermal performance, using a scale from one to five, where one corresponds to the best result and five to the worst.

Table 7.7: Annual thermal performance comparison between all Forms models' design – for all ground integrations

Design Effect - Models' Annual Savings (%) per Ground Integration and Models Overall Performance

Models		Levels of Ground Integration							Overall Results		Scale*
		01	02	03	04	05	06	07	Average Savings*	Perfor.**	
F01		11.49	16.87	15.02	14.91	12.96	14.37	7.49	13.30	= 2	
F02		4.26	2.62	5.80	5.85	8.93	2.40	4.87	4.96	= 3	→
F03		13.62	14.21	**14.70**	**14.69**	15.28	**13.78**	12.66	14.14	**= 1**	1 to 5
F04		2.02	4.03	2.79	2.68	1.48	0.00	0.89	1.98	= 4	↓
F05		0.00	0.00	0.00	0.00	0.00	0.04	0.00	0.01	= 5	

*Average annual savings % per model; ** Performance Scale 1 to 5 (1= Best performace & 5= Worst performance).

Two main findings emerge from these results. Firstly, there are two models that produce good results at this location: Models F01 and F03 share the highest number of best results. The long shape model achieves its best performance with ground integrations 02, 03, 04 and 06, while the compact model results show that this

shape is better with the remaining ground integrations 01, 05 and 07. Both models share similar results with integrations 03, 04 and 06. Model F01 has the second best annual average savings with 13.30%. As for Model F03, it has the best values, achieving savings of 14.14%. These two structures' performances are followed by those of Models F02 and F04, while lastly, the courtyard shape Model F05 produced the worst results.

7.1.2.2. Seasonal Results

The monthly average loads per season were calculated in order to identify the main energy consumption patterns generated by the different ground integrations. In Figure 7.2 it is evident that the heating demand is the largest source of energy consumption. The highest energy need is found in winter, followed by the autumn values. Conversely, spring is the season with the lowest energy needs.

It can also be observed that during winter, spring, and autumn increasing ground integration improves the thermal performance of all models. However, during these seasons a total underground integration only produces the second best results. The overall pattern of results in the summer showed that the higher the ground contact the lower is the energy needs of a model. For the two highest ground integrations the energy consumption in summer is null or almost null.
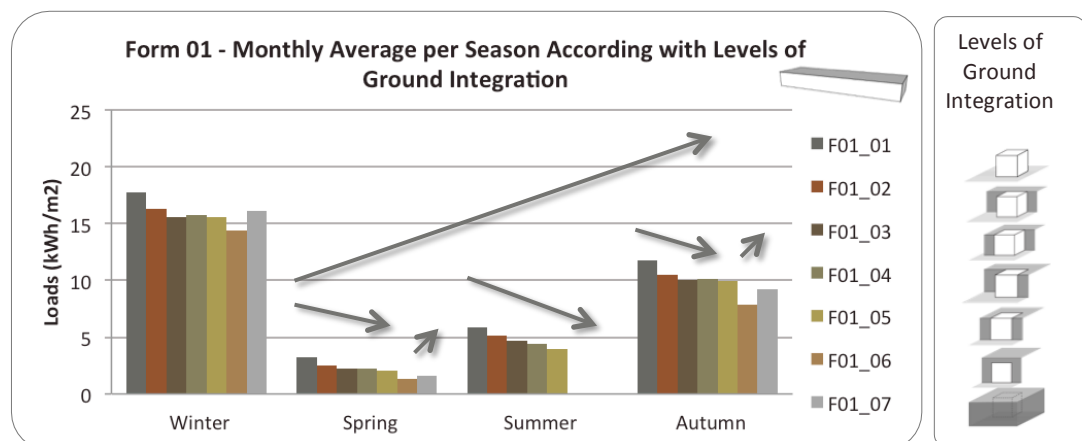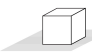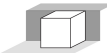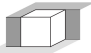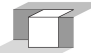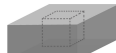
Figure 7.2: Ground integration effect on model' monthly average loads per season – Form 01

The monthly average results per season for each model are compiled in Table 7.8. All models' results show a similar pattern for each season except Model F01, a model that shows particular results during the winter season.

Table 7.8: Forms models' season thermal performance according with ground integration

Ground Effect – Models Season Thermal Performance

Season		Levels of Ground Integration						
		01	02	03	04	05	06	07
Winter	F01	7	6	2**	4**	2**	1	5
Winter	F02 to F05	7	6	3	5	4	1	2
Spring		7	6	4**	4**	3	1	2
Summer		7	6	5	4	3	1 (Null or almost null)	1 (Null)
Autumn		7	6	4	5	3	1	2
Scale*				← 1 to 7 →				

* Performance Scale 1 to 7 (1= Best performance & 7= Worst performance); **Equal or very similar results.

Generally, for all seasons, the highest energy demand is found in models with reduced ground integration such as 01 and 02. The best ground integration is 06, which achieve the lowest energy consumption with all models. The second best ground integration is the totally underground integration (07). This level of integration works well in summer, with no cooling needs. However, during winter, in the case of Model F01, the total underground integration (07) achieved the worst results when compared with minor ground integrations such as 03, 04 and 05. Although the performance of the totally underground (07) integration is good at spring and autumn, the values are not far behind models with lower levels of ground integration. This leads to the conclusion that if construction costs are a concern, ground integration 05 can be a good choice in terms of energy efficiency, as it produces a stable performance during all seasons.

The difference between the performances of ground integrations 03 and 04 is linked with the seasons. Using a seasonal energy loads analysis it was found that ground integration 03 (with north and west ground-integrated walls) gave a better

performance in winter and autumn. Whereas ground integration 04 (with north and east ground-integrated walls), has a better performance than 03, particularly during spring and summer. Therefore, the author concluded that ground integration 03 works better as a heating strategy and ground integration 04 is a good option when applied as part of a cooling strategy.
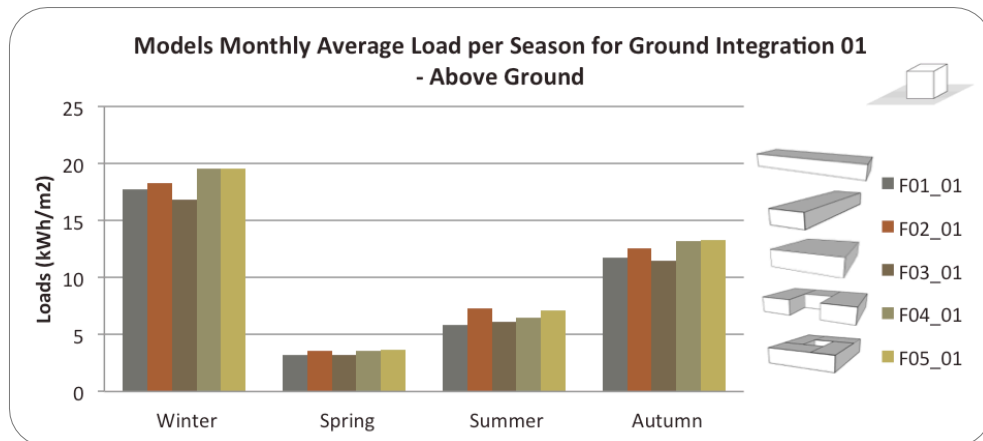
Figure 7.3: Seasonal loads comparison between all Forms models' design – Above Ground

A comparison between the seasonal results of all forms was made according with the levels of ground integration. Looking at the example of the results of ground integration 01 (Figure 7.3), it is clear that the seasonal loads are lower during spring, increases in summer and autumn, and produces the highest energy demand during winter. These patterns are found with all ground integrations. It is also clear that the differences between the results of different models are minor, and in some cases the outcomes are almost identical.
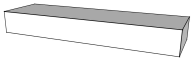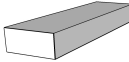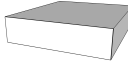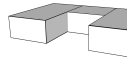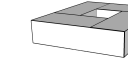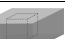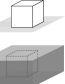
The average monthly loads per season of each model and for all ground integrations are compiled in Table 7.9. These results show that in winter, when the forms have the highest energy demands, the best model is F03 followed by F02. Therefore, it is clear that the larger the perimeter of the model the worse the model's results. However in spring, summer and autumn the results are diverse.

During spring the models' performances change according with shape and levels of ground integration. The performance of model F01 is the best, especially with small

ground integrations such as 02, 03 and 04. However as the ground integration increases the performance of the model declines. Model F02 is the best shape when using medium ground integrations such as 05. The Model F03 achieves the most stable results. This is the best shape to use when there is no ground integration, as in 01 and with a ground integration 04. With all other ground integrations Model F03 achieves the second best results. On the other hand, Model F05 achieved the best spring results with the highest ground integrations, 06 and 07.

Table 7.9: Comparison between all Form models' design – Seasonal loads

Design Effect - Models' Seasonal Thermal Performance per Ground Integration

Seasons and Levels of Ground Integration		Model F01	Model F02	Model F03	Model F04	Model F05
Winter – all levels		2	3	1	4**	5**
Spring	01	2	4	1	3	5
	02	1	4	2	3	5
	03	1	3	2	4	5
	04	1	3	1	4	5
	05	3	1	2	5	4
	06	3	4	2	5	1
	07	5	3	2	4	1
Summer	01	1	5	2	3	4
	02	1	4	2	3	5
	03	1	4	2	3	5
	04	3	1	2	4	5
	05	3	1	2	4	5
	06	3 Almost null	1 (Null)	1 (Null)	4 Almost null	5 Almost null
	07	1 (Null)	1 (Null)	1 (Null)	5 Almost null	1 (Null)
Autumn	01 & 07	2	3	1	4	5
	02 & 04	1	4	2	3	5
	03, 05 & 06	1	3	2	5	5
Scale*				01		

*Performance Scale 1 to 5 (1= Best performance; 5= Worst performance); **Reverse order for Ground Integration 06.

During summer, Model F01 produces the best results with lower ground integrations such as 01 to 03, while Model F02 has the best results when used with higher ground integrations such as 04 and 05. For all models, the cooling loads with the greatest integration (such as 06 and 07) are null or almost non-existent. In autumn, Model F03 produces the best performances for the lowest as well as the highest ground integrations, 01 and 07 respectively. Model F01 generates the best performance with the remaining ground integrations, 02, 03, 04, 05, and 06. Model F05, with its courtyard shape, achieves the worst results for all ground integrations.

In summary, Models F01 and F03 achieve the best seasonal results with almost all ground integrations. Nevertheless, the results for the compact model are more consistent whereas the performance of Model F01 is more irregular. Whenever Model F03 is not the best option, it is always the second best.

7.1.3. Findings and Conclusions

The study above shows that, for this particular climate, direct ground contact effects have a greater impact on the thermal performance of buildings than building design effect, since ground integration can produce up to 2.6 times higher average annual savings than design effects. A building shape can, by itself, contribute to improving the thermal performance of a building, producing average annual energy savings of up to 14.14%. However, it was found that the ground effect can produce average annual energy savings of up to 37.87%.

The total annual energy demand of each model was compared, firstly, to understand how building shapes respond to different levels of ground integration and, secondly, to identify the best shape for a temperate climate such as Lisbon. The study analysis presented above shows that different levels of ground integration produce different thermal performances, and therefore the higher the ground integration the better the annual thermal performance of each model. However, the total

underground integration (07) proves to be the exception to this trend, since it only achieves the second best performance. The reason why ground integration 06 performs better than a total underground model is because of the heating load period. During the coldest season this integration is able to receive extra heating gains through the south-facing wall through solar exposure. Therefore, the author concluded that for this climate, better annual results can be achieved through greater levels of direct ground contact, but also that a totally underground building is not the best solution. Concerning the medium ground integrations such as 03 and 04, and although both integrations produced equal annual results, the seasonal loads analysis revealed a different behaviour. It was found that as a heating strategy ground integration 03 is more efficient than 04 and that, as a cooling strategy, ground integration 04 is better than 03.

Regarding the models behaviour it was found that for this location Model F01 and F03 are the two best shapes producing average annual savings of 13.30% and 14.14% respectively. Although the results for the compact form (Model F03) are more consistent, both long and compact forms (Model F01 and F03) are revealed to be equally efficient for the study climate and location. Therefore, these two shapes are used as the base models on the following studies. Additionally, in most cases the two walls (03 and 04) and three walls (05) ground integration revealed very similar results with average saving differences of around only 4%. For this reason the following case studies use a reduced number of ground integrations, by excluding both two walls ground integrations.

7.2. FLOORS STUDY

The distribution of floor area per number of stories produces different layouts and therefore different exterior surface areas. This section of the chapter looks at how the number of floors can affect the thermal performance of ground-integrated buildings.

The long and compact Models F01 and F03, identified above as the most efficient shapes, are used as the base models for the Floors study. In this section all models share equal total area and volume. As previously discussed in Chapter 5, the single-family residence is the most common type of dwelling in Portugal, a dwelling that has a slightly higher incidence value in Portugal than the European average. Also, the average number of floor per dwelling on the Portuguese mainland is 2.1, with the lowest value of 1.6 in the southern areas of Alentejo, and the highest average of 2.6 around Lisbon. Therefore, this study focuses on three building floor types: a single floor, similar to the base models, a model with two floors, and another with three floors, which is the tallest model.

Both base models (CompF_1F and LongF_1F) were reshaped based on two factors, depth (A) and proportion (B). The variations based on models depth keep the depth value of the base models constant while changing the length and number of floors. The variations based on the models proportion keep the base models ratio while changing the number of floors.

7.2.1. Models Description and Levels of Ground Integration

For the Compact Form, the models variations that keep the base models proportions (CompF_2FA and CompF_3FA) have a lower perimeter than the ones based on the models' depth (CompF_2FB and CompF_3FB), as show on Table 7.10. Table 7.11 shows the models' details such as name, dimensions and type of ground integration,

as well as reference number for each model simulation.

Table 7.10: Models characteristics – Floors study
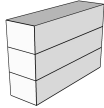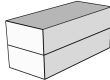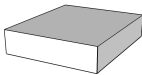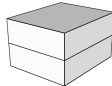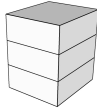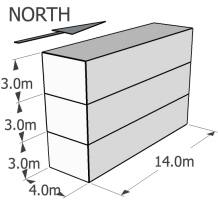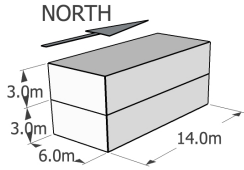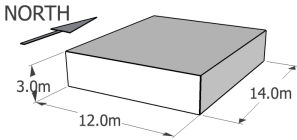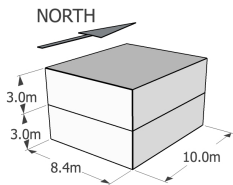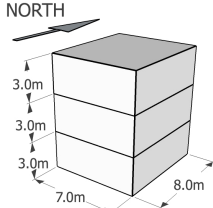
	A - Equal Depth		Base Model	B - Equal Proportion	
Number of Floors	3 Floors	2 Floors	1 Floor	2 Floors	3 Floors
Model Name	**CompF_3FA**	**CompF_2FA**	**CompF_1F**	**CompF_2FB**	**CompF_3FB**
Models					
Total Area (m^2)	168	168	168	168	168
Area per Floor (m^2)	56	84	168	84	56
Floor Perimeter (m)	36	40	52	36.8	30
Floor Ratio A/P	1.55	2.1	3.23	2.28	1.87

Table 7.11: Models details – Floors study

		Models Dimensions	Ground Integration	Ref. Name
Compact Model Depth and Proportion variations	**A – Equal Depth** / CompF_3FA		01- Above Ground	CompF_3FA_01
			02 - North Wall	CompF_3FA_02
			03 - North, West & East Wall	CompF_3FA_03
			04 - North, West & East Wall	CompF_3FA_04
			05 - 'Total Underground'	CompF_3FA_05
	CompF_2FA		01- Above Ground	CompF_2FA_01
			02 - North Wall	CompF_2FA_02
			03 - North, West & East Wall	CompF_2FA_03
			04 - North, West & East Wall	CompF_2FA_04
			05 - 'Total Underground'	CompF_2FA_05
	Base Model / CompF_1F		01- Above Ground	CompF_1F_01
			02 - North Wall	CompF_1F_02
			03 - North, West & East Wall	CompF_1F_03
			04 - North, West & East Wall	CompF_1F_04
			05 - 'Total Underground'	CompF_1F_05
	B – Equal Proportion / CompF_2FB		01- Above Ground	CompF_2FB_01
			02 - North Wall	CompF_2FB_02
			03 - North, West & East Wall	CompF_2FB_03
			04 - North, West & East Wall	CompF_2FB_04
			05 - 'Total Underground'	CompF_2FB_05
	CompF_3FB		01- Above Ground	CompF_3FB_01
			02 - North Wall	CompF_3FB_02
			03 - North, West & East Wall	CompF_3FB_03
			04 - North, West & East Wall	CompF_3FB_04
			05 - 'Total Underground'	CompF_3FB_05

In the case of the Long Form model, the variations that keep the same proportions as the base model, such as LongF_2FB and LongF_3FB, have higher perimeters

than those based on the models' depth, which is the case of LongF_2FA and LongF_3FA (Table 7.12).

Table 7.12: Models characteristics – Comparison
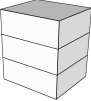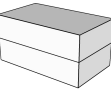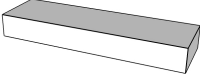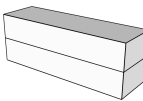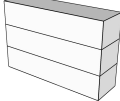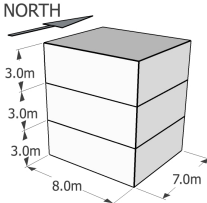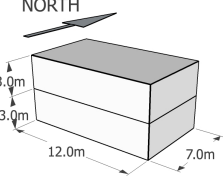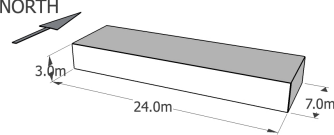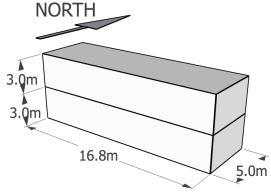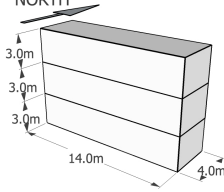
	A - Equal Depth		Base Model	B - Equal Proportion	
Number of Floors	3 Floors	2 Floors	1 Floor	2 Floors	3 Floors
Model Name	**LongF_3FA**	**LongF_2FA**	**LongF_1F**	**LongF_2FB**	**LongF_3FB**
Models					
Total Area (m2)	168	168	168	168	168
Area per Floor (m2)	56	84	168	84	56
Floor Perimeter (m)	30	38	62	43.6	36
Floor Ratio A/P	1.87	2.21	2.7	1.93	1.55

Table 7.13: Models details – Comparison

		Models Dimensions	Ground Integration	Ref. Name
Long Model Depth and Proportion variations	**A – Equal Depth** — **LongF_3FA**	NORTH · 3.0m · 3.0m · 3.0m · 8.0m · 7.0m	01- Above Ground	LongF_3FA_01
			02 - North Wall	LongF _3FA_02
			03 - North, West & East Wall	LongF _3FA_03
			04 - North, West & East Wall	LongF _3FA_04
			05 - 'Total Underground'	LongF _3FA_05
	LongF_2FA	NORTH · 3.0m · 3.0m · 12.0m · 7.0m	01- Above Ground	LongF _2FA_01
			02 - North Wall	LongF _2FA_02
			03 - North, West & East Wall	LongF _2FA_03
			04 - North, West & East Wall	LongF _2FA_04
			05 - 'Total Underground'	LongF _2FA_05
	Base Model — **LongF_1F**	NORTH · 3.0m · 24.0m · 7.0m	01- Above Ground	LongF _1F_01
			02 - North Wall	LongF _1F_02
			03 - North, West & East Wall	LongF _1F_03
			04 - North, West & East Wall	LongF _1F_04
			05 - 'Total Underground'	LongF _1F_05
	B – Equal Proportion — **LongF_2FB**	NORTH · 3.0m · 3.0m · 16.8m · 5.0m	01- Above Ground	LongF _2FB_01
			02 - North Wall	LongF _2FB_02
			03 - North, West & East Wall	LongF _2FB_03
			04 - North, West & East Wall	LongF _2FB_04
			05 - 'Total Underground'	LongF _2FB_05
	LongF_3FB	NORTH · 3.0m · 3.0m · 3.0m · 14.0m · 4.0m	01- Above Ground	LongF _3FB_01
			02 - North Wall	LongF _3FB_02
			03 - North, West & East Wall	LongF _3FB_03
			04 - North, West & East Wall	LongF _3FB_04
			05 - 'Total Underground'	LongF _3FB_05

The Long Form models' details such as name, dimensions, type of ground

integration and reference number are show in Table 7.13.

Table 7.14: Level of ground integration – Floors study with ground integration

Levels of Ground Integration	Sections ⟶ N	Plans N	Perspectives ⟋ N	Walls Depth
01 – No Ground Integration				0 m
02 – North Wall (1 Side)				3 m
03 – North, West & East Walls (3 Sides)				
04 – North, West & East Walls (3 Sides)				3.5 m
05 – North, West, East & South Walls (4 Sides – 'total underground')				

As illustrated by Table 7.14, there are five levels of ground integration. The initial level is ground integration 01, when the all walls are above the ground. This integration is followed by a single wall with ground integration (02). With ground integration 03 and 04 three walls have direct ground contact but the walls depth differ, for ground integration 03 the depth is 3 m and for ground integration 04 the depth is 3.5 m. Lastly, with ground integration 05 the whole models are placed 3.5 m below ground.

7.2.2. Results Analysis

7.2.2.1. Annual Results – Compact Form
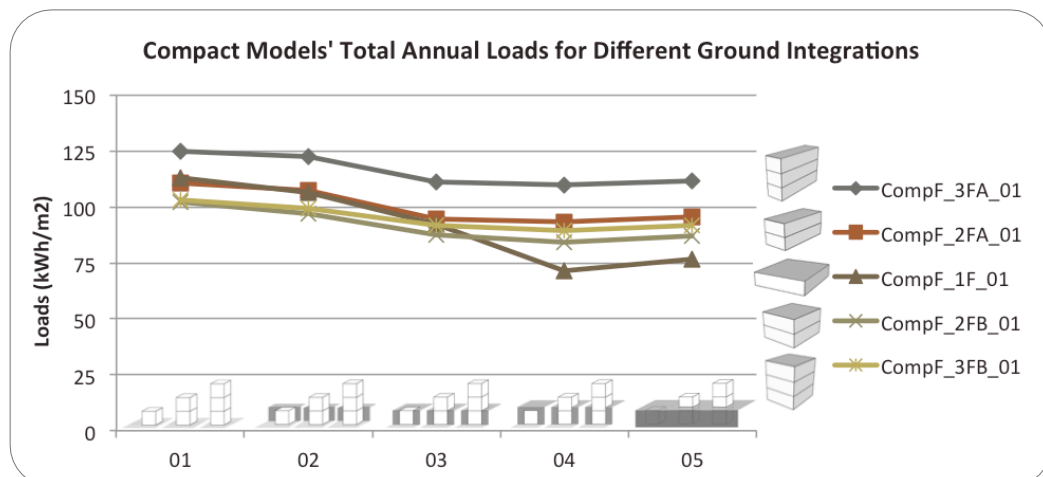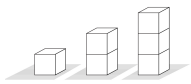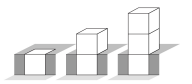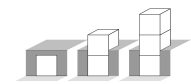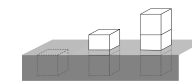
Figure 7.4: Ground effect on Compact Form models' total annual load

A clear pattern is found in this analysis of the total annual loads results (Figure 7.4). The annual thermal performance of the compact models improves in accordance with the ground integration level. However, with 'total underground' integration (05) this tendency is broken and the thermal performance worsens. This pattern reoccurs for all compact form results and is summarised in Table 7.15.

Table 7.15: Compact Form models' annual thermal performance according with ground integration

Effect of Ground Integration on Models Annual Thermal Performance

01	02	03	04	05
No Integration	1 Wall (3m)	3 Walls (3m)	Roof + 3 Walls (3.5m)	'Total Und.' (3.5m)
5	4	2**	1	3**
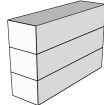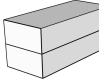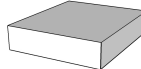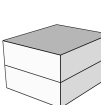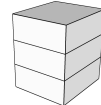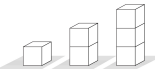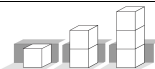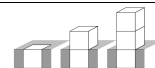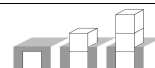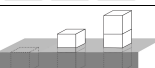
← Scale 1 to 5 →

* Performance Scale 1 to 5 (1= Best performance & 5= Worst performance); ** For CompF_1F & CompF_2FB the order is reverse.

Through this analysis, it was revealed that all models' best results were achieved with ground integration 04. The second best results are divided between integration 03 and 05. With CompF_1F and CompF_2FB, the results for total ground integration (05) is the second best and for the other models it proved to be the third best. With the exception of model CompF_1F, in all cases ground integration 03 and 05 results are very similar, showing very small energy saving differences between the two integrations (Table 7.16). That results leads the author to claim that the greater ground integration might not be cost effective when compared with a reduced ground integration option such as 03.

The ground effect on the energy saving potential of the models is higher with the single floor model, which achieves the highest value of 36.76% with ground integration 04. The same ground integration can provide energy savings of up to 17.44% for models with two floors, and up to 13.40% for models with three floors. The main reason why the ground impact decreases as the number of floors

increases is because the surface area of the model with ground contact also decreases.
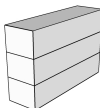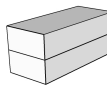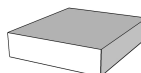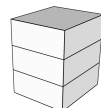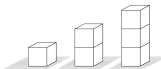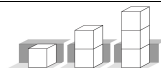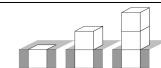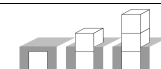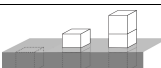
Table 7.16: Compact Form models' annual savings percentage according with ground integration

Ground Effect - Annual Savings (%) per Model

Model Name	**A** - Equal Depth		Base Model	**B** - Equal Proportion		Overall Results		
	CompF_3FA	CompF_2FA	CompF_1F	CompF_2FB	CompF_3FB	Average Savings*	Perfor.**	Scale
Models								
01	0.00	0.00	0.00	0.00	0.00	0.00	= 5	
02	1.79	3.09	5.53	4.80	3.97	3.84	= 4	↑
03	11.19	14.38	18.48	14.14	11.04	13.85	= 3	1 to 5
04	12.03	15.70	36.76	17.44	13.40	19.07	= 1	↓
05	10.69	13.56	32.31	14.78	10.89	16.45	= 2	

(Row labels under "Levels of Ground Integration")

* Average savings % per ground integ.; **Performance Scale 1 to 5 (1= Best performance & 5= Worst performance).

Looking into the effect of the models' design through the annual savings percentage (Table 7.17) it becomes clear that the shape of the model and its number of floors can produce result gaps of up to 18.36%. Furthermore, two main patterns can be observed. Firstly, the models based on equal proportions that keep a more compact form achieve better results than the ones based on an equal depth with a less compact form. Secondly, for both variations, namely equal depth and equal proportion, the models with two floors achieved better performance than the corresponding model with three floors. It is also visible that the single floor model is greatly affected by ground integration. Its performance improves when the level ground integration increases, as it is the model with the largest surface area with direct ground contact with integrations 04 and 05. The best average savings are shared between CompF_1F and CompF_2FB both of which generate results of around 21%. Overall, however, the savings produced by models CompF_2FB and CompF_3FB are better for lower ground integrations.

Table 7.17: Annual thermal performance comparison between all Compact Form models' design – for all ground integrations

Design Effect - Models' Annual Savings (%) per Ground Integration and Models Overall Performance

		A - Equal Depth		Base Model	**B** - Equal Proportion	
Model Name		CompF_3FA	CompF_2FA	CompF_1F	CompF_2FB	CompF_3FB
Models						
Levels of Ground Integration	01	0.00	11.35	9.61	18.36	17.34
	02	0.00	12.52	13.05	20.86	19.17
	03	0.00	14.53	17.03	21.07	17.19
	04	0.00	15.04	35.02	23.38	18.62
	05	0.00	14.20	31.49	22.10	17.53
Overall Results	Average Savings*	0.00	13.53	21.24	21.16	17.97
	Perfor.**	= 5	= 4	= 2	= 1	= 3
Scale		← 1 to 5 →				

* Average savings % per model; **Performance Scale 1 to 5 (1= Best performance & 5= Worst performance).

7.2.2.2. Seasonal Results – Compact Form
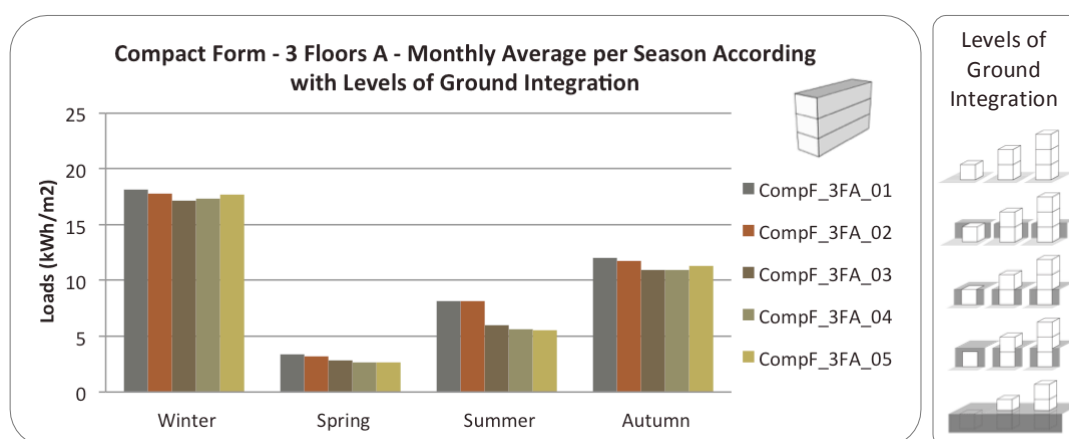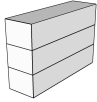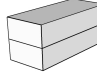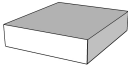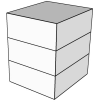
Figure 7.5: Ground integration effect on model' monthly average loads per season – Compact Form – 3 Floors A

The energy loads distribution per season of each model, exemplified by the CompF_3FA results (Figure 7.5) indicate that heating, especially the winter, is the largest contributor to the energy requirements of each model, while spring is the season with the lowest energy demands. Per season and for each model the best ground integrations are identified and compiled on the following table.

In Table 7.18, it can be seen that ground integration 04 is the most efficient, with a good performance in winter and autumn, and a very good performance in spring and summer. Ground integration 03 proved to be better as a heating strategy since it works well in winter and autumn. During summer, ground integration 05 achieved the best results. However this is not sufficient to highlight the performance of this ground integration because 03 and 05 produced similar annual results. Consequently, ground integration 05 might not be a better solution than 03 when considering construction costs.

Table 7.18: Compact Form models' season thermal performance – Best ground integration

Season Ground Effect - Models Best Ground Integration per Season

Model Name	**A** - Equal Depth		Base Model	**B** - Equal Proportion	
	CompF_3FA	CompF_2FA	CompF_1F	CompF_2FB	CompF_3FB
Forms					
Winter	03	03	04	04	04
Spring	04	04	04	05	04
Summer	05	05	04/05 Null	05	05
Autumn	03/04	04	04	04	04
Best Annual	04	04	04	04	04

The best ground integration for each model according with season: 01= No Integration; 02= 1 Wall (3m); 03=3 Walls (3m); 04= ; Roof + 3 Walls (3.5m) 05= 'Total Und.' (3.5m).
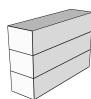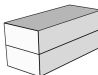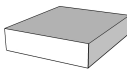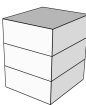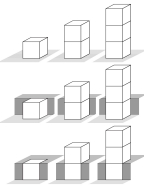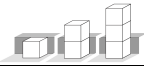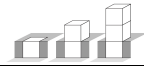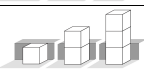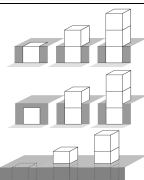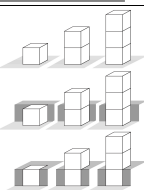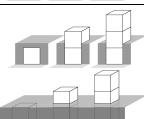
Figure 7.6: Seasonal loads comparison between all Compact Form models' design – Above Ground

The annual results patterns are repeated with the monthly average loads per season. The above figure, which corresponds to ground integration 01, shows that the models based on equal proportion (CompF_2FB and CompF_3FB) register the best performance at all seasons.

Table 7.19: Comparison between all Compact Form models' design – Seasonal loads

Design Effect - Models' Season Thermal Performance per Ground Integration

		A - Equal Depth		Base Model	B - Equal Proportion	
Model Name		CompF_3FA	CompF_2FA	CompF_1F	CompF_2FB	CompF_3FB
Forms						
Winter	01 to 03	5	3	4	1	2
	04	5	4	2	1	3
	05	5	4	3	1	2
Spring	01	5	3	4	2**	1**
	02	5	4	3	1	2
	03	5	4	1	2	3
	04 & 05	5	3	1	2	4
Summer	01	5	4	3	2	1
	02	5	4	3	1**	2**
	03 to 05	5	4	1	2	3
Autumn	01 to 03	5	3	4	1	2
	04 & 05	5	4	1	2	3
Scale*				← 1 to 5 →		

* Performance Scale 1 to 5 (1= Best performance & 5= Worst performance).

All results are summarised in Table 7.19, which is based on the performance of each model per ground integration. It is immediately visible that both models with equal depth, namely the longest ones, provide the worst results. However, while the

results for model ComF_3FA are always the least effective, performance results for model ComF_2FA are better in winter and autumn with none or low levels of ground integration.

Looking to the best performance, it is found that the results change according with season and level of ground integration. Overall, for all seasons ComF_2FB and ComF_3FB have good performance, but in spring, summer and autumn the base model achieves the best performance with the greater levels of ground integrations.

7.2.2.3. Annual Results – Long Form
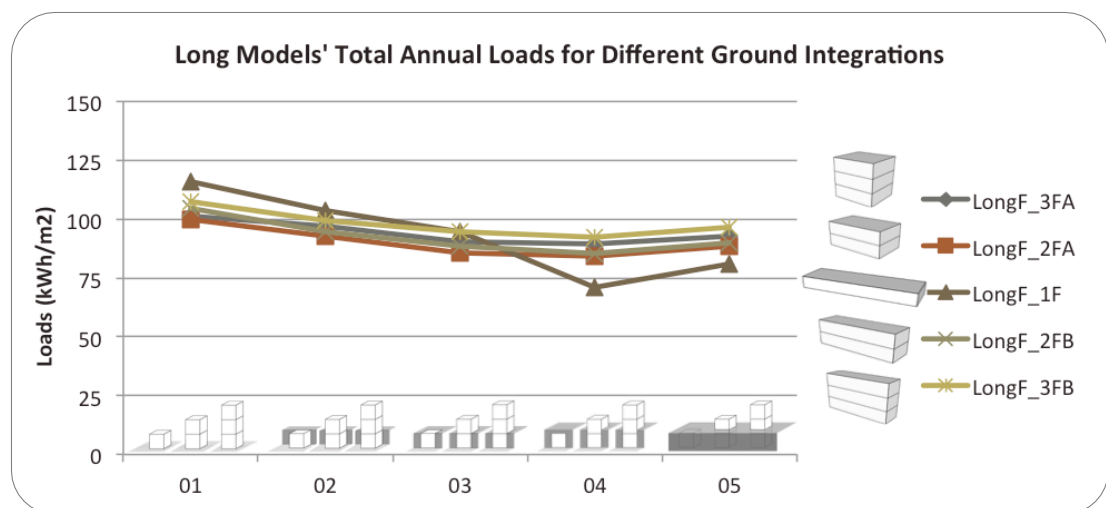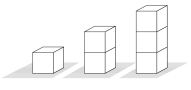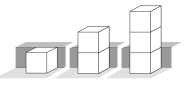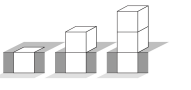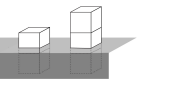
Figure 7.7: Ground effect on Long Form models' total annual load

As can be observed in Figure 7.7, the long form results repeat the same patterns as those found for compact forms. As summarised in the following table, for all floor plans the annual best performance is achieved with ground integration 04.

Table 7.20: Long Form models' annual thermal performance according with ground integration
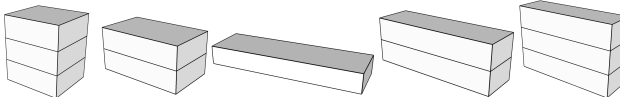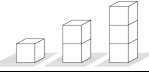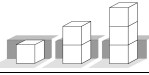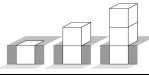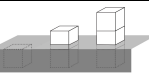
Effect of Ground Integration on Models Annual Thermal Performance				
01	02	03	04	05
No Integration	1 Wall (3m)	3 Walls (3m)	Roof + 3 Walls (3.5m)	'Total Und.' (3.5m)
5	4	2**	1	3**
← Scale 1 to 5 →				

* Performance Scale 1 to 5 (1= Best performance & 5= Worst performance); ** For LongF_1F the order is reverse.

With the exception of model LongF_1F, the second best results are found with ground integration 03. Once again, and for all models, the best annual performance was not registered in the highest ground integration. Increasing the ground coverage from 04 to 05 shows a regression in the annual results. The thermal performance of this particular integration (05) is less efficient than 03 and in cases of two floor models it is very similar to ground integration 02, which only has one wall with ground contact. This leads the author to argue that models' annual performance benefits from the south facing wall solar exposure. Therefore, the balance between solar exposure and ground contact should be always considered on an early design stage.
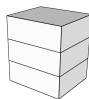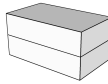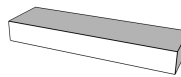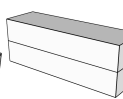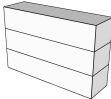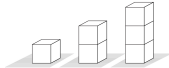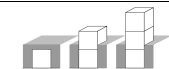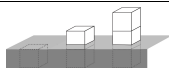
Table 7.21: Long Form models' annual savings percentage according with ground integration

Ground Effect - Annual Savings (%) per Model

		A - Equal Depth		Base Model	B - Equal Proportion		Overall Results		
Model Name		LongF_3FA	LongF_2FA	LongF_1F	LongF_2FB	LongF_3FB	Average Savings*	Perfor.**	Scale
Models									
Levels of Ground Integration	01	0.00	0.00	0.00	0.00	0.00	0.00	= 5	1 to 5 ↑ ↓
	02	4.62	7.01	10.63	9.23	7.44	7.79	= 4	
	03	11.11	14.38	18.36	15.07	11.82	14.15	= 2	
	04	12.03	15.68	38.72	18.17	14.11	19.75	= 1	
	05	8.69	11.23	30.03	13.68	10.01	14.73	= 3	

* Average savings %per ground integ.; **Performance Scale 1 to 5 (1= Best performance & 5= Worst performance).

With Table 7.21 it can be observed that a ground integration such as 04 can produce energy savings up to 38.72% with the single floor model. For a two-floor model, the energy potential of this ground integration can reach 18.17%, and for a three-floor model the value can go up to 14.11%.

Table 7.22: Annual thermal performance comparison between all Long Form models' design – for all ground integrations

Design Effect - Models' Annual Savings (%) per Ground Integration and Models Overall Performance

		A - Equal Depth		Base Model	**B** - Equal Proportion	
Model Name		LongF_3FA	LongF_2FA	LongF_1F	LongF_2FB	LongF_3FB
Models						
Levels of Ground Integration	01	12.30	13.77	0.00	9.80	7.13
	02	6.41	10.27	0.00	8.40	3.82
	03	4.80	9.85	0.32	6.46	0.00
	04	3.28	8.85	23.18	7.47	0.00
	05	4.18	8.40	16.28	6.83	0.00
Overall Results	Average Savings*	6.19	10.23	7.96	7.79	2.19
	Perfor.**	= 4	= 1	= 3	= 2	= 5
Scale				← 1 to 5 →		

* Average savings % per model; **Performance Scale 1 to 5 (1= Best performance & 5= Worst performance).

When comparing the models design effect through the correspondent annual energy saving results (Table 7.22), it was found that by changing the shape and number of floors the energy savings could be improved up to 13.77%. The best performance was reached with model LongF_2FA, with average savings of 10.23%. Again, the two-floor models provide better results than the correspondent three-floor model. Additionally, it can be observed that the models that kept the initial depth have better results than the models that maintained the base model proportions. This pattern shows that for the study climate, longer forms have lower thermal efficiency comparing with a more compacted form.

7.2.2.4. Seasonal Results – Long Form
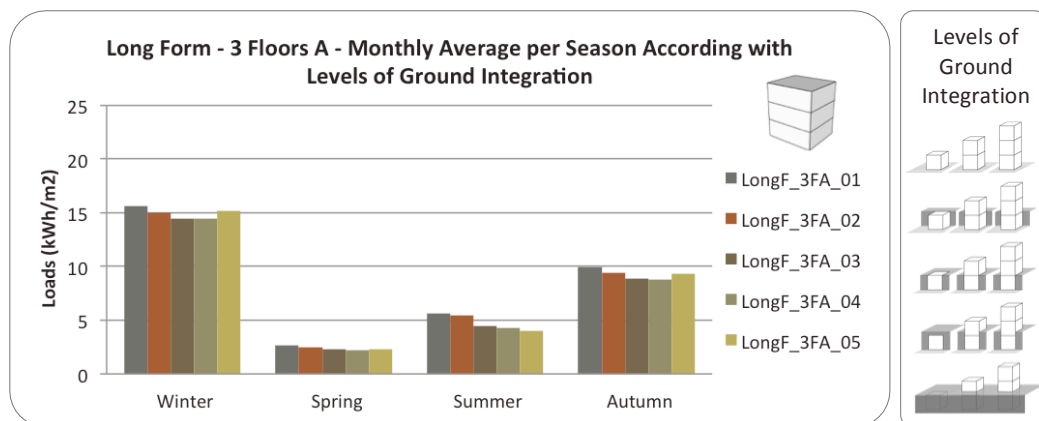
Figure 7.8: Ground integration effect on model' monthly average loads per season – Long Form – 3 Floors A

In the example of model LongF_03A, seasonal results according to models' levels of ground integration (Figure 7.8), it can be seen that ground integration 04 had the best results for spring and autumn and achieving the second best results in summer. In winter this is the only model that achieves its best performance with ground integration 03, which shares an almost equal value with ground integration 04.

Table 7.23: Long Form models' season thermal performance – Best ground integration

Season Ground Effect - Models Best Ground Integration per Season

	A - Equal Depth		Base Model	**B** - Equal Proportion	
Model Name	LongF_3FA	LongF_2FA	LongF_1F	LongF_2FB	LongF_3FB
Forms					
Winter	03	03/04	04	04	04
Spring	04	04	04	04	04
Summer	05	05	04/05 Null	05	05
Autumn	04	04	04	04	04
Best Annual	04	04	04	04	04

The best ground integration for each model according with season: 01= No Integration; 02= 1 Wall (3m); 03=3 Walls (3m) ; 04= ; Roof + 3 Walls (3.5m) 05= 'Total Und.' (3.5m).

Table 7.23 summarises the best ground integration by season for each model. The results presented in this table make clear that almost all models produce the same results. Ground integration 04 is the best annual ground integration and achieves the best results during spring, autumn and winter – corresponding to the three heating seasons. Ground integration 05 provides the best results in summer, which

corresponds to the cooling season. These results, therefore, make this particular integration ideal for a cooling strategy. However, during winter and autumn, the performance of ground integration 05 drops and is surpassed by integrations with lower levels of ground contact such as ground integration 03 and in some cases 02.
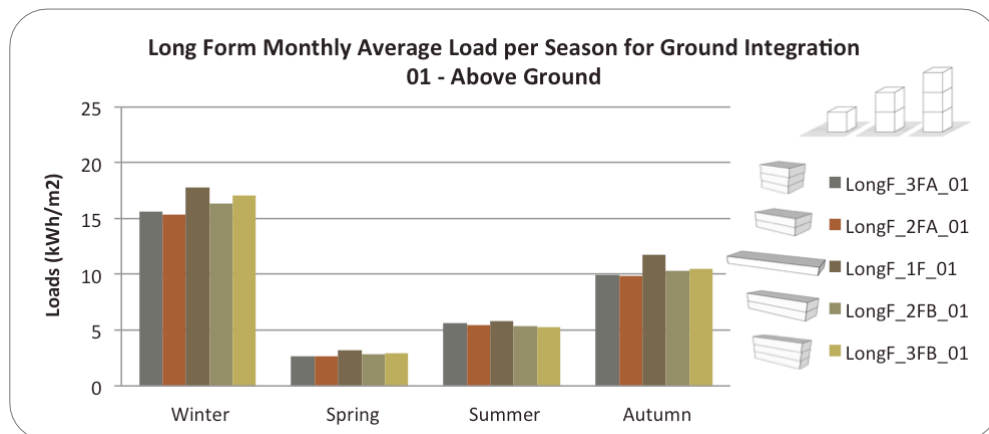
Figure 7.9: Seasonal loads comparison between all Long Form models' design – Above Ground
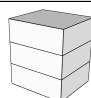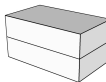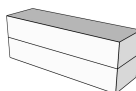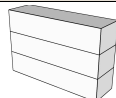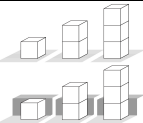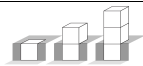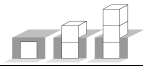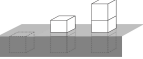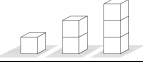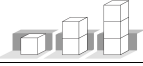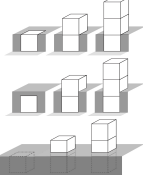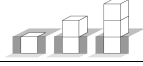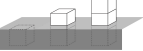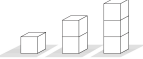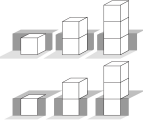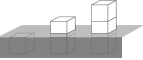
The comparison of the seasonal thermal performance of each model according with ground integration allows for the observation of several patterns, which occur throughout the year. In Figure 7.9 it is visible that without ground integration (01) the single floor model produces the worst results. During the heating periods of autumn, winter and spring the most compact models (LongF_2FA and LongF_3FA) produce better results than models LongF_2FB and LongF_3FB. Finally, during the summer the opposite was found.

Other patterns become evident in the results presented in Table 7.24, which compiles all the thermal performance of all models, rated from best to worst. As summarised in this table, the performance of base model LongF_1F improves with higher level of ground contact. This is clear in spring, summer and autumn when this model achieves the worst results with the lowest ground integrations but also has its best performance with the highest ground integrations.

During winter, spring and autumn, LongF_2FA shows the best performances, which leads the author to argue that this model is a good design solution for a heating

strategy. In summer LongF_2FB produces a more balance performance with all ground integrations, becoming a good design for a cooling strategy.

Table 7.24: Comparison between all Long Form models' design – Seasonal loads

Design Effect - Models' Season Thermal Performance per Ground Integration

		A - Equal Depth		Base Model	**B** - Equal Proportion	
Model Name		LongF_3FA	LongF_2FA	LongF_1F	LongF_2FB	LongF_3FB
Forms						
Winter	01 & 02	2	1	5	3	4
	03	3	1	5	2	4
	04	4	1	3	2	5
	05	2	1	4	3	5
Spring	01	1	1	5	3	4
	02	3	1	4	2	5
	03 to 05	4	2	1	3	5
Summer	01	4	3	5	2	1
	02	5	3	4	1**	2**
	03	5	2	1	3	4
	04	5	2	1 (Null)	2	4
	05	5	3	1 (Null)	2	4
Autumn	01	2	1	5	3	4
	02 & 03	3	1	5	2	4
	04	4	2	1	1	5
	05	4	1	1	3	5
Scale*				← 1 to 5 →		

* Performance Scale 1 to 5 (1= Best performance & 5= Worst performance); **Similar values.

7.2.3. Findings and Conclusions

The models variations based on the compact and long forms produced similar result patterns. The annual loads results show that the level of ground integration affects the thermal performance of every model. The performance of each model improves with ground contact, but the highest level of ground integration fails to produce the best annual results and only achieves the best seasonal results during the summer. The use of ground integration can improve the thermal performance of a building. However, for this temperate climate during the heating season (and mainly winter and autumn) the solar gains provided by the exposed surface area of the models are also relevant. This is particularly so for the south-facing surface area that was reduced with the highest ground integration. Therefore, a good balance between surface areas with direct ground contact and with solar exposure is the key for achieving the best performance.

The best energy saving potential produced by direct ground contact for the single floor models is found to be 36.76% with the Compact Form, and 38.72% with the Long Form. For the two-floor models, the ground effect can produce savings of up to 17.44% with the Compact Form models, and 18.17%, with the Long Form models. Considering the three-floor models, the best value achieved is of 13.40%, which was registered in the Compact Form models, and 14.11% by the Long Form models. Thus, the lower is the number of floors higher the ground thermal effect, as the surface area of the model with ground contact is greater.

Looking into the design effect produced by the number of floors it is found that it can produce results difference up to 18.36% with the Compact Form models, and up to 13.77% with the Long Form models. In general, models with two floors produce better results than models with three floors. The more compact shapes achieve better annual performance than longer ones, which only produce good results during summer. Therefore, the most compact models are better for this particular climate, and the longer models are efficient as part of a cooling strategy.
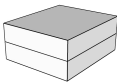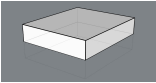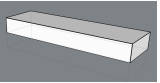
7.3. BASEMENT AND COURTYARD

The previous section demonstrates that ground integration can improve the thermal performance of buildings, but in order to produce the best annual results for the temperate climate studied, it is necessary to produce a good balance between direct ground contact and solar gains. This section looks into this issue, addressing two questions. Firstly, what thermal contributions are produced by an underground construction (e.g. a basement) in comparison with an above ground building with the same characteristics. The second question is if there are any thermal benefits to be gained by introducing an underground courtyard area at the south-facing side of the basement of a building.

This section uses models based on the two best shapes found in the Forms section of this chapter, the Compact and Long form. The study is divided in three groups: Above Ground, Basement and Basement with Courtyard.

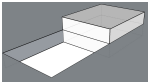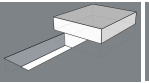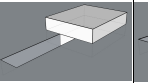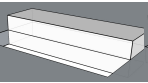### 7.3.1. Models Description and Levels of Ground Integration
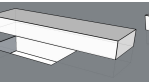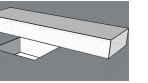
Table 7.25: Models characteristics – Above Ground and Basement

	Above Ground		Basement	
Number of Floors	2 Floors	2 Floors	2 Floors	2 Floors
Model Name	CompF_Abv	LongF_Abv	CompF_Bsmt	LongF_Bsmt
Models				
Total Area (m^2)	336	336	336	336
Area per Floor (m^2)	168	168	168	168
Basement Floor	-	-	1	1
Floor Perimeter (m)	52	62	52	62
Floor Ratio A/P	3.23	2.7	3.23	2.7

The Compact and Long models have the same total area and are designed with two stories (Table 7.25 and 7.26). With the first group that is the Above Ground group, both models are placed over the ground. In the second group named Basement, a basement is introduced in the models, the lower floor is underground and the upper floor is above the ground. In the third group named Basement and Courtyard, the

basement is used with the addition of a courtyard, this is done with the introduction of an open area at the basement south-facing wall.

Table 7.26: Models characteristics – Basement with Courtyard

	Basement with Courtyard					
Number of Floors	2 Floors	2 Floors	2 Floors	2 Floors	2 Floors	2 Floors
Model Name	CompF_01Crt	CompF_02Crt	CompF_03Crt	LongF_01Crt	LongF_02Crt	LongF_03Crt
Models						
Total Area (m2)	336	336	336	336	336	336
Area per Floor (m2)	168	168	168	168	168	168
Basement Floor	1	1	1	1	1	1
Courtyard Area (m2)	168 (1/1)	84 (1/2)	56 (1/3)	168 (1/1)	84 (1/2)	56 (1/3)
Floor Perimeter (m)	52	52	52	62	62	62
Floor Ratio A/P	3.23	3.23	3.23	2.7	2.7	2.7

The courtyards' dimension areas are based on the model's area per floor and are illustrated in Table 7.26 and 7.29. The CompF_01Crt and CompF_01Crt models' courtyard dimensions are equal to the models' ones (1/1). Both 02Crt models have a courtyard area that is half of the model's floor area (1/2). Both 03Crt models' courtyard is one third of the model's floor area (1/3).

The Above Ground, Basement and Basement with Courtyard models' details (such as dimensions, number of simulations, type of ground integration and used simulation reference) are displayed in Table 7.27 to 7.29.
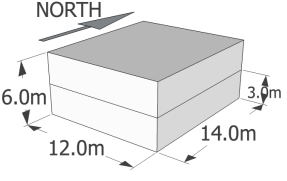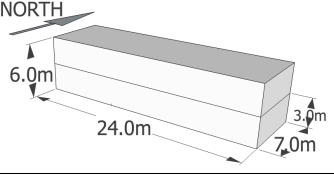
Table 7.27: Models details – Above Ground

	Above Ground Models Dimensions	Ground Integration	Ref. Name
Compact Form		01 – No Ground Integration	CompF_Abv_01
		02 - North, West & East Walls	CompF_Abv_02
		03 - Roof, North, West & East Walls	CompF_Abv_03
Long Form		01 – No Ground Integration	LongF_Abv_01
		02 - North, West & East Walls	LongF_Abv_02
		03 - Roof, North, West & East Walls	LongF_Abv_03

Table 7.28: Models details – Basement

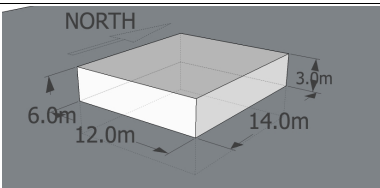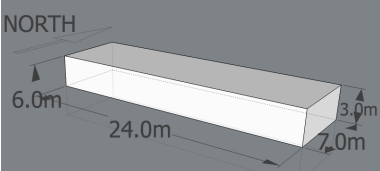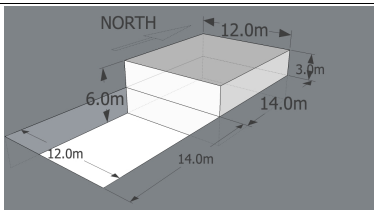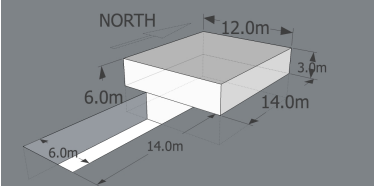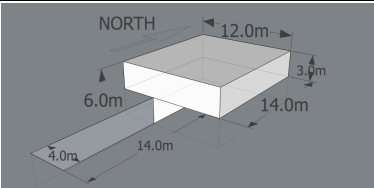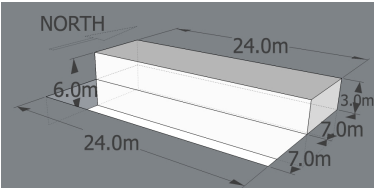| Basement Models Dimensions		Ground Integration	Ref. Name
Compact Form		01 – No Ground Integration	CompF_Bsmt_01
		02 - North, West & East Walls	CompF_Bsmt_02
		03 - Roof, North, West & East Walls	CompF_Bsmt_03
Long Form		01 – No Ground Integration	LongF_Bsmt_01
		02 - North, West & East Walls	LongF_Bsmt_02
		03 - Roof, North, West & East Walls	LongF_Bsmt_03

Table 7.29: Models details– Basement with Courtyard
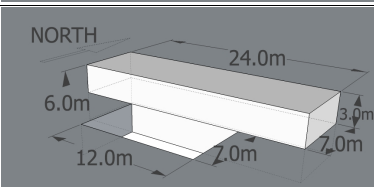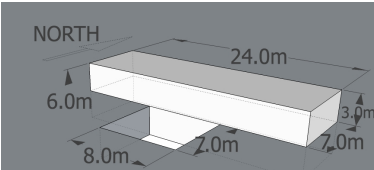
Courtyard Models Dimensions		Ground Integration	Ref. Name
Compact Form Courtyard 1/1		01 – No Ground Integration	CompF_01Crt_01
		02 - North, West & East Walls	CompF_01Crt_02
		03 - Roof, North, West & East Walls	CompF_01Crt_03
Courtyard 1/2		01 – None	CompF_02Crt_01
		02 - North, West & East Walls	CompF_02Crt_02
		03 - Roof, North, West & East Walls	CompF_02Crt_03
Courtyard 1/3		01 – None	CompF_03Crt_01
		02 - North, West & East Walls	CompF_03Crt_02
		03 - Roof, North, West & East Walls	CompF_03Crt_03
Long Form Courtyard 1/1		01 – None	LongF_01Crt _01
		02 - North, West & East Walls	LongF_01Crt _02
		03 - Roof, North, West & East Walls	LongF_01Crt _03
Courtyard 1/2		01 – None	LongF_02Crt _01
		02 - North, West & East Walls	LongF_02Crt _02
		03 - Roof, North, West & East Walls	LongF_02Crt _03
Courtyard 1/3		01 – None	LongF_03Crt _01
		02 - North, West & East Walls	LongF_03Crt _02
		03 - Roof, North, West & East Walls	LongF_03Crt _03

Table 7.30: Level of ground integration – Basement and Courtyard study with ground integration

Levels of Ground Integration	Above Ground	Sections N Basement	Basement with Courtyard	Walls Depth
01 – No Ground Integration				0 m
02 – North, West & East Walls				6 m
03 – Roof, North, West & East Walls				6.5 m

For each stage three types of ground integration are used, including none (01), three walls (02) and roof and three walls (03), as shown in Table 7.30. With no ground integration the walls depth below ground is 0 m for the Above Ground, and 3 m for the Basement and Basement with Courtyard. With ground integration 02 the depth of the larger wall is 6 m, and for the ground integration 03 the depth of the larger wall is 6.5 m.

7.3.2. Results Analysis

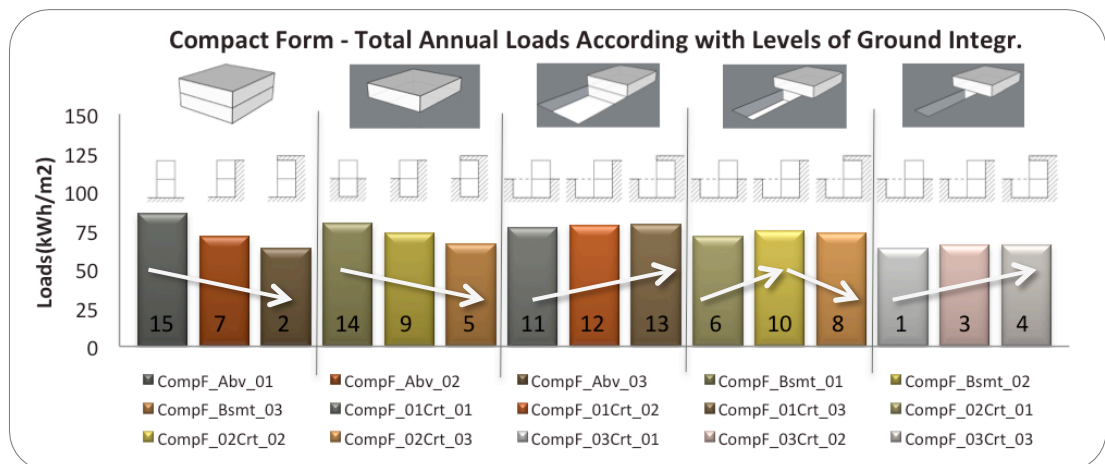#### 7.3.2.1. Annual Results – Compact and Long Form

Figure 7.10: Ground effect on Compact Form models' total annual load – Above Ground, Basement and Basement with Courtyard

The total annual loads of the Above Ground and Basement groups show that for both study forms (Figure 7.10, 7.11 and Table 7.31), the higher the ground

integration the better the models' thermal performance. The energy demand decreases as the level of ground integration increases.
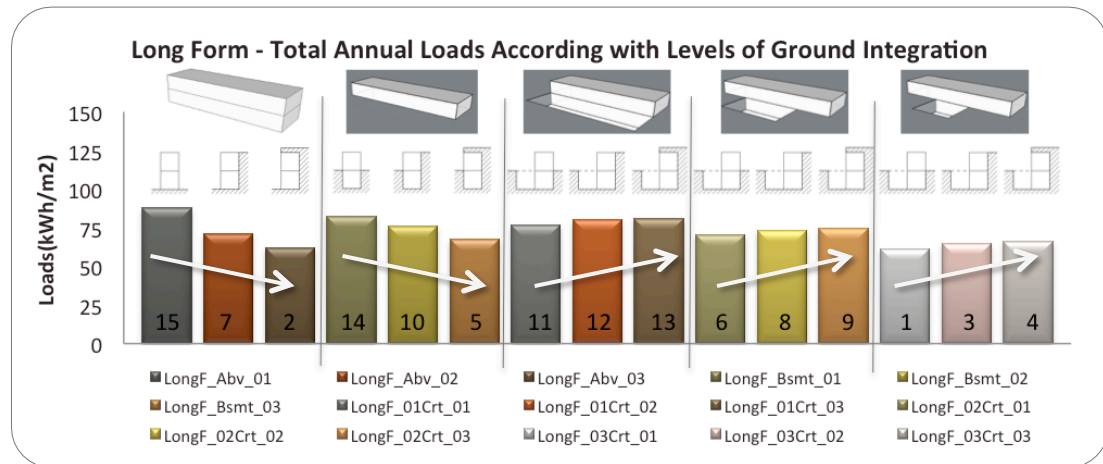

Figure 7.11: Ground effect on Long Form models' total annual load – Above Ground, Basement and Basement with Courtyard

For both compact and long shapes with the lowest ground integration (01), the Basement group models prove to be more energy efficient than the Above Ground models. But by increasing the ground integration (02 and 03) the performance of the Basement models becomes less efficient than the correspondent Above Ground models (Figure 7.10 and 7.11).

Table 7.31: Compact and Long Form models' annual thermal performance according with ground integration

Effect of Ground Integration on Models Annual Thermal Performance

Above Ground and Basement			Basement with Courtyard		
01	02	03	01	02	03
None	3 Walls (6m)	Roof & 3 Walls (6.5m)	None	3 Walls (6m)	Roof & 3 Walls (6.5m)
3	2	1	1	2**	3**
← Scale* 1 to 3 →			← Scale* 1 to 3 →		
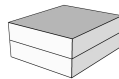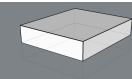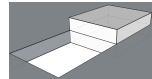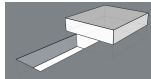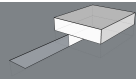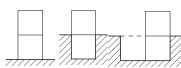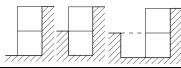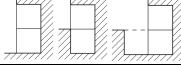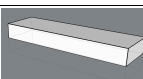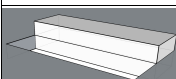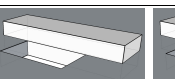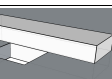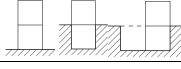
* Performance Scale 1 to 3 (1= Best performance & 3= Worst performance); ** For CompF_02Crt the order is reverse.

Two different patterns can be observed in the Basements with Courtyards group, as displayed in Figure 7.10 and 7.11, and in Table 7.31 and 7.32. Firstly, for both forms the smaller the courtyard, the most efficient the thermal performance of the building. Secondly, the higher the ground integration the higher is the models energy

consumption. These results raise issues in terms of performance and, therefore, it cannot be concluded that the highest levels of ground integrations are energy efficient. Additionally, and for both forms, the best performance is not found in the Basement group, which have the highest ground integration, but in the Basement with Courtyard group.

Regarding the ground effect on the annual savings per model (Table 7.32), in the Above Ground group, the highest ground integration (03) allows the CompF_Abv model to save 25.99% of the initial loads, and the LongF_Abv model is able to save up to 29.41%. For the same ground integration, in the Basement group the model CompF_Bsmt is able to save up to 16.40%, and LongF_Bsmt 1 saves up to 7.92%.

Table 7.32: Compact and Long Form models' annual loads savings percentage according with ground integration
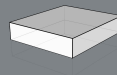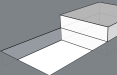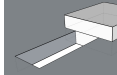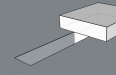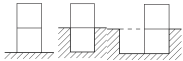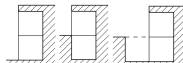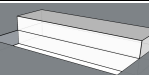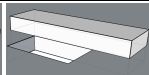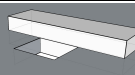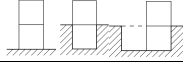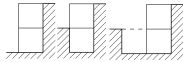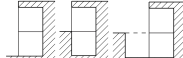
Compact and Long Form - Ground Effect - Annual Savings (%) per Model

	Above Ground	Basement	Basement with Courtyard		
Model Name	CompF_Abv	CompF_Bsmt	CompF_01Crt	CompF_02Crt	CompF_03Crt
Compact Forms					
01	0.00	0.00	2.63	5.00	3.46
02	17.50	7.57	0.62	0.00	0.78
03	25.99	16.40	0.00	2.11	0.00
Model Name	LongF_Abv	LongF_Bsmt	LongF_01Crt	LongF_02Crt	LongF_03Crt
Long Forms					
01	0.00	0.00	5.14	5.71	7.03
02	19.29	7.94	1.33	1.46	1.76
03	29.41	17.92	0.00	0.00	0.00

* Loads savings % per ground integration.

With the Basement and Courtyard group it is clear that the lowest ground integration (01) has the best impact on the annual savings made by the models. For the

compact form the best savings are of up to 5% with model CopF_02Crt, and for the long form the best value is achieved by model LongF_03Crt with 7.03%.

Table 7.33: Annual thermal performance, Compact and Long Form models' design – for all ground integrations

Design Effect – Models' Annual Savings (%) per Ground Integration

		Above Ground	Basement	Basement with Courtyard		
Model Name		CompF_Abv	CompF_Bsmt	CompF_01Crt	CompF_02Crt	CompF_03Crt
Compact Forms						
Levels of Gr.Int.	01	0.00	7.53	10.55	17.67	26.09
	02	9.64	6.38	0.00	5.07	16.80
	03	19.44	15.85	0.00	7.65	16.66
Model Name		LongF_Abv	LongF_Bsmt	LongF_01Crt	LongF_02Crt	LongF_03Crt
Long Forms						
Levels of Gr.Int.	01	0.00	6.28	12.75	20.32	30.28
	02	11.08	4.95	0.00	8.26	18.83
	03	23.26	16.37	0.00	8.13	18.47

*Loads savings % per model for each ground integration.

The annual savings produced by the models' design, illustrated in Table 7.33, shows once again that, for this climate, there is the need to find a balance between ground integration and solar exposure.

For the compact and long models, the Basements with Courtyard group results demonstrate that this balance can be achieved with the addition of this feature on ground-integrated buildings with ground integration 01, which increases savings from 26.09% to 30.28% and, for ground integration 02, increases savings from 16.80% up to 18.83%. Although the basement with the smallest courtyard has a good performance, for ground integration 03, the best annual savings are found with the Above Ground models; CompF_Abv achieves 44% and LongpF_Abv provides savings up to 23.26%.

7.3.2.2. Seasonal Results – Compact and Long Form

Figure 7.12: Ground integration effect on model' monthly average loads per season – Compact Form – Above Ground & Basement
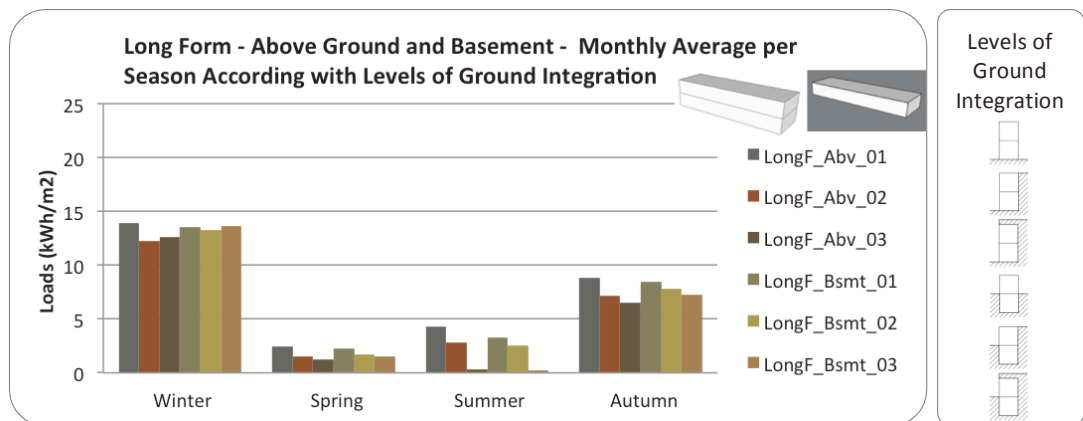
Figure 7.13: Ground integration effect on model' monthly average loads per season – Long Form – Above Ground and Basement

Figure 7.12 and 7.13 respectively display the compact and long form Above Ground and Basement models seasonal results. In these tables it can be observed that winter is the period with highest energy demands, thus it is during this period that the highest ground integrations fail to produce the best performance. This is the case of CompF_Abv and LongF_Abv with ground integration 02, as well as CompF_Bsmt and LongF_Bsmt with ground integration 02 and 03. For the Above Ground and Basement, during summer it is found that the highest ground integration (03) energy loads is null or almost null.

In Table 7.34, the results compilation through the performance order make clear that for both compact and long forms the results for the Above Ground and Basement

models have the same pattern for spring, summer and autumn. The higher the ground integration the better the models' performance.

Table 7.34: Compact and Long Form models' season thermal performance according with integration – Above and Basement

Ground Effect – Models Season Thermal Performance

Seasons		Above			Basement		
		Levels of Ground Integration			Levels of Ground Integration		
		01	02	03	01	02	03
Winter	Comp.Form	3	1	2	1	2	3
	Long Form	3	1	2	2	1	3
Spring		3	2	1	3	2	1
Summer		3	2	1	3	2	1
Autumn		3	2	1	3	2	1
* Scale		← 1 to 3 →			← 1 to 3 →		

* Performance Scale 1 to 3 (1= Best performance & 3= Worst performance).

It is during winter that the performance patterns are mixed. For the Above Ground models both forms have the best performance with ground integration 02, soon followed by ground integration 03. For the Basement models, the compact form achieves the best results with ground integration 01, followed by 02, and the best performance for the long form is achieved with ground integration 02. It needs to be pointed out that this change of pattern does not affect the overall heating performance.
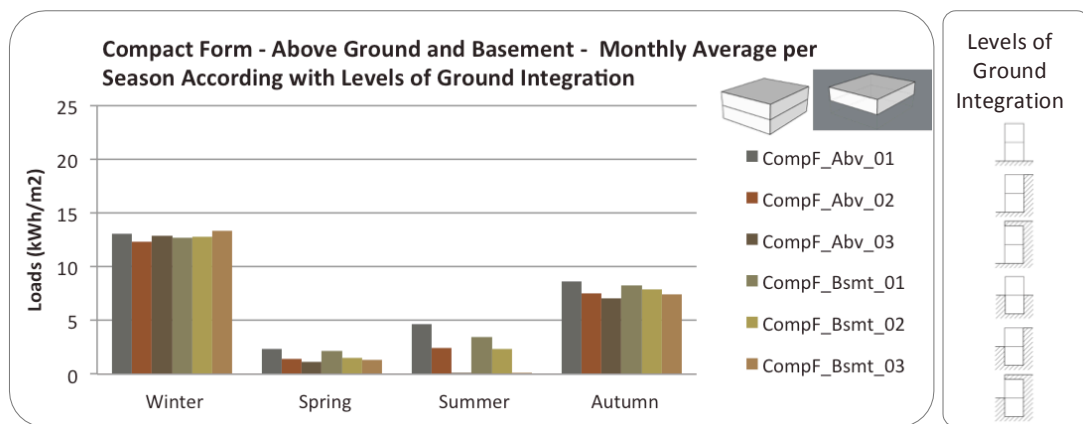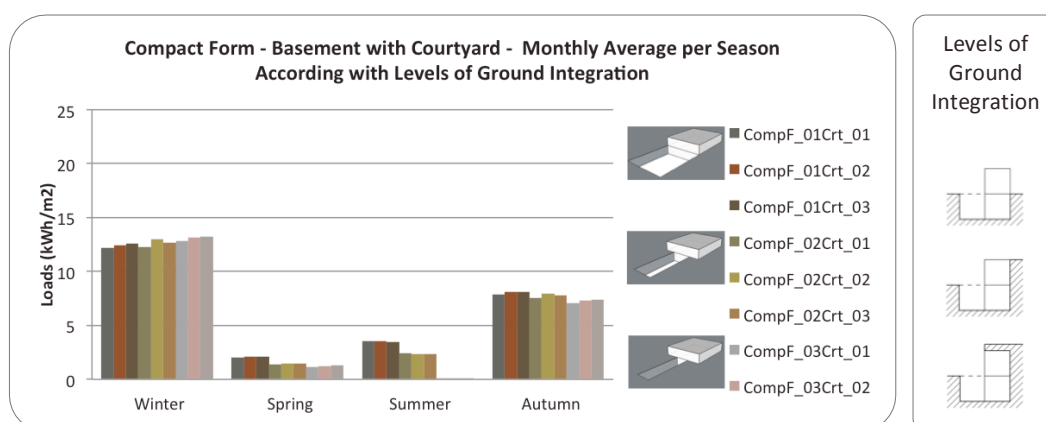

Figure 7.14: Ground integration effect on model' monthly average loads per season – Compact Form – Basement with Courtyard
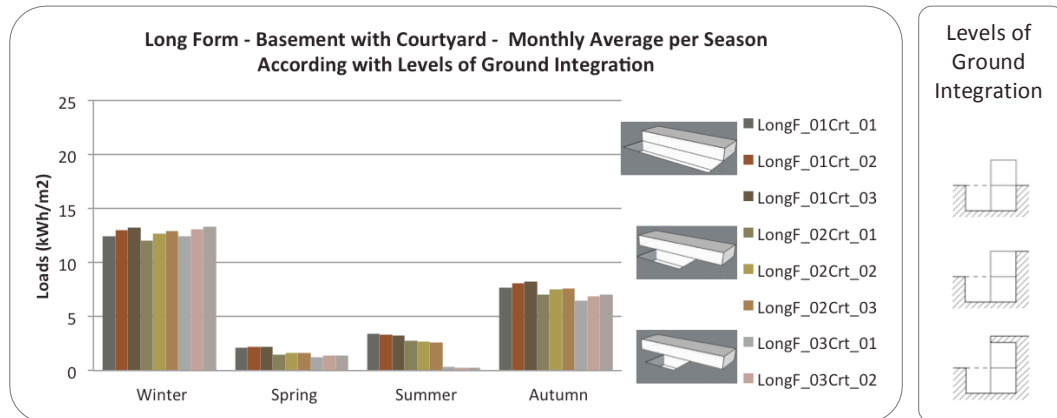
Figure 7.15: Ground integration effect on model' monthly average loads per season – Long Form – Basement with Courtyard

Figure 7.14 and 7.15 shows the seasonal results for compact and long form Basement with Courtyard models. Table 7.35 display the models' performance results summary, organised from best to worst performance.

Table 7.35: Compact and Long Form models' season thermal performance according with integration – Basement with Courtyard

Ground Effect - Models Season Thermal Performance

Season and Model		Courtyard								
		1/1			1/2			1/3		
		Levels of Ground Integration			Levels of Ground Integration			Levels of Ground Integration		
		01	02	03	01	02	03	01	02	03
Winter	Comp.	1	3	4	2	7	5	6	8	9
	Long	2	6	8	1	4	5	3	7	9
Spring		7	8	9	4	5	6	1	2	3
Summer		9	8	7	6	5	4	3	2	1
Autumn	Comp.	6	8	9	4	7	5	1	2	3
	Long	7	8	9	4	5	6	1	2	3
* Scale					← 1 to 9 →					

* Performance Scale 1 to 9 (1= Best performance & 9= Worst performance).

Observing both the figures and the table it is understood that during spring and autumn the pattern is the same. These results make it clear that the smaller the courtyard the better the models thermal performance. Furthermore, it is also clear that the greater the ground integration the lower the thermal performance. The reverse of this pattern was found during the summer. During this season, it is

observed that the smaller the courtyard the better the thermal performance of the model. However, the higher the ground integration the better the thermal performance during this period. During winter, the compact and long forms have different result patterns. For the compact form, the larger the courtyard the better the model's results. Whereas, the performance pattern of the long forms seems to be more linked with the ground integration of the model than the size of the courtyard. It was found that the lower the ground integration the better the model's results.

7.3.3. Findings and Conclusions

This section results shows that a two floor building with a basement has a better thermal performance than models with two floors above ground, even those of the same shape and area. However, when the Above Ground and Basement models were simulated with higher ground integrations, the performances of the Basement models were worse than those of the Above Ground models. For both groups, the annual thermal performance improved with the increasing direct ground contact.

The introduction of an underground courtyard area at the south-facing side of a building basement proved successful in increasing the thermal efficiency of the models, producing energy savings of up to 26.09% for the compact models, and of up to 30.28% for the long models. It was found that smaller courtyards produce better results. However, by increasing the ground integration, the Basement with Courtyard models becomes less efficient.

Once again the results of these simulations indicate that for this climate a good balance between direct ground contact and solar exposure is essential to achieve the best thermal performance.

7.4. CONCLUSIONS

As the findings above demonstrate, ground integration affects the thermal performance of buildings. The higher the ground contact the lower the annual energy loads of the models. However, and for the particular climate studied, evidence reveals that the highest ground integration fails to produce the best thermal performance. It was found that to achieve the best thermal performance, solar gains during the heating season are essential. This is because reduced or null surface areas (in particular south-facing surfaces) with direct solar exposure undermine the performance of these models. Therefore, a good balance between surface areas with direct ground contact and solar exposure needs to be established, in order to achieve greater thermal efficiency.

As the Form study section of this chapter demonstrates, ground coupling improves buildings performance by up to 2.6 times more than the model designs considered in this study, achieving savings up to 37.87% against the design effect maximum of 14.14%. Medium levels of ground integration such as those with two or three walls with direct ground contact show similar values. Between the three correspondent ground integrations, the average annual savings disparity is small, with values of up to 4%. Regarding the annual loads produced by both models with two walls ground integration, the values are equivalent, but the seasonal loads reveal different patterns. Models with north and west ground integration show superior results during the coldest seasons, while models with north and east ground integration are revealed as being ideal as part of a cooling strategy.

The results of the Floor study show that for equal levels of ground integration, the lower the number of floors, the greater the thermal effect of the ground. The reason for this is due to the increased surface area of the model with direct ground contact. Therefore, the single floor models provide the highest energy saving potential, with

values of up to 36.76% for the compact form, and 38.72% for the long form. The annual average savings for the two-floor models are of up to 17.44% for the compact form, and 18.17%, for the long form. In the case of three-floor models, the compact form models with 13.40% produce the best results, and the long models are able to generate savings of up to 14.11%.

Regarding the use of basements, the comparison between a two floor above-ground building and an equal building with a basement floor indicates that the ground coupling provided by the basement is able to improve the thermal performance of the models. The average annual energy savings are up to 7.53% for the compact models, and up to 6.28% for the long models.

In the case of models designs impact, for this climate, different building shapes produce different thermal performances. The best results are achieved with two forms, the compact model (Model F01) and the long model with an East-West axis (Model F03), with correspondent average annual savings values of 14.14% and 13.30%. This is so when compared with the worst thermal results, which are achieved with the model with courtyard (Model F05). The results from the compact form are more stable for all ground integrations during the whole year, while the long forms achieve the best performance during the cooling season.

As also demonstrated by the results analysed in this chapter, the number of floors affects the thermal performance of all models. The author found that models with equal total floor areas but different numbers of floors can have average annual saving differences of up to 18.36% in the compact models, and of up to 13.77% in the long models. The two-floor models achieve the best results, followed by the three-floor models. Overall, the more compact models produce better results than the longer models with the same number of floors.
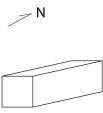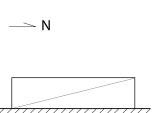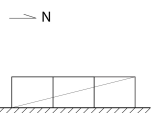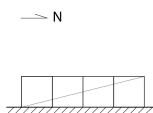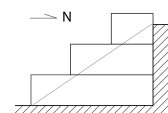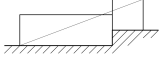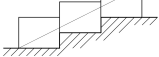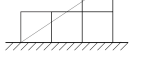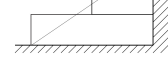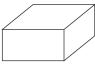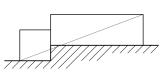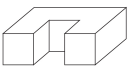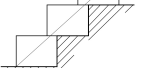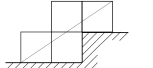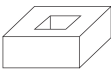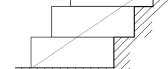
The results of the Basement and Courtyard study allow to found that by introducing an underground courtyard zone adjacent to the building's south-facing wall, the thermal efficiency of the models is improved. In the case of compact models, the annual average savings are of up to 26.09% and, similarly, of up to 30.28% in the long models. Regarding the courtyard size, it is found that smaller courtyards are able to generate better results.

The following chapter analyses the thermal impact produced by ground integration on slope terrains. It analyses its impact on the above studied shapes and introduce new shapes based on slope building designs, which take terrain inclination into consideration.

CHAPTER 8. CASE STUDIES: SLOPE INTEGRATION

8. CASE STUDIES: SLOPE INTEGRATION

Table 8.1: Chapter studies – Forms, Spit Levels, Slope Building Design Adaptation, Configurations and Cross Section Structure

| Forms | Slope Building Designs | | | |
	Spit Levels	Slope Building Design	Configurations	Cross Section Structure
Perspective	Section	Section	Section	Section
Long - long depth	One Level	No Adaptation	Configuration 1	Amanded
Long - Short depth	Two Levels - Diff. Units	Spit Level	Configuration 2	Amanded
Compact	Two Levels - Diff. nits	Cascade - Independent	Configuration 3	Cascade- Γ shape
Semi-courtyard	Two Levels - Equal Units	Cascade - Conected	Configuration 4	Cascade- Semi-step Hill
Courtyard	Three Levels	Amended	Configuration 5	Cascade- Step Hill
			Configuration 6	

This chapter analyses the effect of slope integration on buildings energy consumption, by observing the energy patterns produced by slope degree. In particular, it explains how slope design can affect the thermal performance of a building. This Chapter is organised in five sections: Forms, Split Levels, Slope Building Design, Configurations and Cross Section Structure as illustrated in Table

8.1. Firstly, the Forms section focuses on five models used in Chapter 7 Section 7.1 and discusses how those shapes perform with slope integration. Secondly, the Split Levels section analyses the effect produced by organising the floor area of a building into different levels. Thirdly, the Slope Building Design section combines models with and without slope designs. This section of the chapter compares four model designs that take site inclination into consideration such as spilt level, amends section and cascade or step-hill with a model without slope adaptations. Fourthly, the Configurations study compares six design arrangements with equal numbers of units and areas based on amend and cascade or step-hill sections. Lastly, the Cross Section Structure study compares slope structures integration strategies based on two vertical site integrations, amended sections and cascade sections. For all slope integration studies, when the terrain inclination increases the models surface area with ground contact also increases.

Simulation settings and inputs data:

1. Software Version: EnergyPlus 8.1.
2. Simulation Method: follows the proposed EnergyPlus simulation method for ground-integrated buildings described in Chapter 6.2.
3. Location: Lisbon.
4. Weather File: the weather data described in Chapter 5 Section 5.2.2. uses the Climate Design Data 2009 ASHRAE Handbook design conditions.
5. Internal Gains: no internal gains were used.
6. Ventilation: no ventilation was used.
7. Infiltration: no infiltration was used.
8. Comfort Zone: the annual comfort range at this location it is assumed to be between 20°C to 26°C.
9. HVAC: the heating SetPoint is 20°C and cooling SetPoint is 26°C.
10. Openings: no openings were used.
11. Materials: all surfaced are assumed to be 20 cm concrete, see Table 6.4 in Chapter 6.
12. Seasonal data: it is assumed that winter period correspond to January, February and March; the spring period combines April, May and June; the summer season is formed by July, August and September; the autumn period is formed by October, November and December.

8.1. FORMS WITH SLOPE GROUND INTEGRATION

8.1.1. Models Description and Levels of Slope Integration

This parametric study looks at how different building shapes are affected by slope integration. Following the recommendations presented in Chapter 6, the models previously used in Chapter 7, Section 7.1 are utilised on this section as a separate study. Information regarding the area, perimeter and area to perimeter ratios of the forms can be found in Chapter 7, Section 7.1.1. The details of the models, such as name, dimensions, type of slope integration and its simulation reference name are displayed in Table 8.2.

Table 8.2: Models details - Forms study with slope integration
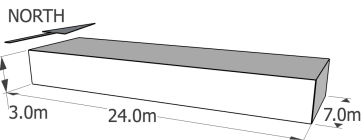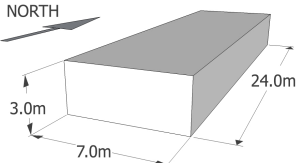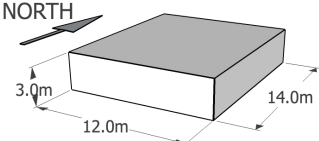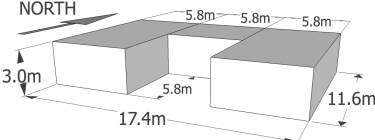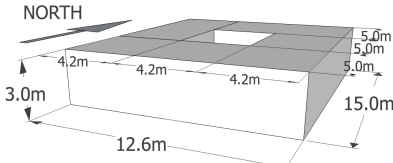
Models Dimensions		Slope Integration	Ref. Name
Model F01		0° Slope	F01_00°
		5° Slope	F01_05°
		10° Slope	F01_10°
		15° Slope	F01_15°
		20° Slope	F01_20°
Model F02		0° Slope	F02_00°
		5° Slope	F02_05°
		10° Slope	F02_10°
		15° Slope	F02_15°
		20° Slope	F02_20°
Model F03		0° Slope	F03_00°
		5° Slope	F03_05°
		10° Slope	F03_10°
		15° Slope	F03_15°
		20° Slope	F03_20°
Model F04		0° Slope	F04_00°
		5° Slope	F04_05°
		10° Slope	F04_10°
		15° Slope	F04_15°
		20° Slope	F04_20°
Model F05		0° Slope	F05_00°
		5° Slope	F05_05°
		10° Slope	F05_10°
		15° Slope	F05_15°
		20° Slope	F05_20°

Table 8.3: Level of slope integration - Forms study with slope integration

Levels of Slope Integration	Sections ⟶N	Plans N	Perspectives ⟶N	Walls Depth
0° Slope				0 m
5° Slope				
10° Slope				Up to 3 m
15° Slope				
20° Slope				

The present case study uses five levels of slope integration with intervals of five degrees, starting with a 0° slope (null) and going up to a 20° slope, as shown in Table 8.3. The total amount of models' exterior surface with ground contact varies not only with the slope gradient but also with the models' shape. The wall ground integration depth can range from 0 m to the highest depth of 3 m. In all cases the roofs of the models have total sun and wind exposure.

8.1.2. Results Analysis – Effects of Slope and Models' Design

8.1.2.1. Annual Results
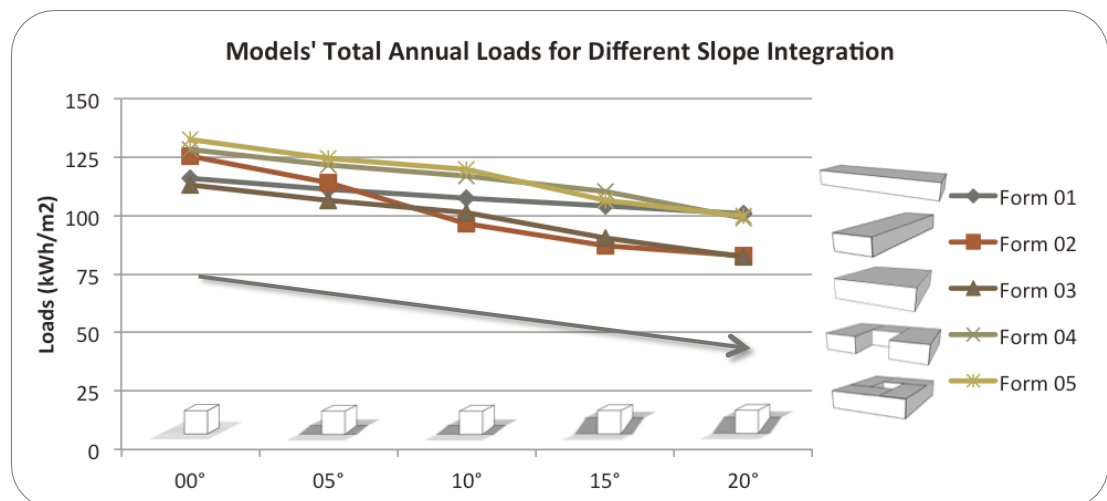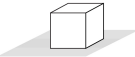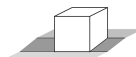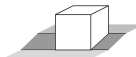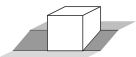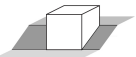
Figure 8.1: Slope effect on Form models' total annual load

The models' total annual loads results reveal one clear pattern. It is immediately obvious from Figure 8.1 that the total energy demand is affected by the degree of

slope integration. It can clearly be seen that a slope gradient increase generates a reduction of energy consumption.
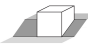
Table 8.4: Form models' annual thermal performance according with slope integration

Annual Slope Effect - Models Thermal Performance According with Slope Integration

0° Slope	5° Slope	10° Slope	15° Slope	20° Slope
5	4	3	2	1

← Scale 1 to 5 →

* Performance Scale 1 to 5 (1= Best performance & 5= Worst performance).

This pattern is reproduced with all models results, as summarised in Table 8.4, in which the slope performance is arranged from best (1) to worst (5). For all models, the higher the slope, the greater the amount of ground integration and the lower the total annual loads. The annual savings per model shown in Table 8.5 indicate that, for all models, any slope-integration has thermal benefits. The highest saving potential is achived with a 20° slope, with an average 24.31%. In shallow slopes, such as 5° and 10°, the correspondent average savings are around 6% and 12% each.

Table 8.5: Form models' annual savings percentage according with slope integration

Slope Effect - Annual Savings (%) per Model
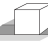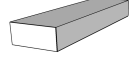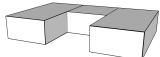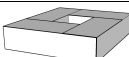
Models		Levels of Slope Integration				
		0°	5°	10°	15°	20°
F01		0.00	4.05	7.12	9.93	**12.93**
F02		0.00	8.93	23.04	30.32	**33.86**
F03		0.00	5.84	10.32	20.06	**27.10**
F04		0.00	5.02	8.66	13.76	**22.87**
F05		0.00	5.97	9.50	19.56	**24.79**
Average Savings % per slope Integration		0.00	5.96	11.73	18.72	**24.31**

In order to assess the design effects, the models annual savings are calculated and compared for each level of slope integration and the corresponding values are

displayed in Table 8.6. The same table also displays the overall average annual savings percentage for each model, and their overall thermal performance using a performance scale from one to five, where one corresponds to the best performance and five to the worst.

Table 8.6: Annual thermal performance comparison between all Forms models' design – for all slopes

Design Effect - Models' Annual Savings (%) per Slope Integration and Models Overall Performance

Models	Levels of Slope Integration					Overall Results		Scale*
	0°	5°	10°	15°	20°	Average Savings*	Perfor.**	
F01	12.68	10.89	10.38	5.65	0.00	7.92	= 3	↑ 1 to 5 ↓
F02	5.55	8.52	19.68	21.05	17.84	14.53	= 2	
F03	14.78	14.66	15.56	18.28	18.30	16.32	**= 1**	
F04	3.34	2.36	2.44	0.00	1.95	2.02	= 4	
F05	0.00	0.00	0.00	3.50	1.08	0.92	= 5	

* Average annual savings % per model; ** Performance Scale 1 to 5 (1= Best performace & 5= Worst performance).

These values show that Model F03 provides the best thermal performance. This model has the best results for slopes 0°, 5° and 20°. This same model has the second best results for slopes 10° and 15°, producing average annual savings of 16.32%. Model F02 has the best results for slopes 10° and 15° and its shape is able to generate the second best average annual savings with 14.53%. The lowest energy savings were produced by Model F05, closely followed by values achieved by Model F04.

8.1.2.2. Seasonal Results
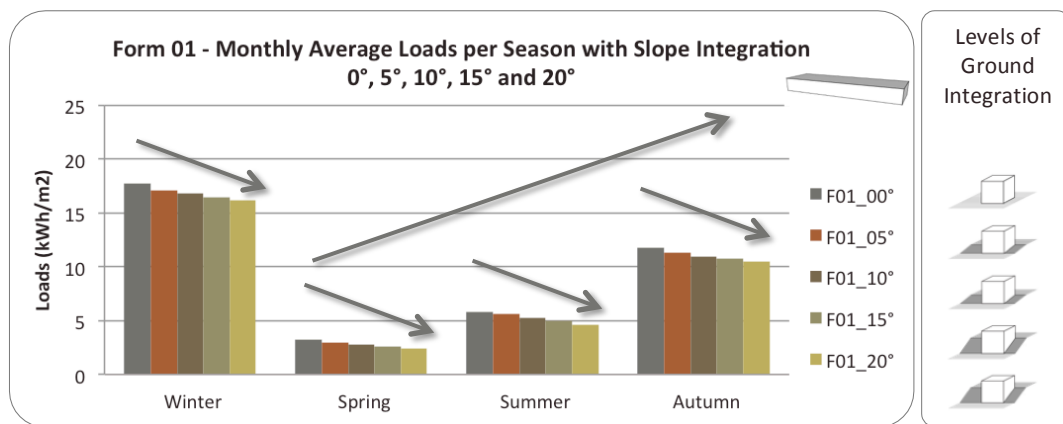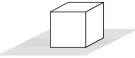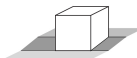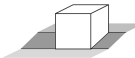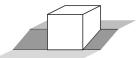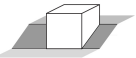
Figure 8.2: Slope effect on model' monthly average loads per season – Form 01

Figure 8.2 shows that the monthly average loads per season change according with the different periods. The lowest loads are produced during spring and the highest during wintertime. It is therefore evident that the heating periods of winter and autumn are the largest contributors to the total annual loads. It is also clear that for all seasons the effect of slope integration is the same because the higher the slope, the lower the energy needs of the model.
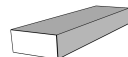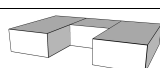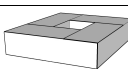
Table 8.7: Forms models' season thermal performance according with slope integration

Season Slope Effect - Models Thermal Performance According with Slope Integration

0° Slope	5° Slope	10° Slope	15° Slope	20° Slope
5	4	3	2	1

← Scale 1 to 5 →

* Performance Scale 1 to 5 (1= Best performance & 5= Worst performance).
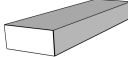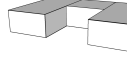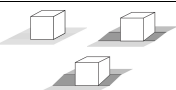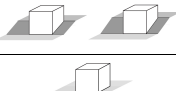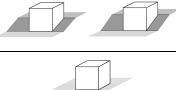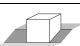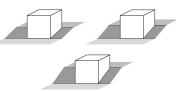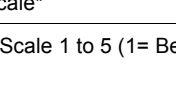
The thermal performance of all models is ranked on a best (1) to worst (5) scale and combined in Table 8.7 according with slope integration. It is clear that for all models, the rise of ground contact due to slope increase improves the thermal performance of all models. This is because the higher the slope the lower the monthly average loads per season.

The same performance scale is applied in Table 8.8, which summarises the average loads per season of each model according with slope integration. Through an

examination of this table it becomes evident that some forms perform better at different seasons. Furthermore, two main patterns can be defined. The first occurs in the coldest seasons and the second is registered during the warmest seasons.

Model F03 produces the best results in the winter and autumn seasons. These results are followed by those registered by Model F01 and F02. In winter Model F01 performs better than Model F02 with null or shallower slopes (5° and 10°). The reverse of these results is found for steeper slopes (15° and 20°), where Model F02 performs better than Model F01. During autumn, the results for Model F01 are better than Model F02 with 0° and 5° slopes. For 10°, 15° and 20° slopes, the performance of Model F02 is better than that of Model F01.

Table 8.8: Comparison between all Form models' design – Seasonal loads

Models's Design Effect - Thermal Performance According with Seasonal Loads

Slope Integration		Form 01	Form 02	Form 03	Form 04	Form 05
Winter	0°, 5° & 10°	2**	3**	1	4	5
	15° & 20°	3	2	1	4	5
Spring	0°	2	4	1	3	5
	5°	3	1	2	4	5
	10°	3	1	2	5	4
	15° & 20°	5	1	2	4	3
Summer	0°	1	5	2	3	4
	5°	3	1	2	4	5
	10°	4	1	2	5	3
	15°	5	1	3	4	2
	20°	5	1	2	4	3
Autumn	0° & 5°	2	3	1	4	5
	10°, 15° & 20°	3**	2**	1	4	5
Scale*				← 1 to 5 →		

* Performance Scale 1 to 5 (1= Best performance; 5= Worst performance); **Equal results with 10° Slope.

Model F02 achieves the best results for all slope integration levels during spring. The exception is found with a 0° slope, where Model F03 has the lowest energy demand. Model F02 has also the best results in summer for all slopes except the null one. These good results are the result of two factors. Firstly, the reduced south wall area minimises the solar gains and, secondly, there is a higher amount of ground contact due to the east and west walls being direct contact with the ground. Model F03 is the second best shape during both spring and summer seasons.

Overall, Model F03 presents the best results. For all slopes it is the model that performs best during winter and autumn and therefore it can be used as part of a heating strategy. Significantly, this is also the model that achieves the second best results in spring and summer. The results for Model F02 show that this shape is the best option as part of a cooling strategy.

8.1.3. Findings and Conclusions

Considering the results discussed above, it is argue that buildings can benefit from slope integration, since the higher the slope gradient, the lower the energy demand of the building integrated into that slope. Through this investigation the author have verified that any degree of slope-integration can produce thermal benefits. Small slopes such as 5° and 10° are still able to generate average annual energy savings of around 6% and 12% each. The highest savings are produced with a 20° slope, which presents an average 24.31% savings.

The best shapes for this type of ground integration are Model F03, followed by Model F02. This finding differs from the Form study results presented in Chapter 6. The average annual savings produced by Model F03 are of 16.32% and by Model F02 of 14.53%. Model F03 performs the best for slope gradients of 0°, 5° and 20°, while Model F02 is the most effective shape for slope gradients of 10° and 15°.
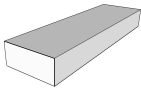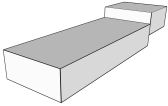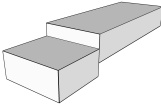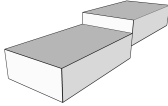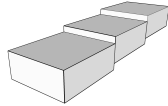
Although the cooling performance is important at this location, a design based on a heating strategy can have a stronger impact on the annual energy demand of a building. The seasonal analysis of this demand allows us to identify Model F03 as the best shape for a heating strategy. This model has the best results for winter and autumn, the seasons in which energy demand is normally higher in this particular location. For spring and summer, Model F03 is the second best model, while Model F02 is the best shape. This makes Model F02 a more effective building form to use as part of a cooling strategy.

8.2. SPLIT LEVELS

The split-level is a commonly used building design type that takes slope site characteristics into consideration. This design is normally used in average slopes and can be shaped by multiple floors levels that follow a slope gradient. This section of the chapter looks into this specific slope design, by focusing on number of levels as well as the position of those levels. It also examines how the slope-integration affects this design if the slope gradient is changed.

8.2.1. Models Description and Levels of Slope Integration
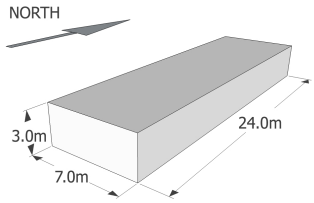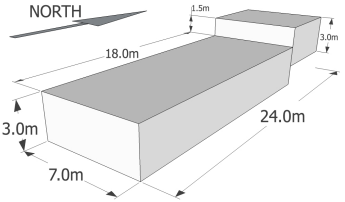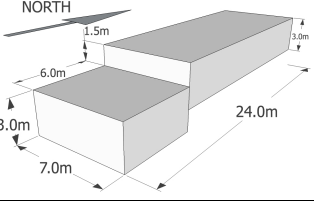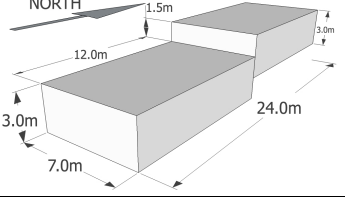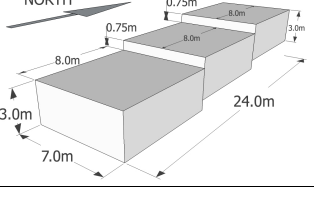
Table 8.9: Models characteristics – Split Level study

Model Name	Split Level 01 (SL01)	Split Level 02 (SL02)		Split Level 03 (SL03)		Split Level 04 (SL04)		Split Level 05 (SL05)		
Models										
Slope Building Desin Type	-	Split-level		Split-level		Split-level		Split-level		
Total Area (m^2)	168	168		168		168		168		
Unit Number	1	2		2		2		3		
Unit Area (m^2)	168	112	56	56	112	84	84	56	56	56
Unit Perimeter (m)	62	46	30	30	46	38	38	30	30	30
Ratio A/P	2.7	2.43	1.87	1.87	2.43	2.21	2.21	1.87	1.87	1.87

This study uses five models with equal total areas. As illustrated in Table 8.9, the base model is SL01, formed by a single level. Models SL02, SL03 and SL04 have two levels, both with equal dimensions but differing in terms of the position of the unit. The levels of Model SL04 have equal areas and, lastly, Model SL05 is formed by three levels with equal areas.

Model SL01 is the only model with a single story 3 m high. As visible in Table 8.10, all other models' height varies with the units. The lower unit height is 3 m and the upper unit height is 4.5 m. All models' dimensions, type of slope integration and correspondent reference name can be found in the same table.

Table 8.10: Models details – Split Level study

Models Dimensions	Slope Integration	Ref. Name
Split Level 01 NORTH 3.0m / 7.0m / 24.0m	0° Slope	SplitLevel01_00°
	5° Slope	SplitLevel01_05°
	10° Slope	SplitLevel01_10°
	15° Slope	SplitLevel01_15°
	20° Slope	SplitLevel01_20°
Split Level 02 NORTH 1.5m / 3.0m / 18.0m / 24.0m / 3.0m / 7.0m	0° Slope	SplitLevel02_00°
	5° Slope	SplitLevel02_05°
	10° Slope	SplitLevel02_10°
	15° Slope	SplitLevel02_15°
	20° Slope	SplitLevel02_20°
Split Level 03 NORTH 1.5m / 3.0m / 6.0m / 24.0m / 3.0m / 7.0m	0° Slope	SplitLevel03_00°
	5° Slope	SplitLevel03_05°
	10° Slope	SplitLevel03_10°
	15° Slope	SplitLevel03_15°
	20° Slope	SplitLevel03_20°
Split Level 04 NORTH 1.5m / 3.0m / 12.0m / 24.0m / 3.0m / 7.0m	0° Slope	SplitLevel04_00°
	5° Slope	SplitLevel04_05°
	10° Slope	SplitLevel04_10°
	15° Slope	SplitLevel04_15°
	20° Slope	SplitLevel04_20°
Split Level 05 NORTH 0.75m / 8.0m / 3.0m / 0.75m / 8.0m / 8.0m / 24.0m / 3.0m / 7.0m	0° Slope	SplitLevel05_00°
	5° Slope	SplitLevel05_05°
	10° Slope	SplitLevel05_10°
	15° Slope	SplitLevel05_15°
	20° Slope	SplitLevel05_20°

The levels of slope integration used in this study are shown in Table 8.11. As in the previous section, there are five different slopes gradients with 5° intervals that range from 0° (null) to a maximum of 20°. The depths of the walls in each model wall change according with their design as well as level of slope integration, with values ranging from 0 m up to a maximum of 8 m.

Table 8.11: Level of slope integration – Split Level study with slope integration

Levels of Slope Integration	Side View ⟍N	Plans N	Perspectives ⟍N	Maximum Walls Depth
0° Slope				0 m
5° Slope				
10° Slope				Up to 8 m
15° Slope				
20° Slope				

8.2.2. Results Analysis

8.2.2.1. Annual Results
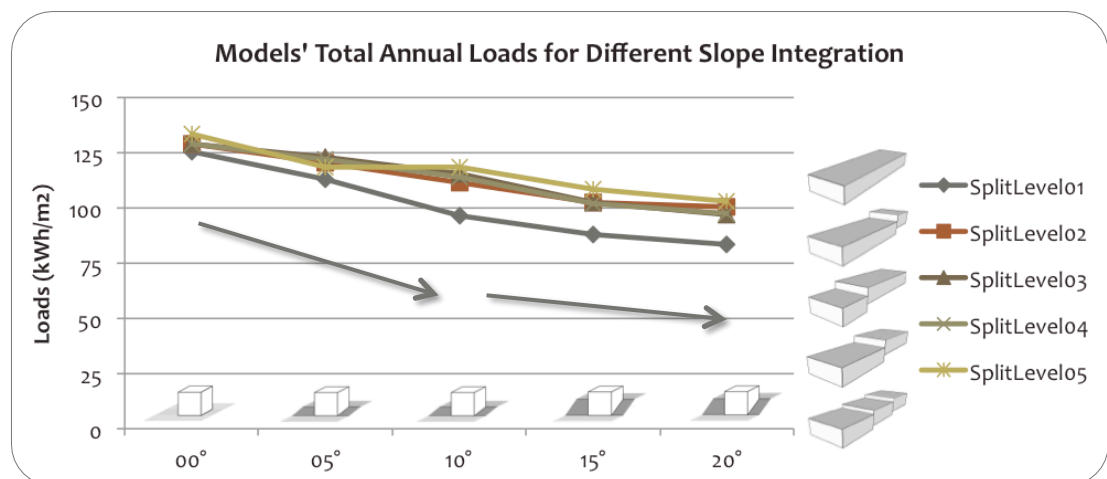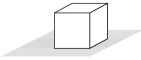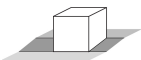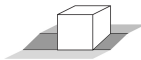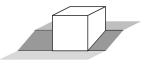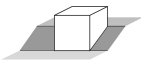
Figure 8.3: Slope effect on Split Level models' total annual load

As illustrated in Figure 8.3, the models' total annual loads show that from 0° to 20° slopes, the higher the slope, the better the thermal performance. However it can also be seen in the same figure that similar results are present in steeper slopes. This pattern is repeated by all models and is summarised in Table 8.12 by using a scale based on best (1) to worst (5) thermal performance. It should be pointed out, however, that the sole exception to this pattern is found in the performance of Model SL05. In this three-unit model, the annual thermal performance for 5° and 10° slopes is the same.

Table 8.12: Split Level models' annual thermal performance according with slope integration

Annual Slope Effect - Models Thermal Performance According with Slope Integration

0° Slope	5° Slope	10° Slope	15° Slope	20° Slope
5	4**	3**	2	1

← Scale 1 to 5 →

* Performance Scale 1 to 5 (1= Best performance & 5= Worst performance); For Split Level 05, 5° and 10° Slope have equal results.

The annual savings produced by slope effect can be observed in Table 8.13. The results presented in this table strengthen the findings which slope-integration can affect the models efficiency, and the higher the slope, the better the thermal performance of each model. The average savings percentage produced by slope integration can go up to 25.61%. It is also observed that the average savings range is larger for 5°, 10° and 15° slopes with a correspondent average increase of 7.51%, 6.46% and 8.1%, and a lower average saving range for a 20° slope, which only produces average savings 3.54% higher than a 15° slope.

Table 8.13: Split Level models' annual savings percentage according with slope integration

Slope Effect - Annual Savings (%) per Model
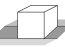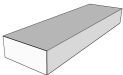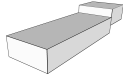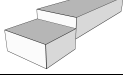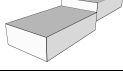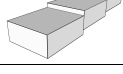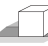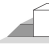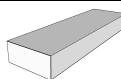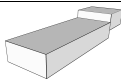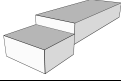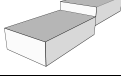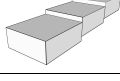
Models		Levels of Slope Integration				
		0°	5°	10°	15°	20°
SplitLevel 01		0.00	9.82	23.06	29.77	33.40
SplitLevel 02		0.00	6.41	13.50	20.41	22.20
SplitLevel 03		0.00	4.58	10.51	20.51	25.01
SplitLevel 04		0.00	5.41	11.50	21.09	24.59
SplitLevel 05		0.00	**11.32**	**11.31**	18.56	22.87
Average Savings % per Slope Integration		0.00	7.51	13.97	22.07	**25.61**
Average Increase Range %		0.00	7.51	6.46	8.1	**3.54**

Table 8.14 displays the average annual savings generated by the models' designs. It is observable in this table that the number of split-levels can affect the thermal

performance of a building. Therefore, the higher the number of split-levels, the lower the thermal performance and average savings of the model. The pattern is confirmed in all slope integrations, excluding a 5° slope. Model SL01 produces the best results for all levels of slope integration, with average savings of 14.13%.

Table 8.14: Annual thermal performance comparison between all Split Level models' design – for all slopes

Design Effect - Models' Annual Savings (%) per Slope Integration and Models Overall Performance

Models		Levels of Slope Integration					Overall Results		Scale*
		0°	5°	10°	15°	20°	Average Savings*	Perfor.**	
SplitLevel 01		6.05	8.23	18.50	18.98	18.88	14.13	= 1	↑ 1 to 5 ↓
SplitLevel 02		**3.31*ˢ**	**1.98**	**5.69**	5.51*ˢ	2.47	3.79	= 3	
SplitLevel 03		3.25*ˢ	0.00	2.37	5.56*ˢ	**5.93*ˢ**	3.42	= 4	
SplitLevel 04		3.30*ˢ	0.92	3.50	**6.30**	5.45*ˢ	3.90	= 2	
SplitLevel 05		0.00	3.94	0.00	0.00	0.00	0.79	= 5	

* Average annual savings % per model; ** Performance Scale 1 to 5 (1= Best performace & 5= Worst performance); *ˢ Equal or similar results.

When comparing the three models with an equal number of levels (i.e. Model SL02, SL03 ad SL04) it is noticeable that all models achieved similar results. The average savings difference between the three models is lower than 0.5%. Model SL02 has better results with shallower slopes, while Models SL03 and SL04 achieve better performance with the highest slopes.

8.2.2.2. Seasonal Results
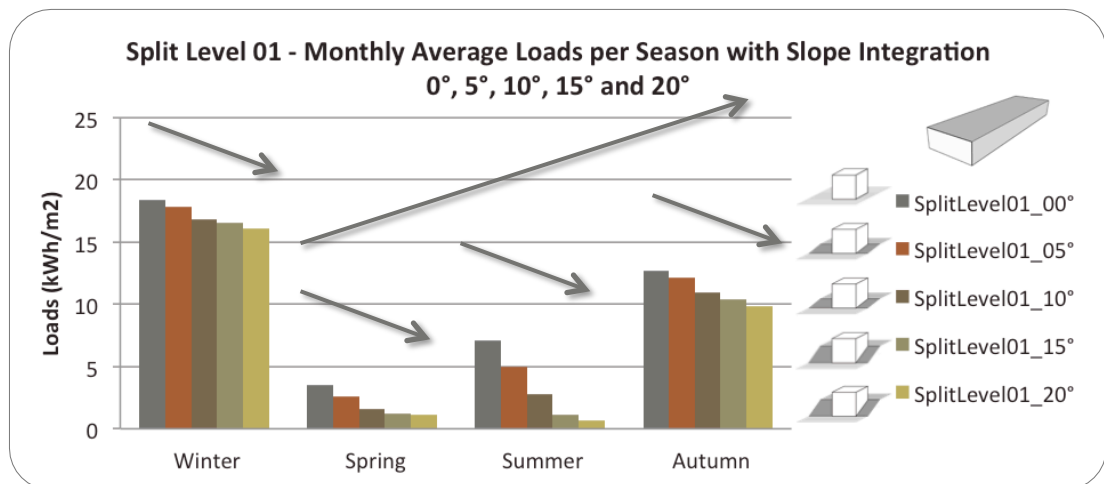
Figure 8.4: Slope effect on model' monthly average loads per season – Split Level 01

The models' monthly average results per season analysis indicate that, for models SL01 to SL04, in all seasons the performance improves as the angle of the slope increases (Table 8.15). This pattern of results can be seen in Figure 8.4, which corresponds to the results of Model SL01. It is clear that the higher the slope gradient the better the models' thermal performance.

During spring and summer, the difference in results between slope gradients of 15° and 20° is reduced. Thus, compared with a 15° slope, the biggest benefit from a 20° slope is linked to the heating seasons of autumn and winter.

Table 8.15: Split Level models' season thermal performance according with slope integration

Season Slope Effect - Models Season Results According with Slope Integration						
Season and Models		0°	5°	10°	15°	20°
SL01 to SL04 All Seasons		5	4	3	2	1
SL05	Winter	5	2	4	3	1
	Spring & Summer	5	4	3	2	1
	Autumn	5	3	4	2	1
Scale*		← Scale 1 to 5 →				

* Performance Scale 1 to 5 (1= Best performance & 5= Worst performance).

Concerning Model SL05 (Table 8.15), the above pattern is only found in spring and summer. Throughout the heating period, in autumn and winter, the highest slope has the best results and the 0° slope produces the lowest results. However, during winter a 5° slope produces better results than 10° and 15° slopes, and in autumn a 5° slope is better than a 10° slope. The reason why 5° and 10° slopes have equal annual results is because a 5° slope has better results in winter and autumn. Therefore, for Model SL05 a shallower slope of around 5° is more efficient as a heating strategy than steeper gradients.
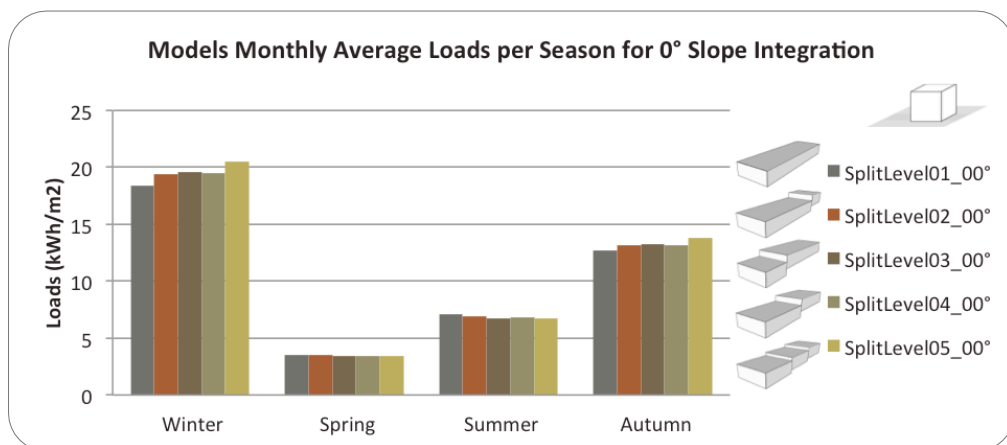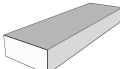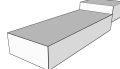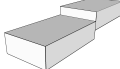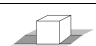
Figure 8.5: Seasonal loads comparison between all Split Level models' design – 0° Slope integration

Through an examination of the models' monthly average loads per season for 0° slope integration, illustrated in Figure 8.5, it can be observed that there is a division in the results according with number of split-levels. The performance of the models worsens when the number of units rises. Again, it is visible that for Models SL02, SL03 and SL04 the results are similar, as the highest gap between these models can be found during winter.

The results presented in Figure 8.5, as well as the results for all other slopes, are summarised in Table 8.16, using a performance scale of best (1) to worst (5). Several patterns can be seen in the results presented in this table. For every single season, Model SL01 has the best results except during spring and summer with 0°

slope. Under this setup this is the model with worst results. Regarding the performance of Model SL05, it is observed that during winter and autumn it produces the worst results. However, during spring and winter the results are mixed. This model achieves good results with shallower slopes, and its performance worsens as the slope gradient increases.

Table 8.16: Comparison between all Split Level models' design – Seasonal loads

Models's Design Effect - Thermal Performance According with Seasonal Loads

	Slope Integration		SplitLevel01	SplitLevel02	SplitLevel03	SplitLevel04	SplitLevel05
Winter/Autumn	0° & 10°		1	2**	4**	3**	5
	5°		1	5	4	3	2
	15°		1	3**	4**	2**	5
	20°		1	4**	3**	2**	5
Spring	0°		5**	4**	2**	3**	1**
	5°		1	3	5	4	2
	10°		1	2**	5	3**	3**
	15°		1	4	2	3	5
	20°		1	5**	2	3**	3**
Summer	0°		5	4	2	3	1
	5°		1	3	5	4	2
	10°		1	2	5	4**	3**
	15°		1	4**	3**	2	5
	20°		1	5	2	3	4
	Scale*			← Scale 1 to 5 →			

* Performance Scale 1 to 5 (1= Best performance & 5= Worst performance); **Equal or similar results at autumn.

The design effect produced by Model SL02, SL03 and SL04 is irregular since a clear pattern cannot be established. It is also clear that the thermal performance difference between models is of reduced significance when comparing these designs. This is because the result values are similar and in some cases identical.

8.2.3. Findings and Conclusions

Concerning the effect of slope-integration, it is found that higher the slope the better the thermal performance of each model, with average annual savings percentage of up to 25.61%. Consequently, it is concluded that slope-integration can improve the thermal performance of these models. It is also observed that the average annual savings amplitude is greater for 5°, 10° and 15° slopes, with correspondent values of 7.51%, 6.46% and 8.1%. For a 20° slope the value is just 3.54% higher than a 15° slope. The seasonal analysis of slope effects reveals that, during all seasons, the performance of all models from SL01 to SL04 improved with the level of slope. With Model SL05, the above pattern is only found in spring and summer, as during winter and autumn the pattern changes.

Observing the design effect, for slope integrations of 0° to 20° it is found that the number of split-levels can affect buildings annual thermal performance. It is identified that the higher the number of split-levels, the worse the results. Model SL01 is the most efficient model, with average savings up to 14.13% in comparison with Model SL05, which is the less efficient model, and produces annual savings of 0.79%. Therefore, it is concluded that a slope design with split-levels should be used only if required. As for a 'gradual' zone division and distribution, this should be used in a reduced number of levels. Between models with equal number of split-levels, such as Model SL02, SL03 and SL04, the annual and seasonal thermal performance is mixed and the results are similar. Overall, the level size and position of the split-level is found to be irrelevant to the models' thermal performance.
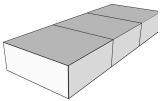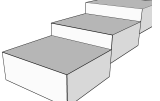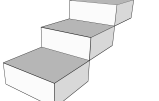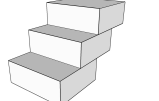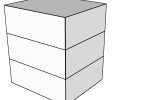
8.3. SLOPE BUILDING DESIGN

As previously discussed in Chapter 4, Section 4.4.2., there are several design solutions when approaching a slope site. This section further explores these solutions, by focusing on site inspired and special designs. It compares four models with slope building designs and a model without slope design. The slope buildings designs used in this section are based on three types of slope design, namely spilt level, amends section, and cascade or step-hill. Examining the efficiency of these models, this section addresses two main questions: firstly, how these designs are affected by site slope degree and, secondly, which slope buildings designs are the most thermally efficient.

8.3.1. Models Description and Levels of Slope Integration
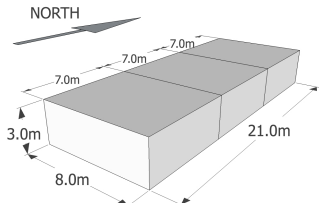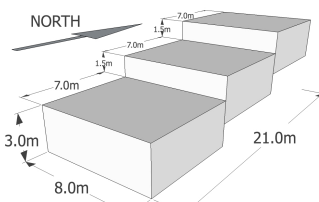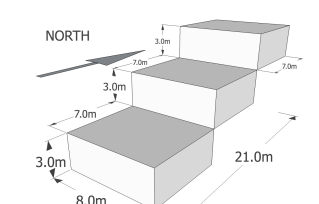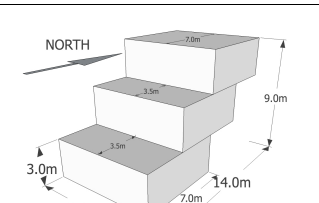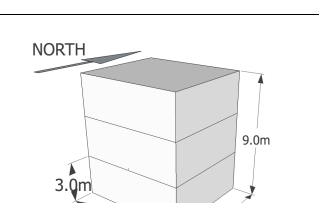
The five models used in this part of the study share the same total area, equal number of zones and unit area as those in Table 8.17. The designs used are a basic single form model (Model SlopeBD 01), a split level model (Model SlopeBD 02), a cascade model with independent units (SlopeBD 03), a cascade model with connected units (SlopeBD 04), and the last model is an amended section structure (SlopeBD 05).

Table 8.17: Models characteristics – Slope Building Design study

Model Name	SlopeBD 01	SlopeBD 02	SlopeBD 03	SlopeBD 04	SlopeBD 05
Models					
Slope Building Desin Type	-	Split-level	Cascade or Step-hill; disconected units	Cascade or Step-hill; linked units	Amended Section
Total Area (m^2)	168	168	168	168	168
Zone N.	3	3	3	3	3
Unit Area (m^2)	56	56	56	56	56
Unit Perimeter (m)	30	30	30	30	30
Ratio A/P	1.87	1.87	1.87	1.87	1.87

The models' dimensions, slope integration and correspondent reference name are listed in the Table 8.18.

Table 8.18: Models details – Slope Building Design study

Models Dimensions	Slope Integration	Ref. Name
SlopeBD 01	0° Slope	SlopeBD01_00°
	10° Slope	SlopeBD01_10°
	20° Slope	SlopeBD01_20°
	30° Slope	SlopeBD01_30°
	40° Slope	SlopeBD01_40°
	50° Slope	SlopeBD01_50°
SlopeBD 02	0° Slope	SlopeBD02_00°
	10° Slope	SlopeBD02_10°
	20° Slope	SlopeBD02_20°
	30° Slope	SlopeBD02_30°
	40° Slope	SlopeBD02_40°
	50° Slope	SlopeBD02_50°
SlopeBD 03	0° Slope	SlopeBD03_00°
	10° Slope	SlopeBD03_10°
	20° Slope	SlopeBD03_20°
	30° Slope	SlopeBD03_30°
	40° Slope	SlopeBD03_40°
	50° Slope	SlopeBD03_50°
SlopeBD 04	0° Slope	SlopeBD04_00°
	10° Slope	SlopeBD04_10°
	20° Slope	SlopeBD04_20°
	30° Slope	SlopeBD04_30°
	40° Slope	SlopeBD04_40°
	50° Slope	SlopeBD04_50°
SlopeBD 05	0° Slope	SlopeBD05_00°
	10° Slope	SlopeBD05_10°
	20° Slope	SlopeBD05_20°
	30° Slope	SlopeBD05_30°
	40° Slope	SlopeBD05_40°
	50° Slope	SlopeBD05_50°

This study uses slope integration levels from null (0°) up to 50°, with 10° intervals between each level, as illustrated in Table 8.19. The maximum wall depth with ground contact goes up to 8 m according to the design of each model, as well as the type of slope. All model simulations assume that the roofs of the buildings have full sun and wind exposure.

Table 8.19: Level of slope integration – Slope Building Design study with slope integration

Levels of Slope Integration	Side View ⟶ N	Plans N	Perspectives ⟶ N	Maximum Walls Depth
0° Slope				0 m
10° Slope				
20° Slope				
30° Slope				Up to 8 m
40° Slope				
50° Slope				

8.3.2. Results Analysis

8.3.2.1. Annual Results
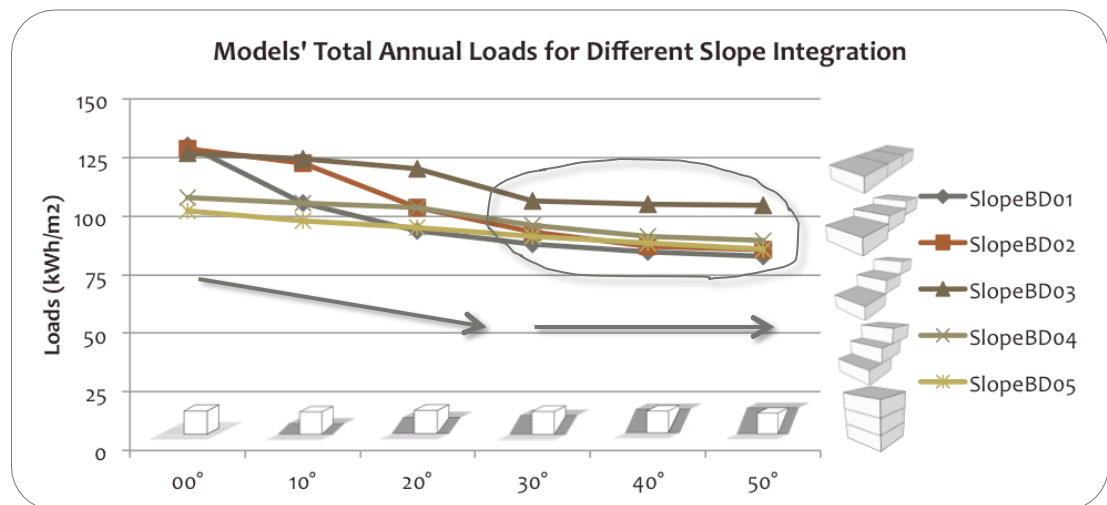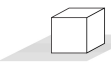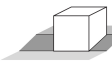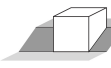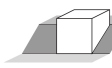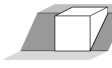
Figure 8.6: Slope effect on Slope Buildng Design models' total annual load

Regarding the slope integration effect, observable in Figure 8.6, for all models it was found that the total annual loads decrease according with slope, and therefore the higher the slope, the lower the annual load of each model. Consequently, the least efficient thermal performances are found with the null slopes and the most efficient are achieved with the highest gradients, which correspond to 50° slopes. However, it can be seen that between a 30°, a 40°, and a 50° slope the results gap is almost negligible. For this reason, the use of slopes between 30° up to 50° should be

considered against other factors, since there are not any noticeable advantages in using steeper slopes.
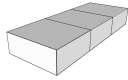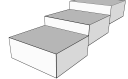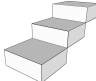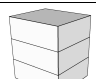
Table 8.20: Slope Building Design models' annual thermal performance according with slope integration

Annual Slope Effect - Models Thermal Performance According with Slope Integration

0° Slope	10° Slope	20° Slope	30° Slope	40° Slope	50° Slope
6	5	4	3	2	1

← Scale 1 to 6 →

* Performance Scale 1 to 6 (1= Best performance & 6= Worst performance).

The annual slope integration effect pattern is reiterated in the results provided in Table 8.20, which provides a summary of the results of all models by using a performance scale which runs from best (1) to worst (6). Table 8.21 shows the annual savings percentage for each model according with the slope level.
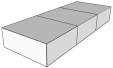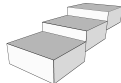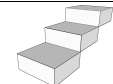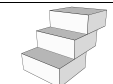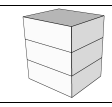
Table 8.21: Slope Building Design models' annual savings percentage according with slope integration

Slope Effect - Annual Savings (%) per Model

Models		Levels of Slope Integration					
		0°	10°	20°	30°	40°	50°
SlopeBD01		0.00	18.81	28.03	32.43	35.09	36.35
SlopeBD02		0.00	4.65	19.27	27.58	32.26	33.53
SlopeBD03		0.00	1.93	5.23	15.81	17.22	17.63
SlopeBD04		0.00	2.22	3.85	11.00	15.22	16.97
SlopeBD05		0.00	4.17	7.07	10.47	13.50	15.93
Average Savings % per Slope Integration		0.00	6.36	12.69	19.46	22.66	24.08
Average Increase Range %		0.00	6.36	6.33	6.77	3.2	1.42

The results in both Table 8.20 and Table 8.21 indicate that slope integration does improve the thermal performance of every model, and it is argued that the higher the slope, the better the models' results. The annual average savings can be of up to

24.08% with a 50° slope. From a null slope up to a 30° slope, for each 10° the average savings difference is around 6.5%. These values drop to 3.2% for 30° to 40° slope, and to 1.42% for 40° to 50° slope.

Table 8.22: Annual thermal performance comparison between all Slope Building Design models' design – for all slopes

Design Effect - Models' Annual Savings (%) per Slope Integration and Models Overall Performance

Models	Levels of Slope Integration						Overall Results		Scale*
	0°	10°	20°	30°	40°	50°	Average Savings*	Perfor.**	
SlopeBD01	0.00	14.92*ˢ	**21.96**	**17.52**	**19.42**	**20.59**	15.74	= 2	
SlopeBD02	1.27	1.36	13.58*ˢ	12.72	16.97*ˢ	18.12*ˢ	10.67	= 4	
SlopeBD03	2.69	0.00	0.00	0.00	0.00	0.00	0.45	= 5	1 to 5 → ↓
SlopeBD04	17.10	15.05*ˢ	13.57*ˢ	9.93	12.75	14.12	13.75	= 3	
SlopeBD05	**21.51**	**21.18**	20.92	14.23	15.72*ˢ	17.68*ˢ	18.54	= 1	

* Average annual savings % per model; ** Performance Scale 1 to 5 (1= Best performace & 5= Worst performance); *ˢ Equal or similar results.

The design effect produced by slope building designs can be observed in Table 8.22, which provides the annual savings value for each model, compared with each model's level of slope lintegration. The amend section design, which corresponds to Model SlopeBD 05, has the best performance, with an average annual savings of 18.54%. These values are followed by the single level Model SlopeBD 01, which reaches 15.74%, Model SlopeBD 04 with a cascade with connected units, which achives 13.75%, the spit level Model SlopeBD 02 that produces savings of 10.67%, and lastly the cascade design with independent unit, Model SlopeBD 03, which achives the worst results. However it should be noted that the performance pattern of each model is different for a null slope. In this case, all models with slope building design produce better results that the single level Model SlopeBD 01.

8.3.2.2. Seasonal Results
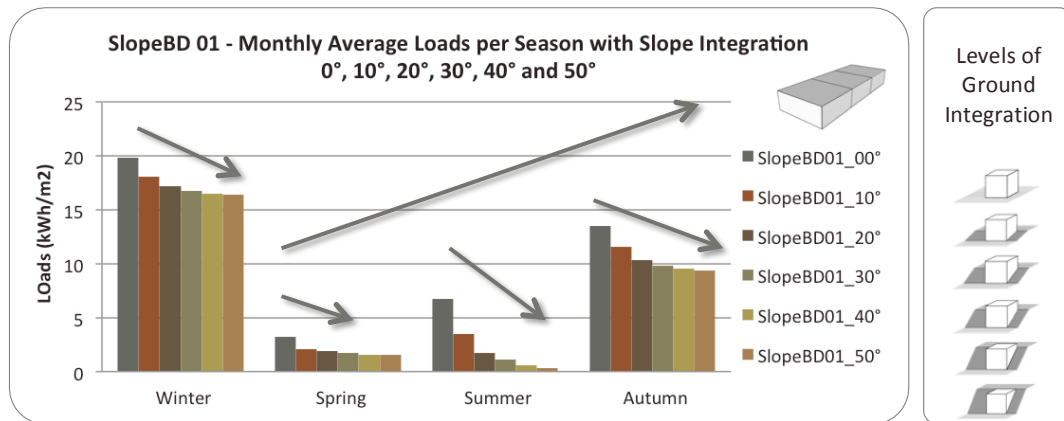
Figure 8.7: Slope effect on model' monthly average loads per season –SlopeBD 01

Looking at the seasonal results produced by Model SlopeBD 01 (Figure 8.7), a main pattern for all seasons can be observed: the steeper the slope the better the results of all models. It should be pointed out that greater results are found between 0° to 30° slopes. The results differences between 30° to 50° slopes are narrowed down in all seasons with almost identical results during winter and spring. This pattern is found in the performance of most models and is displayed in Table 8.23.
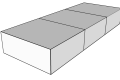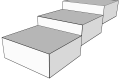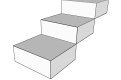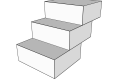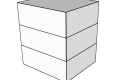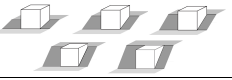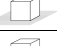
Table 8.23: Slope Building Design models' season thermal performance according with slope integration

Season Slope Effect - Models Season Results According with Slope Integration

	Season and Models		0° Slope	10° Slope	20° Slope	30° Slope	40° Slope	50° Slope
Winter	SlopeBD 01, 02 & 04		6	5	4	3**	2**	1**
	SlopeBD 03		6	5	4	1**	1**	3**
	SlopeBD 05		6	5	4	3**	1**	2**
Spring	SlopeBD 01& 02		6	5	4	3**	1**	1**
	SlopeBD03		6	5	4	3**	1**	2**
	SlopeBD 04 & 05		6	5	4	3**	2**	1**
	Summer – All models		6	5	4	3	2	1
Autumn	SlopeBD 01, 02, 04 & 05		6	5	4	3	2	1
	SlopeBD 03		6	5	4	3**	1**	2**
Scale*				← Scale 1 to 6 →				

* Performance Scale 1 to 6 (1= Best performance & 6= Worst performance); **Equal or very similar results.

The performance summary provided by the above table shows that models' results improve with slope increases for slopes from 0° to 30°. However during spring, autumn, and winter each model produces a distinct pattern with 30° to 50° slopes and, once more, the models results are similar. It should be emphasised that during these seasons, the difference between the results of most models is minimal, and consequently the thermal advantages of using steeper slopes such as 40° or 50° is reduced.

Table 8.24: Comparison between all Slope Building Design models' design – Seasonal loads

Models's Design Effect - Thermal Performance According with Seasonal Loads

Slope Integration			SlopeBD01	SlopeBD02	SlopeBD03	SlopeBD04	SlopeBD05
Winter	0°		5**	3**	3**	2	1
	10° to 50°		3	4	5	2	1
Spring	0°		4**	3**	5**	1	2
	10°		1	4	5	2	3
	20°		1	2	5	3	4
	30°		1	2	4**	3	5**
	40°		1**	1**	4**	3**	4**
	50°		1**	1**	5	3**	4**
Summer	0°		5	4	3	1	2
	10°		1	5	4	2	3
	20°		1	2	5	3**	4**
	30°		1	2	3	4	5
	40° & 50°		1**	1**	4	3	5
Autumn	0°		5	4	3	2	1
	10°		3	4	5	2	1
	20°		2	4	5	3	1
	30°, 40° & 50°		2**	4**	5	3**	1
Scale*			← Scale 1 to 5 →				

* Performance Scale 1 to 5 (1= Best performance & 5= Worst performance); **Similar results.

The complexity of these results increases when comparing the performance of all models according with slope degree. Looking into Table 8.24 and summarising the results of all models from best (1) to worst (5), it becomes evident that the

performance of these models varies between seasons. For all slopes, the single floor model without slope design (Model R SlopeBD 01) has a medium performance in winter, and achieves the best results in spring and summer with slopes of 10° to 50°. The split-level Model SlopeBD 02 produces the best results also during spring and summer with slopes of 40° and 50°. Therefore, both Model SlopeBD 01 and SlopeBD 02 can be used as part of a cooling strategy. Model SlopeBD 02 and SlopeBD 03 have poor results in winter and autumn.

The thermal performance of Model SlopeBD 04 is the most stable throughout the year. This cascade design with connected units also achieves the best results at spring and summer for 10° slopes. The performance of SlopeBD 05 is the most consistent throughout all seasons, as it produces the lowest energy need in winter and autumn. However its overall performance during spring and summer is moderate. If construction costs and issues are to be taken to account, this amended section design becomes the best slope building design choice.

8.3.3. Findings and Conclusions

This section demonstrates that slope integration can affect the thermal performance of building models. In general, the steeper the slope, the better the models' performances. The annual average savings can be of up to 24.08% with the highest slope. However it is found that between 0° to 30° slope for each 10° the average savings difference is approximately 6.5%, while for slope 30° to 50° the results difference is small. The average savings difference is of 3.2% for a 30° to 40° slope, and it falls to 1.42% between 40° and 50° slopes. For this reason, the use of 40° and 50° slopes might not bring many thermal benefits. When looking at the results produced in all seasons it is found that during spring, autumn, and winter and for slopes of between 30° and 50°, each model produces a distinct pattern and, again, all models produce similar results values.

Regarding the design effect produced by slope building designs the author found that the best design structure results is the amended section, Model SlopeBD 05, with average annual savings of 18.54%. The efficiency of this design is followed by the single floor Model SlopeBD 01 with 15.74%, the cascade with connected units Model SlopeBD 04 with 13.75%, the split-level Model SlopeBD 02 with 10.67% and, lastly, the cascade with independent units Model SlopeBD 03 with 0.45%. It is also found that for a 0° slope all models designed for slopes are more efficient than the model without a slope design.
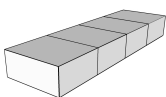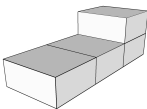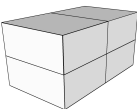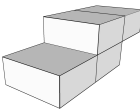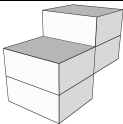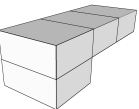
8.4. CONFIGURATIONS

This part of the study explores how different configurations perform against each other, and what patterns of thermal performance are produced when these configurations are simulated as integrated into slopes of different degrees of steepness. The numbers of building configurations are vast and dependent on creativity and project restrictions. Therefore, in this section, six design variations are studied in order to produce a sample of how different configurations designs for slope integration can impact the thermal performance of a building. The configurations are based on amend and cascade or step-hill sections.

8.4.1. Models Description and Levels of Slope Integration
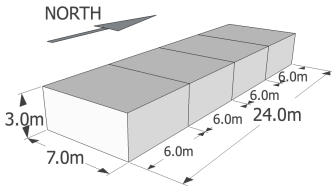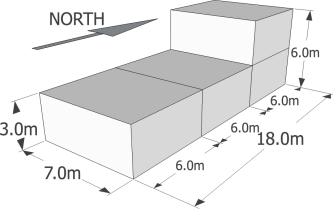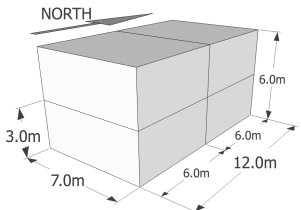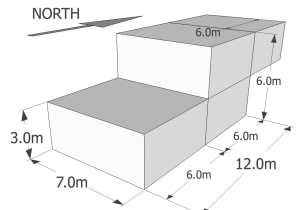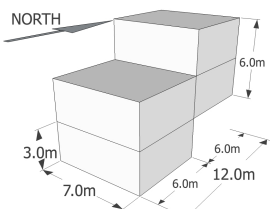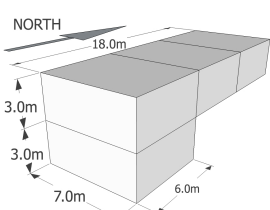
All six models' designs are variations of the single floor Model Confg 01. The models' configurations share the same unit number and area. The units are distributed along the models depth with distinctive positions, as provided in Table 8.25. The number of floors varies from a minimum of one to a maximum of three.

Table 8.25: Models characteristics – Configuration study

Model Name	Confg 01	Confg 02	Confg 03	Confg 04	Confg 05	Confg 06
Models						
Slope Building Desin Type	-	Amended Section	Amended Section	Cascade or Step-hill	Cascade or Step-hill	Cascade or Step-hill
Total Area (m^2)	168	168	168	168	168	168
Floor N.	1	2	2	2	3	2
Zone N.	4	4	4	4	4	4
Unit Area (m^2)	42	42	42	42	42	42
Unit Perimeter (m)	26	26	26	26	26	26
Ratio A/P	1.61	1.61	1.61	1.61	1.61	1.61

Details such as dimensions, level of slope integration, and use reference name for each simulation are displayed in Table 8.26.

Table 8.26: Models details – Configuration study

Models Dimensions	Slope Integration	Ref. Name
Configuration 01	0° Slope	Confg01_00°
	10° Slope	Confg01_10°
	20° Slope	Confg01_20°
	30° Slope	Confg01_30°
	40° Slope	Confg01_40°
	50° Slope	Confg01_50°
Configuration 02	0° Slope	Confg02_00°
	10° Slope	Confg02_10°
	20° Slope	Confg02_20°
	30° Slope	Confg02_30°
	40° Slope	Confg02_40°
	50° Slope	Confg02_50°
Configuration 03	0° Slope	Confg03_00°
	10° Slope	Confg03_10°
	20° Slope	Confg03_20°
	30° Slope	Confg03_30°
	40° Slope	Confg03_40°
	50° Slope	Confg03_50°
Configuration 04	0° Slope	Confg04_00°
	10° Slope	Confg04_10°
	20° Slope	Confg04_20°
	30° Slope	Confg04_30°
	40° Slope	Confg04_40°
	50° Slope	Confg04_50°
Configuration 05	0° Slope	Confg05_00°
	10° Slope	Confg05_10°
	20° Slope	Confg05_20°
	30° Slope	Confg05_30°
	40° Slope	Confg05_40°
	50° Slope	Confg05_50°
Configuration 06	0° Slope	Confg06_00°
	10° Slope	Confg06_10°
	20° Slope	Confg06_20°
	30° Slope	Confg06_30°
	40° Slope	Confg06_40°
	50° Slope	Confg06_50°

This particular case study considers six levels of slope integration, which range from a null slope (0°) up to a 50° slope, using intervals of 10°. The maximum wall depth for surfaces with direct ground contact is dependent on model design and slope

degree, and can go up to 8 m. Table 8.27 illustrates the models' slope integration levels used in this study.

Table 8.27: Level of slope integration – Configuration study with slope integration

Levels of Slope Integration	Side View → N	Plans N↑	Perspectives ⟋N	Maximum Walls Depth
0° Slope				0 m
10° Slope				
20° Slope				
30° Slope				Up to 8 m
40° Slope				
50° Slope				

8.4.2. Results Analysis

8.4.2.1. Annual Results
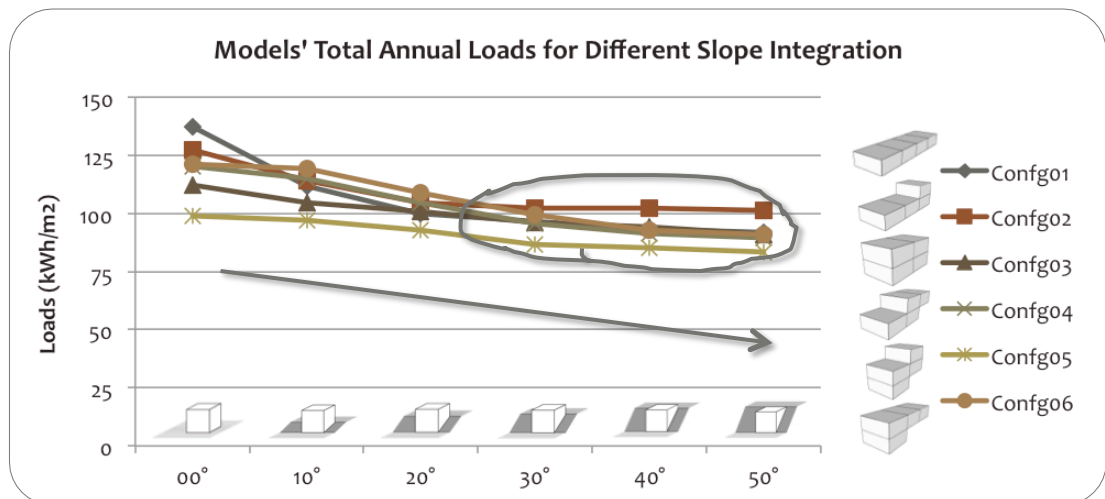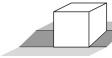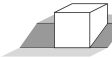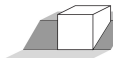
Figure 8.8: Slope effect on Configuration models' total annual load

The simulation results in Figure 8.8 and summarised in Table 8.28 show that for all configurations the higher the slope level the more efficient the annual thermal performance of each model. However, as observed in the previous studies presented, it is clear that between 30°, 40° and 50° slopes the results produced are similar.
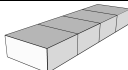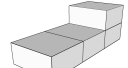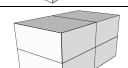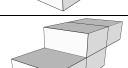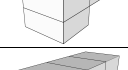
Table 8.28: Cofiguration models' annual thermal performance according with slope integration

Annual Slope Effect - Models Thermal Performance According with Slope Integration

0° Slope	10° Slope	20° Slope	30° Slope	40° Slope	50° Slope
6	5	4	3	2	1

← Scale 1 to 6 →

* Performance Scale 1 to 6 (1= Best performance & 6= Worst performance).

The annual saving percentages produced by the slope effect are displayed in Table 8.29. The highest savings are produced by a 50° slope, with an average value of 23.18%. However, the average range difference between slopes decreases when the slope level is increased.

Table 8.29: Configuration models' annual savings percentage according with slope integration
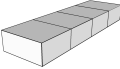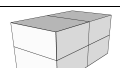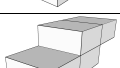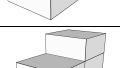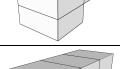
Slope Effect - Annual Savings (%) per Model

Models	Levels of Slope Integration					
	0°	10°	20°	30°	40°	50°
Confg 01	0.00	18.70	27.30	29.72	32.08	**33.27**
Confg 02	0.00	10.32	17.78	19.67	20.25	**20.60**
Confg 03	0.00	6.66	10.29	14.41	16.15	**18.94**
Confg 04	0.00	4.30	12.84	20.41	24.11	**25.52**
Confg 05	0.00	1.80	6.09	12.19	13.76	**15.62**
Confg 06	0.00	1.56	10.36	17.92	23.46	**25.15**
Average Savings % per Slope Integration	0.00	7.22	14.11	19.05	21.63	**23.18**
Average Increase Range %	0.00	**7.22**	6.89	4.94	2.58	1.55

It is visible that for a slope of between 0° and 10° the range of the average increase in thermal performance is 7.22%, which corresponds to the highest value, and between 40° and 50° slopes the thermal performance increases by only 1.55%, the lowest comparative increase. Therefore, all models benefit from any slope

integration, but the lowest slope levels produce the greater impact on the thermal performance of a model.

Table 8.30: Annual thermal performance comparison between all Configuration models' design – for all slopes

Design Effect - Models' Annual Savings (%) per Slope Integration and Models Overall Performance

Models		Levels of Slope Integration						Overall Results		Scale*
		0°	10°	20°	30°	40°	50°	Average Savings*	Perfor.**	
Confg 01		0.00	6.57	8.25	5.69	8.20	9.41	6.35	= 4	↑ 1 to 6 ↓
Confg 02		7.23	4.39	3.74	0.00	0.00	0.00	2.56	= 6	
Confg 03		**18.21**	**12.26**	**7.40**	6.07	7.30	9.99	10.21	= 2	
Confg 04		12.53	3.80	3.80	**6.59**	**10.28**	**11.57**	8.10	= 3	
Confg 05		**27.98**	**18.72**	**11.33**	**15.15**	**16.06**	**17.51**	17.79	**= 1**	
Confg 06		11.60	0.00	0.00	2.64	8.55	10.18	5.50	= 5	

* Average annual savings % per model; ** Performance Scale 1 to 6 (1= Best performace & 6= Worst performance).

The models' design effect can be compared by consulting Table 8.30. This table displays the average annual energy saving percentage per model for each level of slope integration. The table also presents the overall average savings percentage per model and the overall performance, which is displayed on a scale running from best (1) to worst (6).

By comparing these results, It is found that Model Conf 05 produces the best total annual loads with average savings of 17.79%. The results produced by this three floor design is followed by Models Confg 03 and Confg 04. Both these models share the same number of floors and similar results, with corresponding average savings of 10.21% and 8.10%. It can be observed that while Model Confg 03 produces better performances with shallower slopes (0° to 20°), Model Confg 04 achives the best performances with steeper slopes (30° to 50°).

The less efficient results are achieved by Model Confg 02, with 2.56%, and Model Confg 06, with 5.50%. It is relevant to point out that most configurations integrated into slopes of 30° to 50° produced similar results. This leads the author to argue that design effect is more relevant with shallower slopes then with higher ones.

8.4.2.2. Seasonal Results
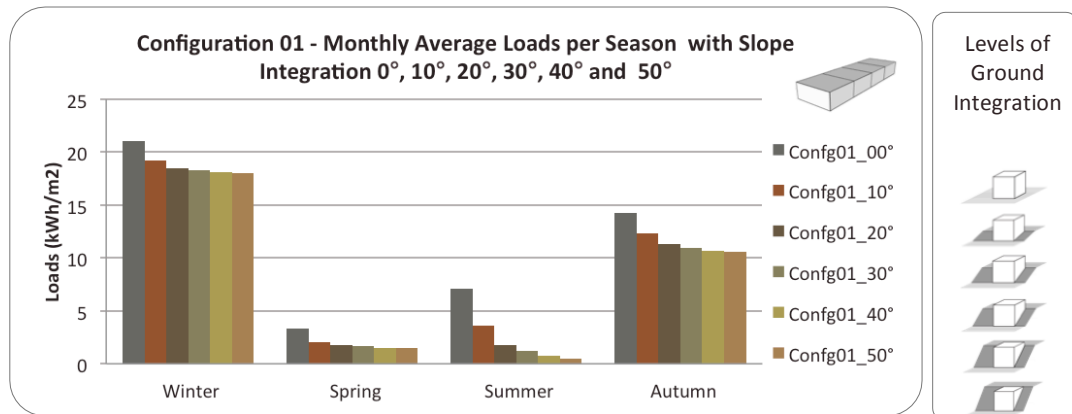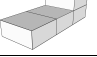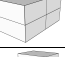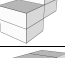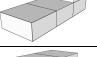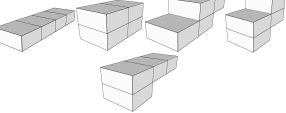
Figure 8.9: Slope effect on model' monthly average loads per season – Configuration 01

In Figure 8.9, the monthly average loads per season for Model Confg 01 show two main patterns, which are present with all models results. These patterns are summarised in Table 8.31.

Firstly, during summer and autumn, the thermal performance of all models improves when the slope degree is increased. The only exception to this pattern is Model Confg 02 during the autumn season. Therefore, during those seasons the higher the slope degree, the better the thermal performance of all models.

Secondly, during winter and spring the performance behaviour differs from model to model. In some cases, integration into a 20°, a 30° or a 40° slope produces the best results during winter. Consequently, the highest slopes might not provide the best thermal performance solution. Moreover, during both seasons, the models' results reinforced the annual findings, since between 30° and 50° slopes most results are similar, producing little or no improvement in thermal performances.

Table 8.31: Configuration models' season thermal performance according with slope integration

Season Slope Effect - Models Season Results According with Slope Integration

Season and Models			0° Slope	10° Slope	20° Slope	30° Slope	40° Slope	50° Slope
Winter	Confg01 & 04		6	5	4	3**	2**	1**
	Confg02		6	2	1	3**	4**	5**
	Confg03		6	3	1	2	4**	4**
	Confg05		6	5	4	1	2**	2**
	Confg06		6	5	4	3	1**	2**
Spring	Confg01, 04, 05 & 06		6	5	4**	3**	2**	1**
	Confg02		6	5	1**	2**	3**	3**
	Confg03		6	5	4	2**	2**	1**
Summer – All models			6	5	4	3	2	1
Autumn	Confg01, 03, 04, 05 & 06		6	5	4	3	2	1
	Confg02		6	5	4**	1**	2**	2**
Scale*			←		Scale 1 to 6		→	
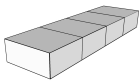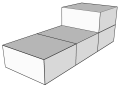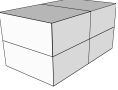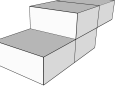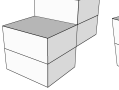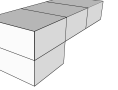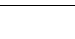
* Performance Scale 1 to 6 (1= Best performance & 6= Worst performance); **Equal or very similar results.

A good example of contrasting results of direct ground contact per season is Model Confg 01. In Table 8.32 it is possible to see that this model does not perform well during the coldest seasons – in actual fact it had the worst performance and winter but it achieved the best results during spring and summer. This is not just because of the model's design, but also because of the large ground integration surface area generated by its slope integration. For this climate a good balance between structural elements with direct ground contact and solar exposure is essential to produce a better thermal performance.

Comparing the results generated by Models Confg 03 and Confg 04 it is clear that the performance of Confg 03 is superior during winter and autumn, which makes it a better design to use as part of a heating strategy. Nonetheless, the results of Model

Confg 04 are more stable throughout the year. Regarding Model Confg 05, the model is able to produce the best results during winter and autumn. However, it is also noticed that during spring and summer Model Confg 05 also produces effective results with shallower slopes, such as those of 0° to 20°.

Table 8.32: Comparison between all Configuration models' design – Seasonal loads

Models's Design Effect - Thermal Performance According with Seasonal Loads

Slope Integration		Confg01	Confg02	Confg03	Confg04	Confg05	Confg06
Winter	0° & 20°	6	5	2	3	1	4
	10°	6	4	2	3	1	5
	30°	5	6	2	3	1	4
	40°	5	6	2	3	1	2
	50°	4	5	5	3	1	2
Spring	0°	6	5	2	4	1	3
	10°	1	4	3	5	2	6
	20°	1	2	6	3	3	5
	30°	1	5	3	2	4	5
	40°	1	5	4	2	3	3
	50°	1	5	5	2	4	3
Summer	0°	6	5	2	4	1	3
	10°	1	3	3	5	2	6
	20°	1	3	6	4	2	5
	30°	1	2	6	3	5	4
	40°	1	3	6	2	5	4
	50°	1	3	3	2	6	5
Autumn	0°	6	5	2	3	1	4
	10°	5	4	2	3	1	6
	20°	4	5	2	3	1	6
	30°	5	6	2	3	1	4
	40°	5	6	3**	2**	1	4
	50°	4	5	5	2	1	3
Scale*				Scale*			

* Performance Scale 1 to 6 (1= Best performance & 6= Worst performance); **Similar results.

8.4.3. Findings and Conclusion

It is found that the thermal performance of the models is affected by the degree of slope integration and that the average annual savings of these models can go up to

23.18% with integration into a 50° slope. The author therefore concluded that for all model designs the higher the ground integration of a model, the better its annual thermal performance.

It is also noted that the average increase range between slopes is greater between shallower slopes and decreases when slope degree increases. Therefore any level of slope integration produces energy savings, but the lowest slope levels produce a greater impact. For slopes of between 0° and 10°, the thermal performance of the models increases by 7.22%, while for 40° to 50° slope this value falls to 1.55%. This saving range decrease means that the results produced with integrations into slopes of between 30° and 50° are similar. The results produced by these slopes show that using the steepest slopes does not provide much advantage. The author therefore concluded that a 30° to 40° slope is preferable to a slope of 50°.

Regarding the design effect it is found that it is more relevant on the building thermal performance with shallower slope integrations then with steeper ones. This is because most configurations integrated on 30° to 50° slopes generate similar results. Model Confg 05 achieves the best annual thermal performance with average savings of 17.79%. This is followed by Model Confg 04 with 10.21% and Confg 03 with 8.10%.

The seasonal analysis shows that during summer and autumn the higher the slope degree the better is the models thermal performance, as during these seasons the steepness of the slopes into which they are integrated exerts a larger influence on a models performance. It is found that the influence of the design in the model thermal performance is higher with shallower slopes and important mainly during winter and spring. In winter and spring the behaviour of the results differ according with the model being studied. Furthermore, the steepest slopes did not always produce the

best results. In some models, shallower slopes such as 20°, 30° or 40° are more efficient, and integrations into 30°, 40° and 50° slopes produced similar values.

Model Confg 05 produces the best results during winter and autumn, and shows stable results in spring and summer with shallower slopes; the configuration of Model Confg 03 is a good design solution as part of a heating strategy, while Confg 04 proved to be the most stable model throughout the year. Model Confg 05 had the best annual results, but these results are closely related to its large number of floors. In order to access these results, this model is used in Section 8.5 where it is compared against models with the same number of floors.
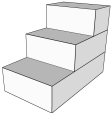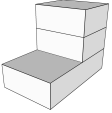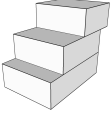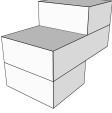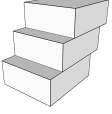
8.5. DIFFERENT CROSS SECTION STRUCTURES

Slope building designs such as cascade and amended sections can have many vertical cross section shapes. This section explores several vertical structures variations, in order to verify more closely how these two site integrations designs can affect buildings thermal performance.

8.5.1. Models Description and Levels of Slope Integration
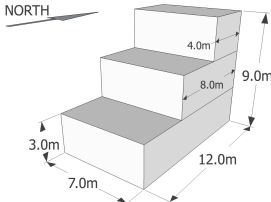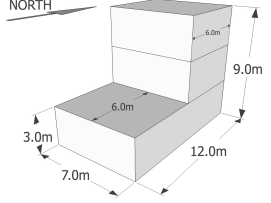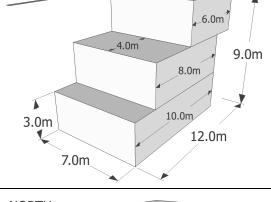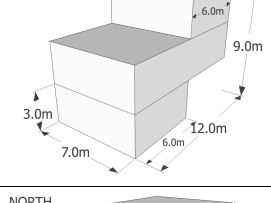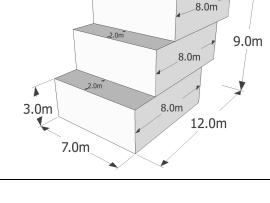
This section presents a case study that compares five cross section structure configurations. As presented in Table 8.33, the case study uses two amended section structures, Model CrossSec 01 and CrossSec 02, and three cascade sections as a Γ shape, a semi step-hill and a step-hill, which correspond to Model CrossSec 03, CrossSec 04 and CrossSec 05, respectively. Although the total area is kept the same, the unit area distribution between levels differs, and all models share the same number of floors.

Table 8.33: Models characteristics – Different cross section structure study

Model Name	Models	Slope Building Desin Type	Total Area (m²)	Floor N.	Zone N.	Unit Area (m²)	Unit Perimeter (m)	Ratio A/P
CrossSection01		Amended Section	168	3	3	28	22	1.27
						56	30	1.86
						84	38	2.21
CrossSection02		Amended Section	168	3	3	42	26	1.61
						42	26	1.61
						84	38	2.21
CrossSection03		Cascade; Γ Shape	168	3	3	42	26	1.61
						56	30	1.86
						70	34	2
CrossSection04		Cascade; semi-step hill	168	3	3	42	26	1.61
						84	38	2.21
						42	26	1.61
CrossSection05		Cascade; step hill	168	3	3	56	30	1.86
						56	30	1.86
						56	30	1.86

The models details such as dimensions, orientation, slope integration and reference name for each individual simulation are listed in Table 8.34.

Table 8.34: Models details – Different cross section structure study

Models Dimensions		Slope Integration	Ref. Name
Cross Section 01		0° Slope	CrossSec01_00°
		30° Slope	CrossSec01_30°
		40° Slope	CrossSec01_40°
		50° Slope	CrossSec01_50°
Cross Section 02		0° Slope	CrossSec02_00°
		30° Slope	CrossSec02_30°
		40° Slope	CrossSec02_40°
		50° Slope	CrossSec03_50°
Cross Section 03		0° Slope	CrossSec03_00°
		30° Slope	CrossSec03_30°
		40° Slope	CrossSec03_40°
		50° Slope	CrossSec03_50°
Cross Section 04		0° Slope	CrossSec04_00°
		30° Slope	CrossSec04_30°
		40° Slope	CrossSec04_40°
		50° Slope	CrossSec04_50°
Cross Section 05		0° Slope	CrossSec05_00°
		30° Slope	CrossSec05_30°
		40° Slope	CrossSec05_40°
		50° Slope	CrossSec05_50°

Although the case studies presented in Sections 8.3 and 8.4 show that the results produced by integration with slopes of between 30° to 50° are similar, the models slope designs for the case study of this section can be integrated into steeper slopes. For this reason the case study uses steep slopes of 30°, 40° and 50° and a null (0°) level of slope integration. With the null inclination the buildings are above the ground, with some north facing walls with direct ground contact. For all models the maximum wall depth can go up to 8 m and it is dependent on slope degree and the design of the model (Table 8.35).

Table 8.35: Level of slope integration – Cross Section Structure study with slope integration

Levels of Slope Integration	Side View N	Plans N	Perspectives N	Maximun Walls Depth
0° Slope				
30° Slope				8 m
40° Slope				
50° Slope				

8.5.2. Results Analysis

8.5.2.1. Annual Results
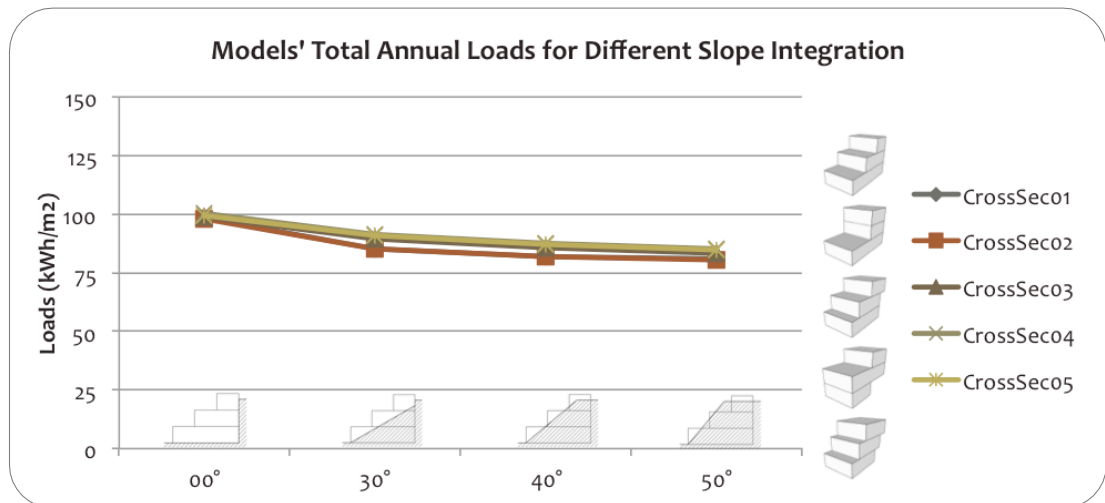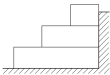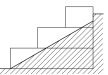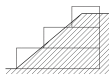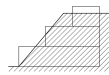
Figure 8.10: Slope effect on Cross Section Structure models' total annual load
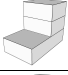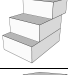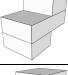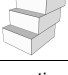
The analysis of the total annual loads results shows that all models are affected by slope integration. As can be seen in Figure 8.10, increasing the steepness of the slope generates an improvement of the models thermal performance, and therefore the highest slope (50° slope) generates the best thermal performances. This pattern was found with all cross section models results and it is summarised in Table 8.36, which use a performance scale running from best (1) to worst (4).

Table 8.36: Cross Section Structure models' annual thermal performance according with slope integration

Annual Slope Effect - Models Thermal Performance According with Slope Integration

0° Slope	30° Slope	40° Slope	50° Slope
4	3	2	1

← Scale 1 to 4 →

* Performance Scale 1 to 4 (1= Best performance & 4= Worst performance).

Regarding the annual saving potential produced by the slopes (show in Table 8.37), it is found that a 50° slope is able to generate average savings of 16.43%, a 40° slope generates 14.42% and a 30° slope produces 10.76%. Once again a pattern can be seen in these results in which the average increase in thermal performance is reduced when the slope degree increases. For slopes of between 30° to 40° the thermal performance improves by 3.66%, while from 40° to 50° the values increases by 2.01%. It is also noticed a second pattern in the differences in results generated by the amended sections Model CrossSec 01 and CrossSec 02 and the cascade Model CrossSec 03, CrossSec 04 and CrossSec 05. Each level of slope integration is able to produce a higher effect on the amended section models results compared with the cascade models.

Table 8.37: Cross Section Structure models' annual savings percentage according with slope integration

Slope Effect - Annual Savings (%) per Model

Models		Levels of Slope Integration			
		0°	30°	40°	50°
CrossSec 01		0.00	13.27	16.66	**17.79**
CrossSec 02		0.00	13.43	16.41	**18.25**
CrossSec 03		0.00	9.77	13.69	**15.95**
CrossSec 04		0.00	8.67	12.66	**15.14**
CrossSec 05		0.00	8.65	12.69	**15.03**
Average Savings % per Slope Integration		0.00	10.76	14.42	**16.43**
Average Increase Range %		0.00	10.76	3.66	2.01

Regarding the design effect, a comparison of the annual energy savings of each model is displayed in Table 8.38. These results once again show that both amended section designs (Model CrossSec 01 and CrossSec 02) are able to provide better thermal performances when compared to all cascade section designs (i.e. Model CrossSec 03, CrossSec 04 and CrossSec 05). For the cascade sections, the best shape is Γ, followed by the step-hill and lastly the semi step-hill.

Table 8.38: Annual thermal performance comparison between all Cross Section Structure models' design – for all slopes

Design Effect - Models' Annual Savings (%) per Slope Integration and Models Overall Performance

Models		Levels of Slope Integration				Overall Results		Scale*
		0°	30°	40°	50°	Average Savings*	Perfor.**	
CrossSec 01		1.73*ˢ	6.68*ˢ	6.23*ˢ	4.80*ˢ	4.86	= 2	↑ 1 to 5 ↓
CrossSec 02		2.06*ˢ	7.16*ˢ	6.27*ˢ	5.66*ˢ	5.29	**= 1**	
CrossSec 03		1.12*ˢ	2.31	2.29	2.08	1.95	= 3	
CrossSec 04		0.00*ˢ	0.00	0.00	0.00*ˢ	0.00	= 5	
CrossSec 05		0.69*ˢ	0.66	0.72	0.56*ˢ	0.65	= 4	

* Average annual savings % per model; ** Performance Scale 1 to 5 (1= Best performace & 5= Worst performance); *ˢ Equal or similar results.

The average savings difference between the amended section Model CrossSec 01 and CrossSec 02 is of 0.43%, thus reduced and almost identical with a 40° slope, As for Model CrossSec 02 and CrossSec 04, which correspond to the best and the worst structures, the average savings difference is of 5.29%, and this value decreases as slope angle increases. This leads the author to conclude that the higher the slope the less impact is provided by the cross section designs.

It is noted that Model CrossSec 04, which has the worst performance, corresponds to the best design presented in Chapter 8 Section 8.3 – that is Model Confg 05. This shows that the number of floors strongly affects the thermal potential of these models.

8.5.2.2. Seasonal Results
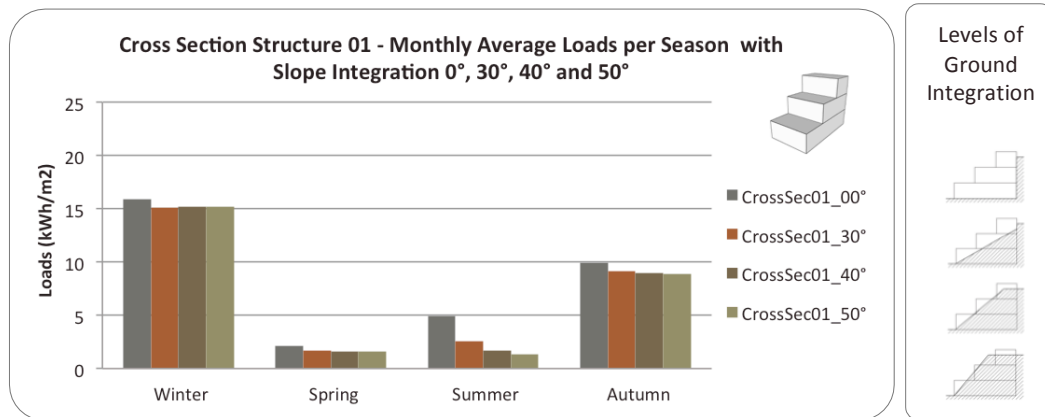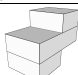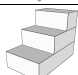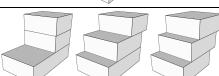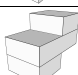
Figure 8.11: Slope effect on model' monthly average loads per season – Cross Section Structure 01

The seasonal results analysis indicates that the slope effect produces two main patterns. Firstly, the slope degree has a greater effect on the models' results during summer and autumn. It can be observed that for all models, the higher the angle of the slope the better the thermal performance of the model. This is observed in Model CrossSec 01, exemplified in Figure 8.11 and summarised in Table 8.39 according with all models' result performances ranked from best (1) to worst (4).
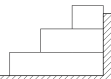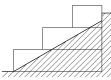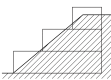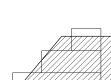
Secondly, during winter and spring, almost every model generated its own pattern of results. As can be seen in Table 8.39, it is not always the steepest slope that is able to produce the best performance. The author emphasise that apart from summer, when the results gap between different slope degrees is clearly visible, the difference between the results generated by slopes of 30°, 40°, and 50° is normally small. Thus, apart from summer, the advantage of using steeper slopes is minimal.

Table 8.39: Cross Section Structure models' season thermal performance according with slope integration

Season Slope Effect - Models Season Results According with Slope Integration

Season and Models		0° Slope	30° Slope	40° Slope	50° Slope
Winter	CrossSec 01	4	1**	2**	3**
	CrossSec 02	4	2**	3**	1**
	CrossSec 03 & 05	4	3**	1**	1**
	CrossSec 04	4	3**	2**	1**
Spring	CrossSec 01	4	3**	1**	2**
	CrossSec 02, 03 & 05	4**	3**	2**	1**
	CrossSec 04	4	3**	2**	1**
Summer/Autumn – All models		4	3	2**Aut	1**Aut
Scale*		← Scale 1 to 4 →			

- Performance Scale 1 to 4 (1= Best performance & 4= Worst performance);** Equal or similar results; **Aut Similar results at autumn.

Regarding the structural effect, Models CrossSec 01 and CrossSec 02 have the best seasonal results as can be observed in Table 8.40. While the amended Model CrossSec 01 achieves better performance during spring and summer, the amended Model CrossSec 02 achieves the best results during the coldest periods. This leads the author to conclude that Model CrossSec 01 is the best structure to use as part of a cooling strategy and that Model CrossSec 02 is an ideal slope building design to use as part of a heating strategy. Model CrossSec 03 achieves the most stable results with a medium performance.

Table 8.40: Comparison between all Cross Section Structure models' design – Seasonal loads

Models's Design Effect - Thermal Performance According with Seasonal Loads

Slope Integration		CrossSec01	CrossSec02	CrossSec03	CrossSec04	CrossSec05
0° Slope	Winter & Autumn	2	1	3	5	4
	Spring	1	2	3	5	4
	Summer	4	5	2	3	1
30° Slope	Winter & Autumn	2	1	3	5	4
	Spring & Summer	1	2	3	4	5
40° Slope	Winter	2	1	**3**	5	**3**
	Spring	1	2	3	4	5
	Summer	1	2	3	5	4
	Autumn	2	1	3	5	4
50° Slope	Winter	2	1	**3**	5	**3**
	Spring	1	2	3	4	5
	Summer	1	2	3	5	4
	Autumn	2	1	3	5	4
Scale*				← Scale 1 to 5 →		

Performance Scale 1 to 5 (1= Best performance & 5= Worst performance).

8.5.3. Findings and Conclusions

The annual results show that all models are affected by slope integration since the steeper the slope, the better the thermal performance of the model integrated into it. The author found that a 50° slope can produce average annual savings of 16.43%, a 40° slope produces 14.42% and a 30° slope is able to generate energy savings of 10.76%. It is also found that the steeper the slope the lower the impact of the slope on savings. This is because the average increase range is reduced as the slope angle increases. From a 30° to 40° slope the saving difference is 3.66%, and from a 40° to 50° slope it is reduced to 2.01%.

Querying how the vertical cross section, such as the amended and the cascade designs, affects the thermal performance of buildings it was found that the amended section models produced better results when compared with the cascade section models. The average annual savings difference between Models CrossSec 02 and

CrossSec 04, which correspond to the best and the worst models, is 5.29%, a number that only decreases as the slope angle increases. This leads the author to conclude that the impact provided by the cross section designs reduce as the angle of the slope increases. Regarding the annual performance of the different cascade designs, it was found that the best design is Model CrossSec 03 that has a Γ shape, followed by Model CrossSec 05 with a step-hill design and lastly, Model CrossSec 04 with a semi step-hill design.

The seasonal results show two main patterns produced by the slope effect. During summer and autumn the steepness of the slope has a greater effect on models results, since the steeper the slope the better the results. In winter and spring these patterns change according with model, and the steepnest slope does not always produce the best results. The differences between the results generated by integration into 30°, 40°, and 50° slopes are normally small, except in summer, reducing the advantage of using steeper slopes. The performance of Model CrossSec 01 is better during spring and summer and the results produced by CrossSec 02 are better during winter and autumn.

8.6. CONCLUSIONS

This chapter analysed the energy saving potential of slope-integrated buildings by observing the effect produced by slopes and building design. Regarding the slope parameter, all case studies show that the thermal performance of these buildings can benefit from integration into slopes off all degrees of steepness. In general, it was found that the steeper the slope, the higher the energy savings produced through integration into it. However, it was also evident that the average saving potential produced by slopes decreases as the angle of the slope increases, which means that shallower slopes have greater savings impact. For all studies, building design can affect the thermal performance of these models. However, its impact decreases as the steepness of that slope increases. Therefore, a greater attention to building design is essential with shallower slope-integrations.

According to the Form study, the average annual saving potential of shallow slopes of 5° to 10° is around 6% and 12% each, and for a 20° slope, this saving is of 24.31%. Regarding the design performance, the two best shapes are Model F03 and F02, with average annual savings of 16.32% and 14.53% respectively. Through the analysis of these seasonal results, it is clear that Model F03 has the best results during winter and autumn, and Model F02 is the best shape for spring and summer. Therefore Model F03 is the best design for a heating strategy, while Model F02 is the best design as part of a cooling strategy.

The results from the Split Level study, which uses slopes of up to 20°, show that the highest slope generates an average increase in annual energy savings of 25.61%. Between 0° to 10° the average annual savings amplitude value is 7.51%, while between 15° to 20° the value is reduced to 3.54%, indicating that the saving potential amplitude decreases as the angle of the slope increases. Regarding the effect produced by a slope building design as split-levels, for slope integrations of

between 0° and 20° it is clear that the split-levels quantity can affect the thermal performances of buildings, since the higher the number of split-levels the worse the performance of the model. The average annual savings difference between the best and the worst models, corresponding to Model SL01 and SL05, is 14.13%. Overall, the author concluded that split-levels slope design should be used cautiously and in a small number of levels. However, the position of the split-level within the building layout was proved to be irrelevant to the thermal performance of the models.

The Slope Building Designs case study shows that the annual average savings can be up to 24.08% with the steepest slope of 50°. For slopes of between 0° and 30°, each 10° increase corresponds to an average saving of approximately 6.5%. However for slopes of between 30° and 40° the different in results is 3.2% and it falls further to only 1.42% for 40° and 50° slopes. This indicates that the use of 40° and 50° slopes might not provide a better thermal benefit than a 30° slope. Considering the effect generated by slope building designs it is found that the best design structure results is achieved by the amended section. The coresponding Model SlopeBD 05 produces average annual savings of 18.54%, when compared with the less effective designs. This value indicates how relevant a slope building design can be to the thermal performance of a building.

Concerning the Configuration case study, the slope effect analysis indicate that all studied inclinations produce an increase of average annual savings, which can go up to 23.18% with a 50° slope. However, the lowest slope levels produce greater impacts. This is because the average increase range between slopes is greater between shallower slopes and decreases when slope degree increases. Between 0° and 10° slopes the range is 7.22%, while for 40° to 50° slopes the value is 1.55%, and integrations between 30° to 50° slope generate similar results. This calculation leads the author to the conclusion that a 30° to 40° slope is preferable to 50° slope.

With regard to design effect, similar results are found on most configurations integrated into slopes of between 30° and 50°. This leads the author to conclude that design effects have a greater relevance for the thermal performance of buildings with shallower slope integrations than those with higher ones. The best annual thermal performance is produced by Model Confg 05, with average annual savings of 17.79% when compared to the less effective performances. The results of this design are followed by Model Confg 03 and Confg 04, with 10.21% and 8.10% respectively. Model Confg 05, which has the highest number of floors produces the best annual results, with a superior performance during winter and autumn. Model Confg 03 is a good design solution as part of a heating strategy and Confg 04 proved to be more stable throughout the year.

Through the analysis of these seasonal results, it is clear that during summer and autumn the models thermal performance is highly affected by the slope whereas during winter and spring, the building design has a greater impact on the thermal performances of the models with shallower slope integrations. In winter and spring it is also found that the best results do not always correspond to the steepest slopes. In some models, shallower slopes such as 20°, 30° or 40° are more effective, and slopes integrations with 30°, 40° and 50° generate similar results.

The Cross Sections Structure case study shows that a 50° slope is able to generate annual average saving of 16.43%, while a 40° slope produces 14.42%, and a 30° slope 10.76%. As in previous case studies, it is found that steeper the slope the lower the energy saving potential increase. Between 30° to 40° slopes the saving range is 3.66%, and in 40° to 50° slopes the saving range is 2.01%.

Regarding the thermal performance difference between a vertical cross section as the amended and the cascade designs, it is observable that the amended section models produce superior performances. However the author would also point out

that the average annual savings difference between the best and worst designs, which correspond Models CrossSec 02 and CrossSec 04, is of only 5.29%, and this value decreases with the steepest. Therefore, the difference between amended and the cascade designs is small and it becomes even less significant when the slope increases.

Lastly, the results of the seasonal analysis show that two patterns are generated. Firstly, during summer and autumn, the steeper the slope, the better the thermal performance of the models and, consequently, the slope degree has a greater effect on models results. Secondly, in winter and spring, the patterns of results change according with the model and the steepest slopes do not always produce the best results. During winter, spring and autumn the results difference produced by 30° to 50° slopes is small, something which decreases the advantage of steeper slopes-integrations. The model CrossSec 01 performance is better during spring and summer, while CrossSec 02 is better in winter and autumn.

-260-

CHAPTER 9. CONCLUSIONS AND FURTHER WORK

9. CONCLUSIONS AND FURTHER WORK

Far from being a new way to control building thermal comfort, ground integrated buildings on slope terrains are a long established part of vernacular architecture. Examples of urban areas built on hillsides or mountains can be traced all around the globe and are one of the earliest settlement configurations, as the case of Mardin (Turkey), Alicante (Spain), Santorini (Greece) and Matera (Italy). In most cases, the buildings in these settlements are not just constructed over the inclined surface but also explore the below ground areas of the site by incorporating part of their buildings into the ground. The advantages of ground-integrated buildings are also well known. The energy benefits generated by these constructions have been researched since the 1970s. However, only a limited number of studies have focused on ground-integrated buildings on slope terrains.

The particular importance of ground-integrated buildings on slopes is due to three factors. Firstly, the thermal benefits produced by the actual site are a crucial advantage compared to buildings constructed on flat terrain. It is well known that topography affects the climate near the ground and, as a consequence of that, climate also affects the thermal potential of the ground. In temperate climates, buildings constructed on hillsides or mountains can benefit from a more moderate climate than buildings constructed on flat or valley sites. Sites on flat land or in valleys are typically subject to higher air temperature amplitudes than those on hillsides and, therefore, the heating and cooling demands of buildings constructed in these locations tend to be higher. Secondly, ground integrated buildings have been

identified as ideal to construct on sharply inclined sites. These integrated buildings on slopes reduce or even eliminate the risk of flooding, provide better ventilation and can offer better view and light access compared to ground integrated buildings constructed on a flat site. Thirdly, ground integrated buildings on slopes contribute to the efficient use of the available land. The relevance of slope-integrated buildings for efficient land use strategies is growing considerably due to two well-known and linked factors, the growth of both global and urban populations. On average a flat settlement occupies twice the area of a slope settlement with the same characteristics. Higher construction density can be achieved in slope terrains without compromising solar access and external view.

The rising world population and the increasing tendency of that population to live in urban areas are both contributing to a rapid growth in urban settlements all around the globe. The higher demand for construction land and urban infrastructure is leading to the appropriation of agricultural land. This practice also intensifies forecasted food shortages due to the growing global population. Considering this issue, the use of underground areas for construction its one approach that can contribute to more efficient land use. Another relevant approach is to construct in hillside sites, as these sites are significantly less suitable for farming.

This thesis explores both approaches in two distinct ways. Firstly, it looks into the ground thermal effect produced on buildings with direct ground contact, focusing on how buildings are affected by ground integration and terrain inclination. Secondly, this study examines the thermal effect produced by building design, looking at aspects such as construction shape, number of floors, basements, and courtyards and finally slope building designs, particularly the case of *spilt level*, *amended section* and *cascade* or *step-hill* designs.

This research elucidates on the thermal benefits of ground-integrated buildings on slope terrains and this was accomplished by fulfilling the thesis objectives. Initially, through the literature review on ground thermal energy, the advantages and

disadvantages of ground-integrated architecture and the benefits of slope-integrated architecture it was identified a lack of knowledge on how terrain inclination affects the ground thermal potential. Furthermore, it also was demonstrate how building design can enhance the thermal performance of ground-integrated architecture.

Consequently, the ground thermal potential on slope terrains was investigated. Firstly, the ground thermal potential in Portugal was verified through the study of the ground temperature at different depths. This was done by using a mathematical model. Secondly, it was demonstrated that terrain inclination affects ground temperatures. It was verified how the received annual and seasonal solar radiation values at Lisbon are affected by terrain inclination. It was also demonstrated that all terrain inclination produce greater ground thermal potential than a flat terrain.

Thereafter, through comparing three building thermal simulation packages, E+ was identified as the simulation tool for investigating ground heat transfer. However it was raised the issue that E+ lacks of input parameters such as terrain inclination and orientation. Consequently, the comparison between ground-integrated models and slope-integrated models should be avoided. Therefore the parametric case studies were divided between ground integration and slope integration, and the designs were based on the finding from the literature review and Portuguese' average building topology retrieved from statistic data.

Lastly, the thermal saving potential produced by ground-integration and building design was identified, and these findings were therefore used to produce the energy efficiency design guidelines provided in this chapter.

9.1. SUMMARY OF THE GROUND THERMAL POTENTIAL AND THERMAL SIMULATION OF GROUND CONTACT STUDIES

Ground integrated buildings benefit from ground heating and cooling through direct contact. This is based on the heat transfers produced between ground and building surfaces. The ground thermal potential is dependent on the temperature difference between the ambient air temperature and the ground temperature at a specific depth. The ground temperature values are determined by location characteristics such as nearby elements and topography in particular altitude, and slope degree and orientation. This relation is also affected by the type of soils present on the site and external factors such as climate conditions, and in particular air temperature and the received solar radiation values.

9.1.1. Ground Thermal Potential

The diversity of Portugal's temperate climates offers a relevant case study to identify ground thermal patterns caused by a particular type of temperate climate. Therefore, the ground thermal potential in Portugal's mainland was examined by calculating the ground temperatures at six locations and by verifying the impact of different soil types. It is found that all locations can benefit from ground thermal potential. Three main ground thermal areas are identified in the course of this research.

The first area includes Oporto and Coimbra and corresponds to the north and centre-north littoral regions of Portugal. This area shows great heating potential but limited cooling potential. This zone has the highest annual precipitation values and has a moderate annual average daily air temperature. The second area includes Bragança and Évora and corresponds to the north and centre interior of the country, which is the area with the greatest ground thermal potential either for heating or cooling. This result is due in large part to the combination of three interrelated factors. Firstly, the greater contrast between the annual air temperature values, with

very cold winters and very hot summers; secondly, the moderate to high annual solar radiation values; and thirdly, the low to moderate annual precipitation values. Lastly, the third ground thermal area identified in this thesis includes Lisbon and Faro and corresponds to the centre-south and south littoral regions of Portugal. This area shows good ground heating potential for both locations; however the ground cooling potential at Lisbon is good, while at Faro it is moderate, something that results from its considerably milder winters.

The impact of soil type on ground thermal potential was found to be of minimal relevance in locations such as Oporto and Coimbra, which are areas with higher annual precipitation. In locations with lower annual precipitation such as Lisbon, Évora and Faro, the soil type has a much larger impact on the ground thermal potential. For these three locations, sandstone-based soils presented the worst ground thermal potential, while heavy clay produced the best thermal results.

9.1.2. Ground Thermal Potential of Slope Terrains

Ground temperatures are largely dependent on topographical characteristics such as slope degree and orientation. It is generally assumed that the ground thermal potential provided by flat and slope terrain are different. To demonstrate this last observation this research project presents two studies that were based on the effect produced by changing a single parameter, more specifically the solar radiation values received according with terrain inclination.

Initially, the annual and seasonal solar radiation received by slopes between 0° to 60° in Lisbon were analysed. As expected, the results show that all inclined surfaces receive higher annual solar radiation than the flat surface, and the maximum solar radiation values were received by a 35° slope. Concerning the seasonal patterns, during winter and autumn, the highest slopes receive the greater amounts of solar

radiation, while the low and medium low slopes recorded the highest values during spring and summer.

Subsequently, the ground temperatures below different terrain inclinations in Lisbon were calculated by using the correspondent received solar radiation values. Firstly it is observed that ground temperatures under slope terrains are different from those below a flat area. Secondly, the study demonstrates that a slope terrain affects the ground temperature of the areas immediately before and after the slope, and therefore generates a transitional zone. It was found that all terrain inclinations generate greater annual ground thermal potential than flat terrains. Finally, it is concluded that 30° to 40° slopes have the optimal inclinations, and therefore provide the best annual ground thermal potential. This finding can be applied in other locations. As rule of thumb, the terrain inclinations with the greatest annual ground thermal potential are close to the latitude of the place.

Regarding the seasonal patterns results, in January all slope terrains produce higher heating potential than flat terrains, and the best heating potential is generated by 30° and 40° slopes. During April, the best ground thermal potential is provided by slopes of between 10° to 40°. In July, the flat terrain has greater cooling potential because it generates the lowest ground temperatures. Nevertheless, firstly, all terrain inclinations can provide good thermal benefits, and secondly, the higher ground temperatures under the slopes show a greater potential of energy storage, essential at this location for using during autumn and winter as heating sources for ground integrated buildings, when the energy demand is higher. During October, the greatest heating potential is provided by a 40° slope.

9.1.3. Summary of the Thermal Simulation of Ground Contact

The studies conducted to establish the software and methodology to use for thermal simulation of ground contact leads to the conclusion that E+ is the most suitable tool

for this research, particularly when compared with other software applications such as Ecotect and Tas. Regarding the ground heat transfer of slope integrated buildings, it was verified that the E+ Basement auxiliary program lacks input parameters such as terrain inclination and orientation. This fact does not reduce its ability to be used as a tool to simulate the thermal performance of buildings with direct ground contact. However, result comparison between ground integration on flat and slope terrains should be avoided. As a consequence, the case studies presented in this study were divided in to ground integration and slope integration, which are analysed in Chapter 7 and Chapter 8, respectively.

9.2. CONCLUSIONS FROM THE GROUND INTEGRATION STUDIES

9.2.1. Ground Integration Studies

The ground integration studies examine the impact of direct ground contact on the thermal performance of buildings. This is done through the analysis of the annual and seasonal results produced by the different levels of ground integration. These studies also inspect the effect produced by the models' design features, and are divided in three sections: Forms, Floors and Basement and Courtyard.

For all three studies, the analysis of the impact of ground integration shows that for this climate, the higher the level of ground integration the better the annual thermal performance of the models. However, the highest ground integration fails to provide the best annual results, showing that during the coldest seasons some source of solar gain is necessary.

Regarding the design impact, the simulations from the Form section of this research have confirmed that the precise configuration of a building affects its thermal performance. The best building shapes for this climate are found to be the compact model and the long model with an East-West axis. Compared with the worst performance, which was delivered by the courtyard model, the compact model can generate average annual energy savings of 14.14%, and the long model provides savings of 13.30%. The main difference between the two forms is that the long form has higher benefits as part of a cooling strategy; while the compact form has a more stable thermal performance throughout the whole year.

The Floor study analysis shows that the ground thermal impact is higher for models with the lowest number of floors, which is caused by a higher surface area with direct ground contact. Concerning the designs impact, the simulation results demonstrate that average annual saving difference varies depending upon the number of floors, with the compact models saving up to 18.36% and the long form

saving up to 13.77%. These values were achieved by the two-floor models. The annual savings provided by both compact and long three-floor models follow these values. It is verified that for buildings with an equal number of floors, the compacted shapes models are able to provide superior results when compared with the longer shapes.

Regarding the Basement and Courtyard study, the results indicate that the ground coupling produced by a basement floor improved the thermal performance of models. Concerning the models designs impact it is found that an underground courtyard area located on the south-facing facade improves the average annual thermal performance by 26.09% for the compact models, and up to 30.28% for the long models. It is also found that the courtyard size affects the models performances, as the best results were achieved with the models with the smallest courtyards.

9.2.2. Slope Integration Studies

The study of ground-integrated buildings on slope terrains is based on the analysis of the thermal impact generated by slope integration and also by building design. The study is divided on five sections: Forms, Split Level, Slope Building Designs, Configuration and Cross Sections Structure.

Regarding the slope impact, it is found that slope steepness affects the thermal performance of buildings. For all studies it is verified that the steeper the slope the better the model's annual thermal performance. In the case of the Split Level, Slope Building Designs, and Configuration studies, the steepest slopes produced annual saving potential of around 23% to 25%. In the case of the Cross Sections Structure the value is around 16%. However it is noted that the average annual saving potential produced by a slope, decreases as the slope angle increases. For example, in the case of the Slope Building Designs, the study shows that between

0° and 30° slope the average savings is approximately 6.5% for each 10° increase. While the savings increase produced by increasing the steepness of the slope from 30° to 50°, is 3.2% for 30° to 40° and actually increases only 1.42% when increasingly the angle from 40° to 50°. This demonstrates that the saving potential range falls when the steepness of the slope increases. Therefore the thermal benefits provided by slopes of 40° and 50° might not be much greater that provided by a 30° slope.

Regarding the design effect, the Form case study simulation analysis indicates that the best forms are the compact model and the long model with South-North axis, which are able to provide average annual savings of 16.32% and 14.53% respectively. The compact model provides the best results during autumn and winter, and therefore is the ideal shape for a heating strategy. On the other hand, the long model is ideal for a cooling strategy, since its performance is superior during spring and summer.

Concerning the impact generated by a slope building design features such as split-levels, the simulation results show that the split-levels quantity affects buildings' thermal performance. The models' performance declines as the number of split-levels increases. The average annual savings difference between the best and worst models is 14.13%. The best results are generated with Model SL01 with no split-levels and the worst results were produced by Model SL05 (with the highest number of split-levels). Therefore, slope design features such as split-levels should be used carefully and designs featuring a large number of levels should be avoided. The location of the split-level within the building layout was found to be irrelevant to the models performance.

According to the Slope Building Designs study the design impact is found to be relevant for a building's thermal performance. The best structure is found to be the

amended section, which generates average annual savings of 18.54%, when compared with the cascade design with an independent unit, which provided the worst results.

The results from the Configuration study show that building design can improve models' average annual savings by up to 17.79%. It is found that most configurations have similar results for slope integration when they are built into slopes of between 30° to 50°. Therefore a parameter such as building design has higher relevance for slopes shallower than 30°. It became clear with the seasonal results analysis that in winter and spring the models configuration has a higher influence on models' results, while in summer and autumn the slope impact on models performance is higher.

The Cross Sections Structure case study shows that slope building design can improve models' annual average savings. The amended section models have superior performance in comparison with the cascade designs. However the design comparison shows that the maximum average annual savings difference between models is just 5.29% and it grows less significant as the steepness of the slope increases. The seasonal results analysis shows that in summer and autumn slopes have a greater impact on models' results than models' design, while during winter and spring, the results differ according with model and the best results are not always registered in the highest slopes.

9.2.3. Overall Conclusions

The simulations conducted as part of the research for this thesis have shown that ground integration affects buildings thermal performance. In general, the thermal performances of these buildings can be improved by increasing the amount of the buildings' surface area with direct ground contact. However, total ground integration of these structures fails to provide the best results, showing that in this particular

climate, solar gains have a relevant impact on the thermal performance of a building, at least during the periods with heating needs. Consequently, to achieve a greater thermal efficiency a good balance is needed between surface areas with direct ground contact and those with solar exposure.

Concerning the levels of slope integration, the five studies featured in this thesis show that all slopes of all angles are able to improve the models' thermal performances. Overall, the steeper the slope the building is constructed into, the greater the average annual savings. However, it is also noted that the average annual saving potential difference between slopes decreases as the steepness of the slope increases. For this reason, between steeper slopes, such as those of between 30° and 50°, the thermal advantages achieved are small. It was concluded that the best annual energy saving potential is achieved with terrain inclinations between 30° to 40°. This finding is particularly relevant, as it means that it can be applied in other locations. As rule of thumb, the best terrain inclinations are close to the latitude of the place. Regarding design impact, for all studies it is found that design affects models' thermal performance. It is also confirmed that design influence decreases as the steepness of the slope increases. Consequently, for shallower slope-integrations a greater attention to building design is needed.

The author therefore conclude that newly-built constructions on hillsides can benefit from the thermal potential provided by slope terrains and also slope building designs. In temperate climates, ground-integrated buildings on slopes terrains reduce the buildings' energy demands for heating and cooling, and therefore mitigate the impact of the built environment on climate change. As design guidelines, the author presents the energy saving potential results provide by ground integration and building design.

9.3. RESULS SUMMARY FOR DESIGN GUIDELINES

Table 9.1: Design guidelines – ground integration and building design

FLOOR STUDY – Compact Form Models

FLOOR STUDY – Long Form Models

FORM STUDY

BASEMENT AND COURTYARD STUDY

Table 9.2: Design guidelines – slope ground integration and slope building design

FORM STUDY (Slope)

	Levels of Slope Integration	0°	5°	10°	15°	20°
Slope Effect — Annual	Thermal Performance	Worst	←	↓	↑	Best
	Average Savings	0.00%	5.96%	11.73%	18.72%	24.31%
	Seasonal Thermal Performance	← The same pattern as the annual thermal performance: for all seasons, higher the level of slope integration better the models thermal performance →				
Design Effect — Annual	Models					
	Thermal Performance	Worst	←	↓	↑	Best
	Average Savings	0.92%	2.02%	7.92%	14.53%	16.32%
	Seasonal Thermal performance	Better at spring and summer; good to be part of a cooling strategy; mix performance at winter and autumn			More efficient at winter and autumn; ideal shape for a heating strategy. Second best results at spring and summer	

SLOPE BUILDING DESIGN STUDY

	Levels of Slope Integration	0°	10°	20°	30°	40°	50°
Slope Effect — Annual	Thermal Performance	Worst	←	↓	↑		Best
	Average Savings	0.00%	6.36%	12.69%	19.46%	22.66%	24.08%
	Seasonal Thermal Performance	Higher the level of slope integration better the models' thermal performance →					
Design Effect — Annual	Models						
	Thermal Performance	Worst	←	↓	↑		Best
	Average Savings	0.45%	10.67%	13.75%	15.74%		18.54%
	Seasonal Thermal Performance	Stable performance during all seasons and with all levels of ground integration	More efficient at spring and summer; ideal shape for a cooling strategy. Weak performance at winter		Best results at winter and autumn; ideal shape for a heating strategy. Weak results at winter		

30° sets a turning point. Except for summer, for slopes between 30° to 50° not always the highest slope produce the best results and overall the results are very similar. Therefore, slopes higher than 30° might not bring much thermal benefit, and the highest slopes are better for a cooling strategy

DIFFERENT CROSS SECTIONS STUDY

	Levels of Slope Integration	0°	30°	40°	50°
Slope Effect — Annual	Thermal Performance	Worst	←	↑	Best
	Average Savings	0.00%	10.76%	14.42%	16.43%
	Seasonal Thermal Performance	← The results are very similar, excepted for summer and autumn not always the highest slope produce the best result →			
Design Effect — Annual	Models				
	Thermal Performance	Worst	←	↓	↑	Best
	Average Savings	0.00%	0.65%	1.95%	4.86%	5.29%
	Seasonal Thermal Performance	Stable performance during all seasons with all levels of slope integration	More efficient at spring and summer; ideal shape for a cooling strategy		Best results at winter and autumn; ideal shape for a heating strategy	

← The average saving difference between slopes is small and becomes less significant as the slope increase →

SPLIT LEVEL STUDY

	Levels of Slope Integration	0°	5°	10°	15°	20°
Slope Effect — Annual	Thermal Performance	Worst	←	↓	↑	Best
	Average Savings	0.00%	7.51%	13.97%	22.07%	25.61%
	Seasonal Thermal Performance	Worst at all seasons				Achieves the best results at all seasons
Design Effect — Annual	Models					
	Thermal Performance	Worst	←	↓	↑	Best
	Average Savings	0.79%	3.42%	3.79%	3.90%	14.13%
	Seasonal Thermal Performance	The higher the number of split levels the worst the models' thermal performance →				Best results at all seasons

← Similar or equal results with an irregular pattern; the location of the split level is found to be irrelevant for the models' thermal performance →

CONFIGURATION STUDY

	Levels of Slope Integration	0°	10°	20°	30°	40°	50°
Slope Effect — Annual	Thermal Performance	Worst	←	↓	↑		Best
	Average Savings	0.00%	7.22%	14.11%	19.05%	21.63%	23.18%
	Seasonal Thermal Performance	Higher the level of slope integration better the models' thermal performance →					
Design Effect — Annual	Models						
	Thermal Performance	Worst	←	↓	↑		Best
	Average Savings	2.56%	5.50%	6.35%	8.10% *	10.21% *	17.79%
	Seasonal Thermal Performance	Better at spring and summer; good for a cooling strategy. Weak at winter and autumn	Stable performance during all seasons with most levels of ground integration		Best results at winter and autumn; ideal shape for a heating strategy		

30° sets a turning point. Except for summer and autumn; slopes between 30° to 50° produce very similar results and not always the greater slope produce the best result

* The cascade model perform better with shallower slopes (0° - 20°) and the compact model produce better results with steeper slopes (30° - 50°)

9.4. RECOMMENDATIONS FOR FUTHER RESEARCH

This research could be expanded in the future by exploring some of the areas left out by the study. These include:

- Further research of the ground thermal potential patterns under slope terrains, by undertaking long term ground temperature measurements at different depths under different slope terrains;

- Undertaking long-term data collection of slope integrated buildings, for validation of the simulations of buildings' ground heat transfer;

- Undertaking long-term data collection of correspondent site weather data to produce weather files to be used on the thermal simulation of buildings;

- For different climates, the use of terrain inclination should be studied in order to optimise the heating and/or cooling efficiency of EAHE systems;

- Lastly, the study on the adding of underground south facing courtyards has shown that this is a good design solution to improve the thermal performance of buildings. Further research on this subject could be done, by looking into the benefits that this feature could bring, particularly regarding the heating and cooling potential of natural ventilation.

REFERENCES

REFERENCES

ADJALI, M. H., DAVIES, M. & LITTLER, J., 1998. Three-dimensional earth-contact heat flows: A comparison of simulated and measured data for buried structure. *Renewable Energy,* 15 (1-4), 356-359.

AL-AJMI, F., LOVEDAY, D. L. & HANBY, V. I., 2006. The cooling potential of earth–air heat exchangers for domestic buildings in a desert climate. *Building and Environment,* 41 (3), 235–244.

AL-MUMIN, A. A., 2001. Suitability of sunken courtyards in the desert climate of Kuwait. *Energy and Buildings,* 33 (2), 103-111.

AL-TEMEEMI, A. A. & HARRIS, D. J., 2003. The effect of earth-contact on heat transfer through a wall in Kuwait. *Energy and Buildings,* 35 (4), 399-404.

AL-TEMEEMI, A. A. & HARRIS, D. J., 2004. A guideline for assessing the suitability of earth-sheltered mass-housing in hot-arid climates. *Energy and Buildings,* 36 (3), 251-260.

AMARA, S., NORDELL, B. & BENYOUCEF, B., 2011. Using Fouggara for Heating and Cooling Buildings in Sahara. *Energy Procedia,* 6 55–64.

ANDOLSUN, S., CULP, C. H., HABERL, J. S. & WITTE, M. J., 2011. EnergyPlus vs DOE-2.1e: The effect of ground coupling on energy use of a code house with basement in a hot-humid climate. *Energy and Buildings,* 53 1663-1675.

ANDOLSUN, S., CULP, C. H., HABERL, J. S. & WITTE, M. J., 2012. EnergyPlus vs DOE-2.1e: The effect of ground coupling on cooling/heating energy requirements of slab-on-grade code houses in four climates of the US. *Energy and Buildings,* 52 189-206.

ANSELM, A. J., 2008. Passive annual heat storage principles in earth sheltered housing, a supplementary energy saving system in residential housing. *Energy and Buildings,* 40 (7), 1214–1219.

ARGIRIOU, A., 1996. Ground cooling. *In:* SANTAMOURIS, M. & ASIMAKOPOULOS, D. N. (eds.), *Passive cooling of buildings* London: James & James, pp. 360-403.

ASCIONE, F., BELLIA, L. & MINICHIELLO, F., 2011. Earth-to-air heat exchangers for Italian climates. *Renewable Energy,* 36 (8), 2177-2188.

ASHRAE, 2011. *2011 ASHRAE Handbook - Heating, Ventilating, and Air-Conditioning Applications.* American Society of Heating, Refrigerating and Air-Conditioning Engineers, Inc.

AUGHENBAUGH, N. B., 1980. Subterranean settlements for arid zones. *In:* GOLANY, G. (ed.) *Housing in arid lands: Design and planning.* London: The Architectural Press, pp. 151-158.

AYDAN, O. & ULUSAY, R., 2003. Geotechnical and geoenvironmental characteristics of man-made underground structures in Cappadocia, Turkey. *Engineering Geology,* 69 (3-4), 245-272

BADESCU, V., 2007. Simple and accurate model for the ground heat exchanger of a passive house. *Renewable Energy,* 32 (5), 845–855.

BALARAS, C., 1996. Cooling in Buildings. *In:* SANTAMOURIS, M. & ASIMAKOPOULOS, D. N. (eds.), *Passive cooling of buildings* London: James & James, pp. 1-34.

BANKS, D., 2008. *An introduction to thermogeology: ground source heating and cooling.* Oxford: Blackwell Publishing.

BANSAL, N. K., HAUSER, G. & MINKE, G., 1994. *Passive building design : a handbook of natural climatic control / Narenda K. Bansal, Gerd Hauser, Gernot Minke.* Elsevier Science.

BANSAL, N. K. & SODHA, M. S., 1986. An Earth-Air Tunnel System for Cooling Buildings. *Tunnelling and Underground Space Technology,* 1 (2), 177-182.

BARKER, M. B., 1986. Using the Earth to Save Energy: Four Underground Buildings. *Tunnelling and Underground Space Technology,* 1 (1), 59-65.

BARTZ, J., 1986. Post-Occupancy Evaluation of Residents of Single- and Multi-Family Earth-Sheltered Housing. *Tunnelling and Underground Space Technology,* 1 (1), 71-88.

BENARDOS, A., ATHANASIADIS, I. & KATSOULAKOS, N., 2014. Modern earth sheltered constructions: A paradigm of green engineering. *Tunnelling and Underground Space Technology,* 41 46-52.

BENNIE, J., HUNTER, B., WILTSHIRE, A., HILL, M. O. & BAXTER, R., 2008. Slope, aspect and climate: Spatially explicit and implicit models of topographic microclimate in chalk grassland. *Ecological Modelling,* 216 47-59.

BHARADWAJ, S. S. & BANSAL, N. K., 1981. Temperature Distribution Inside Ground for Various Surface Conditions. *Building and Environment,* 16 (3), 183-192.

BOJIC, M., TRIFUNOVIC, T. M., PAPADAKIS, T. G. & KYRITSIS, S., 1997. Numerical simulation, technical and economic evaluation of air-to-earth heat exchanger coupled to a building. *Energy,* 22 (12), 1151-1158.

BOYER, L. L., 1982. Earth Sheltered Structures. *Annual Review of Energy,* 7 (1), 201-219.

BOYER, L. L. & GRONDZIK, W. T., 1987. *Earth shelter technology.* Texas: Texas A&M University Press.

BRAGGS, S. A., 1982. Remote prediction of periodic ground temperatures in Australia using isothermal contour maps. *Underground Space,* 7 (2), 127-132.

BROWN, G. & GARNISH, J., 2004. Geothermal Energy. *In:* BOYLE, G. (ed.) *Renewable Energy.* Second ed. Oxford: Oxford University Press, pp. 342-382.

BROWN, G. Z. & NOVITSKI, B.-J., 1981. Climate Responsive Earth-Sheltered Buildings. *Underground Space,* 5 (5), 299-305.

BU, Z., KATO, S. & TAKAHASHI, T., 2010. Wind tunnel experiments on wind-induced natural ventilation rate in residential basements with areaway space. *Building and Environment,* 45 (10), 2263-2272.

BURGER, E., 1987. Geomorphic Architecture: Multifamily Residential Design Solutions. *Tunnelling and Underground Space Technology,* 2 (3), 297-297.

CAÑAS GUERRERO, I. & MAZARRON, F. R., 2009. The effect of traditional wind vents called *zarceras* on the hygrothermal behaviour of underground wine cellars in Spain. *Building and Environment,* 44 (9), 1818-1826.

CAÑAS GUERRERO, I. & OCANA, S. M., 2005. Study ofthe thermal behaviour oftraditional wine cellars: the case ofthe area of"Tierras Sorianas del Cid" (Spain). *Renewable Energy* 30 (1), 44-55.

CARDINALE, N., GUIDA, A. & RUGGIERO, F., 2001. Thermo-hygrometric evaluations in the recovery of rocky buildings of the "Sassi of Matera"(Italy). *Journal of Thermal Envelope and Building Science,* 24 (4), 301-315.

CARDINALE, N., ROSPI, G. & STAZI, A., 2010. Energy and microclimatic performance of restored hypogeous buildings in south Italy: The "Sassi" district of Matera. *Building and Environment,* 45 (1), 94-106.

CARDINALE, N., ROSPI, G. & STEFANIZZI, P., 2013. Energy and microclimatic performance of Mediterranean vernacular buildings: The Sassi district of Matera and the Trulli district of Alberobello. *Building and Environment,* 59 590-598.

CARDINALE, N. & RUGGIERO, F., 2002. A case study on the environmental measures techniques for the conservation in the vernacular settlements in Southern Italy. *Building and Environment,* 37 (4), 405-414.

CARMODY, J. C. & STERLING, R. L., 1987. Design strategies to alleviate negative psychological and physiological effects in underground space. *Tunnelling and Underground Space Technology incorporating Trenchless,* 2 (1), 59-67.

CATALANO, F. & CENEDESE, A., 2010. High-resolution numerical modeling of thermally driven slope winds in a valley with strong capping. *Journal of Applied Meteorology and Climatology,* 49 (9), 1859-1880.

CHANG, J. H., 1958. *Ground temperature.* Massachusetts: Harvard University, Blue Hill Meteorological Observatory.

CHESTER, C. V. & ZIMMERMAN, G. P., 1987. Civil Defense Shelters: a State-of-the-Art Assessment. *Tunnelling and Underground Space Technology incorporating Trenchless,* 2 (4), 401-428.

CHOU, Y., SHENG, Y., LI, Y., WEI, Z., ZHU, Y. & LI, J., 2010. Sunny–shady slope effect on the thermal and deformation stability of the highway embankment in warm permafrost regions. *Cold Regions Science and Technology,* 63 (1–2), 78-86.

ÇORAKBAS, F., 2012. The comparison of rock-cut architecture sites in Turkey and Italy withspecial emphasis on Cappadocia. *World Applied Sciences Journal,* 17 (11), 1445-1453.

DEPARTMENT OF ENERGY, U. S. 2003. Lecture 24 Ground Heat Transfer. *EnergyPlus University Course Teaching Material* [Online]. Available: https://energyplus.net/support [Accessed July 2012].

DEPARTMENT OF ENERGY, U. S. 2012. Auxiliary EnergyPlus Programs: Extra programs for EnergyPlus. Available: http://www.energyplus.gov.

DIMOUDI, A., 1996a. Microclimate. *In:* SANTAMOURIS, M. & ASIMAKOPOULOS, D. N. (eds.), *Passive cooling of buildings* London: James & James, pp. 84-94.

DIMOUDI, A., 1996b. Passive cooling of buildings. *In:* SANTAMOURIS, M. & ASIMAKOPOULOS, D. N. (eds.), *Passive cooling of buildings* London: James & James, pp. 35-55.

DROULIA, F., LYKOUDIS, S., TSIROS, I., ALVERTOS, N., AKYLAS, E. & GAROFALAKIS, I., 2009. Ground temperature estimations using simplified analytical and semi-empirical approaches. *Solar Energy,* 83 (2), 211–219.

EGG, J. & HOWARD, B., 2011. *Geaothermal HVAC: green heating and cooling.* New York: McGraw-Hill.

EL-DIN, M. M. S., 1999. On the heat flow into the ground. *Renewable Energy,* 18 473-490.

ERDEM, A., 2008. Subterranean space use in Cappadocia: The Uchisar example. *Tunnelling and Underground Space Technology,* 23 (5), 492-499.

EUROSTAT. 2015. *EU Statistics* [Online]. Luxembourg: European Commission. Available: http://ec.europa.eu/eurostat/ [Accessed Octobre 2015].

FERREIRA, J. & PINHEIRO, M., 2011. In search of better energy performance in the Portuguese buildings—The case of the Portuguese regulation. *Energy Policy,* 39 (12), 7666-7683.

FITTON, F. M. & BROOKS, C. F., 1931. Soil temperature in the United States. *Monthly Weather Review,* 59 6-16.

FLORIDES, G. & KALOGIROU, S., 2007. Ground heat exchangers—A review of systems, models and applications. *Energy and Buildings,* 32 (15), 2461-2478

FLORIDES, G. A., POULOUPATIS, P. D., KALOGIROU, S., MESSARITIS, V., PANAYIDES, I., ZOMENI, Z., PARTASIDES, G., LIZIDES, A., SOPHOCLEOUS, E. & KOUTSOUMPAS, K., 2011. The geothermal characteristics of the ground and the potential of using ground coupled heat pumps in Cyprus. *Energy,* 36 (8), 5027-5036.

FUENTES PARDO, J. M. & CANAS GUERREIRO, I., 2006. Subterranean wine cellars of Central-Spain (Ribera de Duero): An underground built heritage to preserve. *Tunnelling and Underground Space Technology,* 21 (5), 475-484

FUENTES PARDO, J. M., GALLEGO, E., GARCIA, A. I. & AYUGA, F., 2010. New uses for old traditional farm buildings: The case of the underground wine cellars in Spain. *land Use Policy,* 27 (3), 738-748

GEIGER, R., 1950. *The climate near the ground; a translation by Milroy N. Stewart and others, with revision and enlargements by the author.* Cambridge, Massachusetts: Harvard University Press, for the Blue Hill Meteorological Observatory.

GHOSAL, M. K., TIWARI, G. N., SRIVASTAVA, N. S. L. & SODHA, M. S., 2004. Thermal modelling and experimental validation of ground temperature distribution in greenhouse. *International Journal of Energy Research,* 28 (1), 45-63.

GIVONI, B., 1994. *Passive and low energy cooling of buildings / Baruch Givoni.* John Wiley.

GIVONI, B. & EARTH, L., 1985. Temperatures and underground buildings. *Energy and Buildings,* 8 (1), 15-25.

GOLANY, G., 1980. Subterranean settlements for arid zones. *In:* GOLANY, G. (ed.) *Housing in arid lands: Design and planning.* London: The Architectural Press, pp. 109-122.

GOLANY, G., 1983. Urban form design for arid regions. *In:* GOLANY, G. (ed.) *Design for arid regions.* New York: Van Nostrand Reinhold Company Inc., pp. 1-23.

GOLANY, G., 1992. *Chinese earth-sheltered dwellings: Indigenous lessons for modern urban design.* Honolulu: University of Hawaii Press.

GOLANY, G., 1995. *Ethics and urban design: culture, form, and environment.* New York: J. Wiley & Sons.

GOLANY, G., 1996. Urban design morphology and thermal performance. *Atmospheric Environment,* 30 (3), 455-465.

GOLANY, G., 1998. Introduction. *In:* GOLANY, G., HANAKI, K., AND KOIDE, O (ed.) *Japanese Urban Environment* Oxford: Pergamon, Elsevier Science Lt, pp.

GRINDLEY, P. C. & HUTCHINSON, M., 1996. The thermal behaviours of an earthship. *Renewable Energy,* 8 (1-4), 154-159.

GUIDA, A., PAGLIUCA, A. & ROSPI, G., 2008. Underground spaces and indoor comfort: the case of "Sassi di Matera". *In:* BREBBIA, C. A., KALIAMPAKOS, D. & PROCHÁZKA, P. (eds.), *Underground space: design, engineering and environmental aspects.* Southampton: WIT Press, pp. 149-158.

HASEGAWA, F., YOSHINO, H. & MATSUMOTO, S., 1997. Optimum Use of Solar Energy Techniques in a Semi-Underground House: First-Year Measurement and Computer Analysis. *Earth Shelter & Architecture,* 2 (4), 429-435.

HAYASHI, Y., 1986. The Future of Earth-Sheltered Architecture in China's Farming Villages. *Tunnelling and Underground Space Technology,* 1 (2), 167-169.

HAZBEI, M., NEMATOLLAHI, O., BEHNIA, M. & ADIB, Z., 2015. Reduction of energy consumption using passive architecture in hot and humid climates. *Tunnelling and Underground Space Technology,* 47 16-27.

HERB, W. R., JANKE, B., MOHSENI, O. & STEFAN, H. G., 2008. Ground surface temperature simulation for different land covers. *Journal of Hydrology,* 356 (3-4), 327-343.

HOLLMULLER, P. & LACHAL, B., 2001. Cooling and preheating with buried pipe systems: monitoring, simulation and economic aspects. *Energy and Buildings,* 33 (5), 509-518.

HUNT, D. V. L., JEFFERSON, I. & ROGERS, C. D. F., 2011. Assessing the Sustainability of Underground Space Usage - A Toolkit for Testing Possible Urban Futures. *Journal of Mountain Science,* 8 (2), 211-222.

IMAMOGLU, V., 1980. Microclimatic elements of houses in Turkish arid zones. *In:* GOLANY, G. (ed.) *Housing in arid lands: Design and planning.* London: The Architectural Press, pp. 45-74.

INÁCIO, M., PEREIRA, V. & PINTO, M., 2008. The soil geochemical atlas of Portugal: overview and applications. *Journal of Geochemical Exploration,* 98 22-33.

INE. 2015. *Statistics Portugal* [Online]. Lisboa, Portugal: Instituto Nacional de Estatística. Available: https://www.ine.pt [Accessed Octobre 2015].

IP, K. & MILLER, A., 2009. Thermal behaviour of an earth-sheltered autonomous building – The Brighton Earthship. *Renewable Energy,* 34 (9), 2037-2043.

JACOVIDES, C. P., MIHALAKAKOU, G., SANTAMOURIS, M. & LEWIS, J. O., 1996. On the ground temperature profile for passive cooloing applications in buildings. *Solar Energy,* 57 (3), 167-175.

JAFARIAN, S. M., JAAFARIAN, S. M., HASELI, P. & TAHERI, M., 2010. Performance analysis of a passive cooling system using underground channel (Naghb). *Energy and Buildings,* 42 (5), 559-562.

JANNADI, M. O. & GHAZI, S., 1998. Earth-sheltered housing: The way of the future? *Journal of Urban Planning and Development,* 124 (3), 101-114.

JRC. *Photovoltaic Geographical Information System - Interactive Maps* [Online]. European Commission. Available: http://re.jrc.ec.europa.eu/pvgis/apps4/pvest.php [Accessed 20 May 2015].

JUN, M. & YAN-YUNG, E. 2006. Thermal studies of suitable ecological building in China's loess plateau region. *PLEA2006 - The 23rd Conference on Passive and Low Energy Architecture.* Geneva, Switzerland.

KHAIR-EL-DIN, A.-E.-H. M., 1991. Earth sheltered housing: an approach to energy. *Journal of King Saud University: Architecture & Planning,* 3 (1), 3-18.

KHARRUFA, S. N., 2008. Evaluation of Basement's Thermal Performance in Iraq for Summer Use. *Journal of Asian Architecture and Building Engineering,* 7 (2), 411-417.

KRARTI, M. & KREIDER, J. F., 1996. Analytical model for heat transfer in an underground air tunnel. *Energy Conversion and Management,* 37 (10), 1561-1574.

KUMAR, R., KAUSHIK, S. C. & GARG, S. N., 2006. Heating and cooling potential of an earth-to-air heat exchanger using artificial neural network. *Renewable Energy,* 31 (8), 1139-1155.

KUMAR, R., SACHDEVA, S. & KAUSHIK, S. C., 2007. Dynamic earth-contact building: A sustainable low-energy technology. *Building and Environment,* 42 (6), 2450–2460.

KUSADA, T. & ARCHENBACH, P. R. 1965. Earth temperature and thermal diffusivity at selective stations in the United States. Washington, D. C.: National Bureau of Standards.

KWOK, A. G. & GRONDZIK, W. T., 2011. *The green studio handbook: environmental strategies for schematic design.* Oxford: Architectural Press.

LABBÉ, M. & DUFFAUT, P., 1995. Underground space inside a hilltop: the summit hotel project, St. Michael Peak, France. *Tunnelling and Underground Space Technology incorporating Trenchless,* 10 (2), 155-161.

LABS, K., 1979. Underground building climate. *Solar Age,* 4 (10), 44-50.

LABS, K., 1980. Terratypes: underground housing for arid zones. *In:* GOLANY, G. (ed.) *Housing in arid lands: Design and planning.* London: The Architectural Press, pp. 123-140.

LABS, K., 1982. Regional analysis of ground and above-ground climate. *Underground Space,* 6 (6), 397-422.

LABS, K. & HARRINGTON, K., 1982. Comparison of ground and above-ground climates for identifying appropriare cooling strategies. *Passive Solar Journal,* 1 (1), 4-11.

LEE, S. W. & SHON, J. Y., 1988. The Thermal Environment in an Earth-Sheltered Home Korea. *Tunnelling and Underground Space Technology,* 5 (4), 409-416.

LEMBO, F., MARINO, F. P. R. & CALCAGNOA, C. 2011. Semi-underground house models as new concepts for urban sustainable environment. *In:* ENGINEERING, P. (ed.) *2001 International Conference on Green Buildings and Sustainable Cities.*

LEWIS, T. J. & WANG, K., 1992. Influence of terrain on bedrock temperatures. *Palaeogeography, Palaeoclimatology. Palaeoecology (Global and Planetary Change Section),* 98 87-100.

LI, Y. & WU, W. C. 2011. Energy-efficient land-saving and low-carbon art of dwelling environment - Research from the underneath type earth cave dwelling in Bai She Village, San Yuan County of Shaanxi Province. Brussels.

LITTLEFAIR, P. J., SANTAMOURIS, M. & ALVAREZ, S., 2011. *Site layout planning for daylight and sunlight : a guide to good practice.* Bracknell BRE Press.

LIU, C., SHI, B., TANG, C. & GAO, L., 2011. A numerical and field investigation of underground temperatures under Urban Heat Island. *Building and Environment,* 46 (5), 1205-1210.

LIU, J., ZHU, X., YANG, L. & HU, R., 2010. Exemplary project of green cave dwellings in Loess Plateau. *Frontiers of Energy and Power Engineering in China,* 4 (1), 122-130.

LUO, W., 1987. Seismic Problems of Cave Dwellings on China's Loess Plateau. *Tunnelling and Underground Space Technology,* 2 (2), 203-208.

LUO, Z. & LI, Y., 2001. Passive urban ventilation by combined buoyancy-driven slope flow and wall flow: Parametric CFD studies on idealized city models. *Atmospheric Environment,* 45 (32), 5946-5956.

MANNERS, J., VOSPER, S. B. & ROBERTS, N., 2012. Radiative transfer over resolved topographic features for high-resolution weather prediction. *Quarterly Journal of the Royal Meteorological Society,* 138 (664), 720-733.

MAZARRON, F. R. & CAÑAS, I., 2008. Exponential sinusoidal model for predicting temperature inside underground wine cellars from a Spanish region. *Energy and Buildings,* 40 (10), 1931-1940.

MAZARRON, F. R. & CAÑAS, I., 2009. Seasonal analysis of the thermal behaviour of traditional underground wine cellars in Spain. *Renewable Energy,* 34 (11), 2484-2492.

MAZARRON, F. R., CID-FALCETO, J. & CAÑAS, I., 2012. An assessment of using ground thermal inertia as passive thermal technique in the wine industry around the world. *Applied Thermal Engineering,* 33-34 (1), 54-61.

MCHENRY, P. G., JR, 1980. Building materials and technology in arid lands. *In:* GOLANY, G. (ed.) *Housing in arid lands: Design and planning.* London: The Architectural Press, pp. 97-106.

MIHALAKAKOU, G., 2002. On estimating soil surface temperature profiles. *Energy and Buildings,* 34 (3), 251-259.

MIHALAKAKOU, G., LEWIS, J. O. & SANTAMOURIS, M., 1996a. The influence of different ground covers on the heating potential of earth-to-air heat exchangers. *Renewable Energy,* 7 (1), 33-46.

MIHALAKAKOU, G., SANTAMOURIS, M. & ASIMAKOPOULOS, D., 1998. Modeling ambient air temperature time series using neural networks. *Journal of Geophysical Research,* 103 (D16), 19509-19517.

MIHALAKAKOU, G., SANTAMOURIS, M., LEWIS, J. O. & ASIMAKOPOULOS, D. N., 1997. On the application of the energy balance equation to predict ground temperature profiles. *Solar Energy,* 60 (3-4), 181-190.

MINISTÉRIO DAS OBRAS PÚBLICAS & COMUNICAÇÕES, T. E. 2006. Decreto-Lei 80/2006, Regulamento das Características de Comportamento Térmico dos Edifícios. Diário da República.

MOUKALLED, F. & SALEH, Y., 2006. Heat and Mass Transfer in Moist Soil, Part I. Formulation and Testing. *Numerical Heat Transfer,* 49 (5), 467-486.

NASSAR, Y., ELNOAMAN, A., ABUTAIMA, A., YOUSIF, S. & SALEM, A., 2006. Evaluation of the underground soil thermal storage properties in Libya. *Renewable Energy,* 31 (5), 593–598.

OCANA, S. M. & CAÑAS GUERRERO, I., 2005. Comparison of hygro-thermal conditions in underground wine cellars from a Spanish area. *Building and Environment,* 40 (10), 1384-1394.

OCANA, S. M. & CAÑAS GUERRERO, I., 2006. Comparison of analytical and on site temperature results on Spanish traditional wine cellars. *Applied Thermal Engineering,* 26 (7), 700-708.

OLGYAY, V., 1963. *Design with climate: bioclimatic approach to architecture regionalism.* Princeton: Princeton University Press.

OZGENER, L., 2011. A review on the experimental and analytical analysis of earth to air heat exchanger (EAHE) systems in Turkey. *Renewable and Sustainable Energy Reviews,* 15 (9), 4483-4490.

PERRIER, F., MORAT, P. & LE MOUEL, J.-L., 2001. Pressure induced temperature variations in an underground quarry. *Earth and Planetary Science Letters,* 191 (1-2), 145-156.

PFAFFEROTT, J., 2003. Evaluation of earth-to-air heat exchangers with a standardised method to calculate energy efficiency. *Energy and Buildings,* 25 (10), 971-983.

POPIEL, C. O., WOJTKOWIAK, J. & BIERNACKA, B., 2001. Measurements of temperature distribution in ground. *Experimental Thermal and Fluid Science,* 25 (5), 301-309.

POULOUPATIS, P. D., FLORIDES, G. & TASSOU, S., 2011. Measurements of ground temperatures in Cyprus for ground thermal applications. *Renewable Energy,* 36 (2), 804-814.

RANTALA, J., 2005. Estimation of the Mean Temperature Distribution Underneath a Slab-on-ground Structure. *Journal of Building Physics,* 29 (1), 51-68.

REES, S. W., ADJALI, M. H., ZHOU, Z., DAVIES, M. & THOMAS, H. R., 2000. Ground heat transfer effects on the thermal performance of earth-contact structures. *Renewable and Sustainable Energy Reviews,* 4 (3), 213-265.

REES, S. W., ZHOU, Z. & THOMAS, H. R., 2007. Ground heat transfer: A numerical simulation of a full-scale experiment. *Building and Environment,* 42 (3), 1478-1488

RUDOFSKY, B., 1964. *Architecture without architects : an introduction to nonpedigreed architecture / by Bernard Rudofsky.* Museum of Modern Art.

RUIZ-ARIAS, J. A., POZO-VÁZQUEZ, D., SANTOS-ALAMILLOS, F. J., LARA-FANEGO, V. & TOVAR-PESCADOR, J., 2011. A topographic geostatistical approach for mapping monthly mean values of daily global solar radiation: A case study in southern Spain. *Agricultural and Forest Meteorology,* 151 (12), 1812-1822.

ŠAFANDA, J., 1999. Ground surface temperature as a function of slope angle and slope orientation and its effect on the subsurface temperature field. *Tectonophysics,* 306 (3-4), 367-375.

SELECÇÕES DO READER'S, D. & INSTITUTO GEOGRÁFICO, C., 1988. *Atlas de Portugal: cartas do Instituto Geográfico e Cadastral.* Selecções do Reader's Digest.

SHUKLA, A., TIWARI, G. N. & SODHA, M. S., 2006. Parametric and experimental study on thermal performance of an earth–air heat exchanger. *International Journal of Energy Research,* 30 (6), 365-379.

SIMPSON, B. J. & PURDY, M. T., 1984. *Housing on sloping sites: a design guide.* London and New York: Construction Press.

SOBOTKA, P., YOSHINO, H. & MATSUMOTO, S., 1996. Thermal Comfort in Passive Solar Earth Integrated Rooms. *Building and Environment,* 31 (2), 155-166.

STANIEC, M. & NOWAK, H., 2011. Analysis of the earth-sheltered buildings' heating and cooling energy demand depending on type of soil. *ARCHIVES OF CIVIL AND MECHANICAL ENGINEERING,* 11 (1), 221-235.

STASINOPOULOS, T. N., 2014. The four elements of Santorini's architecture. *In:* WEBER, W. & YANNAS, S. (eds.), *Lessons from vernacular architecture.* New York: Routledge, pp. 11-36.

STEAD, P., 1980. Lessons in traditional and vernacular architecture in arid zones. *In:* GOLANY, G. (ed.) *Housing in arid lands: Design and planning.* London: The Architectural Press, pp. 33-44.

STEEMERS, T. C., 1991. The State of the Art in Passive Cooling. *International Journal of Solar Energy,* 10 (1-2), 5-14.

STERLING, R., CARMODY, J. C. & ELNICKY, G., 1981. *Earth sheltered community design: Energy-efficient residential development.* New York: Van Nostrand Reinhold Company Limited.

SZOKOLAY, S. V., 2014. *Introduction to architectural science: the basis of sustainable design.* Abingdon; New York, NY: Routledge.

TANG, Z. & FANG, J., 2006. Temperature variation along the northern and southern slopes of Mt. Taibai, China. *Agricultural and Forest Meteorology,* 139 (3–4), 200-207.

THAKUR, A. K. S., 1982. Modification of Ground Temperature Distribution due to Various Parameters. *Building and Environment,* 17 (4), 301-302.

TIAN, Y. Q., DAVIES-COLLEY, R. J., GONG, P. & THORROLD, B. W., 2001. Estimating solar radiation on slope of arbitrary aspect. *Agricultural and Florrest Meteorology,* 109 67-74.

TINTI, F., BARBARESI, A., BENNI, S., TORREGGIANI, D., BRUNO, R. & TASSINARI, P., 2014. Experimental analysis of shallow underground temperature for the assessment of energy efficiency potential of underground wine cellars. *Energy and Buildings,* 80 451-460.

TITTELEIN, P., ACHARD, G. & WURTZ, E., 2009. Modelling earth-to-air heat exchanger behaviour with the convolutive response factors method. *Applied Energy,* 86 (9), 1683-1691.

TONG, L. & CHEN, Z., 2012. Ancient energy-saving housing-earth-dwelling cave residences. *Advanced Materials Research,* 347-353 4104-4108.

TONG, L., CHEN, Z. & LI, W., 2011. Approach to folk construction techniques of earth-dwelling caves. *Advanced Materials Research,* 255-260 1644-1648.

TROMBE, A., PETTIT, M. & BOURRET, B., 1991. Air cooling by earth tube heat exchanger: experimental approach. *Renewable Energy,* 1 (5-6), 699-707.

TRZASKI, A. & ZAWADA, B., 2011. The influence of environmental and geometrical factors on air-ground tube heat exchanger energy efficiency. *Building and Environment,* 46 (7), 1436-1444.

TSILINGIRIDIS, G. & PAPAKOSTAS, K., 2014. Investigating the relationship between air and ground temperature variations in shallow depths in northern Greece. *Energy,* 73 1007-1016.

TURAN, M. H., 1983. Architectural and environmental adaptation in slope settlements. *In:* GOLANY, G. (ed.) *Design for arid regions.* New York: Van Nostrand Reinhold Company Inc., pp. 141-165.

UN-HABITAT, U. N. C. F. H. S., 1987. *Global Report on Human Settlements.* Oxford, New York: Oxford University Press.

UN-HABITAT, U. N. S. P., 2011. *Cities and Climate Change: Global Report on Human Settlements 2011.* London, Washington: Earthscan.

UNDERGROUND SPACE CENTER, U. M., 1979. *Earth Sheltered Housing Design: Guidelines, Examples and References.* New York: Van Nostrand Reinhold Company.

VAN DER MEER, W. J., 1980. Possibilities for subterranean housing in arid zones. *In:* GOLANY, G. (ed.) *Housing in arid lands: Design and planning.* London: The Architectural Press, pp. 141-150.

VAN DER RYN, S., 1979. Preface. *In:* WATSON, D. (ed.) *Energy conservation through building design.* USA: McGraw-Hill, Inc., pp.

VAN DRONKELAAR, C., CÓSTOLA, D., MANGKUTO, R. A. & HENSEN, J. L. M., 2014. Heating and cooling energy demand in underground buildings: Potential for saving in various climates and functions. *Energy and Buildings,* 71 (0), 129-136.

VELOSO DA VEIGA, P. 2009. *Solar Energy Potential of Clustered Building Forms on Sloped Terrains.* Ph. D., University of Nottingham.

WANG, F. & LIU, Y., 2002. Thermal environment of courtyard stile cave dwelling in winter. *Energy and Buildings,* 34 985-1001.

WANG, J. & BRAS, R. L., 1999. Ground heat flux estimated from surface soil temperature. *Journal of Hydrology,* 216 (3-4), 214–226.

WANG, S. Year. Study on astronomical solar radiation over rugged terrain using DEM data. *In*, 2009. pp. 2184-2187.

WENDT, R. L. 1982. Earth-shelteredhousing, an evaluation of energy-conservation potential. Oak Ridge, Tennesee: Department of Energy.

WORLD HEALTH ORGANIZATION, W. & UN-HABITAT 2016. Global report on urban health: equitable, healthier cities for sustainable development. http://www.who.int/en/.

WORLD RESOURCES INSTITUTE, W., 1988. *World resources: an assessment of the resource base that supports the global economy. 1988-89 by the World Resources Institute.* New York: Basic Books, Inc.

WORLD RESOURCES INSTITUTE, W., 1990. *World resources: a guide to the global environment. 1990-91 by the World Resources Institute.* New York, Oxford: Oxford University Press.

WORLD RESOURCES INSTITUTE, W., 1994. *World resources: a guide to the global environment. 1994-95 by the World Resources Institute.* New York, Oxford: Oxford University Press.

WU, H., WANG, S. & ZHU, D., 2007. Modelling and evaluation of cooling capacity of earth–air–pipe systems. *Energy Conversion and Management,* 48 (5), 1462-1471.

YAN, H., 1986. The Effects of Cave Dwelling on Human Health. *Tunnelling and Underground Space Technology,* 1 (2), 171-175.

YOSHINO, H., MATSUMOTO, S., NAGATOMO, M. & SAKANISHI, T., 1992. Five-year Measurements of Thermal Performance for a Semi-underground Test House. *Tunnelling and Underground Space Technology,* 7 (4), 339-346.

YUCHENG, Y. & LIU, Y., 1987. Earthquake Damage to and Aseismic Measures for Earth-Sheltered Buildings in China. *Tunnelling and Underground Space Technology,* 2 (2), 209-216.

ZENG, X. D. & SONG, D. M., 2012. From traditional cave to green design of modern earth-sheltered architecture: A case study of Chongqing Empirical Study Center of Building Energy Conservation. *Advanced Materials Research,* 368-373 3486-3489.

ZHANG, H., 2011. Kang Bai-wan's mansions from the ecological perspective. *Advanced Materials Research,* 243-249 6965-6970.

ZHU, X., LIU, J., YANG, L. & HU, R., 2014. Energy performance of a new Yaodong dwelling, in the Loess Plateau of China. *Energy and Buildings,* 70 159-166.

APPENDICES

APPENDIX 1

This appendix provides Chapter 5 additional information, as complete monthly weather data used in Section 5.2, complete thermal properties of selected soils and rocks and monthly solar radiation values for Lisbon used in Section 5.3 and 5.4.

Table Appendices 1: Chapter 5 – Monthly weather data

Oporto - Weather Data		Jan	Feb	Mar	Apr	May	Jun	Jul	Aug	Sep	Oct	Nov	Dec
Temperature - Daily Avg		9.4	10.7	11.6	13.2	14.5	17.8	19	19.4	18	15.5	12.2	10.3
Relative Humidity % - Daily Avg		80	81	78	77	78	75	80	76	82	77	81	82
Wind Speed m/s - Daily Avg		2.8	4	3.9	3.3	4.1	1.6	3.2	2.2	1.9	3.7	3.1	1.9
Mean solar radiation	$Wh/m^2/day$	1960	3050	4590	5600	6730	7340	7360	6620	5270	3550	2270	1730
	Hours with sun	10	11	12	13	14	14	14	13	12	11	10	10
	W/m^2	196.00	277.27	382.50	430.77	480.71	524.29	525.71	509.23	439.17	322.73	227.00	173.00
Braganca - Weather Data		Jan	Feb	Mar	Apr	May	Jun	Jul	Aug	Sep	Oct	Nov	Dec
Temperature - Daily Avg		4.3	6	9.3	10.8	12.9	17.6	21.7	21	17.5	13.2	8.4	5.6
Relative Humidity % - Daily Avg		85	83	62	70	70	65	56	52	56	74	81	88
Wind Speed m/s Daily Avg		3	3	3.3	3	3.4	2.9	2.9	2.6	2.4	2.2	1.6	1
Mean solar radiation	$Wh/m^2/day$	1760	2920	4410	5290	6480	7540	7840	6900	5230	3420	2130	1630
	Hours with sun	10	11	12	13	14	14	14	13	12	11	10	10
	W/m^2	176.00	265.45	367.50	406.92	462.86	538.57	560.00	530.77	435.83	310.91	213.00	163.00
Coimbra - Weather Data		Jan	Feb	Mar	Apr	May	Jun	Jul	Aug	Sep	Oct	Nov	Dec
Temperature - Daily Avg		9.6	11	12.7	13.1	15.6	19	20.8	21.1	20.6	16.9	12.2	11.2
Relative Humidity % - Daily Avg		80	80	70	72	76	74	76	69	74	82	84	81
Wind Speed m/s - Daily Avg		1.9	2.7	2.8	2.5	2.5	2.1	2	2.4	2	1.5	2.5	2.8
Mean solar radiation	$Wh/m^2/day$	2050	3030	4420	5160	6200	6960	7350	6570	5160	3550	2330	1830
	Hours with sun	10	11	12	13	14	14	14	13	12	11	10	10
	W/m^2	205.00	275.45	368.33	396.92	442.86	497.14	525.00	505.38	430.00	322.73	233.00	183.00
Evora - Weather Data		Jan	Feb	Mar	Apr	May	Jun	Jul	Aug	Sep	Oct	Nov	Dec
Temperature - Daily Avg		8.8	10.2	12.5	13.2	17.2	19.8	22.7	23	22	17.2	12.1	10.5
Relative Humidity % - Daily Avg		81	69	65	74	61	61	58	56	61	72	72	82
Wind Speed m/s - Daily Avg		4.6	3.4	5	4.8	4.2	4.6	4.4	4.9	4.4	3.7	4.4	4.4
Mean solar radiation	$Wh/m^2/day$	2340	3420	4870	5780	6800	7850	8130	7170	5510	3980	2710	2100
	Hours with sun	10	11	12	13	14	14	14	13	12	11	10	10
	W/m^2	234.00	310.91	405.83	444.62	485.71	560.71	580.71	551.54	459.17	361.82	271.00	210.00
Lisbon - Weather Data		Jan	Feb	Mar	Apr	May	Jun	Jul	Aug	Sep	Oct	Nov	Dec
Temperature - Daily Avg		10.6	11.5	12.8	14.6	17.3	20.1	22.3	22.6	21.3	17.8	13.6	11
Relative Humidity % - Daily Avg		82	79	77	73	72	70	66	65	70	75	81	8
Wind Speed m/s - Daily Avg		4.9	5	4.9	5.3	5.5	5.8	5.6	5.7	4.8	4.2	4.1	4.1
Mean solar radiation	$Wh/m^2/day$	2180	3210	4640	5680	6680	7450	7620	6880	5400	3800	2510	1950
	Hours with sun	10	11	12	13	14	14	14	13	12	11	10	10
	W/m^2	218.00	291.82	386.67	436.92	477.14	532.14	544.29	529.23	450.00	345.45	251.00	195.00
Faro - Weather Data		Jan	Feb	Mar	Apr	May	Jun	Jul	Aug	Sep	Oct	Nov	Dec
Temperature - Daily Avg		11.8	12.4	14.8	15.8	18.6	21.1	23.9	23.7	21.8	20.2	15.5	13.2
Relative Humidity % - Daily Avg		75	81	72	71	72	70	59	66	74	78	74	7
Wind Speed m/s - Daily Avg		3.4	3.8	3.6	4.3	3.8	4	3.4	2	2.9	4.2	4.1	3.8
Mean solar radiation	$Wh/m^2/day$	2590	3680	5230	6250	7240	8010	8040	7190	5700	4280	2960	2320
	Hours with sun	10	11	12	13	14	14	14	13	12	11	10	10
	W/m^2	259.00	334.55	435.83	480.77	517.14	572.14	574.29	553.08	475.00	389.09	296.00	232.00

Table Appendices 2: Chapter 5 - Thermal properties of selected soils and rocks by ASHRAE (2011, p. 34.15)

Class	Material	Dry Density (kg/m^3)	Conductivity (W/(m K))	Diffusivity (m2/day)
Soils	Heavy clay, 15% water	1925	1.4 to 1.9	0.042 to 0.061
	5% water	1925	1.0 to 1.4	0.047 to 0.061
	Light clay, 15% water	1285	0.7 to 1.0	0.055 to 0.047
	5% water	1285	0.5 to 0.9	0.056 to 0.056
	Heavy sand, 15% water	1925	2.8 to 3.8	0.084 to 0.11
	5% water	1925	2.1 to 2.3	0.093 to 0.14
	Light sand, 15% water	1285	1.0 to 2.1	0.047 to 0.093
	5% water	1285	0.9 to 1.9	0.055 to 0.12
Rocks	Granite	2650	2.3 to 3.7	0.084 to 0.13
	Limestone	2400 to 2800	2.4 to 3.8	0.084 to 0.13
	Sandstone		2.1 to 3.5	0.65 to 0.11
	Shale, wet	2570 to 2730	1.4 to 2.4	0.065 to 0.084
	Shale, dry	2570 to 2730	1.0 to 2.1	0.055 to 0.074

Table Appendices 3: Chapter 5 – Lisbon, solar radiation data

00° Slope		Jan	Feb	Mar	Apr	May	Jun	Jul	Aug	Sep	Oct	Nov	Dec
Mean solar radiation	Wh/m^2/day	2180	3210	4640	5680	6680	7450	7620	6880	5400	3800	2510	1950
	Hours with sun	10	11	12	13	14	14	14	13	12	11	10	10
	W/m^2	218	292	387	437	477	532	544	529	450	345	251	195
10° Slope		Jan	Feb	Mar	Apr	May	Jun	Jul	Aug	Sep	Oct	Nov	Dec
Mean solar radiation	Wh/m^2/day	2640	3740	5140	5910	6780	7450	7670	7160	5880	4340	3040	2430
	Hours with sun	10	11	12	13	14	14	14	13	12	11	10	10
	W/m^2	264	340	428	455	484	532	548	551	490	395	304	243
20° Slope		Jan	Feb	Mar	Apr	May	Jun	Jul	Aug	Sep	Oct	Nov	Dec
Mean solar radiation	Wh/m^2/day	3060	4200	5480	6060	6750	7290	7560	7260	6230	4790	3500	2860
	Hours with sun	10	11	12	13	14	14	14	13	12	11	10	10
	W/m^2	306	382	457	466	482	521	540	558	519	435	350	286
30° Slope		Jan	Feb	Mar	Apr	May	Jun	Jul	Aug	Sep	Oct	Nov	Dec
Mean solar radiation	Wh/m^2/day	3400	4550	5700	6070	6560	6970	7260	7190	6420	5130	3880	3220
	Hours with sun	10	11	12	13	14	14	14	13	12	11	10	10
	W/m^2	340	414	475	467	469	498	519	553	535	466	388	322
40° Slope		Jan	Feb	Mar	Apr	May	Jun	Jul	Aug	Sep	Oct	Nov	Dec
Mean solar radiation	Wh/m^2/day	3650	4800	5780	5940	6230	6490	6800	6940	6460	5340	4160	3510
	Hours with sun	10	11	12	13	14	14	14	13	12	11	10	10
	W/m^2	365	436	482	457	445	464	486	534	538	485	416	351
50° Slope		Jan	Feb	Mar	Apr	May	Jun	Jul	Aug	Sep	Oct	Nov	Dec
Mean solar radiation	Wh/m^2/day	3820	4920	5730	5670	5760	5860	6180	6510	6320	5410	4330	3700
	Hours with sun	10	11	12	13	14	14	14	13	12	11	10	10
	W/m^2	382	447	478	436	411	419	441	501	527	492	433	370
60° Slope		Jan	Feb	Mar	Apr	May	Jun	Jul	Aug	Sep	Oct	Nov	Dec
Mean solar radiation	Wh/m^2/day	3880	4910	5530	5260	5150	5110	5420	5920	6020	5340	4390	3790
	Hours with sun	10	11	12	13	14	14	14	13	12	11	10	10
	W/m^2	388	446	461	405	368	365	387	455	502	485	439	379

APPENDIX 2

This appendix provides the model materials used in Chapter 6 Section 6.1 initial case study thermal simulations.
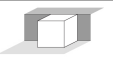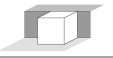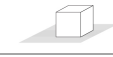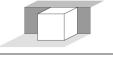
Table Appendices 4: Chapter 6 – Initial case models - materials

	Material	Width (mm)	Conductiv. (W/m.°C)	Convec. Coeff. (W/m^2.°C)	Density (Kg/m^3)	Specific Heat (J/Kg.°C)	Thermal Resist. (m^2.°C/W)
Roof	1-Tiles	4	0.23	0.001	1500	1300	0.0174
	2- Insulation	80	0.04	0.001	30	850	2.0000
	3- Concrete	200	2.1	0.001	2400	850	0.0952
	Total thermal resistance						2.1126
	U value (W/m^2.°C)						0.431
External Wall	1- Gyp board	15.88	0.16	0.001	800.923	1088.57	0.0993
	2- Insulation	89.41	0.046	0.001	19.222	962.964	1.9437
	3- Concrete	203.2	0.26	0.001	464.535	879.228	0.7815
	Total thermal resistance						2.8245
	U value (W/m^2.°C)						0.335
Floor	1-Tiles	20	0.42	0	1200	837	0.0476
	2- Concrete screed	50	1.28	0	2100	1000	0.0391
	3- Concrete	125	0.87	0	1800	920	0.1437
	Total thermal resistance						0.2304
	U value (W/m^2.°C)						2.209
Internal Wall	1- Plaster	25	0.079	0	400	837	0.3165
	2- Foamed slag con.	100	0.317	0	1040	1050	0.3155
	3- Plaster	25	0.079	0	400	837	0.3165
	Total thermal resistance						0.9484
	U value (W/m^2.°C)						0.894
Window frame	1- Wood	25	0.138	0	500	2805	0.1812
	U value (W/m^2.°C)						2.848
Windows	1- Glass	4	1	0.001	0		0.004
	2- Air	16	0.01	1.76E-05	0		1.6
	3- Glass (low-e)	4	1	0.001	0		0.004
			Solar Trans.	Ext. Solar Refl.	Int. Solar Refl.	Ext. Emiss	Int. Emiss
			0.816	0.089	0.089	0.84	0.84
	U value (W/m^2.°C)	0.463	0	0	0	0	0
			0.62	0.082	0.082	0.84	0.1

APPENDIX 3

This appendix presents the monthly, seasonal and annual energy demand results from Chapter 7, Section 7.1, Section 7.2 and Section 7.3.

Table Appendices 5: Section 7.1 - Forms heating and cooling results

Forms - F1

		F01_01		F01_02		F01_03		F01_04		F01_05		F01_06		F01_07	
		Heating	Cooling	Heating	Cooling	Heating	Cooling	Heating	Cooling	Heating	Cooling	Heating	Cooling	Heating	Cooling
Monthly	Jan	24.40	0.00	22.62	0.00	21.73	0.00	21.86	0.00	21.62	0.00	18.86	0.00	20.76	0.00
	Feb	16.78	0.00	15.46	0.00	14.74	0.00	14.95	0.00	14.82	0.00	14.01	0.00	15.84	0.00
	Mar	12.08	0.00	10.82	0.00	10.25	0.00	10.42	0.00	10.31	0.00	10.36	0.00	11.83	0.00
	Apr	4.70	0.02	3.85	0.00	3.58	0.00	3.67	0.00	3.60	0.00	3.79	0.00	4.90	0.00
	May	0.89	0.96	0.59	0.62	0.51	0.46	0.55	0.44	0.50	0.29	0.10	0.00	0.02	0.00
	Jun	0.05	3.03	0.02	2.43	0.01	2.11	0.01	1.96	0.01	1.64	0.00	0.00	0.00	0.00
	Jul	0.00	7.36	0.00	6.37	0.00	5.74	0.00	5.50	0.00	4.93	0.00	0.00	0.00	0.00
	Aug	0.00	7.18	0.00	6.43	0.00	5.83	0.00	5.54	0.00	5.02	0.00	0.08	0.00	0.00
	Sep	0.00	2.97	0.00	2.68	0.00	2.37	0.00	2.29	0.00	2.00	0.00	0.00	0.00	0.00
	Oct	1.20	0.07	0.79	0.04	0.70	0.03	0.72	0.02	0.66	0.01	0.01	0.00	0.00	0.00
	Nov	11.52	0.00	10.04	0.00	9.55	0.00	9.60	0.00	9.42	0.00	7.23	0.00	9.12	0.00
	Dec	22.54	0.00	20.65	0.00	19.83	0.00	19.93	0.00	19.68	0.00	16.45	0.00	18.43	0.00
Annual	Total	94.16	21.60	84.82	18.57	80.89	16.54	81.71	15.74	80.62	13.88	70.80	0.08	80.90	0.00
	H+C	115.76		103.38		97.43		97.45		94.50		70.87		80.90	
Season Aver.	Winter	17.75	0.00	16.30	0.00	15.57	0.00	15.74	0.00	15.58	0.00	14.41	0.00	16.14	0.00
	Spring	1.88	1.34	1.48	1.02	1.37	0.85	1.41	0.80	1.37	0.64	1.30	0.00	1.64	0.00
	Summer	0.00	5.84	0.00	5.16	0.00	4.65	0.00	4.44	0.00	3.98	0.00	0.03	0.00	0.00
	Autumn	11.75	0.02	10.49	0.01	10.03	0.01	10.08	0.01	9.92	0.00	7.90	0.00	9.19	0.00

Forms - F2

		F02_01		F02_02		F02_03		F02_04		F02_05		F02_06		F02_07	
		Heating	Cooling	Heating	Cooling	Heating	Cooling	Heating	Cooling	Heating	Cooling	Heating	Cooling	Heating	Cooling
Monthly	Jan	25.69	0.00	25.46	0.00	23.91	0.00	24.58	0.00	23.74	0.00	21.16	0.00	21.66	0.00
	Feb	17.42	0.00	17.35	0.00	16.17	0.00	17.17	0.00	16.61	0.00	15.90	0.00	16.35	0.00
	Mar	11.75	0.00	11.66	0.00	10.60	0.00	11.46	0.00	10.94	0.00	11.35	0.00	11.63	0.00
	Apr	4.12	0.05	4.05	0.02	3.43	0.00	3.91	0.00	3.48	0.00	4.05	0.00	4.20	0.00
	May	0.60	1.55	0.57	1.20	0.36	0.62	0.48	0.42	0.29	0.09	0.01	0.00	0.02	0.00
	Jun	0.03	4.40	0.02	3.81	0.00	2.87	0.00	2.03	0.00	1.22	0.00	0.00	0.00	0.00
	Jul	0.00	9.71	0.00	8.79	0.00	7.03	0.00	5.64	0.00	4.12	0.00	0.00	0.00	0.00
	Aug	0.00	9.02	0.00	8.23	0.00	6.63	0.00	5.13	0.00	3.77	0.00	0.00	0.00	0.00
	Sep	0.00	3.14	0.00	2.76	0.00	1.93	0.00	1.50	0.00	0.80	0.00	0.00	0.00	0.00
	Oct	1.25	0.05	1.18	0.03	0.90	0.00	1.03	0.00	0.77	0.00	0.00	0.00	0.00	0.00
	Nov	12.40	0.00	12.21	0.00	11.28	0.00	11.65	0.00	11.13	0.00	9.41	0.00	9.90	0.00
	Dec	24.04	0.00	23.77	0.00	22.27	0.00	22.81	0.00	21.93	0.00	18.91	0.00	19.43	0.00
Annual	Total	97.29	27.92	96.27	24.83	88.91	19.09	93.11	14.72	88.88	10.00	80.79	0.00	83.19	0.00
	H+C	125.21		121.10		108.00		107.83		98.88		80.79		83.19	
Season Aver.	Winter	18.29	0.00	18.16	0.00	16.89	0.00	17.74	0.00	17.09	0.00	16.14	0.00	16.55	0.00
	Spring	1.58	2.00	1.55	1.68	1.26	1.17	1.46	0.82	1.25	0.44	1.36	0.00	1.40	0.00
	Summer	0.00	7.29	0.00	6.59	0.00	5.20	0.00	4.09	0.00	2.90	0.00	0.00	0.00	0.00
	Autumn	12.56	0.02	12.39	0.01	11.48	0.00	11.83	0.00	11.28	0.00	9.44	0.00	9.78	0.00

Forms - F3

		F03_01		F03_02		F03_03		F03_04		F03_05		F03_06		F03_07	
		Heating	Cooling	Heating	Cooling	Heating	Cooling	Heating	Cooling	Heating	Cooling	Heating	Cooling	Heating	Cooling
Monthly	Jan	23.54	0.00	22.64	0.00	21.60	0.00	21.86	0.00	21.43	0.00	18.76	0.00	19.70	0.00
	Feb	16.01	0.00	15.34	0.00	14.56	0.00	15.00	0.00	14.77	0.00	14.05	0.00	14.95	0.00
	Mar	11.02	0.00	10.36	0.00	9.71	0.00	10.05	0.00	9.84	0.00	10.15	0.00	10.84	0.00
	Apr	3.97	0.03	3.52	0.01	3.19	0.00	3.37	0.00	3.21	0.00	3.65	0.00	4.17	0.00
	May	0.63	1.23	0.48	1.05	0.38	0.63	0.43	0.57	0.35	0.24	0.02	0.00	0.02	0.00
	Jun	0.03	3.61	0.02	3.31	0.00	2.60	0.01	2.26	0.00	1.60	0.00	0.00	0.00	0.00
	Jul	0.00	8.08	0.00	7.58	0.00	6.29	0.00	5.74	0.00	4.57	0.00	0.00	0.00	0.00
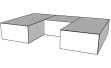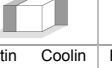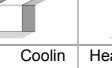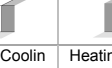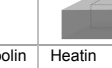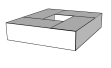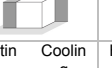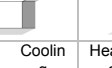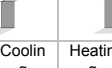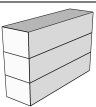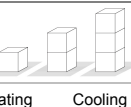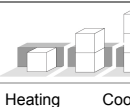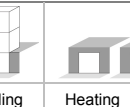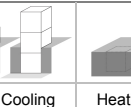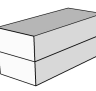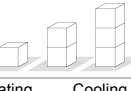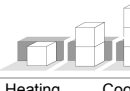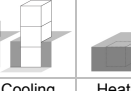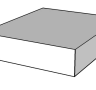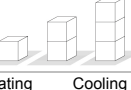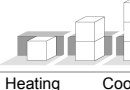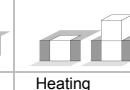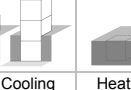
		Heating	Cooling	Heating	Cooling	Heating	Cooling	Heating	Cooling	Heating	Cooling	Heating	Cooling	Heating	Cooling
	Aug	0.00	7.56	0.00	7.19	0.00	6.01	0.00	5.36	0.00	4.32	0.00	0.00	0.00	0.00
	Sep	0.00	2.75	0.00	2.60	0.00	1.99	0.00	1.83	0.00	1.28	0.00	0.00	0.00	0.00
	Oct	1.18	0.05	0.96	0.03	0.82	0.00	0.86	0.00	0.75	0.00	0.00	0.00	0.00	0.00
	Nov	11.31	0.00	10.57	0.00	9.99	0.00	10.10	0.00	9.83	0.00	8.05	0.00	9.01	0.00
	Dec	21.97	0.00	21.02	0.00	20.04	0.00	20.24	0.00	19.79	0.00	16.69	0.00	17.68	0.00
Annual	Total	89.66	23.31	84.92	21.78	80.28	17.52	81.93	15.77	79.97	12.01	71.36	0.00	76.38	0.00
	H+C	112.97		106.69		97.80		97.70		91.98		71.36		76.38	
Season Aver.	Winter	16.86	0.00	16.11	0.00	15.29	0.00	15.64	0.00	15.35	0.00	14.32	0.00	15.17	0.00
	Spring	1.54	1.62	1.34	1.46	1.19	1.08	1.27	0.94	1.19	0.61	1.22	0.00	1.40	0.00
	Summer	0.00	6.13	0.00	5.79	0.00	4.76	0.00	4.31	0.00	3.39	0.00	0.00	0.00	0.00
	Autumn	11.49	0.02	10.85	0.01	10.28	0.00	10.40	0.00	10.12	0.00	8.25	0.00	8.90	0.00

Forms - F4

		F04_01		F04_02		F04_03		F04_04		F04_05		F04_06		F04_07	
		Heating	Cooling	Heating	Cooling	Heating	Cooling	Heating	Cooling	Heating	Cooling	Heating	Cooling	Heating	Cooling
Monthly	Jan	26.90	0.00	25.68	0.00	24.66	0.00	24.89	0.00	24.57	0.00	21.73	0.00	22.64	0.00
	Feb	18.61	0.00	17.70	0.00	16.92	0.00	17.29	0.00	17.13	0.00	16.22	0.00	16.98	0.00
	Mar	13.13	0.00	12.22	0.00	11.58	0.00	11.88	0.00	11.74	0.00	11.76	0.00	12.23	0.00
	Apr	5.07	0.02	4.41	0.00	4.08	0.00	4.25	0.00	4.13	0.00	4.20	0.00	4.39	0.00
	May	0.93	1.09	0.69	0.83	0.59	0.53	0.64	0.50	0.56	0.25	0.09	0.00	0.04	0.00
	Jun	0.05	3.50	0.02	3.08	0.01	2.52	0.01	2.25	0.00	1.72	0.00	0.00	0.00	0.00
	Jul	0.00	8.36	0.00	7.68	0.00	6.64	0.00	6.21	0.00	5.29	0.00	0.05	0.00	0.02
	Aug	0.00	7.97	0.00	7.46	0.00	6.51	0.00	5.98	0.00	5.15	0.00	0.22	0.00	0.07
	Sep	0.00	2.99	0.00	2.79	0.00	2.28	0.00	2.15	0.00	1.68	0.00	0.00	0.00	0.00
	Oct	1.41	0.05	1.09	0.03	0.95	0.01	0.99	0.01	0.89	0.00	0.04	0.00	0.03	0.00
	Nov	13.02	0.00	11.96	0.00	11.39	0.00	11.48	0.00	11.26	0.00	9.17	0.00	9.99	0.00
	Dec	25.03	0.00	23.72	0.00	22.77	0.00	22.94	0.00	22.60	0.00	19.31	0.00	20.29	0.00
Annual	Total	104.17	23.97	97.48	21.88	92.96	18.49	94.36	17.10	92.88	14.09	82.50	0.27	86.58	0.09
	H+C	128.14		119.36		111.45		111.46		106.97		82.77		86.67	
Season Aver.	Winter	19.55	0.00	18.53	0.00	17.72	0.00	18.02	0.00	17.81	0.00	16.57	0.00	17.28	0.00
	Spring	2.02	1.54	1.71	1.31	1.56	1.02	1.63	0.92	1.57	0.66	1.43	0.00	1.48	0.00
	Summer	0.00	6.44	0.00	5.98	0.00	5.15	0.00	4.78	0.00	4.04	0.00	0.09	0.00	0.03
	Autumn	13.16	0.02	12.26	0.01	11.70	0.00	11.80	0.00	11.58	0.00	9.50	0.00	10.10	0.00

Forms - F5

		F05_01		F05_02		F05_03		F05_04		F05_05		F05_06		F05_07	
		Heating	Cooling	Heating	Cooling	Heating	Cooling	Heating	Cooling	Heating	Cooling	Heating	Cooling	Heating	Cooling
Monthly	Jan	27.20	0.00	26.29	0.00	25.14	0.00	25.43	0.00	25.01	0.00	22.02	0.00	23.07	0.00
	Feb	18.66	0.00	17.96	0.00	17.09	0.00	17.58	0.00	17.35	0.00	16.21	0.00	17.20	0.00
	Mar	12.93	0.00	12.23	0.00	11.49	0.00	11.88	0.00	11.66	0.00	11.39	0.00	12.13	0.00
	Apr	4.78	0.03	4.28	0.01	3.88	0.00	4.08	0.00	3.89	0.00	3.53	0.00	4.02	0.00
	May	0.80	1.28	0.63	1.09	0.49	0.67	0.55	0.61	0.45	0.28	0.02	0.00	0.01	0.00
	Jun	0.04	3.95	0.02	3.66	0.00	2.92	0.01	2.55	0.00	1.85	0.00	0.00	0.00	0.00
	Jul	0.00	9.22	0.00	8.76	0.00	7.41	0.00	6.81	0.00	5.60	0.00	0.22	0.00	0.00
	Aug	0.00	8.79	0.00	8.47	0.00	7.23	0.00	6.51	0.00	5.43	0.00	0.47	0.00	0.01
	Sep	0.00	3.27	0.00	3.14	0.00	2.49	0.00	2.30	0.00	1.70	0.00	0.00	0.00	0.00
	Oct	1.33	0.05	1.09	0.04	0.91	0.01	0.97	0.01	0.83	0.00	0.01	0.00	0.00	0.00
	Nov	13.05	0.00	12.26	0.00	11.58	0.00	11.69	0.00	11.40	0.00	9.17	0.00	10.20	0.00
	Dec	25.40	0.00	24.43	0.00	23.34	0.00	23.55	0.00	23.12	0.00	19.70	0.00	20.81	0.00
Annual	Total	104.19	26.59	99.19	25.18	93.92	20.73	95.74	18.79	93.71	14.87	82.05	0.69	87.44	0.01
	H+C	130.78		124.37		114.65		114.53		108.57		82.74		87.45	
Season Aver.	Winter	19.60	0.00	18.83	0.00	17.91	0.00	18.29	0.00	18.01	0.00	16.54	0.00	17.47	0.00
	Spring	1.87	1.75	1.64	1.59	1.46	1.20	1.55	1.05	1.45	0.71	1.18	0.00	1.34	0.00
	Summer	0.00	7.10	0.00	6.79	0.00	5.71	0.00	5.21	0.00	4.24	0.00	0.23	0.00	0.00
	Autumn	13.26	0.02	12.59	0.01	11.94	0.00	12.07	0.00	11.78	0.00	9.63	0.00	10.34	0.00

Table Appendices 6: Section 7.2. Compact forms – heating and cooling results

Compact Form - CompF_3FA

		CompF_3FA_01		CompF_3FA_02		CompF_3FA_03		CompF_3FA_04		CompF_3FA_05	
		Heating	Cooling	Heating	Cooling	Heating	Cooling	Heating	Cooling	Heating	Cooling
Monthly	Jan	25.19	0.00	24.82	0.00	23.62	0.00	23.79	0.00	24.22	0.00
	Feb	17.31	0.00	17.02	0.00	16.49	0.00	16.70	0.00	17.10	0.00
	Mar	11.94	0.00	11.65	0.00	11.45	0.00	11.59	0.00	11.86	0.00
	Apr	4.35	0.07	4.13	0.07	3.88	0.06	3.88	0.06	4.03	0.05
	May	0.54	1.22	0.49	1.19	0.42	1.02	0.39	0.89	0.38	0.88
	Jun	0.03	3.88	0.03	3.82	0.03	3.03	0.02	2.73	0.02	2.70
	Jul	0.00	10.51	0.00	10.42	0.00	7.73	0.00	7.25	0.00	7.18
	Aug	0.00	10.30	0.00	10.26	0.00	7.60	0.00	7.18	0.00	6.98
	Sep	0.00	3.66	0.00	3.65	0.00	2.72	0.00	2.51	0.00	2.42
	Oct	0.81	0.08	0.75	0.08	0.65	0.07	0.60	0.06	0.61	0.06
	Nov	11.85	0.00	11.53	0.00	10.68	0.00	10.64	0.00	11.02	0.00
	Dec	23.23	0.00	22.84	0.00	21.54	0.00	21.64	0.00	22.09	0.00
Annual	Total	95.27	29.71	93.26	29.47	88.76	22.23	89.26	20.68	91.34	20.28
	H+C	124.98		122.74		110.99		109.94		111.62	
Season Aver.	Winter	18.15	0.00	17.83	0.00	17.19	0.00	17.36	0.00	17.73	0.00
	Spring	1.64	1.72	1.55	1.69	1.44	1.37	1.43	1.23	1.48	1.21
	Summer	0.00	8.16	0.00	8.11	0.00	6.02	0.00	5.65	0.00	5.53
	Autumn	11.97	0.03	11.71	0.03	10.96	0.02	10.96	0.02	11.24	0.02

Compact Form - CompF_2FA

		CompF_2FA_01		CompF_2FA_02		CompF_2FA_03		CompF_2FA_04		CompF_2FA_05	
		Heating	Cooling	Heating	Cooling	Heating	Cooling	Heating	Cooling	Heating	Cooling
Monthly	Jan	22.64	0.00	22.07	0.00	20.64	0.00	20.79	0.00	21.43	0.00
	Feb	15.52	0.00	15.07	0.00	14.37	0.00	14.52	0.00	15.11	0.00
	Mar	10.66	0.00	10.23	0.00	9.93	0.00	9.97	0.00	10.36	0.00
	Apr	3.71	0.08	3.40	0.08	3.09	0.06	3.04	0.02	3.24	0.02
	May	0.45	1.20	0.38	1.17	0.32	1.00	0.27	0.79	0.26	0.75
	Jun	0.03	3.47	0.03	3.36	0.02	2.64	0.01	2.33	0.01	2.27
	Jul	0.00	8.93	0.00	8.76	0.00	6.02	0.00	5.58	0.00	5.44
	Aug	0.00	8.65	0.00	8.56	0.00	5.83	0.00	5.44	0.00	5.14
	Sep	0.00	3.04	0.00	3.00	0.00	2.12	0.00	1.90	0.00	1.75
	Oct	0.76	0.08	0.67	0.08	0.58	0.06	0.51	0.04	0.54	0.02
	Nov	10.65	0.00	10.17	0.00	9.29	0.00	9.22	0.00	9.81	0.00
	Dec	20.94	0.00	20.34	0.00	18.88	0.00	18.96	0.00	19.64	0.00
Annual	Total	85.35	25.45	82.36	25.00	77.13	17.73	77.30	16.10	80.38	15.38
	H+C	110.80		107.37		94.86		93.40		95.77	
Season Average	Winter	16.27	0.00	15.79	0.00	14.98	0.00	15.09	0.00	15.63	0.00
	Spring	1.40	1.58	1.27	1.54	1.15	1.23	1.11	1.05	1.17	1.01
	Summer	0.00	6.87	0.00	6.77	0.00	4.66	0.00	4.31	0.00	4.11
	Autumn	10.78	0.03	10.40	0.03	9.58	0.02	9.56	0.01	9.99	0.01

Compact Form - CompF_1F

		CompF_1F_01		CompF_1F_02		CompF_1F_03		CompF_1F_04		CompF_1F_05	
		Heating	Cooling	Heating	Cooling	Heating	Cooling	Heating	Cooling	Heating	Cooling
Monthly	Jan	23.54	0.00	22.65	0.00	21.45	0.00	18.77	0.00	19.72	0.00
	Feb	16.01	0.00	15.34	0.00	14.78	0.00	14.06	0.00	14.96	0.00
	Mar	11.02	0.00	10.36	0.00	9.86	0.00	10.16	0.00	10.85	0.00
	Apr	3.97	0.03	3.53	0.01	3.22	0.00	3.66	0.00	4.18	0.00
	May	0.63	1.23	0.48	1.05	0.35	0.24	0.02	0.00	0.02	0.00
	Jun	0.03	3.61	0.02	3.31	0.00	1.60	0.00	0.00	0.00	0.00
	Jul	0.00	8.08	0.00	7.59	0.00	4.57	0.00	0.00	0.00	0.00
	Aug	0.00	7.56	0.00	7.19	0.00	4.32	0.00	0.00	0.00	0.00
	Sep	0.00	2.75	0.00	2.60	0.00	1.28	0.00	0.00	0.00	0.00
	Oct	1.18	0.05	0.96	0.03	0.75	0.00	0.00	0.00	0.00	0.00
	Nov	11.31	0.00	10.57	0.00	9.84	0.00	8.06	0.00	9.03	0.00
	Dec	21.97	0.00	21.03	0.00	19.82	0.00	16.71	0.00	17.71	0.00
Annual	Total	89.66	23.31	84.94	21.78	80.07	12.02	71.44	0.00	76.47	0.00
	H+C	112.97		106.72		92.09		71.44		76.47	
Season Average	Winter	16.86	0.00	16.12	0.00	15.37	0.00	14.33	0.00	15.18	0.00
	Spring	1.54	1.62	1.34	1.46	1.19	0.62	1.23	0.00	1.40	0.00
	Summer	0.00	6.13	0.00	5.79	0.00	3.39	0.00	0.00	0.00	0.00
	Autumn	11.49	0.02	10.85	0.01	10.14	0.00	8.26	0.00	8.91	0.00
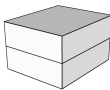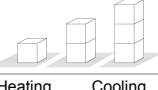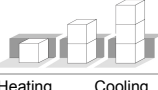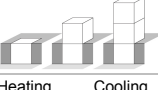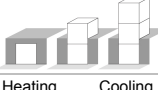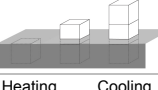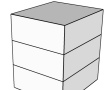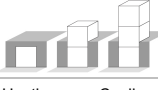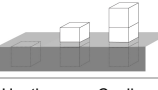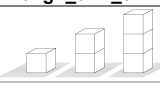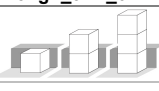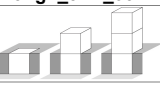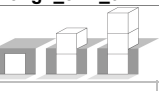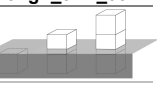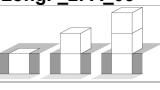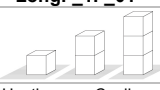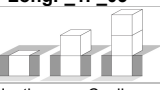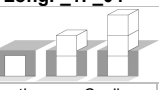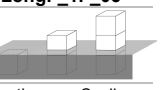
Compact Form - CompF_2FB										
		CompF_2FB_01		**CompF_2FB_02**		**CompF_2FB_03**		**CompF_2FB_04**		**CompF_2FB_05**
		Heating	Cooling	Heating	Cooling	Heating	Cooling	Heating	Cooling	Heating	Cooling
Monthly	Jan	21.16	0.00	20.34	0.00	19.11	0.00	18.78	0.00	19.55	0.00
	Feb	14.60	0.00	13.96	0.00	13.29	0.00	13.09	0.00	13.83	0.00
	Mar	10.27	0.00	9.69	0.00	9.36	0.00	9.21	0.00	9.74	0.00
	Apr	3.72	0.06	3.29	0.06	3.05	0.05	2.97	0.02	3.25	0.01
	May	0.50	1.00	0.40	0.97	0.35	0.87	0.32	0.69	0.31	0.61
	Jun	0.03	2.81	0.03	2.68	0.02	2.32	0.02	1.99	0.02	1.88
	Jul	0.00	7.56	0.00	7.28	0.00	5.40	0.00	4.82	0.00	4.54
	Aug	0.00	7.44	0.00	7.27	0.00	5.34	0.00	4.81	0.00	4.33
	Sep	0.00	2.75	0.00	2.67	0.00	2.02	0.00	1.78	0.00	1.54
	Oct	0.70	0.08	0.59	0.08	0.53	0.07	0.48	0.04	0.53	0.02
	Nov	9.87	0.00	9.20	0.00	8.43	0.00	8.17	0.00	8.93	0.00
	Dec	19.48	0.00	18.63	0.00	17.39	0.00	17.04	0.00	17.86	0.00
Annual	Total	80.32	21.71	76.11	21.02	71.53	16.07	70.08	14.15	74.01	12.94
	H+C	102.03		97.13		87.60		84.23		86.95	
Season Average	Winter	15.34	0.00	14.66	0.00	13.92	0.00	13.70	0.00	14.37	0.00
	Spring	1.41	1.29	1.24	1.24	1.14	1.08	1.10	0.90	1.19	0.83
	Summer	0.00	5.92	0.00	5.74	0.00	4.25	0.00	3.80	0.00	3.47
	Autumn	10.02	0.03	9.47	0.03	8.78	0.02	8.56	0.01	9.11	0.01

Forms - CompF_3FB										
		CompF_3FB_01		**CompF_3FB_02**		**CompF_3FB_03**		**CompF_3FB_04**		**CompF_3FB_05**
		Heating	Cooling	Heating	Cooling	Heating	Cooling	Heating	Cooling	Heating	Cooling
Monthly	Jan	21.47	0.00	20.78	0.00	19.81	0.00	19.54	0.00	20.19	0.00
	Feb	14.95	0.00	14.42	0.00	13.91	0.00	13.76	0.00	14.41	0.00
	Mar	10.80	0.00	10.32	0.00	10.09	0.00	10.00	0.00	10.48	0.00
	Apr	4.23	0.04	3.86	0.04	3.73	0.04	3.67	0.04	3.96	0.03
	May	0.64	0.77	0.54	0.75	0.48	0.70	0.46	0.64	0.45	0.62
	Jun	0.03	2.38	0.03	2.28	0.03	2.06	0.03	1.86	0.03	1.79
	Jul	0.00	7.35	0.00	7.11	0.00	5.73	0.00	5.28	0.00	5.09
	Aug	0.00	7.45	0.00	7.32	0.00	5.83	0.00	5.42	0.00	5.08
	Sep	0.00	2.89	0.00	2.83	0.00	2.29	0.00	2.10	0.00	1.91
	Oct	0.66	0.08	0.58	0.07	0.53	0.07	0.50	0.06	0.53	0.06
	Nov	9.95	0.00	9.38	0.00	8.71	0.00	8.50	0.00	9.12	0.00
	Dec	19.61	0.00	18.89	0.00	17.89	0.00	17.61	0.00	18.30	0.00
Annual	Total	82.34	20.96	78.79	20.41	75.19	16.72	74.07	15.40	77.46	14.59
	H+C	103.31		99.20		91.91		89.46		92.05	
Season Average	Winter	15.74	0.00	15.17	0.00	14.60	0.00	14.43	0.00	15.03	0.00
	Spring	1.63	1.07	1.47	1.03	1.41	0.94	1.39	0.84	1.48	0.82
	Summer	0.00	5.90	0.00	5.75	0.00	4.61	0.00	4.27	0.00	4.03
	Autumn	10.08	0.03	9.62	0.02	9.05	0.02	8.87	0.02	9.31	0.02

Table Appendices 7: Section 7.2. Long forms – heating and cooling results

Long Form - LongF_3FA										
		LongF_3FA_01		LongF_3FA_02		LongF_3FA_03		LongF_3FA_04		LongF_3FA_05
		Heating	Cooling	Heating	Cooling	Heating	Cooling	Heating	Cooling	Heating	Cooling

		Heating	Cooling	Heating	Cooling	Heating	Cooling	Heating	Cooling	Heating	Cooling
Monthly	Jan	21.21	0.00	20.42	0.00	19.51	0.00	19.52	0.00	20.36	0.00
	Feb	14.82	0.00	14.22	0.00	13.72	0.00	13.76	0.00	14.58	0.00
	Mar	10.86	0.00	10.31	0.00	10.07	0.00	10.09	0.00	10.71	0.00
	Apr	4.34	0.04	3.93	0.04	3.81	0.04	3.77	0.03	4.12	0.03
	May	0.70	0.71	0.58	0.69	0.53	0.65	0.49	0.60	0.47	0.58
	Jun	0.03	2.16	0.03	2.06	0.03	1.90	0.03	1.77	0.03	1.71
	Jul	0.00	6.89	0.00	6.60	0.00	5.44	0.00	5.19	0.00	5.01
	Aug	0.00	7.08	0.00	6.91	0.00	5.62	0.00	5.41	0.00	5.06
	Sep	0.00	2.85	0.00	2.78	0.00	2.28	0.00	2.19	0.00	1.97
	Oct	0.65	0.08	0.56	0.08	0.52	0.07	0.49	0.07	0.51	0.06
	Nov	9.78	0.00	9.13	0.00	8.51	0.00	8.39	0.00	9.12	0.00
	Dec	19.32	0.00	18.48	0.00	17.55	0.00	17.51	0.00	18.38	0.00
Annual	Total	81.72	19.80	77.67	19.16	74.24	16.01	74.04	15.27	78.28	14.43
	H+C	101.52		96.83		90.25		89.31		92.71	
Season Average	Winter	15.63	0.00	14.98	0.00	14.43	0.00	14.46	0.00	15.22	0.00
	Spring	1.69	0.97	1.51	0.93	1.46	0.86	1.43	0.80	1.54	0.78
	Summer	0.00	5.61	0.00	5.43	0.00	4.45	0.00	4.26	0.00	4.01
	Autumn	9.92	0.03	9.39	0.03	8.86	0.02	8.80	0.02	9.34	0.02

Long Form - LongF_2FA										
		LongF_2FA_01		LongF_2FA_02		LongF_2FA_03		LongF_2FA_04		LongF_2FA_05
		Heating	Cooling	Heating	Cooling	Heating	Cooling	Heating	Cooling	Heating	Cooling

		Heating	Cooling	Heating	Cooling	Heating	Cooling	Heating	Cooling	Heating	Cooling
Monthly	Jan	20.95	0.00	19.76	0.00	18.71	0.00	18.70	0.00	19.94	0.00
	Feb	14.55	0.00	13.64	0.00	13.01	0.00	13.01	0.00	14.19	0.00
	Mar	10.58	0.00	9.77	0.00	9.41	0.00	9.35	0.00	10.20	0.00
	Apr	4.05	0.05	3.46	0.05	3.26	0.04	3.17	0.02	3.58	0.01
	May	0.64	0.84	0.48	0.82	0.43	0.76	0.38	0.65	0.35	0.55
	Jun	0.03	2.35	0.03	2.22	0.03	2.05	0.02	1.89	0.01	1.77
	Jul	0.00	6.69	0.00	6.25	0.00	5.02	0.00	4.79	0.00	4.46
	Aug	0.00	6.79	0.00	6.50	0.00	5.17	0.00	4.99	0.00	4.33
	Sep	0.00	2.74	0.00	2.62	0.00	2.11	0.00	2.01	0.00	1.63
	Oct	0.68	0.09	0.55	0.10	0.51	0.09	0.45	0.07	0.50	0.03
	Nov	9.64	0.00	8.68	0.00	8.00	0.00	7.87	0.00	8.95	0.00
	Dec	19.14	0.00	17.90	0.00	16.86	0.00	16.80	0.00	18.10	0.00
Annual	Total	80.27	19.55	74.27	18.56	70.22	15.25	69.75	14.41	75.83	12.79
	H+C	99.82		92.83		85.47		84.17		88.62	
Season Average	Winter	15.36	0.00	14.39	0.00	13.71	0.00	13.69	0.00	14.78	0.00
	Spring	1.57	1.08	1.32	1.03	1.24	0.95	1.19	0.85	1.31	0.78
	Summer	0.00	5.41	0.00	5.13	0.00	4.10	0.00	3.93	0.00	3.48
	Autumn	9.82	0.03	9.05	0.03	8.46	0.03	8.37	0.02	9.19	0.01

Long Form - LongF_1F										
		LongF_1F_01		LongF_1F_02		LongF_1F_03		LongF_1F_04		LongF_1F_05
		Heating	Cooling	Heating	Cooling	Heating	Cooling	Heating	Cooling	Heating	Cooling

		Heating	Cooling	Heating	Cooling	Heating	Cooling	Heating	Cooling	Heating	Cooling
Monthly	Jan	24.40	0.00	22.63	0.00	21.62	0.00	18.87	0.00	20.78	0.00
	Feb	16.78	0.00	15.46	0.00	14.82	0.00	14.02	0.00	15.86	0.00
	Mar	12.08	0.00	10.83	0.00	10.31	0.00	10.38	0.00	11.85	0.00
	Apr	4.70	0.02	3.85	0.00	3.60	0.00	3.79	0.00	4.90	0.00
	May	0.89	0.96	0.59	0.62	0.50	0.29	0.10	0.00	0.02	0.00
	Jun	0.05	3.03	0.02	2.43	0.01	1.64	0.00	0.00	0.00	0.00
	Jul	0.00	7.36	0.00	6.38	0.00	4.93	0.00	0.00	0.00	0.00
	Aug	0.00	7.18	0.00	6.43	0.00	5.02	0.00	0.08	0.00	0.00
	Sep	0.00	2.97	0.00	2.68	0.00	2.00	0.00	0.00	0.00	0.00
	Oct	1.20	0.07	0.79	0.04	0.66	0.01	0.01	0.00	0.00	0.00
	Nov	11.52	0.00	10.05	0.00	9.42	0.00	7.24	0.00	9.14	0.00
	Dec	22.54	0.00	20.66	0.00	19.68	0.00	16.46	0.00	18.45	0.00
Annual	Total	94.16	21.60	84.88	18.58	80.62	13.88	70.86	0.08	80.99	0.00
	H+C	115.76		103.46		94.50		70.94		80.99	
Season Average	Winter	17.75	0.00	16.31	0.00	15.58	0.00	14.42	0.00	16.16	0.00
	Spring	1.88	1.34	1.48	1.02	1.37	0.64	1.30	0.00	1.64	0.00
	Summer	0.00	5.84	0.00	5.16	0.00	3.98	0.00	0.03	0.00	0.00
	Autumn	11.75	0.02	10.50	0.01	9.92	0.00	7.90	0.00	9.20	0.00
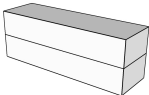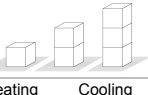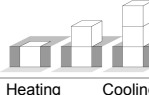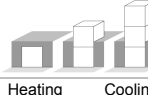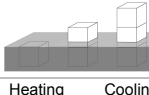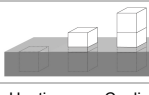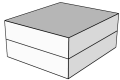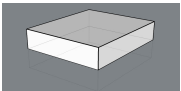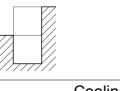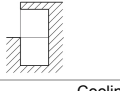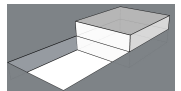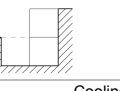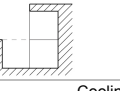
Long Form - LongF_2FB									
LongF_2FB_01		**LongF_2FB_02**		**LongF_2FB_03**		**LongF_2FB_04**		**LongF_2FB_05**	
Heating	Cooling	Heating	Cooling	Heating	Cooling	Heating	Cooling	Heating	Cooling

		LongF_2FB_01		LongF_2FB_02		LongF_2FB_03		LongF_2FB_04		LongF_2FB_05	
		Heating	Cooling	Heating	Cooling	Heating	Cooling	Heating	Cooling	Heating	Cooling
Monthly	Jan	22.04	0.00	20.39	0.00	19.44	0.00	19.01	0.00	20.50	0.00
	Feb	15.42	0.00	14.16	0.00	13.54	0.00	13.25	0.00	14.72	0.00
	Mar	11.59	0.00	10.48	0.00	10.07	0.00	9.85	0.00	10.96	0.00
	Apr	4.72	0.04	3.91	0.04	3.72	0.03	3.59	0.02	4.18	0.00
	May	0.88	0.73	0.64	0.71	0.59	0.68	0.55	0.56	0.50	0.42
	Jun	0.05	2.07	0.04	1.95	0.04	1.86	0.03	1.64	0.03	1.43
	Jul	0.00	6.36	0.00	5.74	0.00	4.91	0.00	4.51	0.00	3.90
	Aug	0.00	6.70	0.00	6.28	0.00	5.34	0.00	4.99	0.00	3.91
	Sep	0.00	3.00	0.00	2.85	0.00	2.43	0.00	2.28	0.00	1.61
	Oct	0.71	0.12	0.54	0.12	0.52	0.12	0.45	0.10	0.53	0.04
	Nov	10.01	0.00	8.68	0.00	8.08	0.00	7.75	0.00	8.97	0.00
	Dec	19.97	0.00	18.23	0.00	17.30	0.00	16.85	0.00	18.43	0.00
Annual	Total	85.39	19.03	77.08	17.69	73.30	15.38	71.34	14.09	78.82	11.31
	H+C	104.41		94.77		88.68		85.44		90.13	
Season Average	Winter	16.35	0.00	15.01	0.00	14.35	0.00	14.04	0.00	15.39	0.00
	Spring	1.88	0.95	1.53	0.90	1.45	0.86	1.39	0.74	1.57	0.62
	Summer	0.00	5.35	0.00	4.96	0.00	4.23	0.00	3.93	0.00	3.14
	Autumn	10.23	0.04	9.15	0.04	8.63	0.04	8.35	0.03	9.31	0.01

Long Form - LongF_3FB											
		LongF_3FB_01		LongF_3FB_02		LongF_3FB_03		LongF_3FB_04		LongF_3FB_05	
		Heating	Cooling	Heating	Cooling	Heating	Cooling	Heating	Cooling	Heating	Cooling
Monthly	Jan	22.74	0.00	21.35	0.00	20.60	0.00	20.25	0.00	21.50	0.00
	Feb	16.08	0.00	15.03	0.00	14.54	0.00	14.29	0.00	15.56	0.00
	Mar	12.47	0.00	11.56	0.00	11.24	0.00	11.06	0.00	12.07	0.00
	Apr	5.48	0.02	4.81	0.02	4.67	0.02	4.56	0.02	5.17	0.02
	May	1.19	0.52	0.94	0.51	0.90	0.50	0.86	0.47	0.79	0.44
	Jun	0.05	1.59	0.05	1.51	0.05	1.47	0.05	1.36	0.04	1.28
	Jul	0.00	6.01	0.00	5.51	0.00	4.92	0.00	4.62	0.00	4.22
	Aug	0.00	6.64	0.00	6.30	0.00	5.59	0.00	5.33	0.00	4.53
	Sep	0.00	3.24	0.00	3.13	0.00	2.79	0.00	2.67	0.00	2.09
	Oct	0.69	0.13	0.56	0.13	0.55	0.12	0.51	0.11	0.55	0.09
	Nov	10.26	0.00	9.15	0.00	8.66	0.00	8.37	0.00	9.27	0.00
	Dec	20.39	0.00	18.93	0.00	18.19	0.00	17.81	0.00	19.12	0.00
Annual	Total	89.35	18.17	82.39	17.12	79.39	15.41	77.75	14.59	84.08	12.67
	H+C	107.51		99.51		94.80		92.34		96.75	
Season Average	Winter	17.09	0.00	15.98	0.00	15.46	0.00	15.20	0.00	16.38	0.00
	Spring	2.24	0.71	1.93	0.68	1.87	0.66	1.82	0.62	2.00	0.58
	Summer	0.00	5.30	0.00	4.98	0.00	4.43	0.00	4.21	0.00	3.61
	Autumn	10.45	0.04	9.55	0.04	9.13	0.04	8.90	0.04	9.65	0.03

Table Appendices 8: Section 7.3. Compact form – Above Ground, Basement and Basement with Courtyard - heating and cooling results

		Compact Form – Above Ground					
		CompF_Abv_01		**CompF_Abv_02**		**CompF_Abv_03**	
		Heating	Cooling	Heating	Cooling	Heating	Cooling
Monthly	Jan	17.99	0.00	16.63	0.00	16.54	0.00
	Feb	12.46	0.00	11.91	0.00	12.61	0.00
	Mar	8.74	0.00	8.29	0.00	9.35	0.00
	Apr	3.10	0.06	2.68	0.00	3.50	0.00
	May	0.38	0.94	0.13	0.24	0.05	0.00
	Jun	0.02	2.42	0.00	1.16	0.00	0.00
	Jul	0.00	6.09	0.00	3.21	0.00	0.10
	Aug	0.00	5.87	0.00	3.10	0.00	0.26
	Sep	0.00	2.03	0.00	1.02	0.00	0.00
	Oct	0.62	0.06	0.24	0.00	0.00	0.00
	Nov	8.58	0.00	7.29	0.00	6.72	0.00
	Dec	16.64	0.00	15.06	0.00	14.50	0.00
Annual	Total	68.53	17.47	62.22	8.73	63.29	0.36
	H+C	86.00		70.95		63.65	
Season Average	Winter	13.06	0.00	12.28	0.00	12.84	0.00
	Spring	1.17	1.14	0.94	0.47	1.18	0.00
	Summer	0.00	4.66	0.00	2.44	0.00	0.12
	Autumn	8.61	0.02	7.53	0.00	7.07	0.00
		Compact Form - Basement					
		CompF_Bsmt_01		**CompF_Bsmt_02**		**CompF_Bsmt_03**	
		Heating	Cooling	Heating	Cooling	Heating	Cooling
Monthly	Jan	17.09	0.00	17.14	0.00	17.04	0.00
	Feb	12.18	0.00	12.42	0.00	13.13	0.00
	Mar	8.74	0.00	8.72	0.00	9.80	0.00
	Apr	3.22	0.04	3.01	0.00	3.88	0.00
	May	0.28	0.80	0.12	0.22	0.03	0.00
	Jun	0.02	2.07	0.00	1.13	0.00	0.00
	Jul	0.00	4.58	0.00	3.10	0.00	0.08
	Aug	0.00	4.28	0.00	2.98	0.00	0.22
	Sep	0.00	1.56	0.00	0.96	0.00	0.00
	Oct	0.54	0.04	0.26	0.00	0.00	0.00
	Nov	8.32	0.00	7.85	0.00	7.28	0.00
	Dec	15.76	0.00	15.60	0.00	15.03	0.00
Annual	Total	66.15	13.38	65.12	8.39	66.19	0.30
	H+C	79.53		73.51		66.49	
Season Average	Winter	12.67	0.00	12.76	0.00	13.32	0.00
	Spring	1.17	0.97	1.04	0.45	1.30	0.00
	Summer	0.00	3.47	0.00	2.35	0.00	0.10
	Autumn	8.21	0.01	7.90	0.00	7.44	0.00
		Compact Form – Basement with Courtyard - 01Crt					
		CompF_01Crt_01		CompF_01Crt_02		CompF_01Crt_03	
		Heating	Cooling	Heating	Cooling	Heating	Cooling
Monthly	Jan	16.56	0.00	16.88	0.00	16.98	0.00
	Feb	11.64	0.00	11.96	0.00	12.06	0.00
	Mar	8.29	0.00	8.56	0.00	8.64	0.00
	Apr	2.90	0.05	3.08	0.05	3.14	0.05
	May	0.29	0.82	0.28	0.81	0.28	0.81
	Jun	0.02	2.11	0.02	2.09	0.02	2.08
	Jul	0.00	4.67	0.00	4.62	0.00	4.61
	Aug	0.00	4.41	0.00	4.34	0.00	4.32
	Sep	0.00	1.64	0.00	1.59	0.00	1.58
	Oct	0.50	0.05	0.52	0.04	0.53	0.04
	Nov	7.76	0.00	8.10	0.00	8.21	0.00
	Dec	15.22	0.00	15.55	0.00	15.65	0.00
Annual	Total	63.18	13.75	64.97	13.55	65.52	13.48
	H+C	76.93		78.52		79.00	
Season Average	Winter	12.16	0.00	12.47	0.00	12.56	0.00
	Spring	1.07	0.99	1.13	0.98	1.15	0.98
	Summer	0.00	3.58	0.00	3.52	0.00	3.50
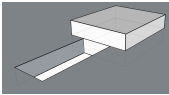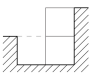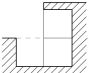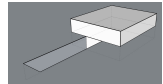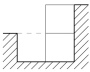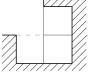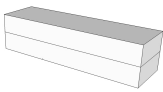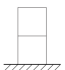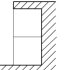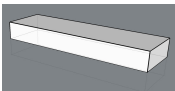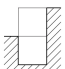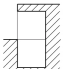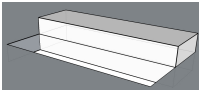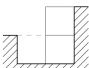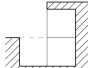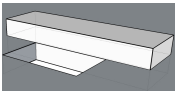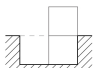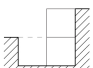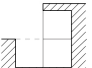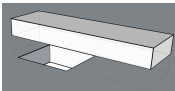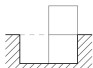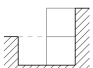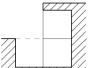
| | Autumn | 7.83 | 0.02 | 8.06 | 0.01 | 8.13 | 0.01 |

Compact Form – Basement with Courtyard - 02Crt

		CompF_02Crt_01		CompF_02Crt_02		CompF_02Crt_03	
		Heating	Cooling	Heating	Cooling	Heating	Cooling
Monthly	Jan	16.61	0.00	17.45	0.00	17.03	0.00
	Feb	11.88	0.00	12.62	0.00	12.31	0.00
	Mar	8.26	0.00	8.86	0.00	8.62	0.00
	Apr	2.68	0.00	3.03	0.00	2.93	0.00
	May	0.13	0.24	0.13	0.23	0.12	0.23
	Jun	0.00	1.15	0.00	1.13	0.00	1.14
	Jul	0.00	3.18	0.00	3.13	0.00	3.12
	Aug	0.00	3.09	0.00	3.02	0.00	3.01
	Sep	0.00	1.01	0.00	0.98	0.00	0.97
	Oct	0.24	0.00	0.25	0.00	0.26	0.00
	Nov	7.29	0.00	7.87	0.00	7.74	0.00
	Dec	15.06	0.00	15.84	0.00	15.49	0.00
Annual	Total	62.14	8.66	66.05	8.48	64.49	8.47
	H+C	70.81		74.53		72.96	
Season Average	Winter	12.25	0.00	12.98	0.00	12.65	0.00
	Spring	0.94	0.46	1.05	0.45	1.02	0.45
	Summer	0.00	2.43	0.00	2.37	0.00	2.37
	Autumn	7.53	0.00	7.99	0.00	7.83	0.00

Compact Form – Basement with Courtyard - 03Crt

		CompF_03Crt_01		CompF_03Crt_02		CompF_03Crt_03	
		Heating	Cooling	Heating	Cooling	Heating	Cooling
Monthly	Jan	16.52	0.00	16.84	0.00	16.89	0.00
	Feb	12.59	0.00	12.91	0.00	13.00	0.00
	Mar	9.32	0.00	9.60	0.00	9.69	0.00
	Apr	3.52	0.00	3.73	0.00	3.82	0.00
	May	0.04	0.00	0.03	0.00	0.03	0.00
	Jun	0.00	0.00	0.00	0.00	0.00	0.00
	Jul	0.00	0.09	0.00	0.09	0.00	0.08
	Aug	0.00	0.25	0.00	0.23	0.00	0.22
	Sep	0.00	0.00	0.00	0.00	0.00	0.00
	Oct	0.00	0.00	0.00	0.00	0.00	0.00
	Nov	6.72	0.00	7.07	0.00	7.21	0.00
	Dec	14.50	0.00	14.83	0.00	14.90	0.00
Annual	Total	63.22	0.35	65.01	0.32	65.54	0.30
	H+C	63.56		65.33		65.84	
Season Average	Winter	12.81	0.00	13.12	0.00	13.20	0.00
	Spring	1.19	0.00	1.25	0.00	1.28	0.00
	Summer	0.00	0.12	0.00	0.11	0.00	0.10
	Autumn	7.07	0.00	7.30	0.00	7.37	0.00

Table Appendices 9: Section 7.3. Long form – Above Ground, Basement and Basement with Courtyard - heating and cooling results

		Long Form – Above Ground					
		LongF_Abv_01		LongF_Abv_02		LongF_Abv_03	
		Heating	Cooling	Heating	Cooling	Heating	Cooling
Monthly	Jan	18.69	0.00	16.53	0.00	16.28	0.00
	Feb	13.12	0.00	11.70	0.00	12.28	0.00
	Mar	9.73	0.00	8.45	0.00	9.35	0.00
	Apr	3.86	0.04	2.90	0.00	3.55	0.00
	May	0.65	0.73	0.26	0.27	0.16	0.00
	Jun	0.04	1.94	0.00	1.17	0.00	0.00
	Jul	0.00	5.28	0.00	3.34	0.00	0.25
	Aug	0.00	5.37	0.00	3.55	0.00	0.58
	Sep	0.00	2.21	0.00	1.51	0.00	0.16
	Oct	0.63	0.09	0.20	0.02	0.00	0.00
	Nov	8.66	0.00	6.58	0.00	5.70	0.00
	Dec	17.05	0.00	14.61	0.00	13.88	0.00
Annual	Total	72.42	15.65	61.23	9.86	61.18	0.99
	H+C	88.08		71.09		62.18	
Season Average	Winter	13.85	0.00	12.22	0.00	12.63	0.00
	Spring	1.52	0.90	1.06	0.48	1.23	0.00
	Summer	0.00	4.29	0.00	2.80	0.00	0.33
	Autumn	8.78	0.03	7.13	0.01	6.53	0.00

		Long Form - Basement					
		LongF_Bsmt_01		LongF_Bsmt_02		LongF_Bsmt_03	
		Heating	Cooling	Heating	Cooling	Heating	Cooling
Monthly	Jan	17.95	0.00	17.54	0.00	17.28	0.00
	Feb	12.97	0.00	12.74	0.00	13.32	0.00
	Mar	9.74	0.00	9.34	0.00	10.27	0.00
	Apr	3.99	0.03	3.56	0.00	4.33	0.00
	May	0.45	0.62	0.23	0.23	0.13	0.00
	Jun	0.03	1.71	0.00	1.11	0.00	0.00
	Jul	0.00	4.08	0.00	3.15	0.00	0.20
	Aug	0.00	3.97	0.00	3.24	0.00	0.48
	Sep	0.00	1.64	0.00	1.34	0.00	0.09
	Oct	0.54	0.06	0.23	0.02	0.00	0.00
	Nov	8.46	0.00	7.60	0.00	6.73	0.00
	Dec	16.32	0.00	15.67	0.00	14.93	0.00
Annual	Total	70.45	12.10	66.91	9.09	66.99	0.77
	H+C	82.55		75.99		67.76	
Season Average	Winter	13.55	0.00	13.21	0.00	13.62	0.00
	Spring	1.49	0.79	1.26	0.45	1.49	0.00
	Summer	0.00	3.23	0.00	2.58	0.00	0.26
	Autumn	8.44	0.02	7.83	0.01	7.22	0.00
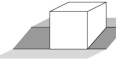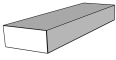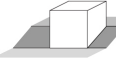
		Long Form – Basement with Courtyard - 01Crt					
		LongF_01Crt_01		LongF_01Crt_02		LongF_01Crt_03	
		Heating	Cooling	Heating	Cooling	Heating	Cooling
Monthly	Jan	16.78	0.00	17.43	0.00	17.64	0.00
	Feb	11.76	0.00	12.44	0.00	12.65	0.00
	Mar	8.71	0.00	9.27	0.00	9.46	0.00
	Apr	3.30	0.04	3.64	0.03	3.77	0.03
	May	0.48	0.67	0.46	0.64	0.46	0.64
	Jun	0.03	1.76	0.03	1.73	0.03	1.72
	Jul	0.00	4.24	0.00	4.16	0.00	4.13
	Aug	0.00	4.24	0.00	4.08	0.00	4.04
	Sep	0.00	1.83	0.00	1.72	0.00	1.69
	Oct	0.47	0.08	0.51	0.07	0.52	0.06
	Nov	7.31	0.00	7.93	0.00	8.15	0.00
	Dec	15.15	0.00	15.81	0.00	16.02	0.00
Annual	Total	64.00	12.85	67.52	12.43	68.71	12.31
	H+C	76.85		79.95		81.02	
Season Average	Winter	12.42	0.00	13.05	0.00	13.25	0.00
	Spring	1.27	0.82	1.38	0.80	1.42	0.80
	Summer	0.00	3.44	0.00	3.32	0.00	3.28
	Autumn	7.65	0.03	8.08	0.02	8.23	0.02

Long Form – Basement with Courtyard - 02Crt					
LongF_02Crt_01		**LongF_02Crt_02**		**LongF_02Crt_03**	
Heating	Cooling	Heating	Cooling	Heating	Cooling

		Heating	Cooling	Heating	Cooling	Heating	Cooling
Monthly	Jan	16.37	0.00	17.02	0.00	17.23	0.00
	Feb	11.54	0.00	12.21	0.00	12.43	0.00
	Mar	8.30	0.00	8.87	0.00	9.06	0.00
	Apr	2.86	0.00	3.21	0.00	3.34	0.00
	May	0.26	0.26	0.24	0.25	0.24	0.24
	Jun	0.00	1.15	0.00	1.13	0.00	1.12
	Jul	0.00	3.30	0.00	3.22	0.00	3.19
	Aug	0.00	3.48	0.00	3.34	0.00	3.31
	Sep	0.00	1.50	0.00	1.40	0.00	1.38
	Oct	0.19	0.02	0.21	0.02	0.22	0.02
	Nov	6.45	0.00	7.07	0.00	7.29	0.00
	Dec	14.51	0.00	15.15	0.00	15.37	0.00
Annual	Total	60.48	9.70	63.99	9.36	65.18	9.26
	H+C	70.18		73.34		74.43	
Season Average	Winter	12.07	0.00	12.70	0.00	12.91	0.00
	Spring	1.04	0.47	1.15	0.46	1.19	0.45
	Summer	0.00	2.76	0.00	2.66	0.00	2.63
	Autumn	7.05	0.01	7.48	0.01	7.62	0.01

Long Form – Basement with Courtyard - 03Crt					
LongF_03Crt_01		**LongF_03Crt_02**		**LongF_03Crt_03**	
Heating	Cooling	Heating	Cooling	Heating	Cooling

		Heating	Cooling	Heating	Cooling	Heating	Cooling
Monthly	Jan	16.12	0.00	16.76	0.00	16.98	0.00
	Feb	12.12	0.00	12.79	0.00	13.00	0.00
	Mar	9.20	0.00	9.79	0.00	9.98	0.00
	Apr	3.52	0.00	3.95	0.00	4.10	0.00
	May	0.15	0.00	0.13	0.00	0.12	0.00
	Jun	0.00	0.00	0.00	0.00	0.00	0.00
	Jul	0.00	0.24	0.00	0.21	0.00	0.21
	Aug	0.00	0.56	0.00	0.52	0.00	0.51
	Sep	0.00	0.15	0.00	0.12	0.00	0.11
	Oct	0.00	0.00	0.00	0.00	0.00	0.00
	Nov	5.57	0.00	6.20	0.00	6.42	0.00
	Dec	13.78	0.00	14.42	0.00	14.63	0.00
Annual	Total	60.46	0.95	64.04	0.85	65.23	0.82
	H+C	61.41		64.89		66.05	
Season Average	Winter	12.48	0.00	13.11	0.00	13.32	0.00
	Spring	1.22	0.00	1.36	0.00	1.41	0.00
	Summer	0.00	0.32	0.00	0.28	0.00	0.27
	Autumn	6.45	0.00	6.87	0.00	7.02	0.00

APPENDIX 4

This appendix displays all Chapter 8 simulation results, as monthly, seasonal and annual energy loads.

Table Appendices 10: Section 8.1. – Slope Forms heating and cooling results

Slope Forms - F01											
		F01_00°		F01_05°		F01_10°		F01_15°		F01_20°	
		Heating	Cooling	Heating	Cooling	Heating	Cooling	Heating	Cooling	Heating	Cooling
Monthly	Jan	24.40	0.00	23.66	0.00	23.22	0.00	22.82	0.00	22.41	0.00
	Feb	16.78	0.00	16.19	0.00	15.92	0.00	15.60	0.00	15.33	0.00
	Mar	12.08	0.00	11.55	0.00	11.34	0.00	11.03	0.00	10.78	0.00
	Apr	4.70	0.02	4.40	0.01	4.27	0.00	4.07	0.00	3.90	0.00
	May	0.89	0.96	0.80	0.86	0.76	0.72	0.68	0.61	0.63	0.47
	Jun	0.05	3.03	0.04	2.84	0.03	2.56	0.02	2.35	0.02	2.08
	Jul	0.00	7.36	0.00	7.01	0.00	6.53	0.00	6.17	0.00	5.70
	Aug	0.00	7.18	0.00	6.88	0.00	6.51	0.00	6.16	0.00	5.75
	Sep	0.00	2.97	0.00	2.86	0.00	2.71	0.00	2.55	0.00	2.36
	Oct	1.20	0.07	1.07	0.06	0.97	0.05	0.90	0.04	0.81	0.03
	Nov	11.52	0.00	11.03	0.00	10.61	0.00	10.36	0.00	10.03	0.00
	Dec	22.54	0.00	21.81	0.00	21.30	0.00	20.92	0.00	20.49	0.00
Annual	Total	94.16	21.60	90.55	20.52	88.43	19.09	86.40	17.87	84.40	16.40
	H+C	115.76		111.07		107.52		104.27		100.79	
Season Average	Winter	17.75	0.00	17.13	0.00	16.83	0.00	16.48	0.00	16.17	0.00
	Spring	1.88	1.34	1.75	1.24	1.69	1.10	1.59	0.99	1.52	0.85
	Summer	0.00	5.84	0.00	5.58	0.00	5.25	0.00	4.96	0.00	4.60
	Autumn	11.75	0.02	11.30	0.02	10.96	0.02	10.73	0.01	10.45	0.01
Slope Forms - F02											
		F02_00°		F02_05°		F02_10°		F02_15°		F02_20°	
		Heating	Cooling	Heating	Cooling	Heating	Cooling	Heating	Cooling	Heating	Cooling
Monthly	Jan	25.69	0.00	24.92	0.00	23.33	0.00	22.28	0.00	21.62	0.00
	Feb	17.42	0.00	17.05	0.00	16.41	0.00	16.02	0.00	15.70	0.00
	Mar	11.75	0.00	11.35	0.00	10.84	0.00	10.79	0.00	10.71	0.00
	Apr	4.12	0.05	3.86	0.00	3.41	0.00	3.31	0.00	3.18	0.00
	May	0.60	1.55	0.49	0.79	0.25	0.03	0.14	0.00	0.07	0.00
	Jun	0.03	4.40	0.01	3.01	0.00	0.89	0.00	0.05	0.00	0.00
	Jul	0.00	9.71	0.00	7.33	0.00	3.89	0.00	1.92	0.00	1.07
	Aug	0.00	9.02	0.00	6.79	0.00	3.66	0.00	1.86	0.00	1.10
	Sep	0.00	3.14	0.00	2.14	0.00	0.72	0.00	0.09	0.00	0.00
	Oct	1.25	0.05	1.08	0.00	0.63	0.00	0.37	0.00	0.23	0.00
	Nov	12.40	0.00	11.95	0.00	10.81	0.00	10.12	0.00	9.60	0.00
	Dec	24.04	0.00	23.27	0.00	21.48	0.00	20.30	0.00	19.53	0.00
Annual	Total	97.29	27.92	93.97	20.05	87.17	9.19	83.33	3.92	80.64	2.17
	H+C	125.21		114.02		96.37		87.25		82.81	
Season Average	Winter	18.29	0.00	17.78	0.00	16.86	0.00	16.36	0.00	16.01	0.00
	Spring	1.58	2.00	1.45	1.27	1.22	0.31	1.15	0.02	1.08	0.00
	Summer	0.00	7.29	0.00	5.42	0.00	2.76	0.00	1.29	0.00	0.72
	Autumn	12.56	0.02	12.10	0.00	10.98	0.00	10.26	0.00	9.79	0.00
Slope Forms - F03											
		F03_00°		F03_05°		F03_10°		F03_15°		F03_20°	
		Heating	Cooling	Heating	Cooling	Heating	Cooling	Heating	Cooling	Heating	Cooling
Monthly	Jan	23.54	0.00	22.77	0.00	22.35	0.00	21.31	0.00	20.48	0.00
	Feb	16.01	0.00	15.44	0.00	15.24	0.00	14.79	0.00	14.51	0.00
	Mar	11.02	0.00	10.50	0.00	10.29	0.00	9.90	0.00	9.82	0.00
	Apr	3.97	0.03	3.68	0.01	3.54	0.00	3.26	0.00	3.20	0.00
	May	0.63	1.23	0.54	0.95	0.48	0.65	0.34	0.12	0.26	0.00
	Jun	0.03	3.61	0.02	3.08	0.01	2.51	0.00	1.23	0.00	0.30
	Jul	0.00	8.08	0.00	7.17	0.00	6.19	0.00	4.20	0.00	2.52
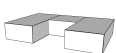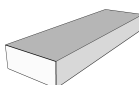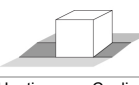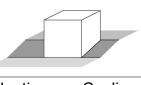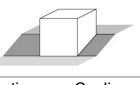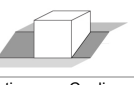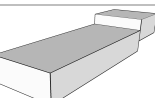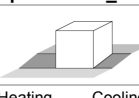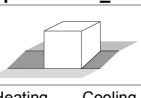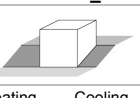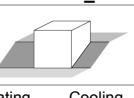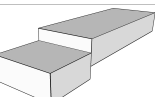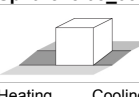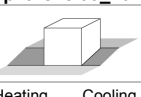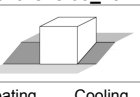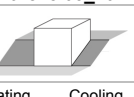
		Heating	Cooling	Heating	Cooling	Heating	Cooling	Heating	Cooling	Heating	Cooling
	Aug	0.00	7.56	0.00	6.73	0.00	5.84	0.00	4.03	0.00	2.50
	Sep	0.00	2.75	0.00	2.39	0.00	1.98	0.00	1.12	0.00	0.44
	Oct	1.18	0.05	1.04	0.02	0.94	0.01	0.67	0.00	0.48	0.00
	Nov	11.31	0.00	10.81	0.00	10.50	0.00	9.72	0.00	9.16	0.00
	Dec	21.97	0.00	21.22	0.00	20.77	0.00	19.62	0.00	18.69	0.00
Annual	Total	89.66	23.31	86.02	20.36	84.13	17.18	79.61	10.70	76.59	5.76
	H+C	112.97		106.38		101.31		90.31		82.35	
Season Average	Winter	16.86	0.00	16.24	0.00	15.96	0.00	15.33	0.00	14.94	0.00
	Spring	1.54	1.62	1.41	1.35	1.34	1.05	1.20	0.45	1.15	0.10
	Summer	0.00	6.13	0.00	5.43	0.00	4.67	0.00	3.12	0.00	1.82
	Autumn	11.49	0.02	11.02	0.01	10.74	0.00	10.01	0.00	9.44	0.00

Slope Forms - F04

		F04_00°		F04_05°		F04_10°		F04_15°		F04_20°	
		Heating	Cooling	Heating	Cooling	Heating	Cooling	Heating	Cooling	Heating	Cooling
Monthly	Jan	26.90	0.00	26.04	0.00	25.59	0.00	24.83	0.00	23.77	0.00
	Feb	18.61	0.00	17.96	0.00	17.68	0.00	17.21	0.00	16.86	0.00
	Mar	13.13	0.00	12.55	0.00	12.27	0.00	11.81	0.00	11.61	0.00
	Apr	5.07	0.02	4.72	0.01	4.53	0.00	4.19	0.00	4.06	0.00
	May	0.93	1.09	0.82	0.88	0.74	0.65	0.61	0.40	0.47	0.02
	Jun	0.05	3.50	0.03	3.10	0.02	2.66	0.01	2.13	0.00	0.66
	Jul	0.00	8.36	0.00	7.64	0.00	6.90	0.00	6.06	0.00	3.70
	Aug	0.00	7.97	0.00	7.34	0.00	6.67	0.00	5.91	0.00	3.76
	Sep	0.00	2.99	0.00	2.72	0.00	2.42	0.00	2.05	0.00	1.01
	Oct	1.41	0.05	1.25	0.03	1.14	0.01	0.94	0.00	0.63	0.00
	Nov	13.02	0.00	12.43	0.00	12.06	0.00	11.46	0.00	10.62	0.00
	Dec	25.03	0.00	24.18	0.00	23.69	0.00	22.90	0.00	21.66	0.00
Annual	Total	104.17	23.97	99.99	21.72	97.72	19.32	93.96	16.55	89.69	9.14
	H+C	128.14		121.71		117.04		110.51		98.83	
Season Average	Winter	19.55	0.00	18.85	0.00	18.51	0.00	17.95	0.00	17.42	0.00
	Spring	2.02	1.54	1.86	1.33	1.77	1.10	1.60	0.84	1.51	0.23
	Summer	0.00	6.44	0.00	5.90	0.00	5.33	0.00	4.67	0.00	2.82
	Autumn	13.16	0.02	12.62	0.01	12.30	0.00	11.77	0.00	10.97	0.00

Slope Forms - F05

		F05_00°		F05_05°		F05_10°		F05_15°		F05_20°	
		Heating	Cooling	Heating	Cooling	Heating	Cooling	Heating	Cooling	Heating	Cooling
Monthly	Jan	27.90	0.00	26.65	0.00	26.66	0.00	25.33	0.00	24.51	0.00
	Feb	19.36	0.00	18.47	0.00	18.57	0.00	17.99	0.00	17.63	0.00
	Mar	13.64	0.00	12.95	0.00	12.90	0.00	12.45	0.00	12.28	0.00
	Apr	5.30	0.01	4.96	0.01	4.84	0.00	4.50	0.00	4.37	0.00
	May	0.99	1.07	0.90	0.87	0.81	0.48	0.59	0.04	0.47	0.00
	Jun	0.06	3.51	0.04	3.09	0.02	2.30	0.00	0.83	0.00	0.24
	Jul	0.00	8.50	0.00	7.68	0.00	6.41	0.00	4.07	0.00	2.78
	Aug	0.00	8.11	0.00	7.40	0.00	6.20	0.00	4.07	0.00	2.89
	Sep	0.00	2.99	0.00	2.72	0.00	2.12	0.00	1.09	0.00	0.56
	Oct	1.49	0.04	1.32	0.03	1.21	0.00	0.81	0.00	0.59	0.00
	Nov	13.58	0.00	12.77	0.00	12.69	0.00	11.63	0.00	11.04	0.00
	Dec	26.02	0.00	24.78	0.00	24.75	0.00	23.24	0.00	22.34	0.00
Annual	Total	108.34	24.22	102.86	21.79	102.45	17.52	96.54	10.10	93.23	6.47
	H+C	132.57		124.65		119.97		106.64		99.70	
Season Average	Winter	20.30	0.00	19.36	0.00	19.38	0.00	18.59	0.00	18.14	0.00
	Spring	2.12	1.53	1.97	1.32	1.89	0.93	1.70	0.29	1.61	0.08
	Summer	0.00	6.53	0.00	5.93	0.00	4.91	0.00	3.08	0.00	2.08
	Autumn	13.70	0.01	12.96	0.01	12.88	0.00	11.89	0.00	11.33	0.00

Table Appendices 11: Section 8.2. –Split Levels heating and cooling results

		Split Levels – SplitLevel01								
		SplitLevel01_00°		SplitLevel01_05°		SplitLevel01_10°		SplitLevel01_15°		SplitLevel01_20°	
		Heating	Cooling	Heating	Cooling	Heating	Cooling	Heating	Cooling	Heating	Cooling
Monthly	Jan	25.79	0.00	24.94	0.00	23.30	0.00	22.44	0.00	21.71	0.00
	Feb	17.54	0.00	17.16	0.00	16.42	0.00	16.20	0.00	15.82	0.00
	Mar	11.88	0.00	11.54	0.00	10.90	0.00	11.05	0.00	10.87	0.00
	Apr	4.20	0.04	4.03	0.00	3.47	0.00	3.51	0.00	3.33	0.00
	May	0.62	1.47	0.55	0.65	0.27	0.03	0.17	0.00	0.08	0.00
	Jun	0.03	4.28	0.01	2.66	0.00	0.87	0.00	0.02	0.00	0.00
	Jul	0.00	9.50	0.00	6.76	0.00	3.85	0.00	1.69	0.00	0.97
	Aug	0.00	8.83	0.00	6.29	0.00	3.63	0.00	1.66	0.00	1.00
	Sep	0.00	3.05	0.00	1.92	0.00	0.71	0.00	0.06	0.00	0.00
	Oct	1.28	0.04	1.12	0.00	0.65	0.00	0.41	0.00	0.24	0.00
	Nov	12.50	0.00	12.00	0.00	10.79	0.00	10.27	0.00	9.71	0.00
	Dec	24.14	0.00	23.28	0.00	21.44	0.00	20.45	0.00	19.63	0.00
Annual	Total	97.99	27.21	94.62	18.28	87.23	9.10	84.50	3.43	81.41	1.97
	H+C	125.20		112.90		96.33		87.93		83.38	
Season Average	Winter	18.40	0.00	17.88	0.00	16.87	0.00	16.57	0.00	16.14	0.00
	Spring	1.62	1.93	1.53	1.10	1.25	0.30	1.23	0.01	1.14	0.00
	Summer	0.00	7.13	0.00	4.99	0.00	2.73	0.00	1.14	0.00	0.66
	Autumn	12.64	0.01	12.13	0.00	10.96	0.00	10.37	0.00	9.86	0.00

		Split Levels – SplitLevel02								
		SplitLevel02_00°		SplitLevel02_05°		SplitLevel02_10°		SplitLevel02_15°		SplitLevel02_20°	
		Heating	Cooling	Heating	Cooling	Heating	Cooling	Heating	Cooling	Heating	Cooling
Monthly	Jan	26.98	0.00	26.49	0.00	25.37	0.00	24.39	0.00	24.15	0.00
	Feb	18.52	0.00	18.35	0.00	17.63	0.00	17.45	0.00	17.37	0.00
	Mar	12.72	0.00	12.62	0.00	11.94	0.00	12.16	0.00	12.15	0.00
	Apr	4.64	0.03	4.64	0.00	4.15	0.00	4.49	0.00	4.53	0.00
	May	0.73	1.23	0.72	0.64	0.51	0.43	0.35	0.17	0.36	0.09
	Jun	0.04	3.86	0.02	2.64	0.00	2.06	0.00	1.20	0.00	0.90
	Jul	0.00	9.09	0.00	7.03	0.00	5.88	0.00	3.67	0.00	3.15
	Aug	0.00	8.59	0.00	6.67	0.00	5.58	0.00	3.48	0.00	2.99
	Sep	0.00	3.00	0.00	2.12	0.00	1.65	0.00	0.95	0.00	0.75
	Oct	1.28	0.04	1.23	0.00	0.95	0.00	0.64	0.00	0.61	0.00
	Nov	12.98	0.00	12.77	0.00	11.88	0.00	11.28	0.00	11.16	0.00
	Dec	25.12	0.00	24.64	0.00	23.44	0.00	22.31	0.00	22.04	0.00
Annual	Total	103.01	25.84	101.49	19.11	95.87	15.59	93.07	9.47	92.36	7.89
	H+C	128.85		120.59		111.46		102.55		100.25	
Season Average	Winter	19.41	0.00	19.15	0.00	18.31	0.00	18.00	0.00	17.89	0.00
	Spring	1.80	1.71	1.80	1.09	1.55	0.83	1.61	0.45	1.63	0.33
	Summer	0.00	6.90	0.00	5.27	0.00	4.37	0.00	2.70	0.00	2.30
	Autumn	13.13	0.01	12.88	0.00	12.09	0.00	11.41	0.00	11.27	0.00

		Split Levels – SplitLevel03								
		SplitLevel03_00°		SplitLevel03_05°		SplitLevel03_10°		SplitLevel03_15°		SplitLevel03_20°	
		Heating	Cooling	Heating	Cooling	Heating	Cooling	Heating	Cooling	Heating	Cooling
Monthly	Jan	27.12	0.00	26.40	0.00	25.91	0.00	24.58	0.00	23.79	0.00
	Feb	18.67	0.00	18.17	0.00	18.03	0.00	17.52	0.00	17.28	0.00
	Mar	12.85	0.00	12.45	0.00	12.34	0.00	12.11	0.00	12.21	0.00
	Apr	4.70	0.01	4.50	0.00	4.42	0.00	4.16	0.00	4.33	0.00
	May	0.74	1.13	0.68	0.90	0.63	0.42	0.40	0.15	0.30	0.12
	Jun	0.04	3.72	0.03	3.24	0.01	2.18	0.00	0.77	0.00	0.56
	Jul	0.00	8.88	0.00	8.03	0.00	6.20	0.00	3.62	0.00	2.09
	Aug	0.00	8.40	0.00	7.60	0.00	5.92	0.00	3.55	0.00	2.15
	Sep	0.00	2.93	0.00	2.58	0.00	1.84	0.00	0.90	0.00	0.74
	Oct	1.33	0.04	1.22	0.02	1.10	0.01	0.69	0.01	0.47	0.01
	Nov	13.12	0.00	12.67	0.00	12.36	0.00	11.51	0.00	11.02	0.00
	Dec	25.25	0.00	24.53	0.00	23.99	0.00	22.51	0.00	21.61	0.00
Annual	Total	103.82	25.11	100.65	22.37	98.80	16.58	93.48	9.01	91.01	5.67
	H+C	128.93		123.03		115.38		102.49		96.69	
Season Average	Winter	19.55	0.00	19.01	0.00	18.76	0.00	18.07	0.00	17.76	0.00
	Spring	1.83	1.62	1.74	1.38	1.69	0.87	1.52	0.31	1.55	0.23
	Summer	0.00	6.74	0.00	6.07	0.00	4.65	0.00	2.69	0.00	1.66
	Autumn	13.23	0.01	12.81	0.01	12.49	0.00	11.57	0.00	11.03	0.00
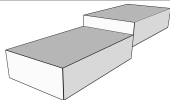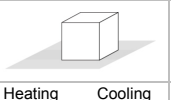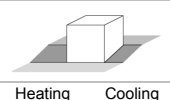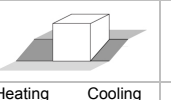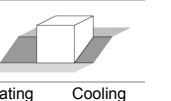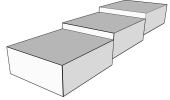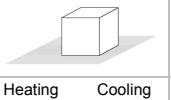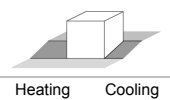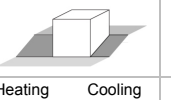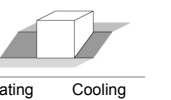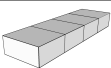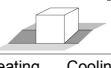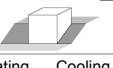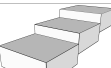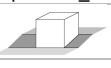
Split Levels – SplitLevel04

		SplitLevel04_00°		SplitLevel04_05°		SplitLevel04_10°		SplitLevel04_15°		SplitLevel04_20°	
		Heating	Cooling	Heating	Cooling	Heating	Cooling	Heating	Cooling	Heating	Cooling
Monthly	Jan	27.07	0.00	26.30	0.00	25.74	0.00	24.35	0.00	23.56	0.00
	Feb	18.61	0.00	18.12	0.00	17.90	0.00	17.42	0.00	17.17	0.00
	Mar	12.80	0.00	12.40	0.00	12.20	0.00	12.14	0.00	12.22	0.00
	Apr	4.67	0.02	4.47	0.00	4.32	0.00	4.29	0.00	4.66	0.00
	May	0.73	1.16	0.67	0.84	0.59	0.43	0.35	0.22	0.26	0.11
	Jun	0.04	3.77	0.02	3.13	0.01	2.14	0.00	1.12	0.00	0.79
	Jul	0.00	8.96	0.00	7.83	0.00	6.10	0.00	3.35	0.00	2.54
	Aug	0.00	8.48	0.00	7.44	0.00	5.81	0.00	3.28	0.00	2.49
	Sep	0.00	2.96	0.00	2.50	0.00	1.77	0.00	1.01	0.00	0.77
	Oct	1.30	0.03	1.18	0.01	1.04	0.01	0.61	0.00	0.42	0.00
	Nov	13.05	0.00	12.54	0.00	12.19	0.00	11.28	0.00	10.80	0.00
	Dec	25.20	0.00	24.42	0.00	23.81	0.00	22.25	0.00	21.37	0.00
Annual	Total	103.48	25.39	100.13	21.76	97.81	16.24	92.70	8.98	90.47	6.71
	H+C	128.86		121.89		114.05		101.69		97.18	
Season Average	Winter	19.49	0.00	18.94	0.00	18.61	0.00	17.97	0.00	17.65	0.00
	Spring	1.81	1.65	1.72	1.33	1.64	0.86	1.55	0.45	1.64	0.30
	Summer	0.00	6.80	0.00	5.92	0.00	4.56	0.00	2.55	0.00	1.93
	Autumn	13.18	0.01	12.71	0.00	12.35	0.00	11.38	0.00	10.86	0.00

Split Levels – SplitLevel05

		SplitLevel05_00°		SplitLevel05_05°		SplitLevel05_10°		SplitLevel05_15°		SplitLevel05_20°	
		Heating	Cooling	Heating	Cooling	Heating	Cooling	Heating	Cooling	Heating	Cooling
Monthly	Jan	28.32	0.00	25.85	0.00	26.81	0.00	25.63	0.00	24.85	0.00
	Feb	19.63	0.00	18.11	0.00	18.79	0.00	18.49	0.00	18.03	0.00
	Mar	13.52	0.00	12.60	0.00	12.87	0.00	13.03	0.00	12.72	0.00
	Apr	4.92	0.01	4.73	0.00	4.52	0.00	4.82	0.00	4.71	0.00
	May	0.73	0.98	0.71	0.59	0.56	0.39	0.34	0.23	0.28	0.09
	Jun	0.03	3.53	0.02	2.43	0.01	2.00	0.00	1.21	0.00	0.77
	Jul	0.00	8.89	0.00	6.89	0.00	6.09	0.00	3.82	0.00	2.94
	Aug	0.00	8.43	0.00	6.66	0.00	5.83	0.00	3.72	0.00	2.90
	Sep	0.00	2.81	0.00	2.16	0.00	1.72	0.00	1.15	0.00	0.79
	Oct	1.31	0.03	1.10	0.02	1.02	0.01	0.60	0.01	0.48	0.00
	Nov	13.76	0.00	12.39	0.00	12.80	0.00	12.05	0.00	11.59	0.00
	Dec	26.35	0.00	23.90	0.00	24.77	0.00	23.42	0.00	22.63	0.00
Annual	Total	108.58	24.68	99.41	18.77	102.15	16.04	98.39	10.14	95.30	7.48
	H+C	133.26		118.18		118.19		108.53		102.78	
Season Average	Winter	20.49	0.00	18.85	0.00	19.49	0.00	19.05	0.00	18.53	0.00
	Spring	1.89	1.51	1.82	1.01	1.69	0.80	1.72	0.48	1.66	0.29
	Summer	0.00	6.71	0.00	5.24	0.00	4.55	0.00	2.90	0.00	2.21
	Autumn	13.81	0.01	12.46	0.01	12.86	0.00	12.03	0.00	11.57	0.00

Table Appendices 12: Section 8.3. – Slope Building Design heating and cooling results

Slope Building Design - SlopeBD01

		SlopeBD01_00°		SlopeBD01_10°		SlopeBD01_20°		SlopeBD01_30°		SlopeBD01_40°		SlopeBD01_50°	
		Heating	Cooling	Heating	Cooling	Heating	Cooling	Heating	Cooling	Heating	Cooling	Heating	Cooling
Monthly	Jan	27.58	0.00	24.68	0.00	22.79	0.00	21.92	0.00	21.49	0.00	21.26	0.00
	Feb	19.06	0.00	17.49	0.00	16.78	0.00	16.34	0.00	16.15	0.00	16.06	0.00
	Mar	12.94	0.00	12.05	0.00	12.10	0.00	11.90	0.00	11.78	0.00	11.80	0.00
	Apr	4.48	0.01	4.08	0.00	4.57	0.00	4.64	0.00	4.58	0.00	4.61	0.00
	May	0.57	1.03	0.32	0.37	0.21	0.17	0.15	0.02	0.12	0.00	0.10	0.00
	Jun	0.02	3.67	0.01	1.57	0.00	0.75	0.00	0.26	0.00	0.02	0.00	0.00
	Jul	0.00	9.11	0.00	4.56	0.00	2.17	0.00	1.35	0.00	0.72	0.00	0.34
	Aug	0.00	8.48	0.00	4.40	0.00	2.22	0.00	1.45	0.00	0.87	0.00	0.50
	Sep	0.00	2.69	0.00	1.40	0.00	0.88	0.00	0.50	0.00	0.23	0.00	0.08
	Oct	1.24	0.03	0.63	0.02	0.27	0.01	0.15	0.00	0.08	0.00	0.04	0.00
	Nov	13.54	0.00	11.56	0.00	10.33	0.00	9.75	0.00	9.41	0.00	9.25	0.00
	Dec	25.77	0.00	22.60	0.00	20.48	0.00	19.56	0.00	19.08	0.00	18.82	0.00
Annual	Total	105.20	25.02	93.41	12.32	87.53	6.19	84.41	3.58	82.68	1.84	81.95	0.93
	H+C	130.22		105.73		93.72		87.98		84.52		82.88	
Season Average	Winter	19.86	0.00	18.07	0.00	17.22	0.00	16.72	0.00	16.47	0.00	16.37	0.00
	Spring	1.69	1.57	1.47	0.65	1.59	0.31	1.60	0.09	1.57	0.01	1.57	0.00
	Summer	0.00	6.76	0.00	3.45	0.00	1.75	0.00	1.10	0.00	0.61	0.00	0.31
	Autumn	13.52	0.01	11.60	0.01	10.36	0.00	9.82	0.00	9.52	0.00	9.37	0.00

Slope Building Design - SlopeBD02

		SlopeBD02_00°		SlopeBD02_10°		SlopeBD02_20°		SlopeBD02_30°		SlopeBD02_40°		SlopeBD02_50°	
		Heating	Cooling	Heating	Cooling	Heating	Cooling	Heating	Cooling	Heating	Cooling	Heating	Cooling
Monthly	Jan	27.61	0.00	26.64	0.00	24.77	0.00	23.00	0.00	22.32	0.00	22.10	0.00
	Feb	19.15	0.00	18.39	0.00	17.65	0.00	16.96	0.00	16.73	0.00	16.65	0.00
	Mar	13.35	0.00	12.67	0.00	12.31	0.00	12.22	0.00	12.04	0.00	12.06	0.00
	Apr	4.97	0.00	4.56	0.00	4.35	0.00	4.66	0.00	4.57	0.00	4.59	0.00
	May	0.82	0.83	0.68	0.73	0.41	0.20	0.20	0.10	0.11	0.00	0.10	0.00
	Jun	0.04	3.09	0.02	2.89	0.00	1.11	0.00	0.57	0.00	0.02	0.00	0.00
	Jul	0.00	8.10	0.00	7.74	0.00	3.73	0.00	1.86	0.00	0.72	0.00	0.34
	Aug	0.00	7.90	0.00	7.55	0.00	3.79	0.00	1.94	0.00	0.87	0.00	0.50
	Sep	0.00	2.84	0.00	2.68	0.00	1.23	0.00	0.76	0.00	0.22	0.00	0.08
	Oct	1.22	0.03	1.06	0.02	0.57	0.01	0.22	0.00	0.08	0.00	0.04	0.00
	Nov	13.10	0.00	12.43	0.00	11.18	0.00	10.11	0.00	9.64	0.00	9.48	0.00
	Dec	25.49	0.00	24.51	0.00	22.47	0.00	20.51	0.00	19.77	0.00	19.52	0.00
Annual	Total	105.75	22.80	100.97	21.61	93.72	10.07	87.88	5.23	85.27	1.82	84.53	0.92
	H+C	128.56		122.58		103.79		93.11		87.09		85.45	
Season Average	Winter	20.04	0.00	19.24	0.00	18.24	0.00	17.39	0.00	17.03	0.00	16.94	0.00
	Spring	1.94	1.31	1.75	1.21	1.59	0.44	1.62	0.22	1.56	0.01	1.56	0.00
	Summer	0.00	6.28	0.00	5.99	0.00	2.92	0.00	1.52	0.00	0.60	0.00	0.31
	Autumn	13.27	0.01	12.67	0.01	11.41	0.00	10.28	0.00	9.83	0.00	9.68	0.00

Slope Building Design - SlopeBD03

		SlopeBD03_00°		SlopeBD03_10°		SlopeBD03_20°		SlopeBD03_30°		SlopeBD03_40°		SlopeBD03_50°	
		Heating	Cooling	Heating	Cooling	Heating	Cooling	Heating	Cooling	Heating	Cooling	Heating	Cooling
Monthly	Jan	27.40	0.00	27.04	0.00	26.81	0.00	25.08	0.00	24.93	0.00	25.00	0.00
	Feb	19.01	0.00	18.75	0.00	18.63	0.00	17.62	0.00	17.59	0.00	17.83	0.00
	Mar	13.59	0.00	13.38	0.00	13.15	0.00	12.44	0.00	12.43	0.00	12.77	0.00
	Apr	5.36	0.00	5.25	0.00	5.01	0.00	4.72	0.00	4.74	0.00	4.99	0.00
	May	1.07	0.71	1.03	0.64	0.89	0.41	0.81	0.12	0.80	0.08	0.89	0.05
	Jun	0.07	2.67	0.06	2.54	0.03	2.07	0.02	1.02	0.01	0.81	0.02	0.58
	Jul	0.00	7.36	0.00	7.12	0.00	6.45	0.00	4.26	0.00	3.81	0.00	3.23
	Aug	0.00	7.50	0.00	7.25	0.00	6.60	0.00	4.46	0.00	3.99	0.00	3.42
	Sep	0.00	3.02	0.00	2.90	0.00	2.52	0.00	1.54	0.00	1.31	0.00	1.05
	Oct	1.22	0.05	1.17	0.04	1.01	0.02	0.84	0.00	0.84	0.00	0.86	0.00
	Nov	12.65	0.00	12.41	0.00	12.11	0.00	11.08	0.00	11.03	0.00	11.14	0.00
	Dec	25.04	0.00	24.67	0.00	24.38	0.00	22.66	0.00	22.53	0.00	22.56	0.00
Annual	Total	105.40	21.31	103.76	20.50	102.03	18.07	95.27	11.41	94.91	9.99	96.04	8.33
	H+C	126.71		124.26		120.09		106.68		104.89		104.37	
Season Average	Winter	20.00	0.00	19.72	0.00	19.53	0.00	18.38	0.00	18.32	0.00	18.53	0.00
	Spring	2.17	1.13	2.12	1.06	1.98	0.83	1.85	0.38	1.85	0.29	1.96	0.21
	Summer	0.00	5.96	0.00	5.76	0.00	5.19	0.00	3.42	0.00	3.03	0.00	2.57
	Autumn	12.97	0.02	12.75	0.01	12.50	0.01	11.53	0.00	11.47	0.00	11.52	0.00
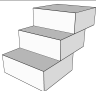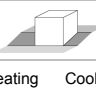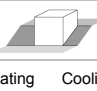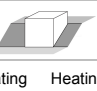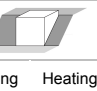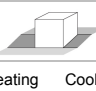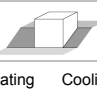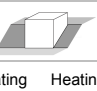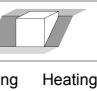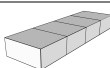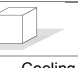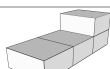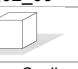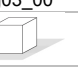
Slope Building Design - SlopeBD04

		SlopeBD04_00°		SlopeBD04_10°		SlopeBD04_20°		SlopeBD04_30°		SlopeBD04_40°		SlopeBD04_50°	
		Heating	Cooling	Heating	Cooling	Heating	Cooling	Heating	Heating	Cooling	Heating	Cooling	Heating
Monthly	Jan	23.76	0.00	23.36	0.00	23.15	0.00	22.26	0.00	21.93	0.00	21.77	0.00
	Feb	16.61	0.00	16.32	0.00	16.19	0.00	15.65	0.00	15.61	0.00	15.62	0.00
	Mar	11.92	0.00	11.69	0.00	11.59	0.00	11.08	0.00	11.11	0.00	11.21	0.00
	Apr	4.59	0.01	4.47	0.01	4.42	0.01	4.05	0.00	4.09	0.00	4.17	0.00
	May	0.82	0.46	0.78	0.44	0.76	0.43	0.60	0.25	0.58	0.11	0.58	0.07
	Jun	0.04	1.76	0.04	1.69	0.03	1.58	0.01	1.10	0.01	0.67	0.00	0.56
	Jul	0.00	6.07	0.00	5.85	0.00	5.55	0.00	4.42	0.00	3.24	0.00	2.67
	Aug	0.00	6.46	0.00	6.23	0.00	5.89	0.00	4.84	0.00	3.65	0.00	3.05
	Sep	0.00	2.45	0.00	2.35	0.00	2.19	0.00	1.78	0.00	1.24	0.00	0.98
	Oct	0.79	0.03	0.75	0.03	0.74	0.03	0.53	0.02	0.45	0.00	0.43	0.00
	Nov	10.69	0.00	10.44	0.00	10.34	0.00	9.58	0.00	9.29	0.00	9.17	0.00
	Dec	21.50	0.00	21.11	0.00	20.91	0.00	19.94	0.00	19.55	0.00	19.35	0.00
Annual	Total	90.70	17.25	88.96	16.60	88.11	15.68	83.68	12.40	82.62	8.90	82.29	7.34
	H+C	107.95		105.56		103.80		96.08		91.52		89.64	
Season Average	Winter	17.43	0.00	17.12	0.00	16.97	0.00	16.33	0.00	16.22	0.00	16.20	0.00
	Spring	1.82	0.74	1.76	0.71	1.74	0.67	1.55	0.45	1.56	0.26	1.58	0.21
	Summer	0.00	4.99	0.00	4.81	0.00	4.54	0.00	3.68	0.00	2.71	0.00	2.24
	Autumn	10.99	0.01	10.77	0.01	10.66	0.01	10.01	0.01	9.76	0.00	9.65	0.00

Slope Building Design - SlopeBD05

		SlopeBD05_00°		SlopeBD05_10°		SlopeBD05_20°		SlopeBD05_30°		SlopeBD05_40°		SlopeBD05_50°	
		Heating	Cooling	Heating	Cooling	Heating	Cooling	Heating	Heating	Cooling	Heating	Cooling	Heating
Monthly	Jan	21.41	0.00	20.73	0.00	20.35	0.00	19.86	0.00	19.57	0.00	19.54	0.00
	Feb	15.04	0.00	14.55	0.00	14.35	0.00	14.04	0.00	13.92	0.00	14.00	0.00
	Mar	11.07	0.00	10.67	0.00	10.56	0.00	10.28	0.00	10.16	0.00	10.16	0.00
	Apr	4.52	0.04	4.26	0.04	4.20	0.04	3.95	0.03	3.78	0.03	3.63	0.01
	May	0.76	0.69	0.68	0.68	0.65	0.65	0.55	0.61	0.47	0.55	0.34	0.41
	Jun	0.03	2.09	0.03	1.99	0.03	1.90	0.03	1.78	0.03	1.57	0.01	1.36
	Jul	0.00	6.70	0.00	6.28	0.00	5.70	0.00	5.34	0.00	4.84	0.00	4.39
	Aug	0.00	6.90	0.00	6.54	0.00	6.00	0.00	5.71	0.00	5.28	0.00	4.89
	Sep	0.00	2.77	0.00	2.63	0.00	2.40	0.00	2.32	0.00	2.17	0.00	2.03
	Oct	0.68	0.08	0.60	0.08	0.56	0.07	0.48	0.07	0.40	0.07	0.23	0.05
	Nov	9.94	0.00	9.41	0.00	9.15	0.00	8.66	0.00	8.19	0.00	7.73	0.00
	Dec	19.49	0.00	18.77	0.00	18.36	0.00	17.79	0.00	17.38	0.00	17.16	0.00
Annual	Total	82.95	19.26	79.70	18.24	78.22	16.76	75.63	15.87	73.90	14.51	72.79	13.13
	H+C	102.21		97.94		94.98		91.50		88.40		85.92	
Season Average	Winter	15.84	0.00	15.32	0.00	15.09	0.00	14.72	0.00	14.55	0.00	14.57	0.00
	Spring	1.77	0.94	1.66	0.90	1.63	0.86	1.51	0.81	1.43	0.72	1.32	0.59
	Summer	0.00	5.45	0.00	5.15	0.00	4.70	0.00	4.46	0.00	4.10	0.00	3.77
	Autumn	10.04	0.03	9.59	0.03	9.36	0.02	8.98	0.02	8.66	0.02	8.37	0.02

Table Appendices 13: Section 8.4. - Configurations heating and cooling results

Configurations - Confg01												
		Confg01_00°		Confg01_10°		Confg01_20°		Confg01_30°		Confg01_40°		Confg01_50°	
		Heating	Cooling	Heating	Cooling	Heating	Cooling	Heating	Cooling	Heating	Cooling	Heating	Cooling
Monthly	Jan	29.15	0.00	26.20	0.00	24.62	0.00	24.09	0.00	23.75	0.00	23.54	0.00
	Feb	20.22	0.00	18.72	0.00	18.15	0.00	17.83	0.00	17.83	0.00	17.76	0.00
	Mar	13.69	0.00	12.69	0.00	12.73	0.00	12.79	0.00	12.69	0.00	12.71	0.00
	Apr	4.72	0.01	4.07	0.00	4.24	0.00	4.51	0.00	4.42	0.00	4.48	0.00
	May	0.57	1.00	0.22	0.33	0.15	0.16	0.12	0.05	0.09	0.00	0.08	0.00
	Jun	0.02	3.76	0.00	1.56	0.00	0.70	0.00	0.41	0.00	0.09	0.00	0.00
	Jul	0.00	9.60	0.00	4.86	0.00	2.17	0.00	1.49	0.00	0.89	0.00	0.51
	Aug	0.00	8.93	0.00	4.64	0.00	2.21	0.00	1.58	0.00	1.02	0.00	0.66
	Sep	0.00	2.74	0.00	1.34	0.00	0.84	0.00	0.63	0.00	0.35	0.00	0.17
	Oct	1.27	0.03	0.54	0.02	0.20	0.01	0.12	0.00	0.06	0.00	0.03	0.00
	Nov	14.36	0.00	12.40	0.00	11.36	0.00	11.05	0.00	10.75	0.00	10.60	0.00
	Dec	27.23	0.00	24.02	0.00	22.26	0.00	21.68	0.00	21.29	0.00	21.06	0.00
Annual	Total	111.22	26.07	98.85	12.76	93.72	6.09	92.32	4.17	90.88	2.36	90.27	1.34
	H+C	137.28		111.61		99.81		96.49		93.24		91.61	
Season Average	Winter	21.02	0.00	19.20	0.00	18.50	0.00	18.28	0.00	18.09	0.00	18.01	0.00
	Spring	1.77	1.59	1.43	0.63	1.46	0.29	1.54	0.15	1.50	0.03	1.52	0.00
	Summer	0.00	7.09	0.00	3.61	0.00	1.74	0.00	1.23	0.00	0.76	0.00	0.45
	Autumn	14.28	0.01	12.32	0.01	11.28	0.00	10.95	0.00	10.70	0.00	10.57	0.00

Configurations - Confg02												
		Confg02_00°		Confg02_10°		Confg02_20°		Confg02_30°		Confg02_40°		Confg02_50°	
		Heating	Cooling	Heating	Cooling	Heating	Cooling	Heating	Heating	Heating	Cooling	Heating	Cooling
Monthly	Jan	26.98	0.00	25.10	0.00	24.73	0.00	24.87	0.00	24.86	0.00	24.86	0.00
	Feb	18.94	0.00	17.77	0.00	17.88	0.00	18.48	0.00	18.63	0.00	18.71	0.00
	Mar	13.42	0.00	12.57	0.00	12.56	0.00	13.50	0.00	13.76	0.00	13.91	0.00
	Apr	5.10	0.02	4.61	0.01	4.41	0.00	5.23	0.00	5.49	0.00	5.64	0.00
	May	0.74	0.90	0.54	0.64	0.28	0.18	0.23	0.11	0.28	0.06	0.32	0.03
	Jun	0.04	2.99	0.03	2.32	0.00	1.05	0.00	0.61	0.00	0.41	0.00	0.28
	Jul	0.00	8.20	0.00	6.36	0.00	4.12	0.00	2.37	0.00	1.82	0.00	1.48
	Aug	0.00	7.95	0.00	6.25	0.00	4.23	0.00	2.51	0.00	1.98	0.00	1.65
	Sep	0.00	2.77	0.00	2.27	0.00	1.39	0.00	0.76	0.00	0.62	0.00	0.54
	Oct	1.10	0.06	0.77	0.05	0.39	0.01	0.28	0.01	0.27	0.00	0.27	0.00
	Nov	13.18	0.00	11.92	0.00	11.13	0.00	11.08	0.00	11.14	0.00	11.20	0.00
	Dec	24.97	0.00	23.01	0.00	22.36	0.00	22.28	0.00	22.25	0.00	22.23	0.00
Annual	Total	104.48	22.88	96.32	17.89	93.73	10.98	95.95	6.37	96.69	4.89	97.14	3.98
	H+C	127.36		114.22		104.71		102.31		101.57		101.13	
Season Average	Winter	19.78	0.00	18.48	0.00	18.39	0.00	18.95	0.00	19.08	0.00	19.16	0.00
	Spring	1.96	1.30	1.73	0.99	1.56	0.41	1.82	0.24	1.92	0.15	1.99	0.10
	Summer	0.00	6.30	0.00	4.96	0.00	3.25	0.00	1.88	0.00	1.47	0.00	1.22
	Autumn	13.08	0.02	11.90	0.02	11.29	0.00	11.21	0.00	11.22	0.00	11.23	0.00

Configurations - Confg03												
		Confg03_00°		Confg03_10°		Confg03_20°		Confg03_30°		Confg03_40°		Confg03_50°	
		Heating	Cooling	Heating	Cooling	Heating	Cooling	Heating	Cooling	Heating	Cooling	Heating	Cooling
Monthly	Jan	23.77	0.00	22.60	0.00	22.12	0.00	22.11	0.00	22.32	0.00	22.15	0.00
	Feb	16.79	0.00	16.00	0.00	15.83	0.00	16.07	0.00	16.59	0.00	16.63	0.00
	Mar	12.02	0.00	11.42	0.00	11.35	0.00	11.52	0.00	12.15	0.00	12.22	0.00
	Apr	4.63	0.02	4.22	0.02	4.26	0.01	4.14	0.01	4.61	0.00	4.70	0.00
	May	0.61	0.77	0.47	0.73	0.38	0.58	0.25	0.34	0.22	0.25	0.19	0.09
	Jun	0.03	2.41	0.02	2.23	0.02	1.91	0.01	1.21	0.01	0.84	0.00	0.51
	Jul	0.00	7.22	0.00	6.30	0.00	5.51	0.00	4.16	0.00	2.78	0.00	1.94
	Aug	0.00	7.11	0.00	6.29	0.00	5.58	0.00	4.36	0.00	3.10	0.00	2.32
	Sep	0.00	2.44	0.00	2.27	0.00	1.99	0.00	1.45	0.00	1.16	0.00	0.87
	Oct	0.89	0.05	0.70	0.05	0.54	0.05	0.29	0.04	0.18	0.03	0.11	0.01
	Nov	11.60	0.00	10.78	0.00	10.41	0.00	10.14	0.00	9.95	0.00	9.61	0.00
	Dec	21.93	0.00	20.71	0.00	20.18	0.00	20.00	0.00	19.97	0.00	19.67	0.00
Annual	Total	92.27	20.02	86.93	17.89	85.09	15.64	84.53	11.57	86.00	8.16	85.29	5.73
	H+C	112.29		104.81		100.73		96.10		94.16		91.02	
Season Average	Winter	17.53	0.00	16.67	0.00	16.43	0.00	16.57	0.00	17.02	0.00	17.00	0.00
	Spring	1.75	1.07	1.57	0.99	1.55	0.84	1.47	0.52	1.61	0.37	1.63	0.20
	Summer	0.00	5.59	0.00	4.95	0.00	4.36	0.00	3.32	0.00	2.35	0.00	1.71
	Autumn	11.47	0.02	10.73	0.02	10.38	0.02	10.14	0.01	10.03	0.01	9.80	0.00
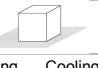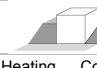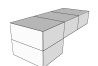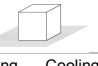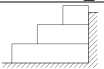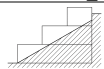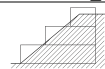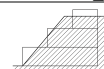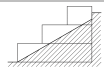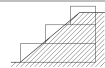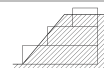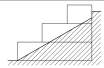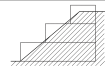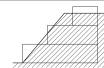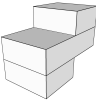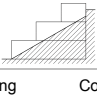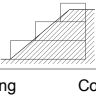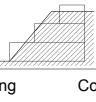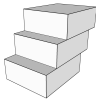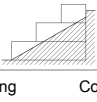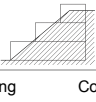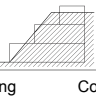
Configurations - Confg04

		Confg04_00°		Confg04_10°		Confg04_20°		Confg04_30°		Confg04_40°		Confg04_50°	
		Heating	Cooling	Heating	Cooling	Heating	Cooling	Heating	Heating	Cooling	Heating	Cooling	Heating
Monthly	Jan	25.68	0.00	24.85	0.00	23.90	0.00	22.98	0.00	22.56	0.00	22.35	0.00
	Feb	17.96	0.00	17.41	0.00	17.09	0.00	16.89	0.00	16.88	0.00	16.84	0.00
	Mar	12.59	0.00	12.23	0.00	12.14	0.00	12.21	0.00	12.38	0.00	12.44	0.00
	Apr	4.60	0.02	4.41	0.01	4.36	0.00	4.62	0.00	4.77	0.00	4.86	0.00
	May	0.64	0.86	0.59	0.77	0.40	0.40	0.27	0.09	0.18	0.05	0.18	0.02
	Jun	0.03	2.82	0.03	2.64	0.01	1.48	0.00	0.63	0.00	0.36	0.00	0.23
	Jul	0.00	7.62	0.00	6.95	0.00	4.71	0.00	2.62	0.00	1.52	0.00	1.13
	Aug	0.00	7.52	0.00	6.84	0.00	4.77	0.00	2.84	0.00	1.78	0.00	1.34
	Sep	0.00	2.70	0.00	2.53	0.00	1.73	0.00	1.10	0.00	0.65	0.00	0.50
	Oct	0.98	0.06	0.90	0.05	0.58	0.03	0.25	0.00	0.12	0.00	0.11	0.00
	Nov	12.33	0.00	11.86	0.00	11.27	0.00	10.41	0.00	9.85	0.00	9.68	0.00
	Dec	23.66	0.00	22.84	0.00	21.79	0.00	20.65	0.00	20.03	0.00	19.76	0.00
Annual	Total	98.47	21.61	95.12	19.79	91.55	13.11	88.29	7.28	86.76	4.37	86.21	3.22
	H+C	120.08		114.91		104.66		95.57		91.13		89.43	
Season Average	Winter	18.74	0.00	18.17	0.00	17.71	0.00	17.36	0.00	17.27	0.00	17.21	0.00
	Spring	1.76	1.23	1.67	1.14	1.59	0.63	1.63	0.24	1.65	0.14	1.68	0.08
	Summer	0.00	5.95	0.00	5.44	0.00	3.74	0.00	2.18	0.00	1.32	0.00	0.99
	Autumn	12.32	0.02	11.87	0.02	11.21	0.01	10.44	0.00	10.00	0.00	9.85	0.00

Configurations - Confg05

		Confg05_00°		Confg05_10°		Confg05_20°		Confg05_30°		Confg05_40°		Confg05_50°	
		Heating	Cooling	Heating	Cooling	Heating	Cooling	Heating	Heating	Cooling	Heating	Cooling	Heating
Monthly	Jan	21.96	0.00	21.62	0.00	20.95	0.00	20.04	0.00	20.18	0.00	20.03	0.00
	Feb	15.76	0.00	15.51	0.00	15.05	0.00	14.54	0.00	14.90	0.00	14.92	0.00
	Mar	11.70	0.00	11.50	0.00	11.14	0.00	10.79	0.00	11.23	0.00	11.29	0.00
	Apr	4.88	0.01	4.77	0.01	4.51	0.01	4.31	0.00	4.70	0.00	4.74	0.00
	May	0.80	0.35	0.76	0.35	0.68	0.34	0.52	0.26	0.52	0.09	0.48	0.05
	Jun	0.04	1.14	0.03	1.13	0.03	1.08	0.02	0.91	0.01	0.54	0.00	0.42
	Jul	0.00	4.54	0.00	4.45	0.00	3.99	0.00	3.19	0.00	2.32	0.00	1.89
	Aug	0.00	4.90	0.00	4.77	0.00	4.35	0.00	3.55	0.00	2.65	0.00	2.18
	Sep	0.00	1.75	0.00	1.69	0.00	1.56	0.00	1.37	0.00	1.00	0.00	0.79
	Oct	0.76	0.03	0.74	0.03	0.61	0.03	0.43	0.02	0.32	0.00	0.26	0.00
	Nov	10.33	0.00	10.13	0.00	9.63	0.00	8.95	0.00	8.88	0.00	8.65	0.00
	Dec	19.93	0.00	19.60	0.00	18.89	0.00	17.91	0.00	17.93	0.00	17.70	0.00
Annual	Total	86.14	12.72	84.66	12.43	81.49	11.35	77.51	9.30	78.66	6.61	78.08	5.34
	H+C	98.87		97.09		92.85		86.81		85.26		83.42	
Season Average	Winter	16.47	0.00	16.21	0.00	15.71	0.00	15.12	0.00	15.43	0.00	15.41	0.00
	Spring	1.90	0.50	1.85	0.50	1.74	0.48	1.62	0.39	1.74	0.21	1.74	0.16
	Summer	0.00	3.73	0.00	3.63	0.00	3.30	0.00	2.70	0.00	1.99	0.00	1.62
	Autumn	10.34	0.01	10.15	0.01	9.71	0.01	9.10	0.01	9.04	0.00	8.87	0.00

Configurations - Confg06

		Confg06_00°		Confg06_10°		Confg06_20°		Confg06_30°		Confg06_40°		Confg06_50°	
		Heating	Cooling	Heating	Cooling	Heating	Cooling	Heating	Heating	Cooling	Heating	Cooling	Heating
Monthly	Jan	26.15	0.00	25.80	0.00	24.66	0.00	23.51	0.00	22.42	0.00	22.36	0.00
	Feb	18.30	0.00	18.05	0.00	17.47	0.00	17.11	0.00	16.57	0.00	16.70	0.00
	Mar	12.80	0.00	12.61	0.00	12.22	0.00	12.27	0.00	12.04	0.00	12.22	0.00
	Apr	4.71	0.01	4.60	0.01	4.29	0.01	4.53	0.01	4.52	0.00	4.70	0.00
	May	0.67	0.74	0.64	0.74	0.45	0.50	0.32	0.32	0.24	0.24	0.23	0.07
	Jun	0.03	2.68	0.03	2.66	0.02	1.73	0.01	1.00	0.01	0.78	0.00	0.42
	Jul	0.00	7.55	0.00	7.42	0.00	5.38	0.00	3.30	0.00	2.22	0.00	1.57
	Aug	0.00	7.41	0.00	7.25	0.00	5.38	0.00	3.43	0.00	2.44	0.00	1.77
	Sep	0.00	2.46	0.00	2.39	0.00	1.72	0.00	1.16	0.00	1.00	0.00	0.72
	Oct	1.07	0.04	1.04	0.04	0.72	0.04	0.39	0.03	0.20	0.02	0.14	0.00
	Nov	12.59	0.00	12.38	0.00	11.64	0.00	10.93	0.00	10.11	0.00	9.99	0.00
	Dec	24.13	0.00	23.79	0.00	22.57	0.00	21.28	0.00	20.05	0.00	19.93	0.00
Annual	Total	100.45	20.91	98.94	20.52	94.03	14.76	90.35	9.25	86.19	6.70	86.28	4.56
	H+C	121.35		119.46		108.79		99.61		92.89		90.84	
Season Average	Winter	19.08	0.00	18.82	0.00	18.12	0.00	17.63	0.00	17.01	0.00	17.10	0.00
	Spring	1.80	1.15	1.76	1.14	1.58	0.75	1.62	0.44	1.59	0.34	1.64	0.16
	Summer	0.00	5.81	0.00	5.69	0.00	4.16	0.00	2.63	0.00	1.89	0.00	1.35
	Autumn	12.60	0.01	12.40	0.01	11.64	0.01	10.87	0.01	10.12	0.01	10.02	0.00

Table Appendices 14: Section 8.5. – Different Cross Sections heating and cooling results

Cross Section – CrossSec01

		CrossSec01_00°		CrossSec01_30°		CrossSec01_40°		CrossSec01_50°	
		Heating	Cooling	Heating	Cooling	Heating	Cooling	Heating	Cooling
Monthly	Jan	21.75	0.00	20.39	0.00	20.25	0.00	20.18	0.00
	Feb	15.16	0.00	14.59	0.00	14.69	0.00	14.77	0.00
	Mar	10.72	0.00	10.46	0.00	10.64	0.00	10.79	0.00
	Apr	3.92	0.00	3.83	0.00	3.93	0.00	4.05	0.00
	May	0.57	0.33	0.50	0.12	0.48	0.03	0.49	0.02
	Jun	0.02	1.55	0.01	0.60	0.01	0.24	0.01	0.17
	Jul	0.00	5.96	0.00	3.00	0.00	1.93	0.00	1.47
	Aug	0.00	6.35	0.00	3.41	0.00	2.35	0.00	1.86
	Sep	0.00	2.38	0.00	1.19	0.00	0.76	0.00	0.56
	Oct	0.54	0.03	0.38	0.02	0.30	0.00	0.29	0.00
	Nov	9.62	0.00	8.75	0.00	8.54	0.00	8.50	0.00
	Dec	19.62	0.00	18.19	0.00	17.95	0.00	17.85	0.00
Annual	Total	81.92	16.60	77.11	8.33	76.79	5.32	76.92	4.07
	H+C	98.52		85.44		82.10		80.99	
Season Average	Winter	15.88	0.00	15.15	0.00	15.19	0.00	15.25	0.00
	Spring	1.50	0.63	1.45	0.24	1.47	0.09	1.52	0.06
	Summer	0.00	4.90	0.00	2.53	0.00	1.68	0.00	1.29
	Autumn	9.93	0.01	9.11	0.01	8.93	0.00	8.88	0.00

Cross Section – CrossSec02

		CrossSec02_00°		CrossSec02_30°		CrossSec02_40°		CrossSec02_50°	
		Heating	Cooling	Heating	Cooling	Heating	Cooling	Heating	Cooling
Monthly	Jan	21.57	0.00	20.14	0.00	19.97	0.00	19.79	0.00
	Feb	15.00	0.00	14.38	0.00	14.44	0.00	14.45	0.00
	Mar	10.61	0.00	10.34	0.00	10.49	0.00	10.59	0.00
	Apr	3.88	0.00	3.81	0.00	3.92	0.00	4.03	0.00
	May	0.56	0.39	0.50	0.23	0.48	0.10	0.49	0.05
	Jun	0.02	1.68	0.02	0.81	0.01	0.52	0.01	0.34
	Jul	0.00	6.05	0.00	3.11	0.00	2.27	0.00	1.75
	Aug	0.00	6.41	0.00	3.47	0.00	2.56	0.00	2.02
	Sep	0.00	2.42	0.00	1.19	0.00	0.83	0.00	0.62
	Oct	0.56	0.03	0.41	0.02	0.35	0.01	0.32	0.00
	Nov	9.52	0.00	8.61	0.00	8.40	0.00	8.31	0.00
	Dec	19.47	0.00	17.97	0.00	17.71	0.00	17.50	0.00
Annual	Total	81.20	16.99	76.17	8.84	75.77	6.30	75.48	4.78
	H+C	98.19		85.00		82.07		80.26	
Season Average	Winter	15.73	0.00	14.95	0.00	14.97	0.00	14.94	0.00
	Spring	1.49	0.69	1.44	0.35	1.47	0.21	1.51	0.13
	Summer	0.00	4.96	0.00	2.59	0.00	1.89	0.00	1.46
	Autumn	9.85	0.01	8.99	0.01	8.82	0.00	8.71	0.00

Cross Section – CrossSec03

		CrossSec03_00°		CrossSec03_30°		CrossSec03_40°		CrossSec03_50°	
		Heating	Cooling	Heating	Cooling	Heating	Cooling	Heating	Cooling
Monthly	Jan	21.87	0.00	20.69	0.00	20.50	0.00	20.37	0.00
	Feb	15.27	0.00	14.69	0.00	14.75	0.00	14.79	0.00
	Mar	10.82	0.00	10.54	0.00	10.65	0.00	10.73	0.00
	Apr	3.99	0.00	3.91	0.00	3.97	0.00	4.02	0.00
	May	0.59	0.38	0.53	0.25	0.51	0.09	0.49	0.04
	Jun	0.02	1.61	0.02	1.09	0.01	0.60	0.01	0.37
	Jul	0.00	5.90	0.00	3.92	0.00	2.82	0.00	2.18
	Aug	0.00	6.29	0.00	4.26	0.00	3.15	0.00	2.49
	Sep	0.00	2.36	0.00	1.58	0.00	1.10	0.00	0.82
	Oct	0.57	0.03	0.46	0.02	0.39	0.01	0.34	0.00
	Nov	9.68	0.00	8.97	0.00	8.74	0.00	8.59	0.00
	Dec	19.73	0.00	18.52	0.00	18.26	0.00	18.07	0.00
Annual	Total	82.55	16.58	78.33	11.11	77.79	7.77	77.41	5.90
	H+C	99.13		89.44		85.56		83.31	
Season Average	Winter	15.99	0.00	15.31	0.00	15.30	0.00	15.30	0.00
	Spring	1.53	0.66	1.49	0.45	1.50	0.23	1.51	0.14
	Summer	0.00	4.85	0.00	3.25	0.00	2.36	0.00	1.83
	Autumn	10.00	0.01	9.32	0.01	9.13	0.00	9.00	0.00

Cross Section – CrossSec04							
CrossSec04_00°		**CrossSec04_30°**		**CrossSec04_40°**		**CrossSec04_50°**	
Heating	Cooling	Heating	Cooling	Heating	Cooling	Heating	Cooling
Jan 22.04	0.00	20.96	0.00	20.74	0.00	20.55	0.00
Feb 15.39	0.00	14.81	0.00	14.85	0.00	14.83	0.00
Mar 10.92	0.00	10.59	0.00	10.67	0.00	10.72	0.00
Apr 4.04	0.00	3.93	0.00	3.98	0.00	4.02	0.00
May 0.59	0.45	0.54	0.29	0.51	0.13	0.50	0.06
Jun 0.02	1.79	0.02	1.22	0.01	0.73	0.01	0.47
Jul 0.00	6.00	0.00	4.39	0.00	3.31	0.00	2.66
Aug 0.00	6.31	0.00	4.64	0.00	3.55	0.00	2.89
Sep 0.00	2.34	0.00	1.64	0.00	1.17	0.00	0.89
Oct 0.59	0.03	0.50	0.02	0.42	0.01	0.38	0.00
Nov 9.82	0.00	9.17	0.00	8.95	0.00	8.79	0.00
Dec 19.92	0.00	18.83	0.00	18.54	0.00	18.31	0.00
Annual Total 83.32	16.93	79.34	12.21	78.67	8.89	78.10	6.98
H+C 100.25		91.56		87.56		85.08	
Season Average Winter 16.11	0.00	15.45	0.00	15.42	0.00	15.37	0.00
Spring 1.55	0.75	1.50	0.51	1.50	0.28	1.51	0.18
Summer 0.00	4.88	0.00	3.56	0.00	2.68	0.00	2.15
Autumn 10.11	0.01	9.50	0.01	9.31	0.00	9.16	0.00

Cross Section – CrossSec05							
CrossSec05_00°		**CrossSec05_30°**		**CrossSec05_40°**		**CrossSec05_50°**	
Heating	Cooling	Heating	Cooling	Heating	Cooling	Heating	Cooling
Jan 21.95	0.00	20.80	0.00	20.56	0.00	20.41	0.00
Feb 15.33	0.00	14.70	0.00	14.72	0.00	14.74	0.00
Mar 10.90	0.00	10.53	0.00	10.62	0.00	10.71	0.00
Apr 4.05	0.01	3.93	0.00	3.99	0.00	4.05	0.00
May 0.60	0.44	0.55	0.37	0.53	0.21	0.51	0.12
Jun 0.02	1.64	0.02	1.29	0.01	0.90	0.01	0.68
Jul 0.00	5.87	0.00	4.28	0.00	3.14	0.00	2.49
Aug 0.00	6.25	0.00	4.61	0.00	3.47	0.00	2.77
Sep 0.00	2.33	0.00	1.67	0.00	1.18	0.00	0.91
Oct 0.59	0.03	0.49	0.03	0.43	0.01	0.38	0.00
Nov 9.74	0.00	9.04	0.00	8.82	0.00	8.66	0.00
Dec 19.81	0.00	18.65	0.00	18.34	0.00	18.14	0.00
Annual Total 82.99	16.58	78.71	12.25	78.02	8.91	77.62	6.98
H+C 99.56		90.96		86.93		84.60	
Season Average Winter 16.06	0.00	15.34	0.00	15.30	0.00	15.29	0.00
Spring 1.56	0.70	1.50	0.55	1.51	0.37	1.52	0.27
Summer 0.00	4.82	0.00	3.52	0.00	2.60	0.00	2.06
Autumn 10.05	0.01	9.39	0.01	9.20	0.00	9.06	0.00